Fabrication & Characterisation Of Enzyme Electrodes For Biosensor & Biofuel Cell Applications

A Thesis Submitted By

James Merotra

For the Degree of Doctor of Philosophy

School of Chemical Engineering and Advanced Materials
Newcastle University

15th August 2013

Abstract

Enzyme electrodes are biochemical transducers. They function by converting biochemical reactions into electrochemical processes. This functionality could potentially give rise to a new generation of implantable medical devices such as biofuel cells and biosensors.

The main aim of this study was to fabricate and characterise enzyme electrodes for potential use in these applications. Specifically, the electrodes were fabricated with a view to addressing current problems with enzyme electrodes, problems such as stability, lifetime, activity, interference and ease of fabrication. The approach involved testing various materials such as different types of enzyme, polymeric electron transfer mediators, enzyme entrapment materials, conductive supports and matrices and biocompatible polymers.

The main enzyme used was Glucose Oxidase. Additional work was also carried out on Bilirubin Oxidase, Pyranose 2-Oxidase Acyl-CoA Oxidase and Acetyl-CoA Synthetase. Various immobilisation methods were used including direct adsorption, covalent binding and physical entrapment.

Polymeric electron transfer mediators were fabricated and tested. The main mediator used was Ferrocene and its derivatives. Coenzyme Q_{10} was also tested as a mediator for enzyme electrodes. The biomimicking polymer poly(2-methacryloyloxyethyl phosphorylcholine-co-n-butyl methacrylate) was also adapted and incorporated into a Glucose Oxidase enzyme electrode. A rapid and straightforward enzyme electrode fabrication method using Ferrocene and Nafion was developed and used to test Pyranose-2-Oxidase for potential use as a glucose oxidising enzyme for enzyme electrodes. This

method was also used to develop an enzymatic biofuel cell using Glucose Oxidase for glucose oxidation at the anode and Bilirubin Oxidase for oxygen reduction at the cathode. Finally, this fabrication method was used with Glucose Oxidase, Acyl-CoA Oxidase and Acetyl-CoA Synthetase for preliminary investigations into the viability of a multi analyte biosensor.

The investigation was based primarily on electrochemical techniques such as voltammetry, amperometry, electrochemical impedance spectroscopy and fuel cell diagnostics.

The materials and immobilisation techniques presented could potentially be used to improve future enzyme electrodes. This may be achieved through the novel use of biocompatible and biomimicking polymers, through simple biofuel cell fabrication and with the use of multi analyte biosensors developed during this investigation.

Contents

Figures

Nomenclature

A	Area
a	Activity
AA	Ascorbic acid
ac	Alternating current
ACOD	Acyl-CoA oxidase
ACS	Acyl-CoA synthatase
AMP	Adenosine monophosphate
APBA	3-aminophenylboronic acid
ATP	Adenosine triphosphate
AuNP	Gold nanoparticle
BMA	Butyl methacrylate
BOD	Bilirubin Oxidase
BSA	Bovine serum albumin
CA	Chronoamperometry
C_{DL}	Double layer capacitance
CE	Counter electrode
C_{LF}	Low frequency capacitance
CNT	Carbon nanotube
CoA	Coenzyme A
CQ_{10}	Coenzyme Q_{10}
CV	Cyclic voltammetry
DC	Direct current
DET	Direct electron transfer
DMF	Dimethylformamide
E_0	Equilibrium potential
$E_{1/2}$	Half wave potential
E_{app}	Applied potential
EBC	Enzymatic biofuel cell
EDC	1-Ethyl-3-(3-dimethylaminopropyl)carbodiimide
EIS	Electrochemical impedance spectroscopy
E_{OPT}	Optimum potential
E_P	Peak potential
FAD	Flavin adenine dinucleotide
Fc	Ferrocene
GA	Glutaraldehyde
GCE	Glassy carbon electrode
GDR	Glucose disposal rate
GOx	Glucose Oxidase
GPE	Graphite paste electrode
GRAS	Generally recognised as safe
HMDA	Hexamethylenediamine

HOPG	Highly ordered pyrolytic graphite
hrs	Hours
IGT	Impaired glucose tolerance
i_P	Peak current
i_{PA}	Anodic peak current
i_{PC}	Cathodic peak current
j	Peak current density
j_{MAX}	Maximum current density
k_B	Boltzmann constant
K_M	Michaelis–Menten constant
L	Polymer thickness
LBL	Layer by layer
LSV	Linear sweep voltammetry
M	Mediator
MCAG	Multi-walled Carbon Nanotube|Chitosan|Gold Nanoparticles|Glucose Oxidase
MPCA	Multi-walled Carbon Nanotube|PMBN| Coenzyme-Q_{10}|Gold Nanoparticles
MPCAG	Multi-walled-Carbon Nanotube|PMBN|Coenzyme-Q_{10}|Gold Nanoparticles|Glucose Oxidase
mV	millivolt
MWCNT	Multi-walled Carbon Nanotube
NAD	Nicotinamide adenine dinucleotide
Nc	Nickelocene
NEFA	Non-esterified fatty acid
NHS	N-hydroxysulfosuccinimide
OA	Oleic acid
OACoA	Oleoyl coenzyme A
OCP	Open circuit potential
P2O	Pyranose-2-oxidase
PA	Palmitic acid
PACoA	Palmitoyl coenzyme A
PBS	Phosphate buffer solution
PC	Phosphorylcholine
PCG	PMBN | Coenzyme Q_{10} | Glucose Oxidase
PDA	Poly(dimethyldiallyammonium chloride)
PEG	Polyethylene glycol
PEI-Fc	Polyethylenimine-Ferrocene
PES	Polyethersulfone
PHF	PMBN|HMDA|Fc
PHFPG	PMBN|HMDA|Fc|PMBN|GOx
P_{MAX}	Maximum power
PMBN	poly[2-methacryloyloxyethyl

	phosphorylcholine-co-n-butyl methacrylate-co-p-nitrophenyloxycarbonyl poly(ethylene glycol) methacrylate]
Ppi	Pyro-phosphate
PQQ	Pyrroloquinoline quinone
q	Charge
QRE	Quasi-Reference Electrode
R	Gas constant
R_{CT}	Charge transfer resistance
RE	Reference electrode
R_F	Film resistance
R_{OPT}	Optimum resistance
R_S	Solution resistance
RTP	Room temperature and pressure
s	Seconds
SPE	Screen printed electrode
SWCNT	Single walled carbon nanotube
T	Temperature
T2D	Type two diabetes
v	Scan rate
V	Volume
VFc	Vinylferrocene
WE	Working electrode
z	Number of moles of electrons
Z’	‘Real’ impedance
Z’’	‘Imaginary’ impedance
Z_W	Warburg impedance

Chapter 1 - Introduction

1.1 Motivation & Aims & Objectives of Research

Electronic devices that can exploit the properties of enzymes could lead to a great improvement in biological and medical technology. Enzymes have properties that are unmatched by conventional low temperature oxidation-reduction catalysts.[1] Perhaps the most important of these properties is the high selectivity of enzymes. This selectivity allows the development of highly specific sensors and of membrane-less biological fuel cell assemblies. The lack of a membrane means the cell design is much simpler and there is no need for fuel pre-treatment. Another advantage enzymes have over conventional catalysts is their activity in physiological conditions. These properties mean that enzyme electrode technology can potentially find application in implantable sensors or as a source of electrical energy in various biological systems.

Current implantable power sources require reactive, corrosive or toxic components and strong cases to house them.[2] The need for a strong case places a restriction on the size of any conventional implantable device.[2] Because of substrate selectivity, membranes and cases are not needed; this allows substantial miniaturisation of enzyme electrode devices. Enzyme electrode devices could therefore be placed directly in human or animal tissue or potentially in plant saps, juices or biological waste streams.

The energy released upon oxidation or reduction of a fuel scales with its mass. Thus the miniaturisation of power sources, even if the oxidant is O_2 from air, can impact only on systems that do not consume much power. The limited effective lifetime of immobilised

enzymes means that application of this technology is best suited to devices that do not operate for long periods.

The key challenges in the design of enzyme electrodes are improving current density and lifetime. These problems can be broken down into a set of design problems that include: obtaining efficient electron conductivity between the macroscopic electrode and the enzyme, achieving high enough volumetric densities of immobilised enzyme that retain activity and stabilising the electrode towards degradation and leaching.[3]

This research attempts to address these areas via investigation of:

- Redox polymers for enzyme immobilisation (Chapters 2 and 3).
- Direct electron transfer (DET) between enzyme active sites and electrodes, in order to improve the operating potential of enzyme electrodes (Chapter 4).

An enzyme electrode developed in Chapter 2 is then tested as the anode in a glucose|oxygen enzymatic biofuel cell (EBC) (Chapter 5) and as a glucose sensor in a duel analyte sensor system (Chapter 6).

1.2 Enzyme Electrode Overview

The development of enzyme electrodes has remained a prime focus of many researchers since the pioneering studies of Clark and Lyons in 1962[4] and by Updike and Hicks in 1967.[5] The majority of the work is focussed on the tailoring of bioelectronic systems via

the assembly of biomaterials on solid conductive supports and the design of the appropriate electrical contact between the biological matrices and the support elements.[6]

All enzyme electrodes must ultimately involve the transfer of electrons to or from the active site of an enzyme and an electrode surface. Electron transfer in enzyme electrodes can be achieved both by tunnelling and by motion in and out of protein chains.[7] For distances of >8 Å tunnelling rates (currents in electrodes) decrease exponentially with the distance between enzyme active sites and electron acceptors (for example oxidized mediators) and also between mediators and electrodes.[7] The successful detection of current arising from electron transfer from an enzyme active site to an electrode is known as electrocatalysis. Electrocatalysis is defined as the promotion of electron transfer rates and efficiencies at electrodes by the properties of the electrode surface.[8] It is the involvement of the electrode in the catalytic cycle of the enzyme. The reaction of enzymes with mediators can be described as an EC' mechanism. That is, an electrochemical (E) /chemical (C) mechanism, with the ' denoting that it is a catalytic process. The electrode generates oxidised mediator (the electrochemical step) which then goes on to react with the reduced enzyme (the chemical step). The chemical step regenerates the oxidised mediator, completing the catalytic process.

A wide variety of electrode materials can be used in enzyme electrode design. The most commonly used materials are Au and C. C has some disadvantages w.r.t. Au such as chemical inertness towards coupling reagents and decreasing mechanical strength with increasing size.[9]

One of the most commonly used electrodes in enzyme electrode research is the glassy carbon electrode (GCE). GCEs have many advantages for use in enzyme electrode research. GCE surfaces can be oxidised to produce COOH groups on the surface which are available for enzyme binding with an activating agent such as 1-Ethyl-3-(3-dimethylaminopropyl)carbodiimide (EDC)[9] (see Section 1.9).

One of the main issues with this work was the reproducibility of the results. The nature of enzyme electrodes means that the results can be highly variable, meaning that it is difficult to determine statistics and error estimates. This is due to the fact that certain parameters, such as enzyme activity, normally assumed to remain constant, may change throughout the timeframe of the experiment.[10] Substrate depletion, enzyme inactivation, low solubility of redox mediators and relativity between mass transport and kinetic control contribute to difficulties in producing repeatable results.[10] In order to compare experimental results it is important to accurately determine and reproducibly control the concentrations of enzyme and mediator immobilised at the electrode surface, a task which, as stated previously, is often difficult to achieve.[10]

1.3 Glucose Oxidase

Molecular weight	150 to 180 KDa[11]
Approximate dimensions	60 Å x 52 Å x 77 Å[11b]
Hydrodynamic radius	43Å[12]
Footprint dimension	5800 Å^2[6]
Isoelectric point	4[6]

The main enzyme used in this study is Glucose Oxidase (GOx). GOx is a dimeric flavoprotein enzyme. It catalyses the oxidation of β-d-glucose by O_2 to d-gluconolactone

which subsequently hydrolyses spontaneously to gluconic acid and hydrogen peroxide.[11b]

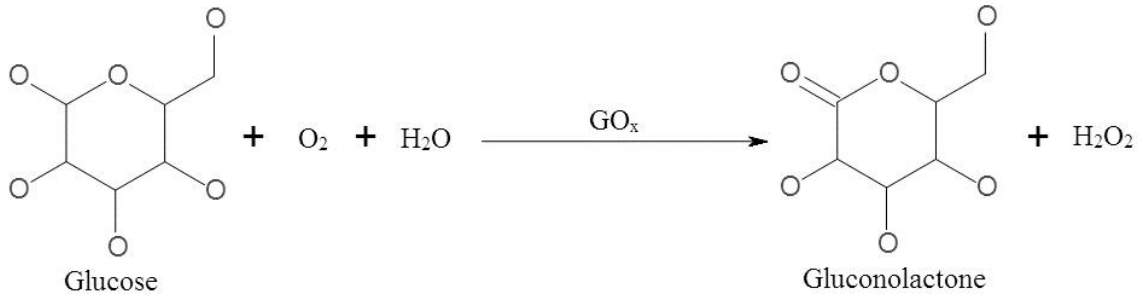

Figure 1.1: The reaction catalysed by GOx

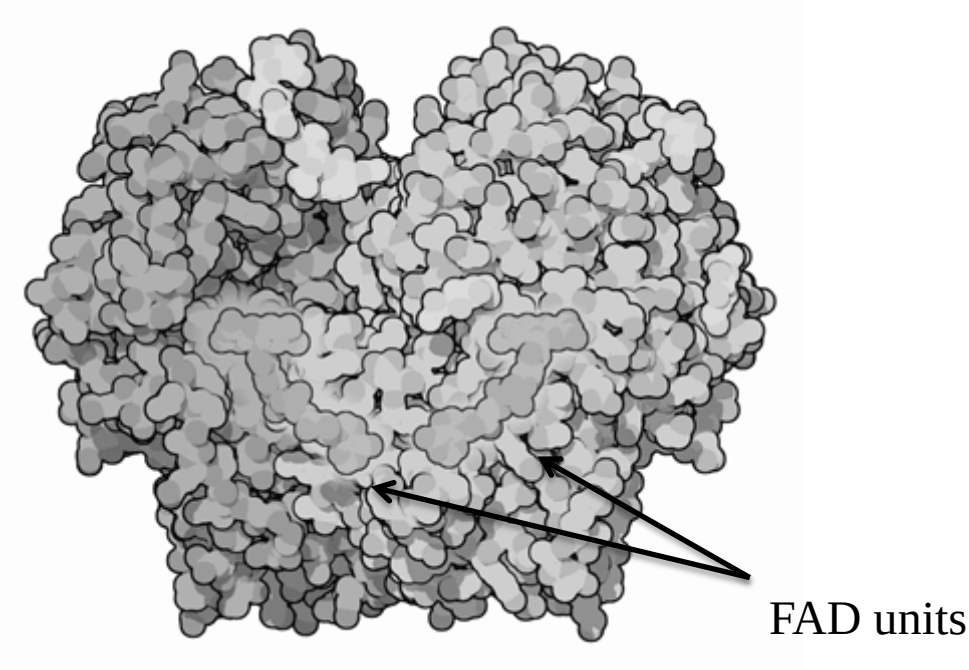

Figure 1.2: The dimeric structure of GOx showing the two FAD units in each dimer.

The enzyme is highly specific for glucose with other saccharides being oxidised at much lower rates.[11b] The reaction can be divided into two different steps, 1) the oxidation of the substrate with the corresponding reduction of the enzyme in the reductive half reaction, 2) the subsequent re-oxidation of the enzyme in the oxidative half reaction. For most substrates the maximum turnover number of the reductive half reaction is

determined by the rate of flavin reduction.[11b] The oxidative half reaction is also governed by one rate constant with no significant contribution from the formation of the enzyme oxygen substrate complex.[11b] The pH optimum for the reaction between GOx and glucose is 5.5, when O_2 is the electron acceptor. At lower pH's than this, protonation of the reduced enzyme leads to an observable decrease in the rate of reaction. At pH >5.5, the reaction rate is also decreased. This is due to the fact that the enzyme becomes deprotonated before it can be re-oxidised, leading to a change in structure, which results in lower activity.

GOx has two flavin adenine dinucleotide (FAD) prosthetic groups per apoenzyme.[13] The FAD groups form strong non-covalent bonds within the enzymes two subunits.[6] The reduction of FAD to $FADH_2$ takes place at -0.05 V vs. SHE.[7] pH has been shown to affect the redox potential (E) of FAD.[6]

GOx is structurally rigid.[12] The rigidity and therefore the ruggedness of the enzyme derive in part from the polysaccharide that forms its outer hydrophilic envelope.[12] The FAD molecule is localized in a cavity deeper than 8 Å, this makes direct contact with the electrode difficult.[11a] Due to the insulating effect of the protein encasing the FAD site, mediators are needed to shuttle electrons from the enzyme active site to the electrode, although direct electron transfer has been demonstrated with GOx.[13] Both cationic groups (lysine and arginine) and anionic groups (aspartic and glutamic acid) are located on the enzymes surface, however, their distribution and relative numbers lead to an essentially negative electrostatic surface potential.[11a] GOx is an excellent choice of enzyme for fuel cell applications as its reduction specifically requires glucose and its oxidation can be brought about by a number of redox partners.[14] Up to 95% of the

carbohydrate content of the enzymes structure can be removed with no effect on activity or stability.[11b] As the active site of the enzyme is located in an insulated pocket, the ability to remove elements of the enzymes structure without any effect on activity or stability is a big advantage. Glucose concentration in human blood plasma ranges from 3.6 mM to 5.8 mM.[15] In most GOx based enzyme electrode assemblies, a current response is observed for glucose concentrations between 0 and 30 mM.[16] This means that GOx is a suitable enzyme for use in devices based on plasma derived glucose.

1.4 Mediated Electron Transfer with GOx

Direct electron transfer between an enzyme active site and an electrode is perhaps most easily achieved by bringing the enzyme close to the electrode surface. However, when brought into contact with a bare metal, a metal oxide or a solid surface in general, proteins tend to deform or even to denature due to interactions between amino acid side chains and the substrate surface.[8] Therefore it is desirable to avoid such interactions, however, in proteins, the rate of electron transfer drops by a factor of 10^4 when the distance between an electron donor and an acceptor is increased from 8Å to 17Å.[12]

Flavoenzymes such as GOx and D-amino-acid oxidase do not directly transfer electrons to conventional electrodes, because the distance between their redox centres and the electrodes' surface exceeds, even on closest approach, the distance across which electrons are transferred at sufficient rates.[7] Also, direct adsorption of GOx onto metal surfaces has been shown to denature the enzyme.[6]

As it is difficult for the electrode to access the FAD site directly, chemical mediators can be used to shuttle electrons from FAD to the electrode. The mediator is shuttled between

the electrode and FAD, transferring the electrons required for the re-oxidation of $FADH_2$ in exchange for the natural electron acceptor O_2.[11a]

Mediated electron transfer involves low RMM redox active species shuttling electrons between the enzyme active site and the electrode. The enzyme catalyses the redox of the mediator (the mediator can be considered a co-substrate). The mediator can then be regenerated at the electrode.

Mediators can be free in solution, physically entrapped behind a membrane immobilised in a matrix along with the biocatalyst or covalently bound to a surface or polymer network (the polymer can be conducting or insulating). In homogeneous solutions, redox enzymes, such as GOx, accept electrons from and transfer electrons to, small oxidisable/reducible ions or molecules but do not exchange electrons with simple metal electrodes.[12] In the absence of adequately fast electron transfer, these electrodes do not respond to variations in substrate (e.g., glucose) concentration.[12]

Fast redox mediators, having redox potentials 0.07-0.55 V positive of the redox potential of immobilised enzymes are effective mediators when covalently or coordinatively bound to the enzyme's proteins groups.[7] The limiting currents, i.e., the currents observed at sufficiently oxidizing potentials and at high substrate concentrations, increase, in general, with the number of mediators per enzyme molecule.[7] The mediators must have redox potentials that are oxidizing relative to the potential of the active centres. Otherwise, oxidation of the active centres by the reduced mediators cannot take place.[7] It is however, beneficial for the redox potential of the mediator to be as reducing as possible, as this helps to avoid interference from non-specific oxidation of interfering components. Low redox potentials also contribute to the efficiency of the electrode.

The most effective mediators are those with fast electron transfer kinetics.[7] This relates to the structure of the mediator and its solvent environment upon oxidation or reduction.[7] Good mediators should also have reversible electrochemistry at the electrode surface.[14] Mediator concentration must be sufficiently high if useable current density is to be achieved.[17] Free floating mediators result in enzyme electrodes that are mass transfer controlled. Immobilising mediators ensures that the catalytic current depends on the active surface area.[18] Obviously it is desirable to have good electron transfer kinetics between electrode, mediator and enzyme so as to make sure that the electron transfer is not the rate-limiting step during enzyme turnover.[8]

Ferrocene (Fc) based mediators can act as rapid oxidants for GOx.[16] Another advantage of Fc as a redox mediator is the fact that its redox potential is independent of pH.[6] However, the rates of the GOx + ferrocenium ion reaction are lower than for the reaction of reduced GOx with O_2 (GOx's natural redox partner).[16] Therefore the presence of O_2 in the vicinity of any GOx|Fc based enzyme electrode will affect the resulting catalytic current.

The mediation of GOx by Fc proceeds in the following manner:

$$Glucose + GOx_{ox} \rightarrow Gluconolactone + GOx_{red} \qquad 1.1$$

GOx is reduced by glucose.

$$GOx_{red} + 2\,FcR^{+} \rightarrow GOx_{ox} + 2FcR + 2H^{+} \qquad 1.2$$

GOx then reduces the Fc mediator.

$$2FcR \leftrightarrow 2FcR^{+} + 2e^{-} \qquad 1.3$$

The Fc mediator is then oxidised by the electrode and is free to be reduced by GOx once again.

Mediators require low solubility in aqueous solution to avoid leeching problems, yet they need to be soluble enough to allow efficient diffusion between the enzyme and the electrode surface.[16] The mediator should also be stable in physiological conditions if it is to be used in an EBC.[16] The formal redox potential of a mediator should be low to reduce interference from reduced compounds present in physiological samples.[16] Low redox potentials mean that the non-specific oxidation of interfering components will be minimised by the efficient bio-electrocatalysed oxidation of glucose.[6] A low formal redox potential is also beneficial as no glucose dependent current can be produced until the potential is positive enough to ionise the mediator.[16]

In a mediated GOx based enzyme electrode, mediator groups must compete with O_2 for oxidation of FAD. If the rate of electron transfer between FAD and O_2 is faster than that of the mediator, no current will be produced. This limits the application of GOx-electrodes to deaerated oxygen-free media. The design of fast electrically communicating relay-modified GOx electrodes could enable their use in oxygenated media. Therefore the enhancement of electron transfer rates between the mediators and the reduced FAD cofactor is of substantial importance in the design of enzyme electrodes.

Apart from Fc, PQQ (methoxatin, 4,5-dihydro-4,5-dioxo-1H-pyrrolo-[2,3-f]-quinoline-2,7,9-tricarboxylic acid) has some of the attributes required to be an effective mediator for GOx based enzyme electrodes. It has a unique heterocyclic o-quinone structure and

undergoes an electrochemically reversible electrochemical reaction,[19] being reduced to the hydroquinone form ($PQQH_2$) and oxidized back with two electrons like the majority of quinones in aqueous solution.[19] PQQ has shown reversible electron transfer when coupled to Nicotinamide adenine dinucleotide (NAD)-dependent enzymes,[20] and has been shown to exhibit good electrochemical properties and electron transfer rates,[21]making it an attractive possibility for use as a mediator in enzyme electrodes.

PQQ has an advantage over Fc because its sequence of reactions for transporting electrons from the FAD site to the electrode does not include one electron transfer steps rather it uses a single two electron transfer step.[6]

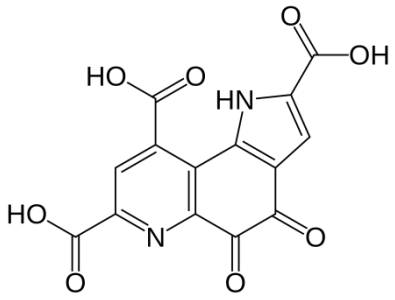

Figure 1.3: The chemical structure of PQQ.

The oxidation of PQQ:[22]

$$PQQH_2 - 2e^- - 2H^+ \leftrightarrow PQQ \qquad 1.4$$

$PQQH_2$ can also be oxidised rapidly by molecular oxygen and hydrogen peroxide in the following reactions:[22]

$$PQQH_2 + O_2 \rightarrow PQQ + H_2O_2 \qquad 1.5$$

$$PQQH_2 + H_2O_2 \rightarrow PQQ + 2H_2O \quad 1.6$$

This oxidation by oxygen and hydrogen peroxide may be a disadvantage, however, the low redox potential of PQQ (as has been observed at a polypyrrole-modified electrode (-110 mV vs. Ag|AgC1)) may reduce possible interference from other electroactive species such as ascorbic acid.[20] Therefore it is still a desirable molecule for use as a mediator.

PQQ can be covalently immobilised via carbodiimide coupling of the PQQ carboxylic groups with amino groups.[19] This enables various methods of covalent immobilisation.

In the case of PQQ containing three carboxylic groups in the molecule, one or two of the carboxylic groups can be involved in the formation of amide bonds with surface amino groups (it is very probable that the third carboxylic group has steric limitations for the formation of a bond with the electrode surface).[19] In the immobilised state, PQQ can be used as an electrochemically reversible electron transfer mediator that can be useful for the development of new, high stability biosensors.[19]

As for the reaction of PQQ with GOx, if electron transfer occurs between the reduced FAD moiety of GOx and oxidized PQQ, sigmoidal catalytic currents should be produced in accordance with the following equations[20]:

$$FADH_2 \rightarrow FAD + 2H^+ + 2e^- \quad 1.7$$

$$PQQ + 2e^- + 2H^+ \rightarrow PQQH_2 \quad 1.8$$

The reduced PQQ as shown in Equation 1.8 can then be oxidised by an electrode producing a sigmoidal catalytic current. The PQQ redox unit therefore acts as an electron relay that electrically contacts the FAD redox-site of the enzyme with the electrode.[23] The electron transfer rate of GOx with an immobilised PQQ layer has been shown to proceed at a rate similar to that of GOx with O_2, another promising characteristic for PQQ as a mediator.[24]

At pH 6 and pH 7 PQQ is no longer protonated and carries a significant negative charge by virtue of its three carboxyl groups. In addition, the net negative charge on the surface of GOx increases as the pH increases beyond the isoelectric point. Consequently a strong electrostatic repulsion between PQQ and GOx has been shown to limit the effectiveness of PQQ as a mediator for GOx at pH6 and pH7.[20] It has been suggested that the carboxylic acid groups of PQQ with a pKa of around 5.0 must be protonated before the appropriate structural interaction between the quinone moiety of PQQ and the FAD moiety of GOx can occur.[20] The resultant charge transfer complex formation facilitates electron transfer from the reduced FAD moiety of GOx to PQQ prior to glucose catalysis.

This is unfortunate as this is inside the range of physiological pH and therefore it is desirable for a mediator to be effective in this range for use in biologically implantable devices.

Co-enzyme Q_{10} (CQ_{10}), or Ubiquinone as it is sometimes known, can be used as a mediator for GOx enzyme electrodes. CQ_{10} is a large molecule (863.34 Da) and therefore has a low rate of diffusion, which improves the stability of CQ_{10} based enzyme

electrodes. CQ_{10} is a naturally occurring compound which fulfils several biological functions in a living cell.[25] It participates in electron and proton transport and Adenosine triphosphate (ATP) synthesis in the mitochondrial reparatory chain.[25] In this process CQ_{10} is reduced to $CQ_{10}H_2$ via semiubiquinone radical $CQ_{10}H^{\cdot}$.[25] The disadvantage of using CQ_{10} as a mediator is its high hydrophobicity, which makes it difficult to incorporate into most common enzyme electrode assemblies (See Chapter 3).

1.5 Chemical Modification of GOx

An increase of the transduced currents of enzyme electrodes requires the improvement of the electrical contact between the enzyme and the electrodes.[6] Access to the active sites of enzymes can be improved by chemical modification.[12] Amperometric glucose sensors can be made with chemically modified enzymes and conventional metal or carbon electrodes.[7]

Electron transfer between the active site of GOx (the FAD site) and electrodes can be improved by chemically modifying GOx with electron mediators. When a sufficient number of electron-relaying centres are attached through covalent bonding to the protein of GOx, electrons are transferred from the enzyme's redox centres to relays that are closer to the periphery of the enzyme.[12] Because some of the relays are located sufficiently close to the enzyme's surface, electrons are transferred at practical rates to the electrode.[12] As a result, a glucose-concentration-dependent current flows in an electrochemical cell made with conventional electrodes when the electrolytic solution contains the relay-modified enzyme.[12] Such a current does not flow when the solution contains the natural enzyme.[12] This type of enzyme modification has been achieved before using ferrocenecarboxylic acid. Specifically, electrical communication was

established between the FAD-FADH, centres of GOx and Au, Pt, or C electrodes through the covalent bonding of an average of 12 molecules of ferrocenecarboxylic acid per GOx molecule.[12] The electron-relaying centres were amides of ferrocenecarboxylic acid and primary protein amines.[12]

The modification of GOx has been achieved by covalent bonding of carboxylic acid groups to the protein part of the enzyme through amide links between carboxylic acid groups and 'free' enzyme amines (such as those of lysine).[7] It has been shown that relays that can be attached to GOx by bonding to lysine, tyrosine, tryptophan or histidine groups on the protein surface and all are effective in accelerating electron transfer between protein and electrode.[7] The small distance between the mediators and FAD (< 10 Å), can lead to a very fast electron tunnelling process by a kind of 'handshaking' between the electron carriers.[7]

It was also shown that after most of the chemical modifications, the enzymes retained 25-75% of their normal catalytic activity of accelerating the reaction of glucose and oxygen, to form gluconolactone and hydrogen peroxide.[7]

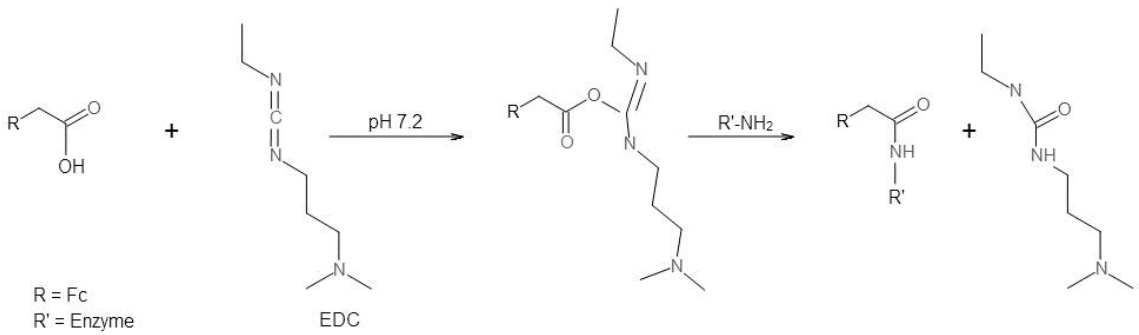

Figure 1.4: Scheme for the addition of FcCOOH to an enzyme.[7]

The bonding of the mediator groups to accessible tyrosine residues of the protein may take place at several places, two of which are fairly close to the active centre (Tyr 68 and 515). Binding mediators at these sites can be undesirable as it would block the entrance path for the substrate.[7]

Mediators attached through amide links to protein amines (usually lysines) through azo bonds to the proteins activated aromatic rings (such as those of tyrosine or tryptophan) or through coordination to the proteins' heterocyclic rings (imidazole rings of histidine) are all effective.[7] Any one of these is sufficient to alter the electrochemical characteristics of the enzyme electrodes that are, prior to enzyme modification, insensitive to change in the concentration, or even to the very presence of substrate.[7]

It has been proposed that in GOx, part of the protein or glycoprotein structure is not essential for enzymatic activity.[7] It has been reported that periodate oxidation of the polysaccharide of GOx decreases the thermal stability of the enzyme but does not reduce its activity.[7] Degani and Heller[7] propose that, beyond providing structural stability, part of the protein or glycoprotein has the simple function of electrically insulating the FAD/$FADH_2$ centres. Such insulation is essential for the survival of any living system: Were different redox enzymes able to transfer electrons to each other in an uncontrolled way, the electrons would cascade thermodynamically downhill.[7] Because of the cascade, enzymes could not be maintained at their proper oxidation potential (i.e., proper oxidation state) to fulfil their role.[7] As a result, the rich inventory of biochemicals in nature would be reduced and synthetic routes, as well as metabolic paths, would close.[7] In addition, the cascade of electrons would drastically reduce the amount of chemically stored free energy available to the organism.[7] The biologically essential insulating shells also

prevent, however, electrical communication between $FADH_2$ centres of native enzymes and metal electrodes.[7] Incorporation of mediators in the shells opens channels for electron transfer to the electrodes.[7] As the modified enzymes retain most or all of their normal catalytic activity, the catalytic core of the enzyme is only mildly affected by the chemical changes in the insulating shell.[7]

Direct electron transfer (DET) between GOx and an electrode does not take place, however subjecting GOx to treatment with urea can facilitate DET. This is due to the denaturation of the enzyme by urea causing partial dissociation of the FAD moiety from the enzyme.[26] Urea treatment results in a weakening of the FAD non-covalent binding to apo-GOx.[26] This leads to increased sensitivity of the enzyme electrode while maintaining the enzymes activity.[26] Treatment with urea can also enhance electron transfer between FAD and adsorbed mediators.[26]

A 2 M concentration of urea reversibly opens the structure of proteins, modification in the presence of 2 M urea has been shown to produce better reproducibility of properties and superior electrochemical characteristics.[7] At a higher (6 M) concentration urea alters the enzymes structure drastically and often irreversibly.[7]

1.6 Polymers in Enzyme Electrodes

As GOx has a negatively charged surface overall[11a], it can form an electrostatic complex with a polycationic redox polymer. GOx can be incorporated into polymeric mediators such as poly(vinylferrocene-co-2-hydroxyethyl methacrylate) (poly(VFc-Co-HEMA)) (see Chapter 2). GOx can also be incorporated into phospholipid polymers which have been modified to include redox active components[21] (see Chapter 2). Another polymer which can be used in enzyme electrode design is Nafion (See Chapter 2). Nafion is a

cation exchanger therefore it can protect enzyme electrodes from anionic interferants.[27] The biocompatible polymer chitosan (CS) has been widely used and is a promising matrix for enzyme immobilization and remains a focus of study in recent years due to its low cost, hydrophilicity, nontoxicity, excellent film-forming ability and remarkable biocompatibility [28]. (See Chapter 4).

GOx can be mixed with redox copolymers forming a carbon paste which can be used as an enzyme electrode that is sensitive to changes in glucose concentration.[15] Glucose in contact with the electrode surface penetrates the carbon paste and is oxidised by the GOx within.[15]

1.7 Stability of GOx Based Enzyme Electrodes

The dominant factor influencing the long term current response of enzyme electrodes is the activity of the enzyme whist immobilised.[29] The activity of the enzyme is affected by many factors such as the nature of the local environment and temperature. Thermal deactivation of GOx occurs above 55°C.[16] Increasing temperature has been shown to increase the steady state current of enzyme electrodes up to 55°C to the effect of 4% ° C^{-1} [16],

It is usually thought that the immobilisation of an enzyme leads to a loss of activity. However immobilisation can sometimes lead to an increase.[30] It is also not always the case that enzymes lose activity when placed in hydrophobic environments, as will be discussed in Chapter 2.

In terms of stability, ferrocene based mediators have many advantages for use in GOx based enzyme electrodes. The optimum pH for other (non-ferrocenium based) foreign electron acceptors is 7.5.[16] The rate of reaction of GOx with ferrocene derivatives is

essentially independent of pH in a physiologically relevant pH range.[16] This is important for physiological applications of GOx based EBCs.[16] O_2 mediated enzyme electrodes show marked pH dependence in the current response, with the maximum occurring at pH 6.5.[16] The difference in behaviour may be due to the fact that no proton transfer is involved in the reduction of the ferrocenium ion.[16]

1.8 Electrochemical Techniques for the Investigation of Enzyme Electrodes

Electrochemical techniques have the advantage of being simpler, cheaper and quicker than other methods of analysis.[31] In the case of GOx, the modified electrodes are investigated by monitoring the faradaic currents associated with the electrochemical re-oxidation of the glucose reduced enzyme.[7] When mediators are used, the addition of glucose produces an anodic current at a potential corresponding to the redox potential of the mediator.[12] When mobile charges (such as mediators) are present, five principal physical processes may influence the data recorded, these are bulk resistive-capacitive effects, electrode reactions, adsorption at the electrodes, bulk generation-recombination effects (e.g. ion-pairing), and diffusion.[32] The current produced depends on the distance between the electron-accepting and transferring centres, on the chemistry (i.e., the phonon spectrum) of the centres, on the medium through which the electrons tunnel, on the energetics of the electron-transfer process, and on the electric field between the centres.[12]

If a mediated enzyme electrode is working correctly, one can observe, at potentials equalling or exceeding the redox potential of the electron mediators, glucose concentration dependent currents.[7]

In the case of GOx, the electron-transfer sequence, on which the measurements are based, involves selective reduction of the FAD centres of the enzyme by the substrate to $FADH_2$, oxidation of the $FADH_2$ centres by the oxidised mediators and electron transfer from the then reduced mediators to the electrode, i.e., electrochemical re-oxidation of the mediator. The current associated with the latter process is measured.[7] The turnover rate of the $FADH_2$ cofactor in GOx by its natural electron acceptor, O_2, (in an aqueous phase equilibrated with air) is ~ 125 times faster than GOx electrodes which use Fc based mediators.[6] Mediator groups must compete with O_2 in real applications. If the turnover rate of $FADH_2$ by O_2 is faster than the turnover rate by the mediator, no current will be produced.[6] Therefore, the enhancement of electron transfer rates between the ferrocenyl cation and reduced FAD cofactor is of substantial importance in the design of GOx based enzyme electrodes[6].

The effect of O_2 limits the investigation of Fc based GOx electrodes to deaerated oxygen-free media. Experiments are usually carried out under an inert atmosphere (such as N_2). The electrolyte is also usually purged of O_2.

In the presence of oxygen and an electron mediator (M), the following reactions occur[31]:

$$\beta - D - Glucose + H_2O + O_2 \xrightarrow{GOx} Gluconic\ acid + H_2O_2 \qquad 1.9$$

The oxidation of glucose is catalysed by GOx.

$$\beta - D - Glucose + M_{ox} + H_2O \xrightarrow{GOx} Gluconic\ acid + M_{red} + 2H^+ \qquad 1.10$$

The oxidation of glucose by GOx using an electron mediator.

The following electrode reactions could occur[31]:

$$M_{red} \rightarrow M_{ox} + 2e^- \qquad 1.11$$

The oxidation of a mediator at an electrode.

$$H_2O_2 \rightarrow O_2 + 2H^+ + 2e^- \qquad 1.12$$

The decomposition of H_2O_2 at an electrode.

$$H_2O_2 + M_{red} + 2H^+ \rightarrow M_{ox} + 2H_2O \qquad 1.13$$

H_2O_2 could also react with the mediator.[31]

Measuring the anodic current at different scan rates can give an indication of the rate of regeneration of the oxidised mediator by the reduced enzyme.[27]

Several other parameters can be measured with electrochemistry. For example the Cotteral equation (equation 1.14) describes the change in current with time, in fixed potential experiments such as chronoamperometry.

$$i = \frac{nFAc_j^0\sqrt{D_j}}{\sqrt{\pi t}} \qquad 1.14$$

Where i =current, n = number of electrons involved in the process, F is the Faraday constant, A is the area of the electrode, c_j^0 is the initial concentration of the redox species present, D is the diffusion coefficient of the redox species present and t is time. It can be used to determine the diffusion coefficient of the redox species involved, as the measured current depends on the rate at which the redox species diffuses to the electrode surface. The Butler-Volmer equation (equation 1.15) relates the measured current at an electrode to the overpotential for both anodic and cathodic processes.

$$j = j_0 \left(e^{\left[\frac{\alpha_a nF\eta}{RT}\right]} - e^{\left[-\frac{\alpha_c nF\eta}{RT}\right]} \right) \quad 1.15$$

Where j =current density, j_0 = exchange current density, T = temperature, η = overpotential, F is the Faraday constant, R is the universal gas constant and α_a and α_c are the anodic and cathodic charge transfer coefficients. The Levich equation (equation 1.16) models the diffusion and solution flow conditions around a rotating disk electrode (RDE).

$$i = 0.620nFAD^{\frac{2}{3}}w^{\frac{1}{2}}v^{\frac{-1}{6}}C \quad 1.16$$

Where i = current, n is the number of electrons transferred in the redox process, F is the Faraday constant, A is the electrode area, D is the diffusion coefficient, w is the angular rotation rate, v is the kinematic viscosity and C is the concentration of the redox species. It can be used to predict the current observed at an RDE, in particular, the Levich equation gives the height of the sigmoidal wave observed in rotating disk voltammetry. The Tafel equation (equation 1.17) relates the rate of an electrochemical reaction to the overpotential.

$$\eta = Aln\frac{j}{j_0} \quad 1.17$$

Where η = overpotential, A is the Tafel slope, j is the current density and j_0 is the exchange current density.

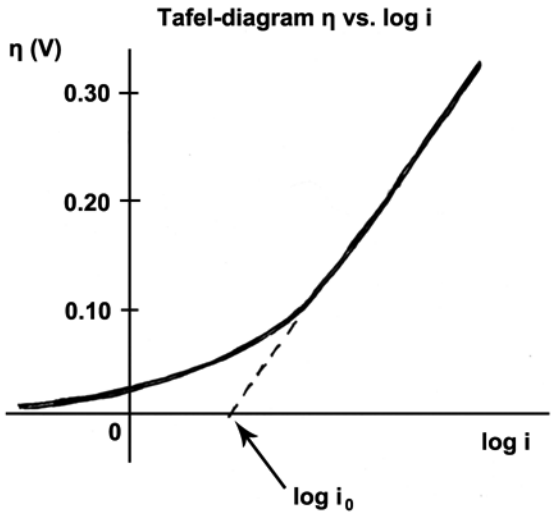

Figure 1.5: An example of a Tafel plot

Measuring the Electroactive Area of an Electrode

The electroactive area of an electrode can be measured by determining the amount of Hydrogen or Oxygen adsorbed on the electrode during potential scanning. This can be achieved by placing the electrode in a three electrode cell and connecting it to a potentiostat. For this procedure the cell must be purged of O_2. This can be achieved by sparging the cell with an inert gas such as N_2. The potential can then be scanned between -0.275 and +0.18V vs Ag|AgCl at a scan rate of 0.25 Vs^{-1}. This should generate H adsorption and desorption peaks. Integrating the area under the desorption peak gives a value for the charge passed (in coulombs) during the desorption. As the desorption of H from the electrode surface is a one electron process, the charge passed (and hence the number of electrons passed) gives the number of H atoms adsorbed on the surface of the electrode. Assuming a monolayer of H is adsorbed, the surface area of the electrode can be calculated, given the area of one H atom, which corresponds to a charge density of 210

μC cm^{-2}. This procedure can also make use of O adsorption by scanning the electrode between 0.12 and 1.0V vs Ag|AgCl at a scan rate of 0.25 Vs^{-1}. This should generate O adsorption and desorption peaks. As described above, integrating the area under the desorption peak gives a value for the charge passed, which corresponds to a charge density of 440 μC cm^{-2}. Therefore using the procedure described above, a value for the true electroactive area of an electrode can be calculated.

1.8.1 Electrolyte

Supporting electrolytes are those electrolytes containing a high concentration of indifferent electrolyte, i.e. electrolytes whose ions generally neither adsorb nor react at the electrodes of the measuring cell. Such an added salt can ensure that the material is very nearly electroneutral everywhere, thus allowing diffusion and reaction effects for a low-concentration ion of interest to dominate the AC response of the system.[32] Support is generally only possible for liquid electrochemical materials: it is often, but not always, used in aqueous electrochemistry. If an electrode is at equilibrium with the solution in which it is immersed, the electrode will have a potential, invariant with time, which is thermodynamically related to the composition of the solution. When choosing the correct buffer concentration to perform experiments, care must be taken to ensure sufficient conductivity whilst preserving enzyme activity.[17]

1.8.2 The Cell Setup

In a material-electrode system without an applied static external potential difference, internal potential differences and fields are, nevertheless, generally present, producing space-charge layers at interfaces. For solids, such regions are known as Frenkel layers and arise from the difference in work function between the electrode and the material.[32]

In an electrolytic cell such static space-charge regions are only absent when the external static potential difference is adjusted so that the charge on the working electrode (WE) is zero, the point of zero charge. Such adjustment is impossible for systems with two symmetrical electrodes because an applied static potential difference increases the space-charge region at one electrode while reducing it at the other. But the use of a working electrode of small area and a large-area counter electrode (CE) ensures that the system is little influenced by what happens at the CE, therefore a CE with a surface area much greater than that of the WE is always used. It is also important to make sure that the electrode surfaces are clean. Cleaning and polishing processes are surface roughening but improve voltammetric responses on both Au and graphitic interfaces.[8] Analyses have been able to confirm, for example, the general phenomenon of increased metalloprotein electrochemical response with increasing surface roughness, and the preferential aggregation of protein at electrode surface discontinuities.[8]

The kinetics of electrode reactions often depend strongly on the static (DC) potential difference between the WE and the bulk, or, equivalently, the WE and the reference electrode (RE), therefore a potentiostat is needed to fix this potential difference to a known and controllable value.[32]

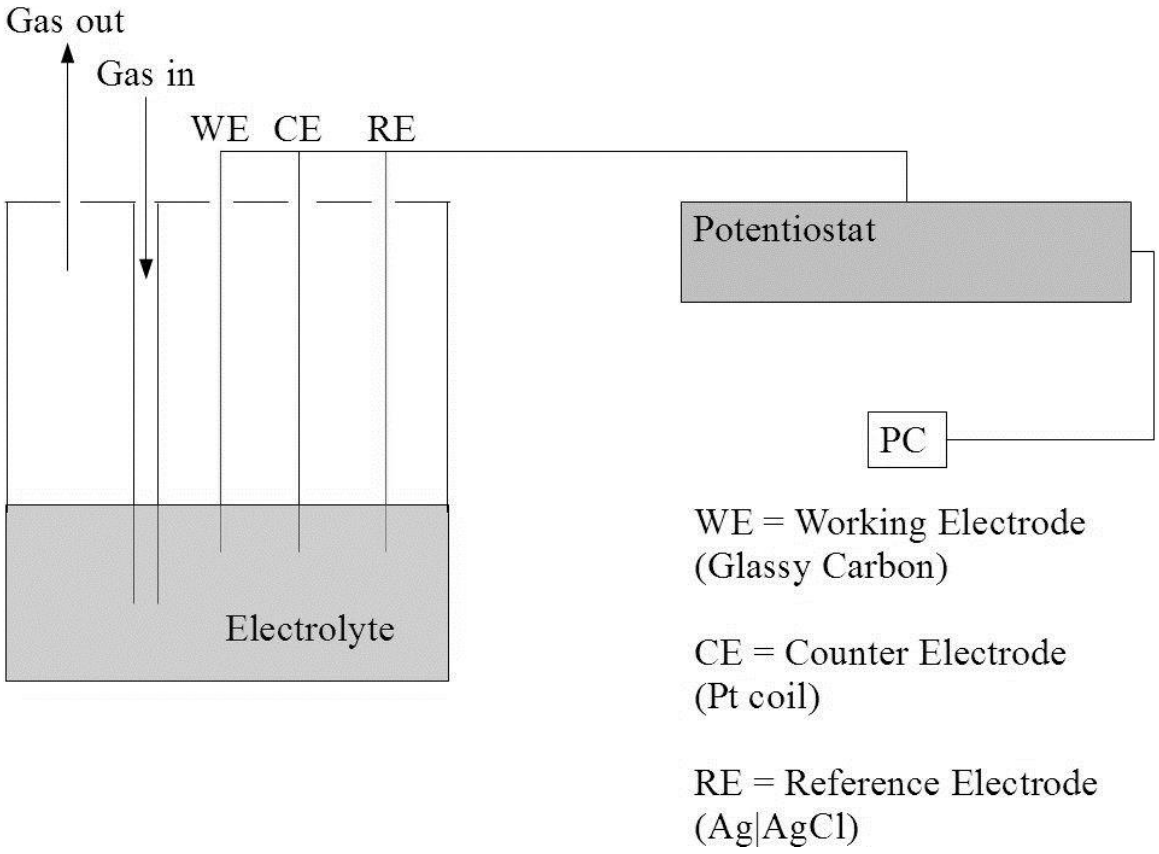

Figure 1.6: A schematic diagram of an electrochemical cell setup.

1.8.3 Voltammetry

A plot of peak current (i_p) vs. scan rate (v) can provide information on the electrochemical processes happening on an electrode during the experiment. The linearity of the slope indicates the degree of surface confinement of the redox material, such that a linear slope indicates a surface confined electrode reaction.

In a three-electrode electrochemical cell, any immobilised redox protein in electrical contact with the electrode is reduced or oxidized depending on the potential difference, V, between the working electrode WE and the RE. The potentials between the WE and the RE, and between the WE and the CE, which carries the current, are controlled by a

potentiostat. The current that flows between CE and WE is measured while a feedback circuit maintains the desired (constant or time-dependent) potential between WE and RE. With increasing sweep rate the peaks start moving apart. Plotting the distance between them as a function of sweep rate results in a ‘‘trumpet plot’’, the shape of which provides the electron transfer rate between electrode and redox active group according to Laviron’s theory.[8]

The potential between the WE and RE is ramped back and forth with a rate v around the midpoint potential of the redox species. This results in two charging processes: 1) a Faradaic process, i.e. the oxidation of the redox molecules upon sweeping from low to high potential and reduction back on the return. This results in a positive and a negative current peak at ¼ of the midpoint potential; 2) the charging of the electrode surface and the ensuing accumulation of counter ions at the surface. This results in a diffuse double layer with a capacitance. Due to the ionic resistance of the solution (in series with the double layer capacitance), a characteristic rise-time is observed at the turning points. The cyclic voltammogram thus is the sum of these two currents, plotted as a function of the applied potential. The width of the Faradaic peaks is 3.5 k_bT /n, where n is the number of electrons transferred in the reaction.[8]

Increasing peak separation with increasing scan rate is also characteristic of a quasi-reversible process, as the rate of the heterogeneous electron transfer is slow compared to the time scale of the experiment. In a reversible process peak current is directly proportional to the square root of the scan rate.

1.8.4 Electrochemical Impedance Spectroscopy (EIS)

Electrochemical impedance spectroscopy (EIS) can be a very important and powerful tool in the analysis of all electrochemical phenomena.[33] It has been known for many years that the application of an alternating voltage or current through a conducting medium such as an electrolyte or an ionic solid gives rise to effects expressible in terms of an electrical impedance.[34] The components of the impedance, resistance and capacitance, follow an inverse function of the frequency of the applied perturbation. As the frequency of the applied perturbation can be scanned over a wide range, information regarding both semi-infinite (high frequency) and finite (very low frequency) diffusional (mass transport) processes can be obtained.[33b] At very high frequencies, kinetic information can also be obtained.[33b] In addition an important advantage of the impedance method is that several parameters can be measured simultaneously as a function of the experimental conditions.[35] Information can be obtained in a single experiment on the charge transfer processes occurring at electrode|polymer interfaces, as well as on the rate of charge transport in polymers. Other important quantities (polymer resistance, double layer capacitance, redox capacitance of the polymer) can also be determined.[35]

EIS is also a very un-intrusive procedure. The system is only marginally perturbed from equilibrium by the low amplitude sinusoidal voltage (several millivolts), whereas other transient techniques usually involve considerably larger perturbations.[33b] This last point is of particular significance with thin films on electrodes, where large voltage perturbations may encompass large variations in the film structure.[33b, 36] EIS has been shown[33b] to be a useful tool for the investigation of processes at polymer- coated electrodes.

The procedure involves placing the electrode material of interest (the working electrode) into an electrolyte solution along with a suitable reference and counter electrode. A potentiostat is then used to apply a voltage to the working electrode. A small amplitude (e.g. 10mV) sinusoidal potential waveform is then applied on top of this voltage. This AC potential perturbation then drives redox processes (if any) at the electrode surface. The amplitude and phase angle of the resulting ac current are measured and used to calculate the real and imaginary components of the impedance.[37] The impedance is the ratio of the applied sinusoidal voltage to the sinusoidal component of the current flowing between the counter and working electrodes as a result of the applied voltage.[38] Unless the system is purely resistive, impedance is a complex quantity because the current will have a different phase from the applied voltage.[38]

Equivalent Circuits

An electrochemical cell (a collection of interfaces) is simply an impedance to a small sinusoidal excitation. It should be possible to represent its performance by an equivalent circuit of resistors and capacitors that pass current with the same amplitude and phase angle that the real cell does under a given excitation.[38] In the evaluation of impedance data, the electrochemical interphase is often described by an equivalent circuit relevant for the conditions of the experiment, using circuit elements that represent the various physical processes present.[33a] For example, the voltage-current characteristics of the solution and charge transfer processes at a fixed potential can be represented accurately with resistors (R_S and R_{CT} respectively), while the space charge characteristics of the electrochemical double-layer (C_{DL}) and dielectric surface layers (e.g., organic coatings

and oxides) can be modelled appropriately with capacitors.[33a] Impedance due to diffusion in a thin film can be considered to be equivalent to a finite transmission line.[33b]

One of the most basic equivalent circuits used to analyse EIS data is the Randles circuit:

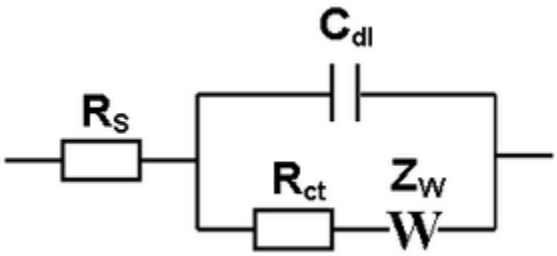

Figure 1.7: Randles circuit.[39] Where R_S is the electrolyte resistance, C_{DL} is the double layer capacitance, R_{CT} is the charge transfer resistance and Z_W is the Warburg impedance.

The Randles circuit is expected to describe a recorded impedance spectrum (especially at high to medium frequencies) when the EIS experiment is carried out at the formal potential of any redox couple present.[40]

C_{DL}, R_{CT} and Z_W are placed in parallel because the current passing through the working electrode is the sum of the distinct independent contributions from these processes. All the current must pass through the uncompensated solution resistance, and therefore R_S is inserted as a series element to represent this effect in the equivalent circuit.[38] In contrast to R_S and C_{DL}, which are nearly ideal circuit elements, the components of the faradaic impedance, R_{CT} and Z_W, are not ideal, because they change with frequency.[38] It should be stressed that a much more complicated behaviour than that predicted from a Randles circuit may be observed in practice. For example, coupling between faradaic and double layer charging processes could exist and the situation may be complicated due to inhomogeneous electrical fields generated by the electrode geometry.[38]

Software can be used to fit data gathered during EIS experiments to the expected shape of a Nyquist plot generated by equivalent circuits such as the Randles circuit. This allows the experimenter to determine values for the various circuit elements which provides information about the electrode.

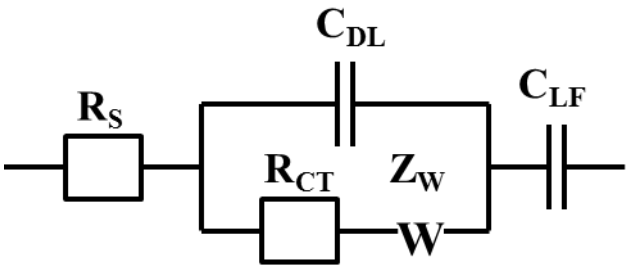

Figure 1.8: Randles circuit modified to include the effects of C_{LF}.[41]

Double Layer Capacitance (C_{DL})

The double layer capacitance (C_{DL}) is a true capacitance in the sense that it results from a separation of charge in space, brought about by the asymmetry generated whenever a metal-solution interphase is formed.

The condition of electroneutrality, which applies everywhere in the bulk solution, is violated at the interphase. There is an excess charge, (q_M) on the metal side of the interphase and an equal but opposite charge (q_S) on the solution side of the interphase.[33a] Electroneutrality is maintained across the interphase, namely, $q_M + q_S = 0$. Adding a small charge (δq_M) to the metal side will induce an equal charge of $-\delta q_M = \delta q_S$ on the solution side. This is achieved by rearrangement of the ions in solution and does not require charge to be transferred across the interphase. The interphase may be leaky, allowing

some faradaic current to flow across it. This is represented as a faradaic resistance (R_{CT}) in parallel with C_{DL}, but the latter still is treated as a pure capacitor.[33a]

Although C_{DL} is inherently independent of frequency (and potential)[42], the phase shift measured experimentally will depend on frequency. This dependence is the result of additional circuit elements in series and in parallel with C_{DL}, in the ideal case, and may be complicated further by frequency dispersion caused by surface roughness, chemical heterogeneity, or other sources of non-uniform current distribution.[33a]

For electrodes modified with polymers, C_{DL} may not always necessarily arise from the double layer capacitance arising from the electrode|polymer interface. C_{DL} effects can also arise from double layers formed between ions in different oxidation states within the polymer layer. During an EIS experiment, as the potential reaches the oxidation potential of a redox species trapped within a polymer, some of the ions (particularly those closest to the electrode) are oxidised. At this point other ions in the polymer will form a double layer near the layer of oxidised ions, giving rise to a capacitance effect. This is confirmed by the fact that as the electrode potential on which the sinusoidal potential is applied is made more oxidising, the capacitance effect decreases, as more and more ions are oxidised, reducing the concentration of reduced ions to form the double layer.[42] The attenuation of this capacitance effect may also be affected by repulsive interactions brought about by the increase in the concentration of oxidised ions.[42]

Charge Transfer Resistance (R_{CT})

Some charge does manage to leak across the double layer due to electrochemical reactions taking place at the interface. Such charge leakage experiences a charge transfer resistance R_{CT}.[38] R_{CT} is frequency independent but varies with the electrode potential.[42]

It has been shown[37] that R_{CT} increases with immobilised film thickness. Therefore monitoring R_{CT} during the immobilisation process can provide information on the progress of the immobilisation.

Warburg Impedance (Z_W)

The Warburg impedance (Z_W) is due to mass transport limitation by diffusion.[33a] Z_W gives rise to a constant phase angle of 45° ($\pi/4$) in a Nyquist plot.[33a] This is true only under the assumption of semi-infinite linear diffusion. If the diffusion field is bounded (e.g. at a rotating disc electrode), Z_W due to mass transport may still be observed and there will be a skewed arc in the Nyquist plot of such a system.[33a] Z_W is observed whenever a reaction is under partial or complete mass transport control by diffusion.[33a] Diffusion gives rise to capacitive behaviour and results in a so-called constant-phase element, namely a phase angle which is independent of frequency.[33a]

It is easy to see why mass transport limitation would lead to an additional resistance in series with R_F in the equivalent circuit representation. The Warburg impedance may arise from mass transport limitations arising from the diffusion like propagation of redox species in the electrolyte or confined within an immobilised polymer.

Adsorption Capacitance (C_{ADS})

The capacitive behaviour associated with adsorption accompanied by charge transfer results from the dependence of coverage on potential for species formed in a charge transfer process. It maintains the two main properties of a capacitance: infinite resistance under direct current (DC) conditions and a phase shift of $-\pi/2$ in response to a sine-wave perturbation. It is regarded as a pseudocapacitance because it is intimately associated with

a faradaic current crossing the interphase and cannot be observed at an ideally polarisable interphase.[33a]

Interpretation of EIS Spectra

Electrodes modified with conducting polymers can be viewed in terms of a redox couple trapped in a polymer film of a certain thickness (which is penetrated readily by the ions of the supporting electrolyte).[43] It is expected[43] that at high frequencies a Randles circuit behaviour will be found, from which the resistance of the solution and the polymer, the double layer capacitance between the electrode and the polymer, the Warburg resistance (corresponding to the diffusion of the components of the redox couple in the polymer) and the charge transfer resistance for electron exchange between the electrode and the redox active constituents of the polymer can be evaluated.

Nyquist Plots

The information gathered during EIS experiments is conveniently displayed as a Nyquist plot. In a Nyquist plot, the real component of the impedance is plotted against the imaginary component of the impedance.

A typical Nyquist plot will show a resistive displacement on the real axis at high frequencies (say in the high kHz range).[41] This displacement is related to the impedance of the electrolyte (the solution resistance). If there is a film on the electrode, the resistance of the film would be expected to be in series with the charge transfer resistance.[44] Therefore the film resistance (R_F) would be observed as part of the high frequency real axis intercept. By comparing the displacement seen when no film is present to that when one is present, the impedance of the film can be determined. If there

is little difference between the resistive displacement with and without the film, this shows that the supporting electrolyte penetrates the film effectively.[43] If there is efficient penetration of the electrolyte in the film, the film resistance can be considered to be negligible.[44]

At high frequencies, the electrode admittance is, in general, great thus the ac signal is damped within a short distance.[45] Therefore, at high frequencies, Nyquist plots are dominated by processes occurring at or very near the electrode surface.

In addition to the typical resistive displacement at high frequencies, the parallel effects of the charge transfer resistance of a redox process and double layer capacitance (both at the electrode surface) can give rise to a semicircular ark in a Nyquist plot as the frequency is lowered.[46] At these frequencies, current is distributed between the charging and discharging of the double layer capacitance and any faradaic charge transfer processes occurring at the electrode surface. The restriction of current flow by heterogeneous electron transfer gives rise to the semicircular ark.[40]

It is important to understand the physical reasons for the existence of the semicircle. It can be shown[47] that by using the Randles equivalent circuit for the simple charge transfer reaction:

$$O + ne^{-} \rightarrow R$$

on separating the in-phase and out-of-phase components of the impedance, that:

$$Z' = R_S + \frac{R_{CT} + \sigma w^{\frac{1}{2}}}{\left(\sigma w^{\frac{1}{2}} C_{DL} + 1\right)^2 + w^2 {C_{DL}}^2 \left(R_{CT} + \sigma w^{\frac{1}{2}}\right)^2} \qquad 1.17$$

$$-Z'' = R_S + \frac{wC_{DL}(R_{CT} + \sigma w^{\frac{1}{2}})^2 + \sigma^2 C_{DL} + \sigma w^{\frac{1}{2}}}{\left(\sigma w^{\frac{1}{2}} C_{DL} + 1\right)^2 + w^2 {C_{DL}}^2 \left(R_{CT} + \sigma w^{\frac{1}{2}}\right)^2} \qquad 1.18$$

where

$$\sigma = \frac{RT}{n^2 F^2 A\sqrt{2}} \left(\frac{1}{D_O^{\frac{1}{2}}[O]_{Bulk}} + \frac{1}{D_R^{\frac{1}{2}} R_{Bulk}} \right) \qquad 1.19$$

and R, T, n and F have their usual meanings and A is the electrode area and *w* is the frequency of the applied perturbation.

It is interesting to consider the two limiting forms of equations 1.14 and 1.15.

1) $w \to 0$

$$Z' = R_S + R_{CT} + \sigma w^{-\frac{1}{2}} \qquad 1.20$$

$$Z'' = -\sigma w^{-\frac{1}{2}} - 2\sigma^2 C_D \qquad 1.21$$

2) $w \to \infty$

$$Z' = R_S + \frac{R_{CT}}{1 + w^2 C_{DL} R_{CT}^2} \qquad 1.22$$

$$Z'' = -\frac{wC_{DL} R_{CT}^2}{1 + w^2 C_{DL}^2 R_{CT}^2} \qquad 1.23$$

At very high frequencies Z'' ($\propto -1/wC_{DL}$) (the y axis in a Nyquist plot) is very small but rises as the frequency diminishes.[47] As the frequency diminishes further, more current passes through the R_{CT} component of the equivalent circuit and the contribution from C_{DL}

becomes lower until it reaches a minimum (the second intercept of the semicircle with the $Z^{'}$ (x) axis).

The lower frequency intercept of the real axis of this semicircular ark gives the charge transfer resistance (R_{CT}) in addition to the solution resistance (R_S). The solution resistance is calculated from the high frequency intercept and therefore by subtraction of R_S from the low frequency intercept the charge transfer resistance can be determined. The frequency at which the maximum height of the semicircle occurs is given by:[41]

$$w = \frac{1}{R_{CT}C_{DL}} \qquad 1.24$$

From which C_{DL} can be determined.

If charge transfer is very inefficient (i.e. without the presence of a redox couple), the double layer capacitance increases the height of the semicircle such that the diameter of the semicircle becomes so large that the Nyquist plot effectively looks like a sloping line at the usual experimental frequencies.[48] Alternatively, a similar effect may be seen in the presence of a redox couple if the charge transfer resistance is extremely efficient (i.e. much smaller than the solution resistance). In this case only mass transport effects would be seen in the Nyquist plot.[28, 37]

If a semi-circle is present in a modified electrode, at intermediate frequencies (i.e. where $w > DL^{-2}$, where w is the frequency, D is the diffusion coefficient of the diffusing species and L is the film thickness) (typically in the Hz range)[41] Warburg impedance can give rise to a distortion of the semicircle, leading to a straight line with a slope of 45°.[48]

For electrodes modified with redox polymers, a Warburg impedance will be apparent at low frequencies if semi-infinite conditions apply, i.e. if $D_{ET}^{1/2} >> L$ (where D_{ET} is the

diffusion coefficient for charge propagation and L is the polymer thickness)[49], in these circumstances, the diffusion layer created by the ac perturbation is much thinner than the redox polymer. In these regions, the ac response is representative of the mass transport properties of the electrode interface.[41]

If semi-infinite conditions do not apply (i.e. when the diffusion layer encompasses the entire film), a Warburg impedance may be very short or not be seen at all at intermediate frequencies, instead there will be a transition to a low frequency capacitance.[50]

Low Frequency Capacitance (C_{LF})

As the frequency becomes lower and lower (i.e. where $w << DL^{-2}$, typically <1Hz[42])(the frequency at which this transition takes places depends on film thickness[44]), in some cases the measured electrode impedance's become very high. This has been attributed to purely capacitive behaviour related to the double layer capacitance at the electrode interface,[43] and the double layer capacitance of the true electrode area[45] (as opposed to the geometric electrode area) or of an entire immobilised film (as opposed to a fraction of the film).[46b] Alternatively, this behaviour arises because at lower frequencies the penetration depth of the ac diffusion wave becomes comparable with film thickness. If this is the case, diffusion across the finite film is accomplished during one-half cycle of the perturbing signal, leading to charge saturation within the film giving rise to the capacitive like behaviour.[41, 44] This capacitance becomes frequency independent at low frequencies (typically <10 Hz[42]), giving rise to a vertical line in the Nyquist plot (a phase angle of $\pi/2$) known as the charge saturation region. The intercept of this line with the real axis is a combination of C_{LF} and C_{DL}. C_{DL} can be calculated by the methods described above allowing the determination of C_{LF}. Usually $C_{LF} >> C_{DL}$ therefore the

intercept of this line ~ C_{LF}.[40] Occasionally, curvatures or finite slopes may be observed in the charge saturation region, this may be due to non-uniform film thickness[44, 50b] and or differences in the rates of diffusion in the immobilised film.[51] This effect may also perturb the Warburg section.[50b]

There exists a thickness range over which both a diffusion controlled region and charge transfer controlled region can be experimentally observed for any given system. For very thin films, the kinetic control region may overlap with the charge saturation region and no diffusion region will be observed. Conversely, with very thick films, charge saturation dominates only at very low frequencies and diffusional control is observed over a large frequency range.[44]

The frequency at which this capacitive behaviour is observed can give an indication of the conductivity of an immobilised polymer. For example the higher the low frequency capacitance is observed, the greater the ability of the polymer to conduct charge.[46a]

The observation of three distinct regions in a Nyquist plot (kinetic control, mass transport control and charge saturation) may not be obtained experimentally due to overlap in the frequency dependence of these processes. The appearance of these distinct regions in a Nyquist plot is also dependent on the nature of the electrode and the potential on which the perturbation is applied.[46a] Even if a non-idealised Nyquist plot is obtained, values for the electrode parameters can still be obtained with the use of data fitting software.

Use of Redox Probes

EIS experiments can be carried out in the absence or presence of a redox probe.[52] In the absence of a redox probe, the measured impedance signal results directly from the

substances that are adherently attached to the electrode surface. In other words, the impedance is influenced by the changes in amount, growth and morphological behaviour of adherent substances.[52] Information about the nature of modified electrodes such as the blocking of an electrode surface by an adsorbed or bound species can be obtained by adding a redox pair (say a 1:1 mixture of $K_3[Fe(CN)_6]$ and $K_4[Fe(CN)_6]$) to the electrolyte before carrying out EIS experiments. In this case, the Nyquist plot of a bare electrode should show a straight line with a slope of 45° which is typical of a diffusion limited electrode process with a fast electron transfer across the electrode|electrolyte interface. The semi-circle arising from R_{CT} in the Nyquist plot should not be visible as the R_{CT} is so low. If material is present on the electrode surface, the access of the redox probe to the electrode is hindered to a higher degree than with an unmodified electrode. Therefore the faradaic reaction of the added redox pair with the electrode will be hindered. This will lead to changes in the measured parameters in the impedance spectra (such as the appearance of a semicircle due to an increase in R_{CT}) of modified electrodes. [53]

The measured parameters of impedance spectra when using redox probes are a function of the convective diffusion of the redox probe in solution, the diffusion of the redox probe through any immobilised film and charge transfer between the film and the redox probe.[46a] Also, at high frequencies, the response of the electrode to the perturbation is insensitive to the presence of any redox probe as long as the frequency is high enough that the sine wave perturbation does not propagate throughout any immobilised film, which appears semi-infinite in length.[36]

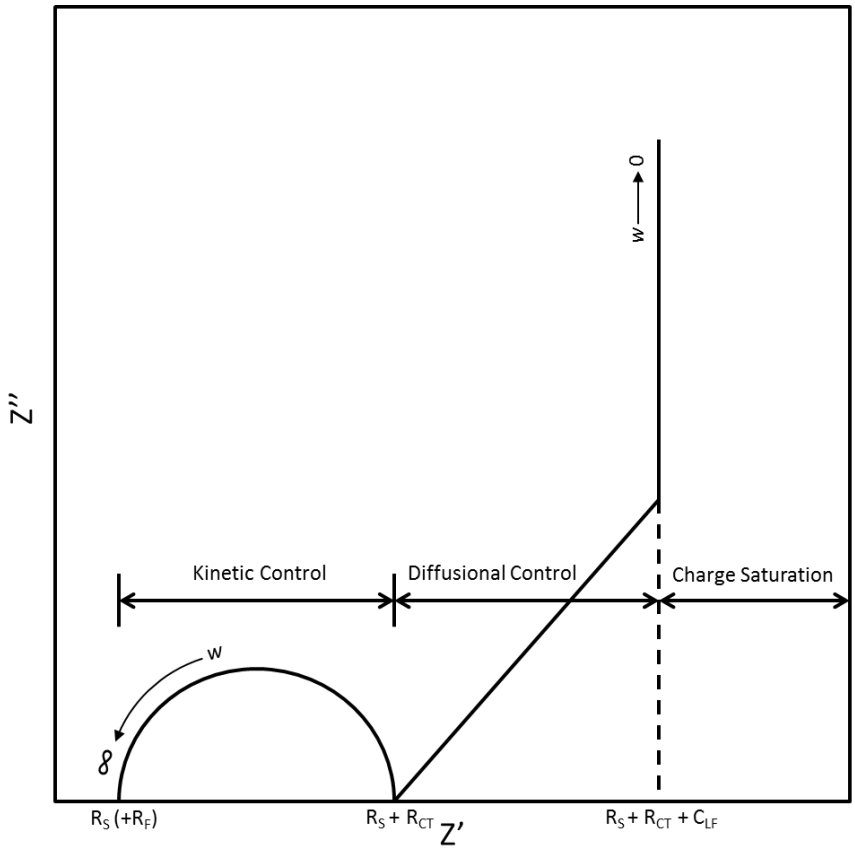

Figure 1.9: An example of an idealised Nyquist plot for an electrode modified with a redox polymer. Z' and Z'' are the real and imaginary components of the impedance respectively. R_S is the electrolyte (or solution) resistance, R_F is the resistance of an immobilised film. R_{CT} is the charge transfer resistance. C_{LF} is the low frequency capacitance and *w* is the frequency.

1.9 Linking Enzymes

The facile immobilisation of enzymes onto electrode surfaces is one of the most crucial aspects of enzyme electrode design. One of the ways this can be achieved is via the used of 1-Ethyl-3-(3-dimethylaminopropyl)carbodiimide (EDC). The mechanism behind the EDC immobilisation process is discussed in this section. EDC can be used to activate carboxylic acid groups for the formation of amide bonds under very mild conditions.[54] It reacts with carboxylic acids to create an active-ester intermediate. In the presence of an amine nucleophile, an amide bond is formed with the release of an isourea by-product.[55]

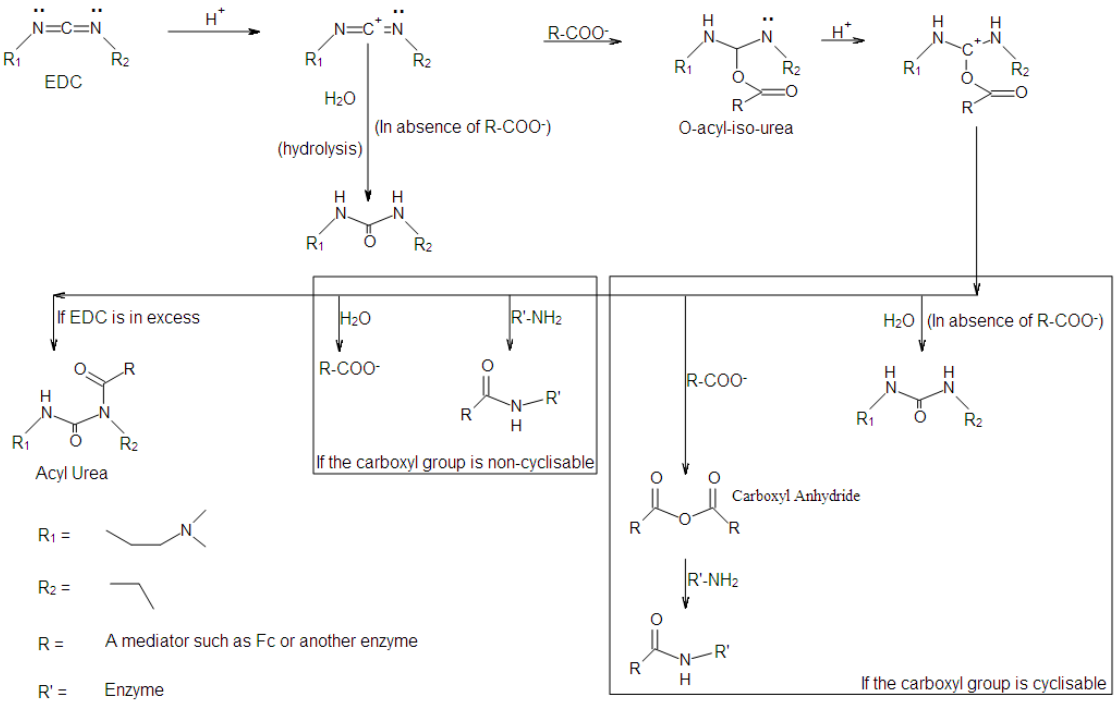

Figure 1.10: The reaction of EDC with carboxylic acid.[54]

The reactions involving H_2O will be prevailing as [H_2O] is much greater than the other reactants.[54] (See Figure 1.4). A narrow pH range such as 3.5-4.5 is, most favourable for the route involving the carboxyl anhydride.[54] A higher pH suppresses the ionization of amine, favouring the one step route, as only unionized amine molecules can react with carboxyl groups pre-treated with carbodiimide. Finally, it should be noted that the two-step method, in which carboxylic anhydride is first prepared from two carboxyl groups by carbodiimide, followed by reaction with amine, may give a variety of selective reactions such as bio-conjugation of enzymes to substrates having carboxyl groups without significant deactivation of enzymes, although the coupling efficiency is lower than that by the one-step method.[54] Carbodiimide-involving modifications can cause some

polymerization of enzymes.[7] The drawback of the use of EDC chemistry is that it is not very specific[8].

1.10 Electrode Modification

Electrodes can be engineered with monolayers of enzyme co-factors covalently linked with mediators. The apo-enzyme (enzyme without the co-factor or active site) can then be introduced to the monolayer to yield an electrically contacted enzyme electrode. This has been achieved using a Au electrode and a FAD-PQQ monolayer.[6]

Using this method of immobilisation and mediator binding, the distance between the mediator and the FAD unit was 2 Å shorter than the best result achieved using random mediator attachment.[6] This reconstitution methodology is beneficial because it provides site specific attachment of the mediator unit.[6] The electron relay unit must be positioned at the electrode surface in an optimised configuration to allow effective electron transport between the biocatalyst active site and the electrode.[6]

Chapter 2 - Enzyme Electrodes Based On Ferrocene Redox Polymers

The aim of the work carried out in this chapter was to test the redox polymer Poly(vinylferrocene-co-2-hydroxyethyl methacrylate) (p(VFc-Co-HEMA) as a possible material for the characterisation of novel genetically engineered strains of GOx. The polymer must be shown to be stable in terms of retention of the mediator at the surface of the electrode, and electrocatalytically active. Once this had been achieved, the aim was to investigate the electrochemical response of the electrode in the presence of biologically relevant interferants. A further aim was to investigate the possibility of improving the properties of the electrode using the biocompatible polymer poly[2-methacryloyloxyethyl phosphorylcholine (MPC)-co -n-butyl methacrylate (BMA)-co-p-nitrophenyloxycarbonyl poly(ethylene glycol) methacrylate (MEONP)] (PMBN). The final objective of this chapter was to investigate the possibility of using redox mediators with more negative redox potentials than Ferrocene, in order to lower the operating potential of possible enzyme electrodes made during this work.

2.1 Introduction

One advantage of using ferrocene (Fc) as an electron transfer mediator in enzyme electrodes as opposed to Fc derivatives is the fact that Fc derivatives (such as ferrocene carboxylic acid and methylated ferrocenes such as 1-1 dimethyl ferrocene) have been shown to be unstable when immobilised on electrode surfaces.[27] In particular, the oxidised forms of the derivatives are soluble in aqueous solutions, which can cause instability in the performance of the enzyme electrode.

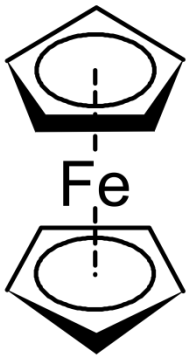

Figure 2.1: Structure of Fc.

Fc has been used as the electron transfer mediator in electrodes modified with covalently attached GOx.[56] The $Fc|Fc^+$ couple was trapped within a membrane at the electrode surface. This electrode successfully catalysed the direct electrochemical oxidation of glucose in the absence of oxygen.

GOx based enzyme electrodes can also be prepared by trapping the $Fc|Fc^+$ couple within a polyacrylamide gel.[56] Entrapment within a polymer in this way allows greater than monolayer loadings of enzyme to be immobilised. Entrapment of the $Fc|Fc^+$ couple within a polymer also has the advantage of allowing greater access of substrate to the immobilized catalytic sites as there is no need for a membrane. Both halves of the $Fc|Fc^+$ couple are stabilized by the polyacrylamide environment at relatively high concentrations.

GOx electrodes can also be fabricated by trapping the enzyme in carbon paste along with a Fc containing siloxane polymer.[57] The properties of the enzyme electrode can be further improved with the addition of a poly(ester-sulphonic acid) cation-exchanger. The mechanism of mediation in this case was thought to be due to the flexible nature of the siloxane backbone

Fc has also been used as the electron transfer mediator for enzyme electrodes based on Horseradish peroxidase.[58] Horseradish peroxidase will reduce H_2O_2 to H_2O and Fc can then act as an electron donor to the oxidised iron in the haem protein. The Fc^+ can then be reduced at an electrode with the reduction current being proportional to substrate concentration.

2.1.1 Poly(vinylferrocene-co-2-hydroxyethyl methacrylate)

The co-polymer Poly(vinylferrocene-co-2-hydroxyethyl methacrylate) (p(VFc-Co-HEMA) is an amphiphilic copolymer, consisting of hydrophobic VFc (which acts as the mediator) and hydrophilic HEMA which can be prepared by radical copolymerisation.

p(VFc-Co-HEMA) is insoluble in water, helping to prevent leakage of the mediator and improving the stability of the redox polymer. However HEMA is hydrophilic, giving the polymer hydrogel like properties. Hydrogels based on HEMA have been shown to be biocompatible.[15] Therefore it is expected that VFc-HEMA copolymers would exhibit favourable biocompatibility.

The redox sites (VFc sites) are covalently attached to a polymer backbone. p(VFc-Co-HEMA) can be used as a redox mediator due to its ability to transfer charge to and from an electrode via electron hopping reactions between ferrocene/ferrocenium sites in the polymer (see Figure 2.3). These electron hopping reactions are aided by the amorphous nature of the polymer, and the local mobility of the VFc sites within the polymer.[59] Therefore p(VFc-Co-HEMA) can be used as a polymeric mediator for transferring charge between $FADH_2$ from GOx and an electrode in a GOx based enzyme electrode. If the electrode is polarised higher than the redox potential of the ferrocenyl group, the ferrocenium ion is generated in the copolymers. The formation of the ferrocenium, site in

the copolymers extends from the surface of the electrode to which it is attached and into the bulk polymeric phase by electron hopping, where it can reach the vicinity of the $FAD/FADH_2$ site in GOx.[15] Since the redox potential of $FAD/FADH_2$ is much lower (E° = -416mV vs. Ag|AgCl)[60], the propagated ferrocenium, sites in the vicinity of $FADH_2$ oxidise it to FAD. By this oxidation reaction, ferrocenium sites in the copolymers are reduced to original ferrocene and the process continues to cycle in the presence of glucose.[15] Thus the catalytic reactions enhance the oxidation current of the enzyme electrodes.[15]

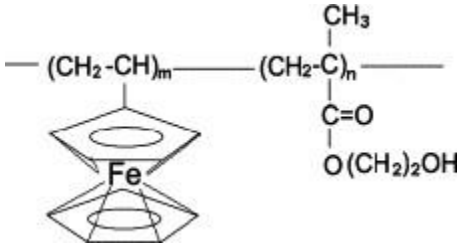

Figure 2.2: Structure of p(VFc-Co-HEMA).

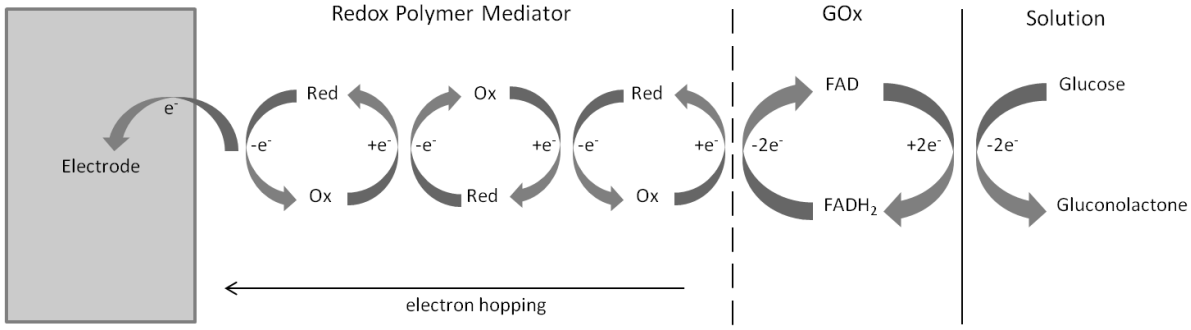

Figure 2.3: Principle of GOx enzyme electrode based on redox-polymer-mediated electron transfer.

In order to immobilise enzymes on p(VFc-Co-HEMA), a spacer arm such as Hexamethylenediamine (HMDA) can be used. Immobilisation of enzymes on p(VFc-Co-HEMA) using this method has been shown to preserve enzyme activity.[61]

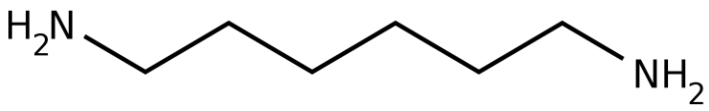

Figure 2.4: Hexamethylenediamine (HMDA).

2.1.2 Ferrocene & Nafion

When GOx based enzyme electrodes are exposed to blood, reversible fouling of the electrode occurs due to adsorption of species from solution such as protein matter or cells.[62] Enzyme electrodes can also be inhibited by reaction of H_2O_2 with catalase released as a result of peroxide induced haemolysis.[62] This has an adverse effect on the performance of enzyme electrodes. Therefore protective membranes such as cellulose and Nafion have been used to reduce effects such as clotting and fibrous encapsulation of the electrode.

Nafion is a perfluorosulfonic acid cation-exchange polymer.[63] It is a complex material which consists of a hydrophilic ionic cluster phase, a hydrophobic Teflon™-like perfluorocarbon backbone with side chains terminated by the hydrophilic SO_3^- groups with counter ions,[64] and an interphase that separates the ionic and chain microphases.[65] Nafion absorbs water and separates into domains of hydrophilic and hydrophobic phases, and ion conductivity takes place through the hydrophilic channels[66].

The pendant sulphonated perfluorovinyl side chains of the Nafion hug the walls of the hydrophilic channels in the polymer, while the sulphonate groups point toward the centre of the hydrophilic phase.[66] At all levels of hydration the pendant perfluorovinyl side chains in Nafion hug the walls of the hydrophilic channels, because in doing so they

allow an increase of water−water interaction.[66] The chemical structure of Nafion is shown in Figure 2.5.

Nafion has many advantages for use in enzyme electrodes. Nafion has excellent properties as an ion conductor, and it provides a biocompatible interface[30].It has many biocompatible characteristics which make it suitable for *in vivo* applications. It has both hydrophilic and hydrophobic properties, is chemically inert, and is subject to relatively little adsorption of species from solution.[62] It has also been shown to be compatible with mammalian tissue.[67]

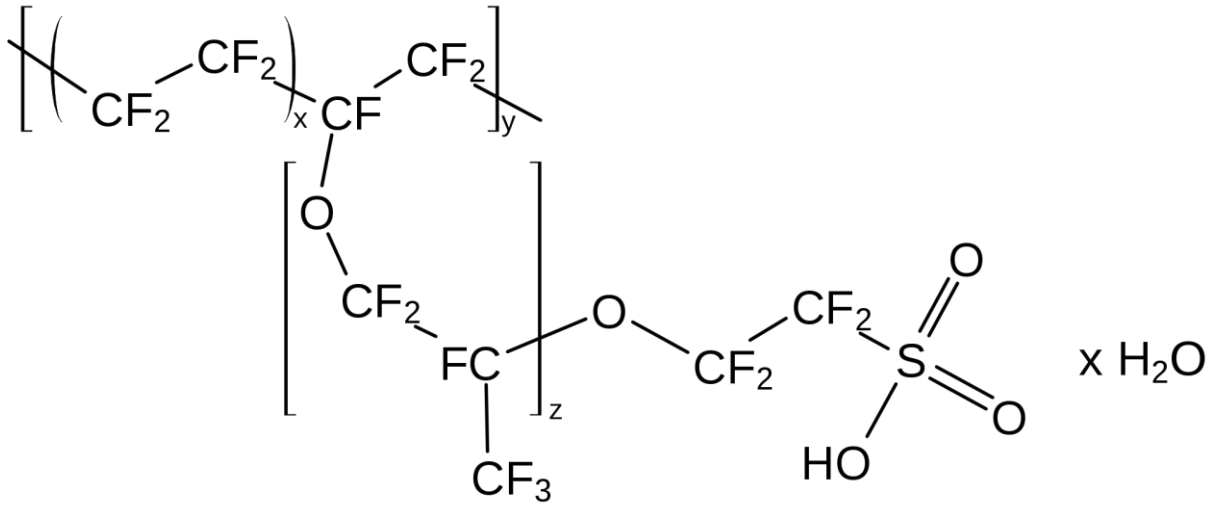

Figure 2.5: Structure of Nafion (x varies between 5 & 14, y varies between 200 & 1000 & z = 1 with the hydration levels encountered in a typical membrane, the hydrated Nafion can hold between 1 and 30 water molecules per SO_3 group.[66]

Nafion's PTFE backbone ensures long-term chemical stability in both reducing and oxidizing environments[66]. Nafion modified electrodes can be easily prepared by solvent casting the polymer directly on the electrode surface and provide several advantages over unmodified electrodes[30]. The method for membrane formation is a simple dipping of the electrode into the polyelectrolyte solution or casting a small volume of the solution onto the electrode surface and allowing the solvent to evaporate. When Nafion is cast onto

electrode surfaces; the resulting membranes possess a high adhesion to the surface and a low swelling in aqueous media.[67b, 68] In addition, the polyelectrolyte membrane stabilizes the ionic strength at the electrode surface which is essential for sensor applications.[68]

The entrapment of positively charged redox-active compounds into Nafion membranes has been reported as early as 1980[69]. The high operation stability of the resulting redox active films allowed the authors to propose them for a variety of electrochemical applications, even as reference electrodes.[70] Cast Nafion films provide an ionically conducting matrix into which many electroactive cations can be incorporated.[63] Unmodified Nafion has a higher affinity for large hydrophobic cations than smaller and more hydrophilic cations[30]. A Nafion containing adsorbed N-methylphenazonium (NMP) layer has been used as a redox polymer for a glucose biosensor containing glucose dehydrogenase.[71] The authors attributed the ability of the Nafion|NMP redox polymer to shuttle electrons between the enzyme and the electrode surface to the relatively weak electrostatic sorption of the NMP cation in the anionic sulphonate centres of the Nafion layer. The weakness of the electrostatic sorption allowed efficient diffusion of the redox mediator within the Nafion layer. Large (up to 1M) amounts of electroactive species can be incorporated into the films by electrostatic binding and extraction.[72]

Ferrocene (Fc) has been incorporated into a Nafion film from an aqueous solution.[72] The authors attributed the absorption of Fc to extraction of the solution species into less polar regions of the polymer film. Electrodes prepared using films of Nafion containing

electroactive species often show diffusion-controlled behaviour[72] (e.g., cyclic voltammetric peak currents proportional to the square root of scan rate).

The authors established that both electron transfer and actual diffusion contribute to the conduction processes in Nafion films.[72] The diffusional behaviour of electroactive cations incorporated in such films was attributed to both physical diffusion and an apparent diffusion due to electron-transfer reactions, with the relative contributions of each depending upon the nature of the incorporated electroactive ion. The electron transfer reactions depend strongly on the self-exchange rate for electron transfer of the cation.[63]

It has been suggested[73] that the diffusion of electroactive species occurs via channels between the ionic clusters of the Nafion membrane. The authors found that the diffusion of electroactive species was fastest when the average number of electroactive species per ionic cluster was <1 and it decreased sharply when the average number is >1. GOx has been immobilised in Nafion and the activity of the enzyme was maintained by diluting the Nafion suspension, however, casting the very dilute Nafion suspensions was shown to form unstable and non-uniform films.[30] Some other problems with Nafion include reducing the active lifetimes of the enzymes within the membranes and as the pH in the solution around the Nafion membrane increases, Nafion will exchange protons back into the membrane, re-acidifying it.[30]

It has been shown[30, 74] that mixing Nafion with quaternary ammonium bromides can increase the electrochemical flux of redox couples through the membrane and allow for larger redox species to diffuse to the electrode surface. The authors proposed that this strategy could be employed to tailor the structure of the Nafion membrane for

immobilizing enzymes in the polymer. For cations with a high affinity for the sulphonic acid groups of Nafion, the modified structure of Nafion could also help to stabilize the enzyme and increase activity by providing a protective outer shell and an ideal chemical environment that resists a decrease in pH within the pore structure.[30] Adding silver salts to Nafion has also been shown[75] to increase pore size and decreases pore density. A similar effect was seen for quaternary ammonium bromides.[74b] Tetrapentylammonium bromide|Nafion membranes are the largest quaternary ammonium bromide that can be employed with Nafion because there comes a point when the micellar pore structure is no longer stable.[30] A downside of using tetrapentylammonium bromide in Nafion films is the destruction of the pore structure due to the restructuring of the membrane that occurs due to the steric hindrance of the quaternary ammonium cations electrostatically binding to every sulphonic acid group.[74b] However, a small (<5%) of the pores remained stable.

During the normal operation of mediated enzyme electrodes, the mediator is re-oxidised at the electrode to its cationic form. If this process were to occur in a Nafion film, one would expect the cations in the film to ion exchange with the cationic constituents of the bulk aqueous electrolyte. Therefore an enzyme electrode based on this process would perform poorly because the mediator would be ion-exchanged out of the film during the enzyme electrode operation. However, Nafion has a high selectivity coefficient for cations with a hydrophobic character,[76] therefore Nafion can provide a potential solution to the problem of mediator leaching.

Nafion's affinity for hydrophobic cations arises from its structural characteristics. When exposed to water or some other hydrophilic solvents (such as buffers), the membrane swells and undergoes microphase segregation, with the ion exchange sites in the polymer

separating from the fluorocarbon backbone.[63-64] The ionic part of the polymer forms into approximately spherical clusters, in which most of the absorbed water and counter-ions reside, forming a hydrophilic subphase around the hydrophilic side chains.[64] These clusters are surrounded by the fluorocarbon backbone regions of the polymer, which constitutes an organic, or hydrophobic subphase.[64]

It has been suggested[77]that because of the large segments of hydrophobic uncharged chain material in the polymer, there is a strong interaction with hydrophobic ions, accounting for the strong retention of hydrophobic cations by Nafion. The high selectivity of Nafion for hydrophobic cations provides a basis for stable mediator incorporation into Nation™ films.[63] In order to improve the retention of cations in the Nafion polymer matrix, molecules can be modified to contain large hydrophobic groups. This has been achieved with ferrocene.[63]

Nafion modified electrodes can be easily prepared by solvent casting the polymer directly on the electrode surface and provide several advantages over unmodified electrodes.[30]

The coating of electrodes with Nafion has also been shown to protect electrodes[78] and also to prevent electrode fowling in whole blood at 37°C.[62] The use of Nafion as an enzyme electrode coating was shown to provide increased performance over conventional cellulose dialysis membranes, with linear responses to glucose up to 28mM and response times of 5-17s.[62] The protective function of the Nafion layer was found to be reproducibly attained, even though the authors reported difficulties with respect to controlling film thickness and uniformity from one electrode preparation to the next.[62]

Nafion has been shown to have permselective properties.[62] Because Nafion is a negatively charged polyelectrolyte matrix; it can reduce the permeability to negatively

charged substances.[68, 78-79] Hence, using Nafion in an enzyme electrode can reduce the influence of reductants such as ascorbate and acetaminophen.[80] Nafion has also been used as a protective, selective coating on electrodes in intracellular fluids in nerve and brain tissue to reduce ascorbic acid response during the determination of various neurotransmitters.[81] The protective effect of Nafion for anionic species such as ascorbate has been attributed to Donnan exclusion.[82]

Nafion films can serve as a stable immobilization matrix that is compatible with the conditions required for an enzyme catalyst to function.[63] It has been used to entrap redox proteins such as cytochrome c[83] and enzymes.[84] Nafion is also able to decrease both precipitation and denaturation of enzymes upon its exposure to concentrated organic solvents.[67b] The polyelectrolyte can wrap up protein macromolecules or their conglomerates, making their solutions in concentrated organic solvents more stable. Nafion can be employed for enzyme immobilization in three different ways.

1. Attachment of the enzyme to the surface of a Nafion modified electrode.
2. Trapping the enzyme between a Nafion membrane and the electrode.

   This is typically accomplished by casting an enzyme solution on an electrode before casting the Nafion suspension on the electrode or by electropolymerising a conducting or redox polymer in the presence of the enzyme before casting the Nafion suspension on the electrode.[78]
3. Entrapment of the enzyme within the Nafion membrane.

One method for immobilising enzymes in Nafion is to suspend enzymes in a water-ethanol mixture with a high (>90%) ethanol content, followed by mixing with dissolved

Nafion and then casting the resulting film onto an electrode surface.[68] Nafion in its commercial form forms an acidic membrane that decreases the lifetime and activity of the enzyme.[30]

It was thought that in order to incorporate enzymes into Nafion films, excessive dilution of the Nafion would be necessary to avoid deactivation of the enzyme by Nafion.[68] This resulted in Nafion solutions that were not properly dissolved. Nafion membranes deposited from such water−organic mixtures with low content of organic solvent were shown to be non-uniform. This was confirmed through the study of ion diffusion[67b].

Using electrode coating solutions where the Nafion is truly dissolved such as solutions containing a high ethanol content, more stable membranes can be obtained.[68] Enzyme electrodes prepared in this way have also shown increased performance compared to enzyme electrodes based on the traditional way of using excessive dilution of Nafion with water.[68] Incorporation of enzymes into Nafion films in this way can improve the stability of the immobilised enzyme[63] and also improve the properties of the Nafion membrane itself.[68]

GOx is a glycoprotein of 160,000 Da which consists of two identical polypeptide chains, each containing an FAD|$FADH_2$ centre.[85] The FAD|$FADH_2$ centre which constitutes the active site, is located in the hydrophobic domains of the enzyme.[73] The outer envelope of the enzyme is hydrophilic and the enzyme is highly soluble in water due to the presence of various negatively charged moieties.[73] It has been proposed[73] that the introduction of hydrophilic macro-molecular GOx into Nafion films generates larger ionic clusters and reduces the overall number of ionic clusters as separated micro ionic

clusters are united by GOx. As a consequence of this, the authors claim that a Nafion|GOx coating is less hydrophobic than a plain Nafion coating.

Nafion is also readily permeable to glucose.[63]

Fc can be dissolved in Nafion and the subsequent FcNafion solution can be used as a redox mediator when a layer of GOx is immobilised onto the FcNafion film.[27] Such a system was used to create a glucose sensor with a response time of less than 20s and a linear range up to 16mM. The properties of the hydrophilic and hydrophobic domains in the Nafion structure mean that both Fc and Fc^+ are retained in the film, which greatly improves the stability of the enzyme electrode. The electrochemical reaction of Fc in the Nafion film can be described as:

$$Fc + SO_3^-/Na^+ \leftrightarrow Fc^+ - SO_3^- + Na^+ + e^- \qquad 2.1$$

In this process, Fc is oxidized to Fc^+ when the potential of the electrode is scanned more positive than the E° of the $Fc|Fc^+$ redox couple (212mV vs. Ag|AgCl).[86] At this point, the Na^+ ions in the sulphonate group of Nafion are replaced by Fc^+. The Na^+ ions then move into the electrolyte and/or anions in the electrolyte enter the FcNafion film to counterbalance the positively charged Na^+ and Fc^+ in the film, which increases in the films conductivity and stability. The voltammetric behaviour of the FcNafion film was found to depend on film thickness. It was also shown[27] that the catalytic current from the oxidation of glucose was still apparent at high scan rates (>100mV s^{-1}) which shows that the regeneration rate of Fc from Fc^+ by reaction with GOx is high. However, the peak currents exhibited a slowly decreasing sensitivity (of about 20%) for the first 8 h of operation.

2.1.3 Ferrocene Derivatives

Interest in using ferrocene/ferricinium (Fc/Fc^+) couples as redox mediators for electron transfer between GOx and electrodes stems from the fact that the ferrocene molecule can replace O_2 as the electron acceptor in the reaction:

$$FADH_2 + O_2 \rightarrow FAD + H_2O_2 \qquad 2.2$$

However this then raises the problem of immobilization of the Fc. Adding a functional group such as COOH to Fc opens up a wide range of possibilities for its immobilisation through covalent binding to COOH. FcCOOH can be covalently bound to GOx itself.[60] Therefore the electrocatalytic current produced results from the oxidation of FcCOOH at the electrode surface and its reduction via intermolecular electron transfer. This was achieved by covalent attachment of FcCOOH to lysine residues on GOx. In order to achieve reproducible derivitisation of GOx with FcCOOH, the reaction is done in the presence of urea. However this can result in a 40% loss of enzyme activity.[60]

FcCOOH can also act as a mediator when bound to a polymer. FcCOOH can be covalently bound to polyallylamine along with GOx.[87] Such an electrode can be used to detect glucose concentrations up to 7mM.

FcCOOH has also been covalently bound to bovine serum albumin (BSA) which was immobilised on an electrode along with horseradish peroxidise in order to produce a reagentless biosensor for the detection of hydrogen peroxide.[88]

2.1.4 Phospholipid Polymers

One way of improving the properties of bioelectronic devices is to use nature as an inspiration in the design of such devices. This is a concept known as biomimicry. With

this in mind, the phospholipid bilayer has many exploitable attributes for use in bioelectronic devices.

A phospholipid bilayer matrix is a natural environment for various enzymes.[89] It is generally believed that the lipid environment is a prerequisite for monitoring or restoring the activity of a number of membrane enzymes.[90] It has been shown that unsaturated lipids can protect enzymes from degradation by atmospheric oxygen or liberated hydrogen peroxide.[90] Therefore it makes sense to use such materials in the design of enzyme electrodes.

Phospholipid bilayers are composed of hydrophilic head groups and hydrophobic acyl substituents. The acyl substituent's of phospholipids provide the hydrophobic environment that is necessary for the function of intrinsic membrane proteins.[91]One of the most common head groups is Phosphorylcholine (PC). PC is a zwitterionic head group that is present, for example, in the form of the phospholipid PC, in the outer lipid bilayer of red cell membranes.[92]

Among phospholipids with various ionic head groups, the PC head group is the only one responsible for blood compatibility.[93] This is based on the fact that phospholipids with an electrically neutral PC head group are predominant in the outer half of the bilayer of cell membranes, while negatively charged phosphatidylserine is almost exclusively found in the inner half of the bilayer.[93] Since densely distributed PC polar head groups exist in the outer lipid surface of red blood cells, (a cell type which shows non-adhesivity toward substrates), it has been hypothesized that the existence of PC head groups on substrates may provide high non-cell adhesivity.[93] The PC head groups are very polar but electrically neutral under physiological conditions, due to zwitterions that can bind a

large amount of water.[93] Therefore, the existence of such phospholipid polar groups provides a strong affinity for phospholipid molecules and a reduction of platelet adhesion, aggregation and suppression of protein adsorption.[94]

It is desirable to utilise the benefits of phospholipid membranes in the design of enzyme electrodes. One way of achieving this is through the use of polymeric phospholipids. Polymeric materials facilitate the creation of a multipurpose interface between biological circumstances and materials, that is biointerfaces.[95] Polymeric phospholipids represent a new class of hybrid biomaterials both of biomembranes (polar surfaces, non-thrombogenic, low antigenic potential and low permeability) and of synthetic polymers (chemical and physical stability).[91]

The incorporation of a phospholipid polymer and an enzyme electrode construct can improve enzyme stability and provides added insulation against electroactive interferants such as ascorbic acid.[96] The protective effect of the lipid layer can also improve electrode lifetime.[90]

Polymerisation inhibits firstly, the rearrangement and decay evident with multilayer's of non-polymerisable lipids, and secondly, the ability to coat an artificial surface with a stable polymeric phospholipid should render the surface more biocompatible, especially when the polymer is engineered to mimic the surface of host cells.[91] When coated from suitable solvent systems, these materials form physiadsorbed coatings on hydrophobic materials that are extremely stable with excellent biocompatibility.[97]

In order for polymeric phospholipids to be of use when immobilised on an electrode surface, they must be perfusable and permit the passage of oxygen, and indeed they have been shown to conform to both of these requirements.[91]

The simplest common feature among the blood-compatible cellular and model membranes is the high content of the electrically neutral phospholipids which contain the PC head group.[91] By mimicking the outer leaflet of a red blood cell, PC-based polymers have been shown to have markedly improved biocompatibility.[97] When sufficient PC is present to provide the necessary levels of biocompatibility, the materials inherently contain a large amount of water associated with the head group and are effectively hydrogels.[97] Furthermore, evidence has been presented to suggest that when proteins contact surfaces containing the PC group, they are not denatured.[97] This is advantageous for the use of such materials in enzyme electrode design.

PC-containing surfaces have demonstrated the ability to reduce adhesion of a number of strains of bacteria.[97] It is logical to assume that PC is preventing the formation of any conditioning layer that might otherwise enable the bacteria to gain anchorage to the surface.[97] This property is of use in many applications where bacterial infection is a problem.

One way to incorporate the PC functional group into a polymer is to use the 2-methacryloyloxyethyl phosphoryl- choline (MPC) and n-butyl methacrylate (BMA) monomers to form poly(MPC-co-BMA). MPC polymers are hydrophilic in nature due to the presence of the PC polar group.[94] The hydrophilicity that is imparted to the copolymer is a function of the molecular weight and molar ratio of MPC relative to BMA.[94] Poly(MPC-co-BMA) coated surfaces have been observed to increase in thickness under wet conditions. This increase in thickness is a result of the poly(MPC-co-BMA) chains adsorbing water molecules.[94]This adsorption of water molecules is facilitated by hydrogen bonding.[94] Because the phosphorylcholine groups in poly-

(MPC) chains are bulky and hydrophilic, they have a large hydration capacity.[98] Therefore it can be said that the copolymers take the hydrogel structure in water.[99] It has also been noted that the permeation of glucose through poly(MPC-co-BMA) based polymers is not affected by the presence of protein.[100] This is beneficial for the use of poly(MPC-co-BMA) based polymers in enzymatic glucose sensing and glucose biofuel cell devices.

Due to the MPC group in poly(MPC-co-BMA), polymers composed of poly(MPC-co-BMA) suppress not only protein adsorption and cell adhesion but also the inflammatory reaction to adherent cells.[101] This is due to the fact that the MPC has the same polar groups as that are of typical phospholipids mainly located at the outer surface of cell membranes.[101a] poly(MPC-co-BMA) modified surfaces are also able to prevent the activation of any adsorbed cells[100] and can effectively suppress the adhesion of blood cells when in contact with both platelet rich plasma and whole blood.[99] So it can be said that polymers comprising poly(MPC-co-BMA) are biocompatible[94] can improve the blood compatibility of biomedical devices[92] and pharmaceutical products[102] and can reduce biofouling.[103] In fact, many other phospholipid polymers containing the PC group possess excellent blood compatibility.[102]

MPC based polymers also have another beneficial effect when used in biomedical devices. Because they have the hydrogel structure when in aqueous environments, they can reduce tissue damage caused by the use of implantable devices by acting as a lubricant between the surface of organs and tissues and any implantable device.[104]

poly(MPC-co-BMA) has also been shown to improve the lifetime of a GOx electrode based on the detection of H_2O_2.[100] Therefore the use of poly(MPC-co-BMA) based polymers may also be able to improve the lifetime of mediated GOx electrodes.

The MPC group also improves the solubility of polymers. Good solubility of a polymer in mild solvents such as water and ethanol is required to facilitate easier modification of electrodes; MPC polymers having more than 30% mole fraction of MPC units are readily able to dissolve in water and possesses enough capability to inhibit nonspecific interactions with various proteins, platelets and cells, therefore the compositions of the designed MPC polymers are usually higher than 30% (mole fraction).[105]

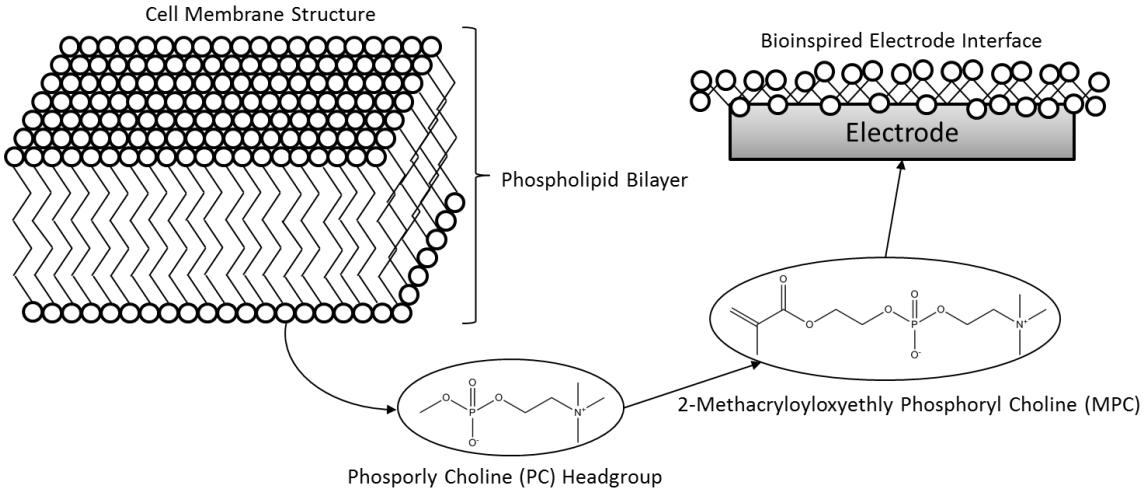

Figure 2.6: A bioinspired electrode interface based the structure of a biological cell membrane.

The phospholipid polymer poly[2-methacryloyloxyethyl phosphorylcholine (MPC)-co -n-butyl methacrylate (BMA)-co-p-nitrophenyloxycarbonyl poly(ethylene glycol) methacrylate (MEONP)] (PMBN) is a polymeric phospholipid whose molecular weight can be in the range of 1.1 to 3.1 x10^5.[106] It contains three polymer chain segments which impart different properties to the polymer[21], MPC, BMA, and MEONP.[107] The MPC moieties in PMBN play an important role in suppressing the activation and adhesion of

platelets.[101b] This is the unit which mimics biomembranes and provides the blood compatibility and biocompatibility.[21] BMA is the hydrophobic unit, and the MEONP unit has an active ester group in the side chain.[21]

It has many advantages for use as a polymer in the fabrication of polymer electrodes. The presence of both the hydrophilic MPC unit and the hydrophobic BMA unit render the polymer amphiphilic.[107] As well as being amphiphilic it is also a hydrogel with a hydrophilic surface.[101b] It has been shown to exhibit excellent hemocompatibility[106] and to be capable of maintaining enzyme activity, these properties are crucial for implantable devices.[21]

Both hydrophobic and hydrophilic compounds can be incorporated into the polymer due to its amphiphilic nature. Also, the MEONP unit can bind biomolecules under very mild conditions.

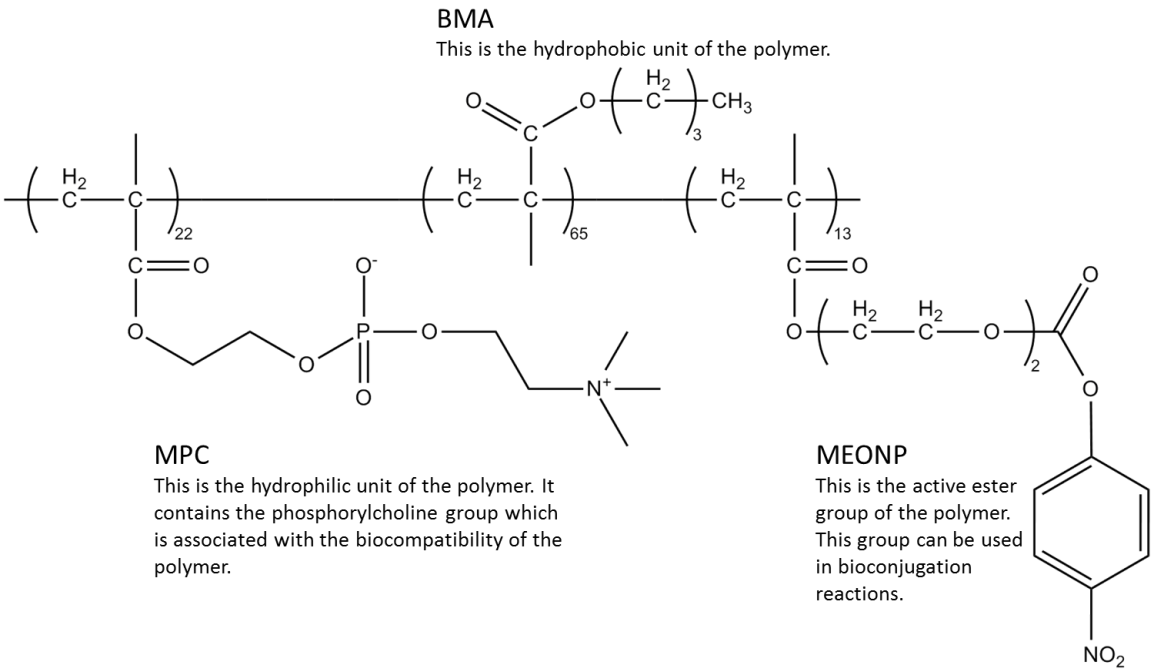

Figure 2.7: Schematic diagram showing the structural elements that make up the phospholipid polymer PMBN.

It has been shown that proteins embedded in phosphorylcholine groups show high structural stability and maintain their activity.[108] Also, PMBN forms films that remain stable for long periods and it comprises units to prevent non-specific adsorption,[109] as well as being stable over a wide pH range (4 – 9).[110] With the potential medical applications of enzyme electrodes in mind, it is notable that PMBN has exhibited high blood compatibility[21].

PMBN was expected to bind to GCE surfaces due to adsorption of the hydrophobic components of the polymer onto the electrode surface and also due to electrostatic attraction of other functional groups on the polymer with the electrode surface.

2.2 Experimental

Materials

p(VFc-Co-HEMA) (number-average molecular weight and molecular weight distribution 3.7×10^4 and 1.2, respectively)[61] and poly[2-methacryloyloxyethyl phosphorylcholine (MPC)-co-n-butyl methacrylate (BMA)-co-p-nitrophenyloxycarbonyl poly(ethylene glycol) methacrylate (MEONP)] (PMBN)[21] were kindly donated by collaborators in Japan.

Dimethylformamide (DMF), Hexamethylenediamine (HMDA), Glucose Oxidase (GOx), 1-Ethyl-3-(3-dimethylaminopropyl)carbodiimide (EDC), Nafion, Ethanol, Ferrocene (Fc), NaOH, NH_4OH Glutaraldehyde (GA), Bovine serum albumin (BSA), $K_3[Fe(CN)_6]$ $K_4[Fe(CN)_6]$, mineral oil and graphite powder were purchased from Sigma-Aldrich (Dorset, UK) and used without further purification.

Universal indicator paper was purchased from VWR International LTD (Leicestershire, UK). N_2 gas was purchased from BOC Gas, (Wallsend, UK).

Electrochemical Tests

All electrochemical tests were carried out with an Autolab potentiostat–galvanostat.

(PGSTAT302). Glassy carbon electrodes (GCE) (diameter = 3mm), Ag|AgCl reference electrodes (RE) (0.208 V vs. NHE) (all electrode potentials are with reference to the Ag|AgCl electrode unless stated otherwise) and graphite paste electrodes (GPE) were purchased from Bioanalytical Systems Ltd. (Warwick, UK). Pt counter electrodes (CE) were purchased from Alfa Aesar, (Heysham, UK).

2.2.1 Fabrication of a Poly(vinylferrocene-co-2-hydroxyethyl methacrylate) Mediated GOx Enzyme Electrode

In order to prepare a p(VFc-Co-HEMA) enzyme electrode, 2µl of p(VFc-Co-HEMA) (1%wt. in DMF) was cast onto a polished GCE. Next 0.4µl of 1%wt. HMDA solution

was added to the p(VFc-Co-HEMA) layer and mixed with the pipette tip, at which time the mixture became turbid. Next 2µl of 1mg ml^{-1} (250 units ml^{-1}) GOx solution containing 6mg of 1-Ethyl-3-(3-dimethylaminopropyl)carbodiimide (EDC) (1.9M) (in 0.1M PBS, pH 7) was added to the electrode. The electrode was then kept at 4°C overnight. After this the electrode was placed in a 3 electrode cell (Pt CE, Ag|AgCl RE) containing PBS solution as the electrolyte. The cell was then sparged with N_2 for at least 10 minutes and a N_2 blanket was maintained throughout all experiments.

2.2.2 Fabrication of a p(VFc-Co-HEMA) Graphite Paste Electrode

24mg of graphite paste was prepared using graphite powder and mineral oil (wt. ratio = 3:2). This was mixed with 150µl of 2%wt. p(VFc-Co-HEMA) in Dimethylformamide (DMF). The DMF was evaporated at 100°C.

2.2.3 Preparation of a Ferrocene|Nafion (FcNafion) Redox Polymer

In order to prepare a FcNafion redox polymer, Nafion was diluted to 1%wt. by dilution of a 5% wt. solution with 90% ethanol. The 1% Nafion was then neutralised to pH 7 with either concentrated NaOH or NH_4OH. This was controlled with universal indicator paper. Fc was then added to the neutralised Nafion solution to make a 50mM FcNafion solution.

2.2.4 Fabrication of an FcNafion Electrode

In order to prepare a FcNafion electrode, 10 µl (applied to the electrode sequentially in 2 µl additions, with time for drying in between addition steps) of 1% w/w Nafion in 90% ethanol containing 50 mM Fc was pippeted onto a polished GCE. The electrode was then placed in a 3 electrode cell (PT CE, Ag|AgCl RE) containing PBS solution (0.1M, pH 7)

as the electrolyte. The cell was then sparged with N_2 for at least 10 minutes and a N_2 blanket was maintained throughout all experiments.

2.2.5 Fabrication of an FcNafion Mediated GOx Enzyme Electrode

In general, FcNafion-GOx enzyme electrodes were prepared as follows:

10 µl of the 1% w/w Nafion solution in 90% ethanol containing 50 mM Fc was deposited onto a polished GCE in 2µl steps with time for drying allowed between the addition steps. Once the electrode was dry it was placed in a 3 electrode cell and subjected to 25 CV scans at 50 mV s^{-1} between -0.2 V and 0.6 V (vs Ag|AgCl). This preconditioning step serves two purposes:

- Accumulating the Fc^+ in the ionic domain of the Nafion
- Decreasing the hydrophobicity of the Nafion layer, allowing a better deposition of the enzyme solution onto the electrode.

Once complete the conditioned Fc-Nafion modified GCE was dried at 35°C for 10 minutes. Next, 10µl of a 5 mg ml^{-1} GOx solution (1250 units ml^{-1}) (in 0.1 M PBS, pH 6.8) was added to the Fc-Nafion modified GCE and dried at 35°C for 10 minutes. The modified GCE was then placed in a 3 electrode cell (Pt coil CE, Ag|AgCl RE) containing PBS as the electrolyte. The cell was de-aerated with N_2 for 10 minutes prior to the start of the measurements and a N_2 blanket was maintained throughout all experiments.

2.2.6 EIS Analysis of FcNafion Mediated GOx Enzyme Electrodes

Electrode Modification

The modification of the electrode with FcNafion is the same as described above. The enzyme was immobilised as follows:

GOx (1mg) and BSA (3 mg) were dissolved in 200µl of 0.1 M PBS (pH 6.8) to create a 2 mg ml^{-1} (500 units ml^{-1}) GOx solution, then 4 µl of a 25% Glutaraldehyde solution (in PBS) was added to this solution with vigorous stirring. 10µl of the freshly prepared mixed solution was added to the Fc-Nafion modified GCE and dried at 35°C for 10 minutes. If PMBN was used, 10µl of 1% wt. in 5% ethanol was added to the electrode after the addition of GOx (BSA was not used).

The modified GCE was then placed in a 3 electrode cell (Pt coil CE, Ag|AgCl RE) with 10 ml of PBS. The cell was de-aerated with N_2 for 10 minutes prior to the start of the measurements and a N_2 blanket was maintained throughout all experiments.

EIS Measurements

EIS experiments were carried out by applying an ac voltage with 5 mV amplitude at the formal potential of the redox couple involved in a frequency range from 0.01 Hz to 100 kHz. For the redox probe, a 5mM $K_3[Fe(CN)_6]$ / $K_4[Fe(CN)_6]$ (1:1) mixture was used.

2.2.7 Fabrication of a FcNafionGOx Electrode

Generally, FcNafionGOx electrodes are prepared by suspending GOx into an FcNafion solution (0.25% Nafion solution in 90% ethanol containing 5mM Fc) to create a 5 mg ml^{-1} enzyme|redox polymer solution. This solution can then be cast onto electrode surfaces. If PMBN was used, a layer of PMBN (0.5µl of a 5% weight PMBN solution in 5% ethanol) was cast on top of the redox polymer|enzyme mixture and allowed to dry. The resulting electrodes were then placed in an electrochemical cell containing PBS and deaerated with N_2 for at least 10 minutes prior to the start of the experiment. A N_2 blanket was maintained throughout all experiments.

2.2.8 Fabrication of a PMBN-HMDA-FcCOOH-PMBN-GOx (PHFPG) Electrode

The fabrication of the PHFPG electrode was based on the binding of the PMBN polymer to a GCE via hydrophobic and electrostatic effects as discussed in section 2.1.4. Once a film of PMBN (1 wt% in 5% ethanol) had been cast on the electrode surface, 1% wt Hexamethylenediamine (HMDA) (a.q.) was added to the film. This allowed the amine from HMDA to react with the active ester of the MEONP group of the PMBN polymer. The modified electrode was then placed in a 5mM FcCOOH solution containing EDC.

After this stage, the electrode was removed from the FcCOOH solution and a solution of 5 mg ml^{-1} GOx (1055 unit's ml^{-1}) in 0.9% wt. PMBN in 5% ethanol was added to the electrode. The enzyme was mixed with the PMBN prior to casting on the electrode to allow amine groups from residues such as lysine on GOx to bind the active ester of the MEONP group of the PMBN polymer. The electrode was allowed to dry, then placed in a three electrode cell (Pt CE, Ag|AgCl RE) containing 0.1M PBS (pH 6.8) as the electrolyte. The reference electrode was isolated from the electrolyte by a salt bridge with a frit of Vicor glass. The cell was then sparged with N_2 for at least 10 minutes and a N_2 blanket was maintained throughout all experiments.

2.2.9 Investigation of Alternative Mediators for use in Enzyme Electrodes

For this investigation, 10mM Fc, 10mM Nickelocene (Nc) (the Nickel analogue of Fc), and 0.4mM CQ_{10} (see figure Figure 3.1) were dissolved in acetone and 10µl aliquots were drop coated onto a polished GCE. The concentrations of the Fc and Nc solutions were used in accordance with Atanasov.[86] The concentration of CQ_{10} was chosen in order to minimise the effect of multilayer electron transfer which can complicate the

voltammogram.[111] The acetone was evaporated and CV scans were then carried out at 50 mV s^{-1} in a three electrode cell (Pt CE, Ag|AgCl RE) containing 0.1M PBS (pH 7).

2.3 Results & Discussion

2.3.1 A Poly(vinylferrocene-co-2-hydroxyethyl methacrylate) Mediated GOx Enzyme Electrode

In this section, the characterisation of p(VFc-Co-HEMA) as a redox polymer for the immobilisation of GOx is described. This electrode was then tested for electrocatalytic activity towards glucose.

Characterisation of the Redox Polymer

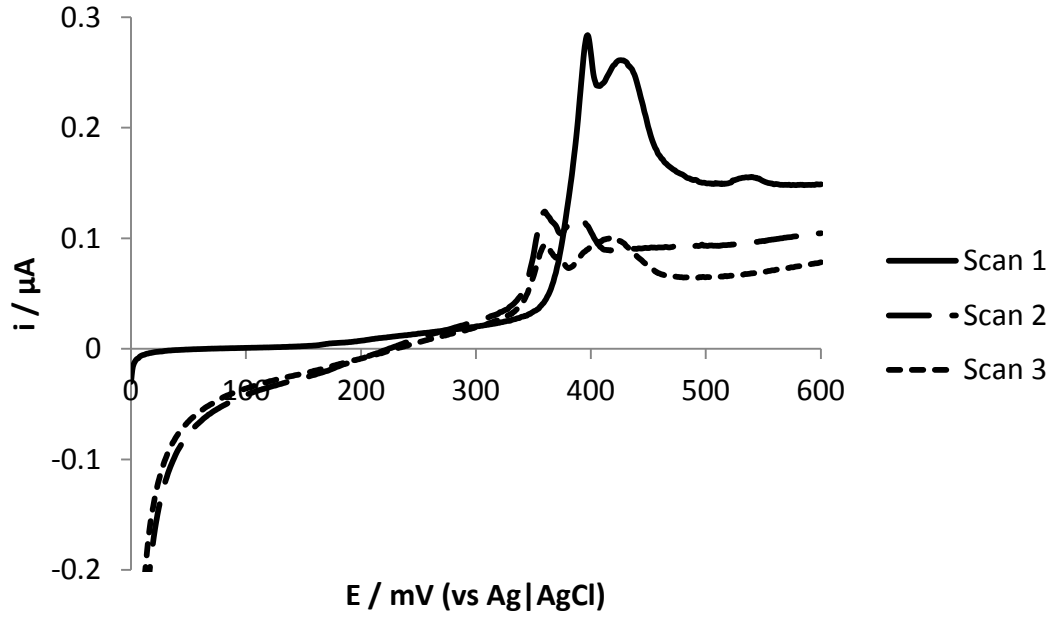

Figure 2.8: Linear sweep voltammograms (LSVs) of p(VFc-Co-HEMA)-HMDA-GOx. Electrolyte was 0.1M PBS; v = 1mV s^{-1}.

Figure 2.8 shows LSVs for the p(VFc-Co-HEMA)-HMDA-GOx electrode. It is noted that the peak current (i_p) drops with increasing scan number. This can be attributed to the mechanical instability of the polymer. As the hydrogel component of the polymer swells

upon exposure to electrolyte, the polymer can break away from the electrode surface, reducing the concentration of VFc redox centres immobilised on the electrode and therefore reducing the peak current over time. Two oxidation peaks are seen in Figure 2.8, the first one roughly corresponds to the oxidation potential of VFc (377mV (vs Ag|AgCl)[15]). The second slightly (~31mV) more positive peak is attributed to VFc units in closer proximity to the hydrophobic domain of the co-polymer. The oxidised form of VFc in these regions will be less stable than those located in the hydrophilic domain of the co-polymer as the hydrophobic domain will be less efficient at screening the excess charge of the VFc unit upon oxidation. Therefore these VFc units will have a slightly more positive oxidation potential.

The slight (~37mV) negative shift in the first oxidation peak potential between scan 1 and scan 2 is attributed to adsorption of electrolyte by the hydrogel component of the co-polymer (as hydrogels are composed of a network of polymer chains that are hydrophilic, they are highly absorbent). This uptake of electrolyte into the polymer structure will improve charge screening of the VFc units upon oxidation and therefore lead to a more favourable oxidation potential.

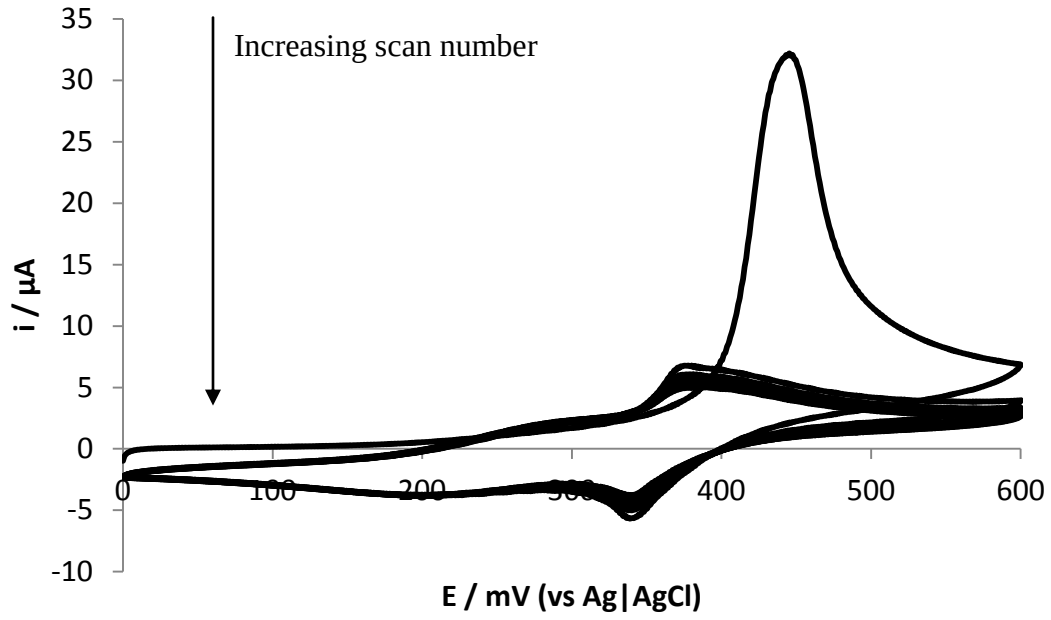

Figure 2.9: Cyclic voltammograms (CVs) of p(VFc-Co-HEMA) in 0.1M PBS; v = 100mV s^{-1} electrode. At this higher scan rate (100mV s^{-1}) the irreversible oxidation of Fc in the VFc units is more obvious.

The Activity of the Enzyme Electrode Towards Glucose

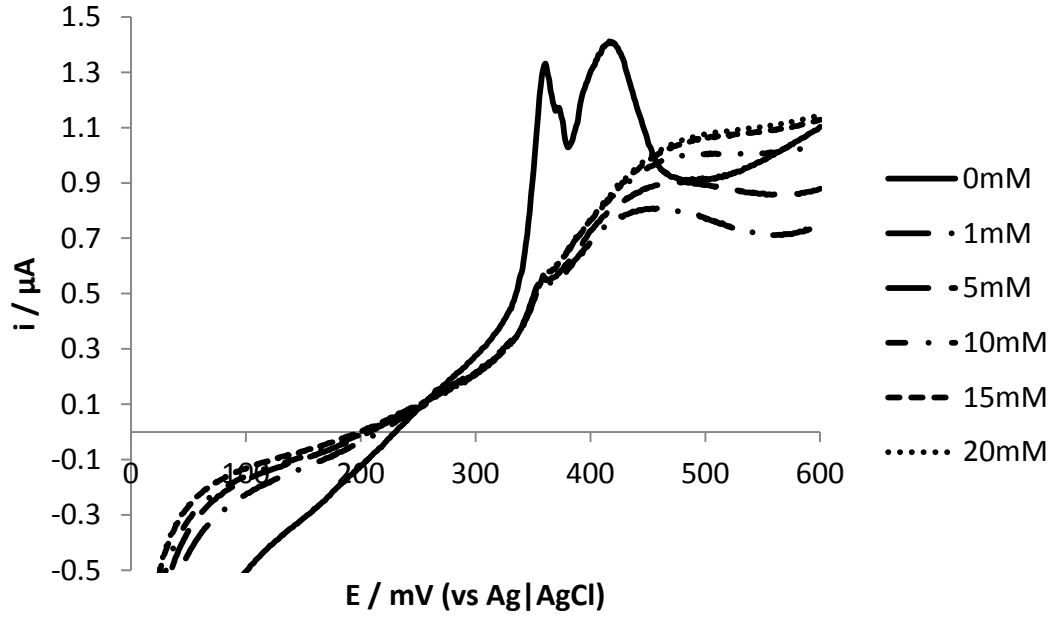

Figure 2.10: LSVs of p(VFc-Co-HEMA)-HMDA-GOx. Electrolyte was 0.1M PBS; v = 1mV s^{-1} with increasing [glucose].

Figure 2.10 shows LSVs for the p(VFc-Co-HEMA)-HMDA-GOx electrode as the cell glucose concentration was increased. The first scan (0mM) is scan 3 from Figure 2.8. Upon the addition of glucose, the current response changes to that of catalytic current, which is dependent on the diffusion of substrate to the electrode. This is most apparent in Figure 2.11 in which the 0mM scan has been removed for clarity. Initially, the ferric ions in the VFc units exist in both the reduced form (Fe^{II}) and oxidised form (Fe^{III}). As the potential of the electrode exceeds that of the oxidation potential of the ferrocenyl group, Fe^{III} is generated in the co-polymer. The formation of the Fe^{III} sites in the co-polymer extends from the surface of the electrode to the bulk polymeric phase via an electron-hopping reaction and reaches the vicinity of the FAD/$FADH_2$ in GOx. Since the redox potential of FAD/$FADH_2$ (-413mV vs Ag|AgCl)[15] is much lower than the Fe^{II}/Fe^{III} couple, the propagated Fe^{III} sites in the vicinity of $FADH_2$ oxidise it to FAD. By this oxidation reaction, Fe^{III} sites in the co-polymer are reduced to Fe^{II}. These successive reactions catalytically cycle, thus the catalytic reaction of GOx increases the detected oxidation current. Therefore, as the substrate concentration is increased, the detected oxidation current will increase, as seen in Figure 2.11. The detected increase in oxidation current reaches a plateau at a glucose concentration of 15mM. This is due to the saturation of GOx with substrate.

It was proposed that a possible solution to the problem of the mechanical instability of p(VFc-Co-HEMA) could be coating the p(VFc-Co-HEMA)-HMDA-GOx layer with another protective polymer such as polyethylene glycol (PEG) (Figure 2.13). PEG has many advantages for use as a protective polymer in enzyme electrodes due to its nontoxic, nonimmunogenic, and amphipathic properties.[112]

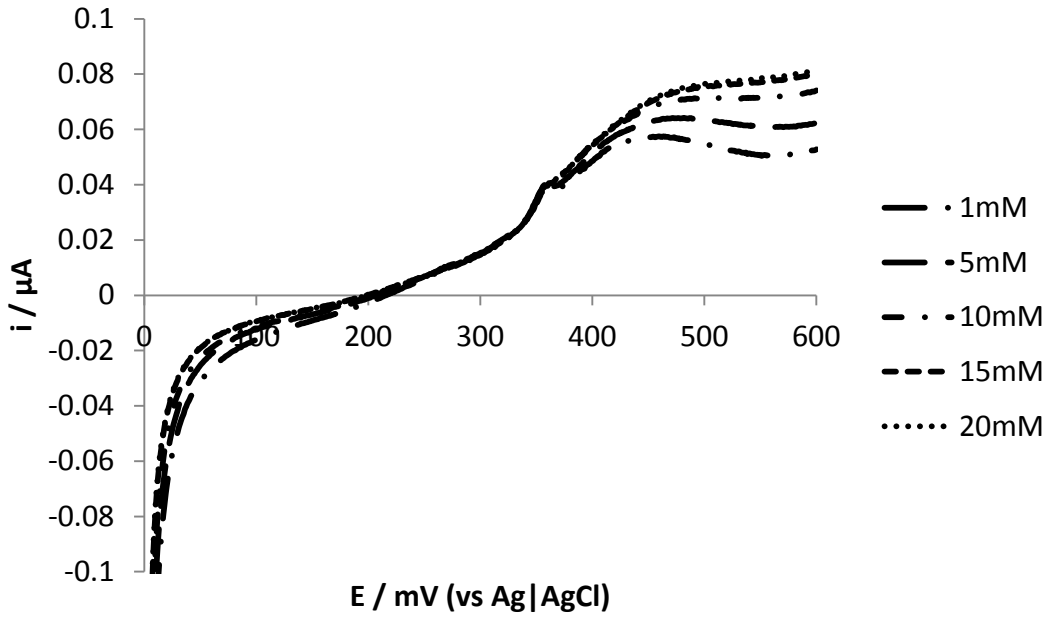

Figure 2.11 LSVs of p(VFc-Co-HEMA)-HMDA-GOx. Electrolyte was 0.1M PBS; v = 1mV s^{-1} with increasing [glucose] (0mM scan omitted for clarity).

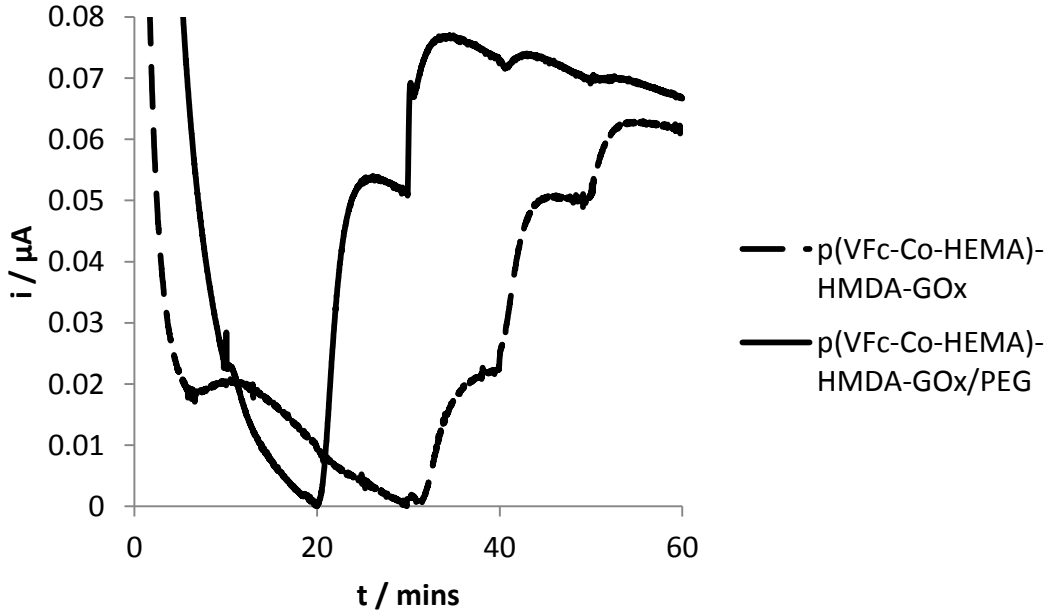

Figure 2.12: Chronoamperometry (CA) experiment for p(VFc-Co-HEMA)-HMDA-GOx & p(VFc-Co-HEMA)-HMDA-GOx/PEG, E = 480mV, electrolyte was 0.1M PBS, glucose added every 10 minutes such that the concentration in the cell was 0, 1, 5, 10, 15 & 20 mM. (Background current subtracted).

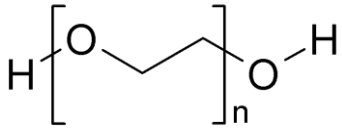

Figure 2.13: Polyethylene glycol (PEG).

It was also proposed that the coverage of the electrode could be improved by adding a larger amount of enzyme solution during electrode preparation. Therefore two p(VFc-Co-HEMA)-HMDA-GOx electrodes were prepared using the procedure outlined in section 2.2.1, except using 10µl of enzyme solution instead of 2µl. A layer of PEG (5µl) was added to one of the electrodes. Figure 2.12 shows the results of CA experiments carried out using the electrodes at 480mV for 1 hr with the addition of glucose every 10 minutes such that the concentration in the cell was 0, 1, 5, 10, 15 and 20 mM. The response time is 10 minutes for p(VFc-Co-HEMA)-HMDA-GOx/PEG and 21.5 minutes for p(VFc-Co-HEMA)-HMDA-GOx. The length of the response time is related to the diffusion of substrate through the film. The shorter response time for p(VFc-Co-HEMA)-HMDA-GOx/PEG is attributed to the hydrogel properties of PEG as the adsorption of electrolyte by the PEG layer will increase the substrate diffusion rate through the polymer film. The upper limit of detection for the electrode modified with PEG is 10mM. The electrode without PEG did not reach its upper limit of detection due to it having a larger response time. The large response times of these enzyme electrodes is likely due to large film thickness. It is desirable to have low film thicknesses but this comes at the expense of enzyme loading. Also, due to the electrode fabrication method, the film thickness was difficult to control.

Investigation of GOx Mutants

The performance of a GOx enzyme electrode can be improved via careful selection and enhancements of the materials chosen for the electrode. However it is also possible to improve the performance of a GOx based enzyme electrode by using different variants of the enzyme itself. One such way of doing this is via directed protein evolution. The principle of directed protein evolution involves the generation of a diverse library of mutants followed by screening for improved protein variants.

Two types of mutant GOx (B11-GOx) have been developed by a collaborating group[113] B11-1 and B11-2. It was proposed that these mutants would be tested for improved electrocatalytic activity (compared to the 'wild type' (WT)) using the p(VFc-Co-HEMA)-HMDA-GOx electrode fabrication method described in section 2.2.1.

Initially, the p(VFc-Co-HEMA)-HMDA-GOx method looked like it would be a suitable method for characterising the mutant enzymes as the results were similar to those described above for commercially available GOx.

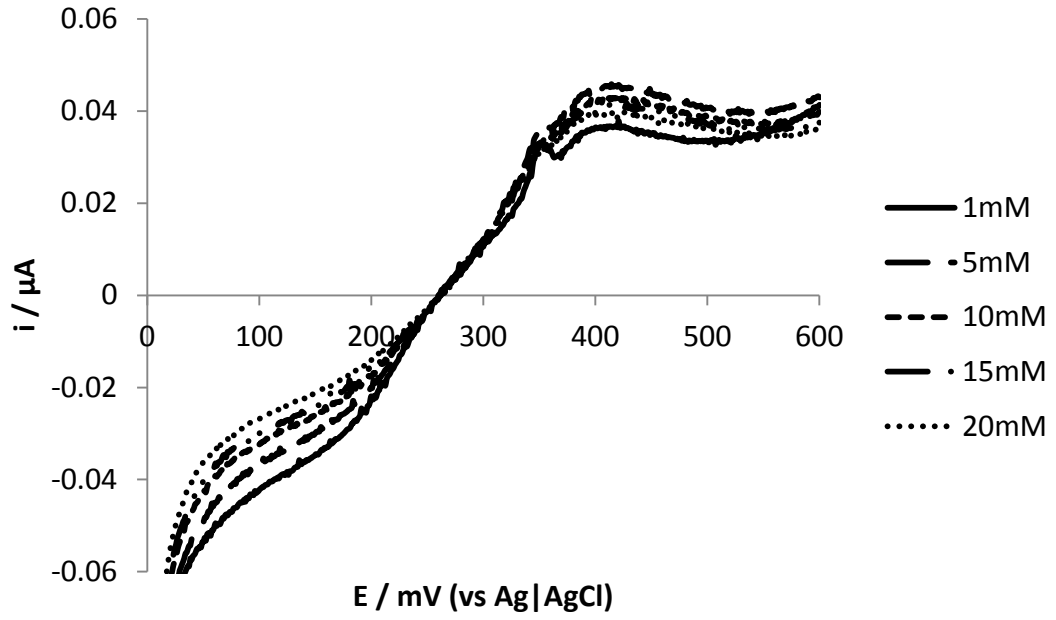

Figure 2.14: LSVs of p(VFc-Co-HEMA)-HMDA-B11-1. Electrolyte was 0.1M PBS; v = 1mV s^{-1} with increasing [glucose] (0mM scan omitted for clarity).

Figure 2.14 shows LSVs for a p(VFc-Co-HEMA)-HMDA-B11-1 at different concentrations of glucose. The maximum current is obtained at a glucose concentration of 5mM. This is lower than for commercially available GOx as the activity of the B11-1 (58 unit's mg^{-1}) is lower than that of commercially available GOx (250 unit's mg^{-1}).

The same procedure was used to characterise B11-2 however the stability of the redox polymer proved problematic. Figure 2.15 shows LSVs carried out under the same conditions as that in Figure 2.14 except using B11-2. The principle of the experiment was to characterise the electrocatalytic activity of B11-2 compared to that of B11-1 and wild type GOx (WT). However it can be seen from Figure 2.15 that the leaching of the VFc units into the electrolyte upon oxidation is the dominant factor in this experiment, masking any information regarding the catalytic activity of the enzyme. Therefore the stability of the redox polymer needed to be improved. One approach was to incorporate

the redox polymer into carbon paste. It was proposed that the hydrophobic nature of carbon paste may help to retain the oxidised VFc units during potential scanning.

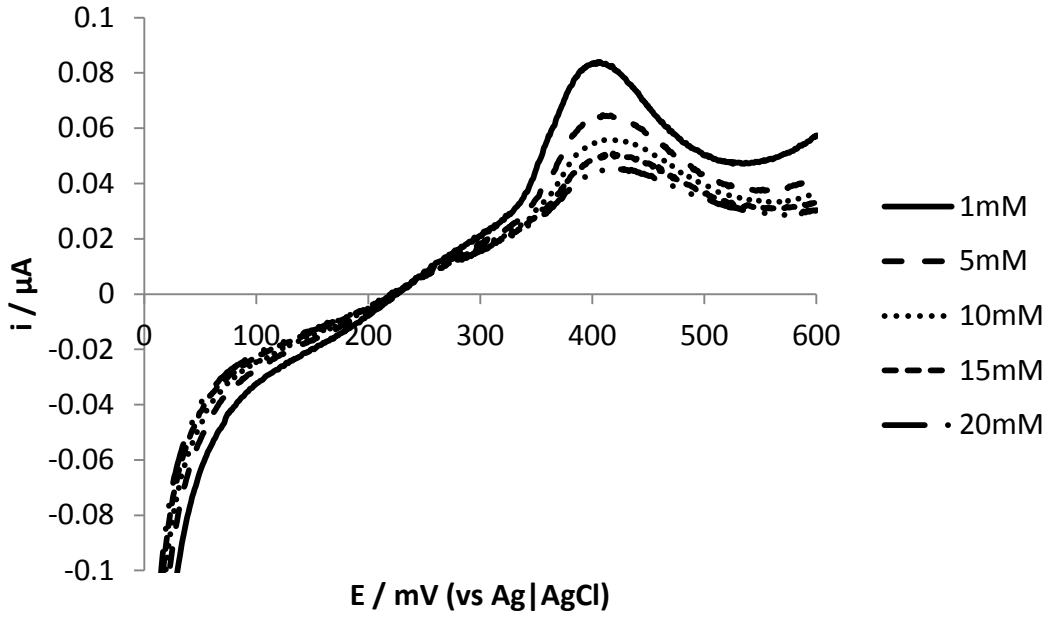

Figure 2.15: LSVs of p(VFc-Co-HEMA)-HMDA-B11-2. Electrolyte was 0.1M PBS; v = 1mV s^{-1} with increasing [glucose] (0mM scan omitted for clarity).

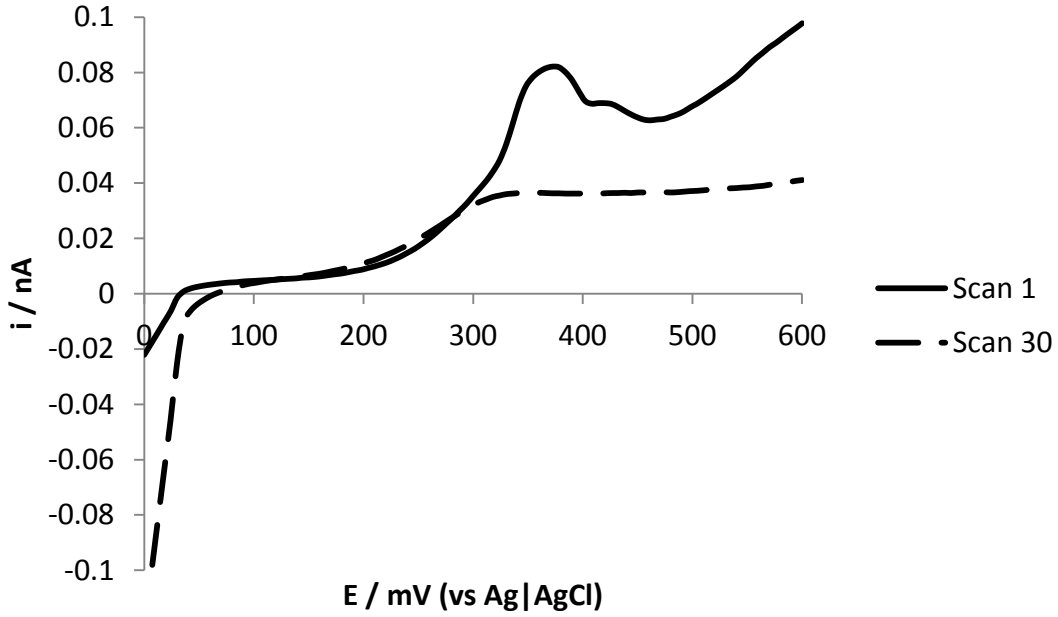

Figure 2.16: LSVs of p(VFc-Co-HEMA) incorporated into graphite paste. Electrolyte was 0.1M PBS; v = 1mV s^{-1}.

A p(VFc-Co-HEMA) graphite paste electrode p(VFc-Co-HEMA)-GPE was prepared as described in Section 2.2.2. The resulting paste was packed into a graphite paste electrode (GPE). Figure 2.16 shows linear sweep voltammograms (LSVs) for the p(VFc-Co-HEMA)-GPE . 30 potential scans were performed and the 1^{st} and 30^{th} scans are shown. It is clear that the VFc units are not retained in the electrode as the peak current has reduced by ~ 66% over the course of the experiment. It is also noted that the current passed during the experiment is several orders of magnitude smaller than previous experiments using planar GCEs (e.g. Figure 2.15). This is likely due to the higher resistance of the graphite paste. It has been noted previously (Section 2.1.2), that Nafion has the ability to retain both forms of the $Fc|Fc^+$ redox couple. Therefore this polymer was used as a basis for forming a stable GOx enzyme electrode.

2.3.2 An FcNafion Mediated GOx Enzyme Electrode

In this section, the characterisation of FcNafion as a redox polymer for the immobilisation of GOx is described. This electrode was then tested for electrocatalytic activity towards glucose.

Properties of FcNafion

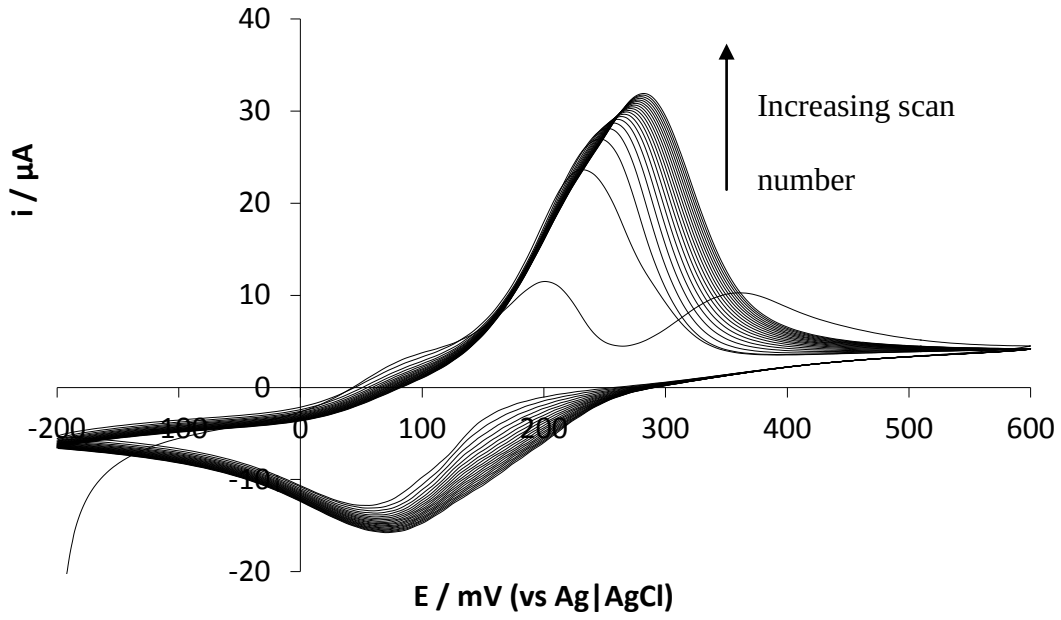

Figure 2.17: CV scans for a FcNafion modified GCE. Scans done in 0.1 M PBS (pH 6.8); v = 50 mV s^{-1}. Coating solution was 10µl of 1% w/w Nafion solution in 90 % ethanol containing 50 mM Fc.

Figure 2.17 shows CVs of a freshly prepared FcNafion modified electrode immersed in PBS (pH 6.8). In the first cycle in the anodic process, two peaks appear; these become one during subsequent scanning. The appearance of two oxidation peaks is due to species residing in different domains of Nafion. As the scan proceeds, the positively charged Fc^+ is accumulated in the ionic clusters, resulting in one oxidation peak. Anodic and cathodic currents rise continuously with potential scans until a distinct redox couple of Fc occurs. With this method it has been reported that the potential scan range influences peak current.[27] The higher the positive potential scan, the higher the peak current. This is due to the number of anions entering the Nafion film. As Fc is oxidised during the anodic scan, it replaces Na^+ in the sulphonate group of Nafion. The Na^+ ions then diffuse into the electrolyte and/or anions from the electrolyte enter the FcNafion film which results in increased conductivity and stability of the film. Cyclic voltammograms obtained in PBS

with the FcNafion modified electrode at different scan rates are shown in Figure 2.18. The scan rate was increased from 10mV s^{-1} (inside scan) to 20, 50, 100, 200 and finally 500mV s^{-1} (outside scan).

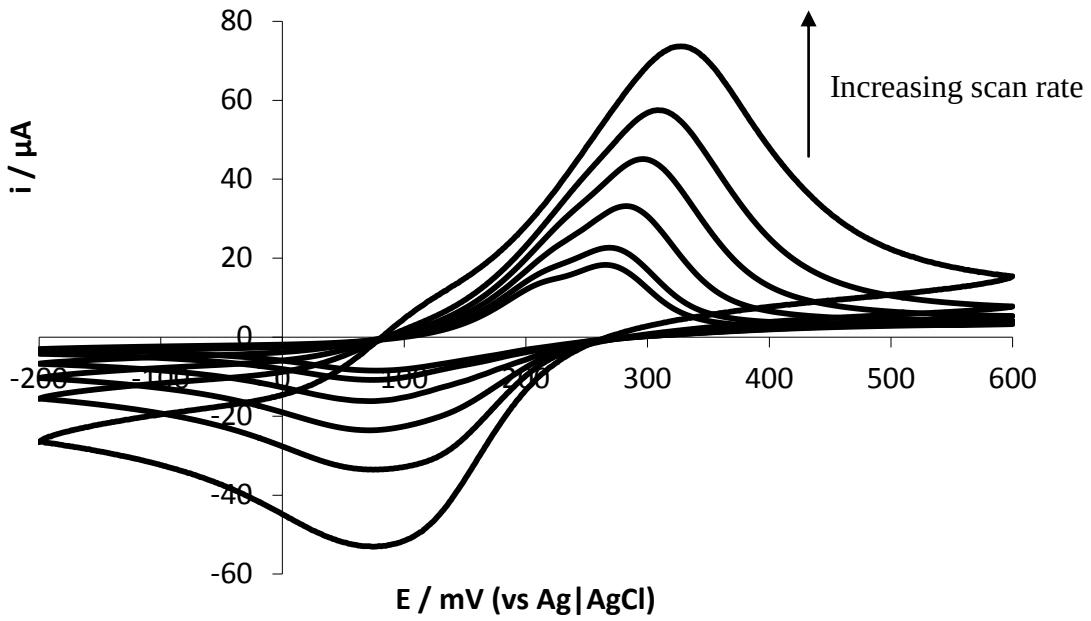

Figure 2.18: CVs of the Fc-Modified GCE at different scan rates. Scans done in 0.1 M PBS (pH 6.8); coating solution was 10µl of 1% w/w Nafion solution in 90 % ethanol containing 50 mM Fc.

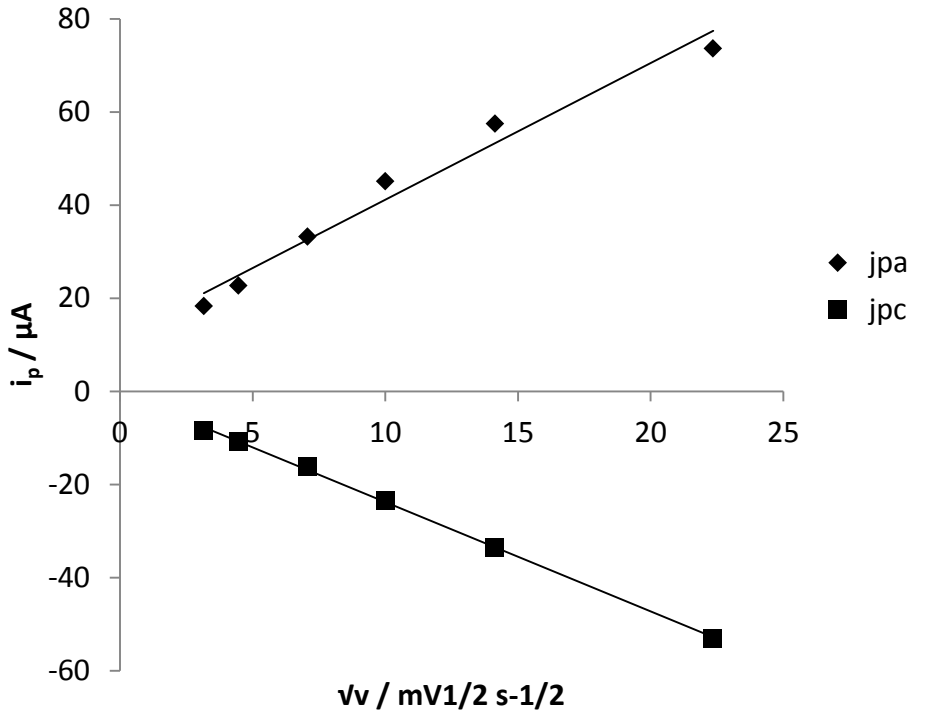

Figure 2.19: A plot of peak current density (j_p) versus square root of scan rate for the FcNafion modified GCE. Data from Figure 2.18.

The observed peak current on the forward potential scan is given for the case of reversible electron transfer by the Randles-Sevcik equation:

$$i_p = 0.4463\, nFAC \left(\frac{nFvD}{RT}\right)^{\frac{1}{2}} \qquad 2.3$$

Where i_p is the peak current, n is the number of electrons transferred in the event, F is the Faraday constant, A is the electrode area, C is the concentration of the electron transferring species, v is the scan rate, D is the diffusion coefficient of the electron transferring species, R is the gas constant and T is temperature.

From equation 2.3 we can see that i_p is proportional to √v in the case of reversible electron transfer. Figure 2.19 shows that both the anodic peak current density (j_{pa}) and the cathodic peak current density (j_{pc}) are proportional to the square root of scan rate (v)

up to 500 mV s^{-1}. The Nernst equation predicts the equilibrium ratio between the reduced and oxidised forms of the redox couple, based on the applied potential:

$$E = E° + \frac{RT}{zF} ln \frac{a_{ox}}{a_{red}} \qquad 2.4$$

Where *E* is the applied potential, *E°* is the formal potential of the redox couple, *z* is the number of moles of electrons transferred in the redox process, *a* is the chemical activity of the relevant species where a_{ox} is the oxidised species and a_{red} is the reduced species. The other symbols have the same meanings as described for equation 2.3.

As the j_p is proportional to √v up to 500mV s^{-1}, this indicates that the electron transfer rate for the FcNafion modified electrode is fast enough to maintain the equilibrium ratio between the reduced and the oxidized forms of the redox couple at least up to this scan rate. This shows that the FcNafion film has good electron transfer properties.

FcNafion as a Redox Mediator for Glucose Oxidase

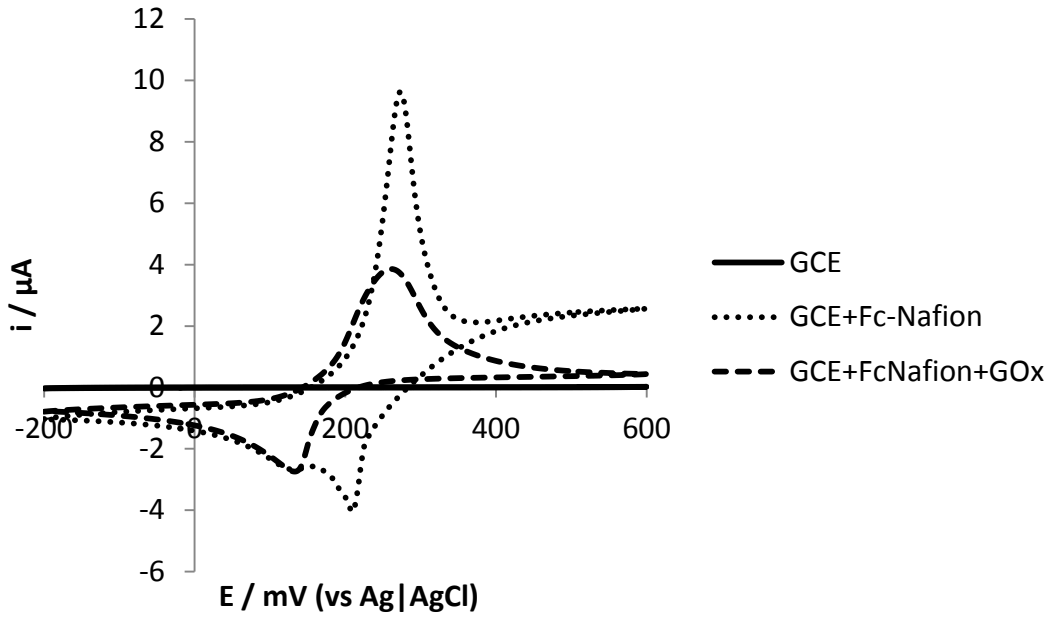

Figure 2.20: CV scans after various stages of the electrode modification process (v = 2mV s^{-1}).

Figure 2.20 shows CV scans after various stages of the electrode modification process. There is a significant drop in accessible redox sites upon addition of the protein layer, consistent with successful immobilisation of the protein.

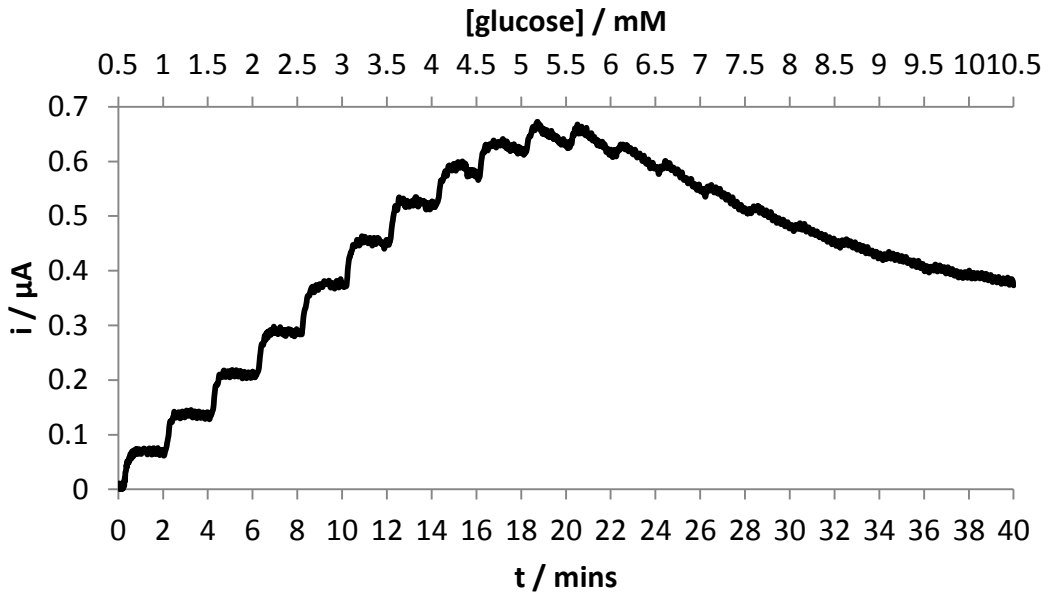

Figure 2.21: Chronoamperometry (CA) experiment for a FcNafion-GOx modified GCE. The [glucose] was increased by 0.5mM every 2 minutes Eapp = 0.37 V (vs Ag|AgCl). (Background current removed).

Figure 2.21 shows a Chronoamperometry (CA) experiment performed on a FcNafion-GOx modified GCE fabricated as described in section 2.2.5. During the experiment the concentration of glucose in the cell was increased by 0.5 mM every 2 minutes.

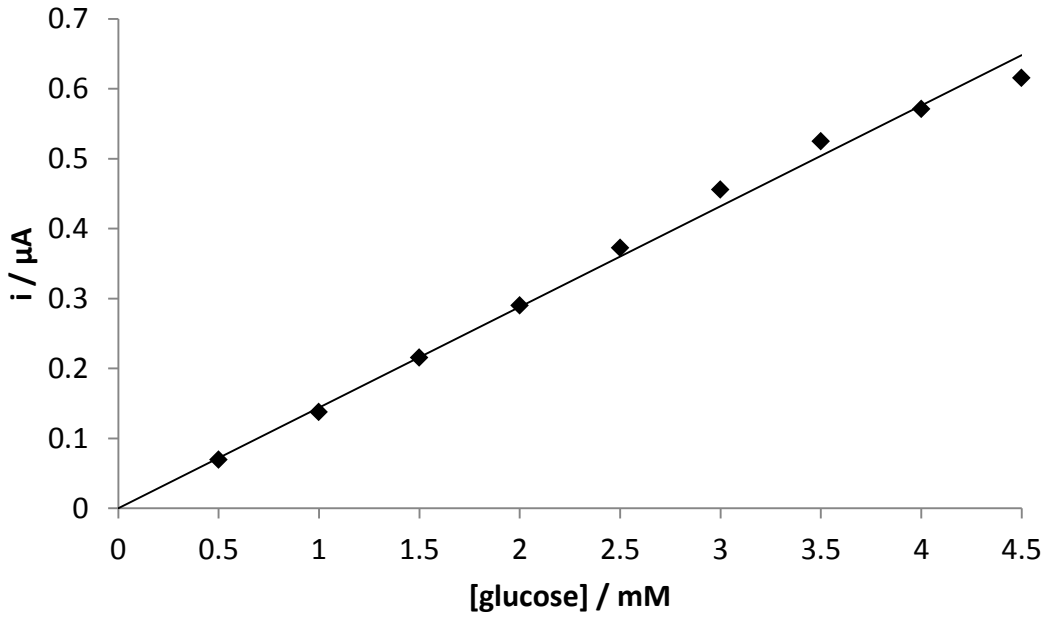

Figure 2.22: Calibration curve for the FcNafion-GOx modified GCE. (Data from Figure 2.21).

The sensitivity of the electrode was 0.14 µA mM^{-1}. Figure 2.21 and Figure 2.22 show that the linear response to glucose peaks at 4.5mM. A useful measure of the effectiveness of the immobilisation process comes from the Michaelis–Menten constant (K_m), where K_m represents the substrate concentration yielding a current response equal to half of its maximum value for infinite substrate concentration.[114] It therefore gives an indication of the immobilised enzyme substrate kinetics. If the rate of the enzymatic reaction is catalysis controlled; K_m may be determined amperometrically using the following Lineweaver-Burk type equation:

$$\frac{1}{i_{ss}} = \left(\frac{K_m}{i_{max}}\right)\left(\frac{1}{C}\right) + \frac{1}{i_{max}} \qquad 2.5$$

Where i_{max} and i_{ss}, are the catalytic currents measured under conditions of substrate saturation and steady state (after the addition of substrate), respectively, for a given

substrate concentration, C. Therefore a plot of l/i_{ss} vs. 1/C will give a straight line with the slope equal to K_m/i_{max} and intercept equal to l/i_{max}.

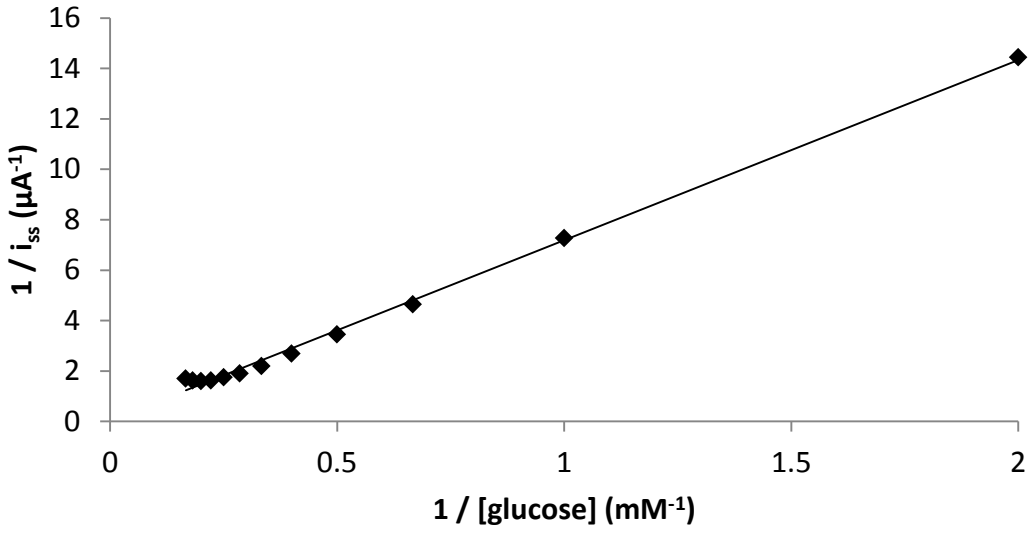

Figure 2.23: Lineweaver Burke plot based on data from Figure 2.22.

The K_m for the immobilised GOx, calculated from Figure 2.23 is 0.30mM. A linear Lineweaver-Burk plot will result if the current is controlled by the catalysis rate.[115] On the other hand, a nonlinear Lineweaver-Burk plot is qualitatively indicative of a either a mass transport limitation,[115] or a kinetic limitation.[116] This could be due to limitations in:

- substrate diffusion through the electrolyte
- substrate diffusion through the polymer layer on the electrode
- the rate of electron transfer of the mediator with the enzyme
- the rate of electron transfer of the mediator with the electrode.

Limitations in the availability of the enzymes active site to either the substrate or the mediator will also have an effect. Determined K_m values are also dependent on the

partition of substrate between the external solution and the polymer layer. If this is the case, determined values of K_m may be larger than their intrinsic value.

Deviations of enzyme characteristics from their intrinsic values when immobilised are not only related to diffusional effects. The secondary and tertiary structure of enzymes is known to play an important role in their activity.[117] Their conformations when they are supported may differ from those in free solution[118] and rearrangement or changes in their structures may result in the enhancement or suppression of enzyme activity.[117]

The above results suggest FcNafion could be a suitable redox mediator for a GOx based enzyme electrode. However, due to concerns about the suitability of the Nafion environment for the enzyme, it is necessary to stabilise the enzyme upon immobilisation. One way of doing this is to co-immobilise the enzyme with bovine serum albumin (BSA). BSA is a well-known inert protein with a 30–35 reactive primary amino groups and can provide thermo-stabilisation to several enzymes.[88] This thermo-stabilisation is likely due to stabilisation of the protein structure by BSA.[119] The mechanism of stabilisation has been linked to hydrophobic interactions.[88]

When immobilised in a redox polymer, BSA has been shown to stabilise the electrochemical response of the polymer.[87] The authors suggested this was due to the prevention of over-swelling of the polymer by BSA.

The experiment outlined in Figure 2.21 was repeated using BSA to stabilise GOx. The GOx solution used in the immobilisation process contained 15 mg ml^{-1} BSA and 25% Glutaraldehyde (GA). GA is used to create cross links between protein molecules.[120] GA is a low molecular weight reagent that produces covalent bonds between itself and amine containing groups such lysine on the outer surfaces of enzymes. It contains an aldehyde

residue at both ends of a 5-carbon chain. Its primary reactivity is toward amine groups, but the reaction may occur by more than one mechanism.[121] Its reaction with amines is rapid in aqueous solution at room temperature, it is also irreversible.[122] It works by converting available protein amines into reactive formyl groups.[121] The subsequent addition of a second protein or another amine-containing molecule causes the activated protein to crosslink with the amines and forms a conjugate.[121] It also may be used in single-step conjugation procedures where the aldehyde-modified protein is not isolated before addition of a second protein. In single- step conjugation both proteins to be crosslinked are together in solution and GA is added to effect crosslinking.

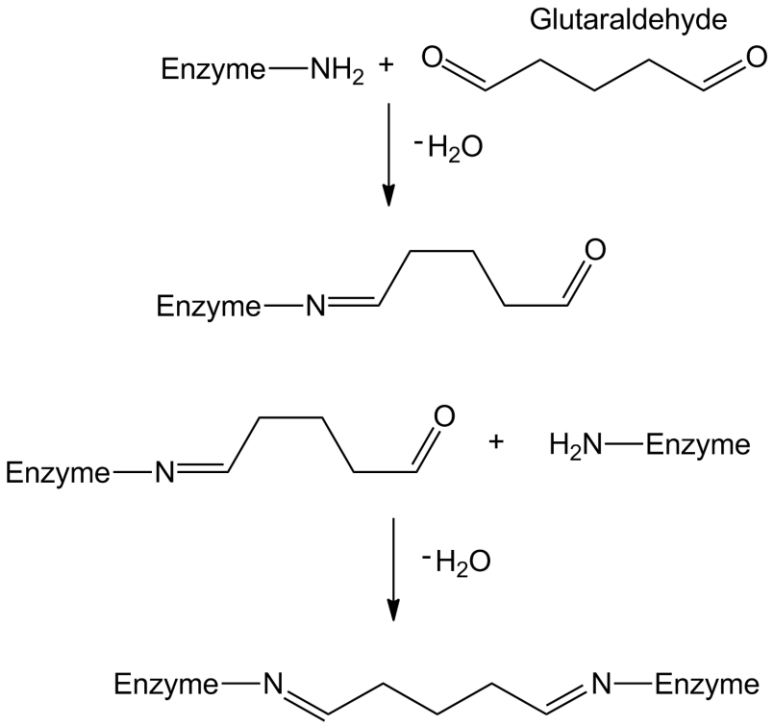

Figure 2.24: The mechanism of protein crosslinking using GA.

The reaction of GA with enzymes can also lead to intramolecular cross links.[123] This is due to the low molecular weight of GA, allowing it to reach gaps in the much larger

enzyme structure. This intramolecular crosslinking can denature the enzyme. Crosslinking with GA has also been shown to produce open lattice type formations of immobilised enzyme.[124] The use of GA to crosslink enzymes makes the subsequent enzyme matrix water insoluble.[125] This can be used to immobilise the enzyme. The cross linking of enzymes can also impart structural rigidity to the enzyme.[126] However it is preferable not to use GA in enzyme electrode design if possible. GA is classified as a toxic substance, and repeated exposure to GA causes irritation of eye, nose, throat, or skin resulting in dermatitis and asthma.[127] Also, using GA can lead to a loss of enzyme activity.[128] Therefore the possibility of fabricating enzyme electrodes without GA is preferable.

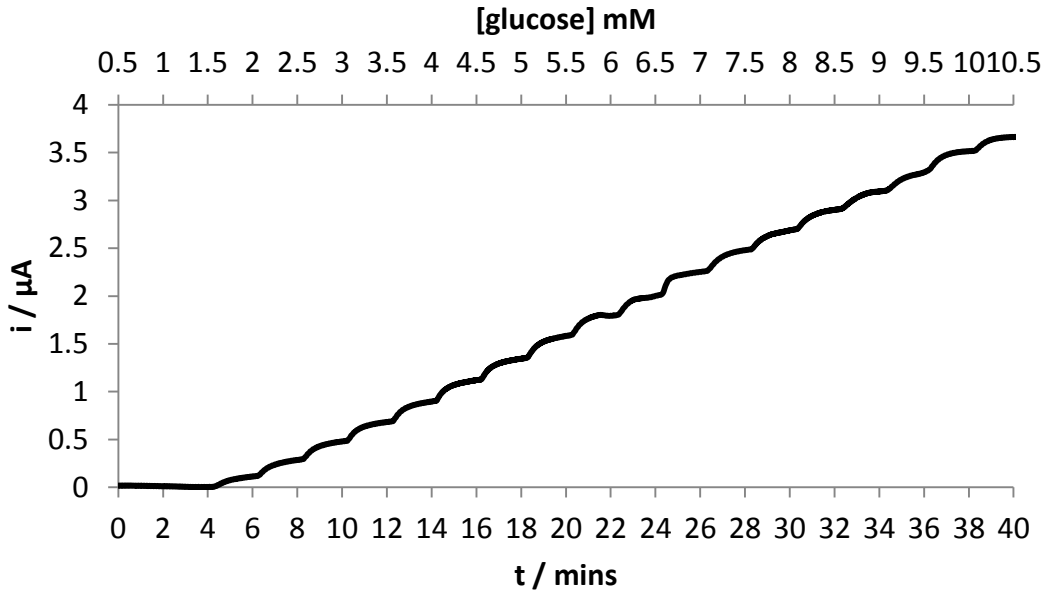

Figure 2.25: Chronoamperometry (CA) experiment for a FcNafion-GOx|BSA modified GCE. The [glucose] was increased by 0.5mM every 2 minutes Eapp = 0.37 V (vs Ag|AgCl). (Background current removed).

Figure 2.25 shows the result of a CA experiment for a FcNafion-GOx|BSA modified electrode carried out under the same conditions as in Figure 2.21. Comparison of Figure

2.25 with Figure 2.21 shows that the linear response region of the electrode has increased from ~ 5mM to ~ 10mM. This is attributed to the stabilising effect of BSA on GOx. However it can be seen in Figure 2.25 that the lower limit of detection has been raised from ~ 0.5mM to ~ 1.5mM (as in Figure 2.21). This is attributed to the presence of BSA. It is suggested that BSA may need to become saturated with glucose before any glucose can be detected by the electrode. This is an undesirable effect. Therefore it is necessary to find a material which can stabilise the electrode without the adverse effect of glucose adsorption. PMBN can be used for this purpose.

Therefore the experiment outlined in Figure 2.25 was repeated without the use of BSA and GA. Instead, after coating with a layer of GOx, 10µl of a 1% wt PMBN solution (in 5% ethanol) was cast onto the electrode. Figure 2.26 shows the results of the experiment. It can be seen that the upper detection limit remains at ~ 10mM but the lower detection limit is now < ~ 0.5mM. This shows that PMBN has the same beneficial stabilising effects on GOx as BSA, but without the problems of glucose adsorption. It can be seen in Figure 2.26 that the resolution between glucose concentrations is lower when compared with Figure 2.25. The presence of the PMBN layer may be increasing the response time of the electrode, decreasing the resolution between glucose concentrations.

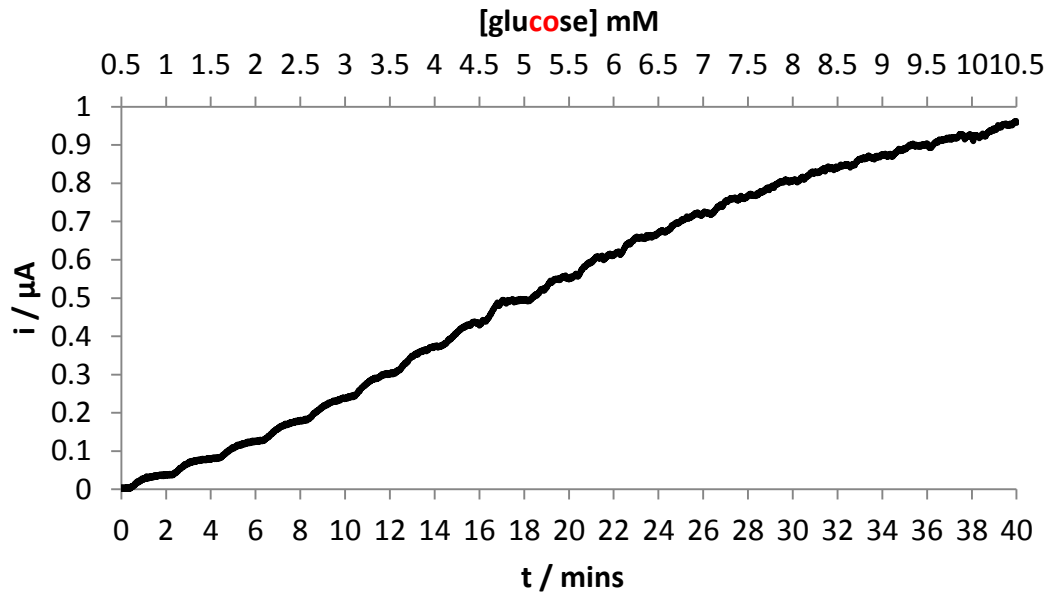

Figure 2.26: Chronoamperometry (CA) experiment for a FcNafion-GOx|PMBN modified GCE. The [glucose] was increased by 0.5mM every 2 minutes Eapp = 0.37 V (vs Ag|AgCl). (Background current removed).

2.3.3 EIS Analysis of FcNafion Mediated GOx Enzyme Electrodes

The electrode fabrication process and the effect of different materials on the properties of the modified electrodes were investigated by EIS with and without the use of a redox probe.

Experiments carried out without a Redox Probe

The experiments carried out without the use of a redox probe provide information on the behaviour of the materials immobilised on the electrode surface.

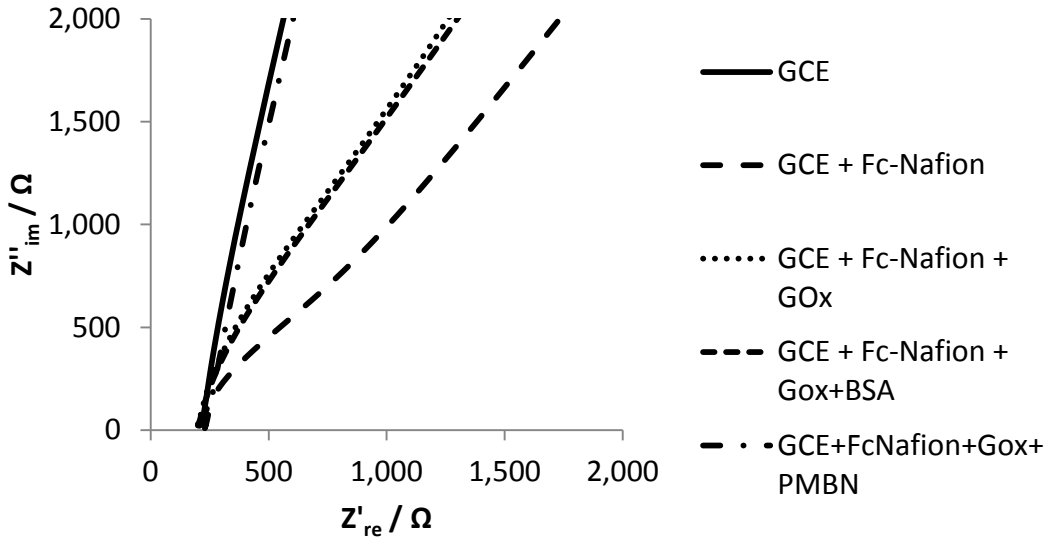

Figure 2.27: EIS spectra of the electrode at different stages of modification (axis decreased to show resistive displacement).

Figure 2.27 shows a subsection of a Nyquist plot for an EIS experiment carried out at the formal potential of the FcNafion redox polymer. It shows a resistive displacement on the real (x) axis resulting from a combination of the electrolyte resistance and the resistance of any immobilised film. It can be seen that there is no significant change in resistance at various stages of the modification process. This indicates that there is a high level of electrolyte adsorption by the immobilised materials. Figure 2.28 shows the data from Figure 2.27 with the axis expanded. The bare electrode exhibits a continuously rising line as the frequency diminishes, indicative of purely capacitive behaviour.

This is because all of the current generated by the applied perturbation goes into charging the double layer formed at the electrode|electrolyte interface. When the FcNafion redox polymer is added to the electrode, the Nyquist plot shows a semicircular ark as the current is now distributed between capacitive charging and the redox processes from FcNafion. When the GOx layer is added to the electrode, the diameter of the semicircle increases, due to a rise in the charge transfer resistance of the redox process. This is to be

expected due to the insulating effect of the GOx protein shell. This increase in R_{CT} indicates the successful immobilisation of the GOx layer.

The experiment was then repeated with the addition of BSA to the GOx solution before immobilisation. It is interesting to note that the R_{CT} drops when BSA is included. This is likely due to an increase in electrolyte adsorption due to the presence of BSA.

The experiment was again repeated with the addition of PMBN to the electrode after the GOx immobilisation step (BSA was not used). Due to the insulating effect of the PMBN layer, the electrode now effectively behaves as a capacitor in the frequency range of the experiment. This is due to the large amount of current needed to charge the PMBN layer.

In order to determine values for R_S, C_{DL} and R_{CT} an equivalent circuit was used to fit the data.

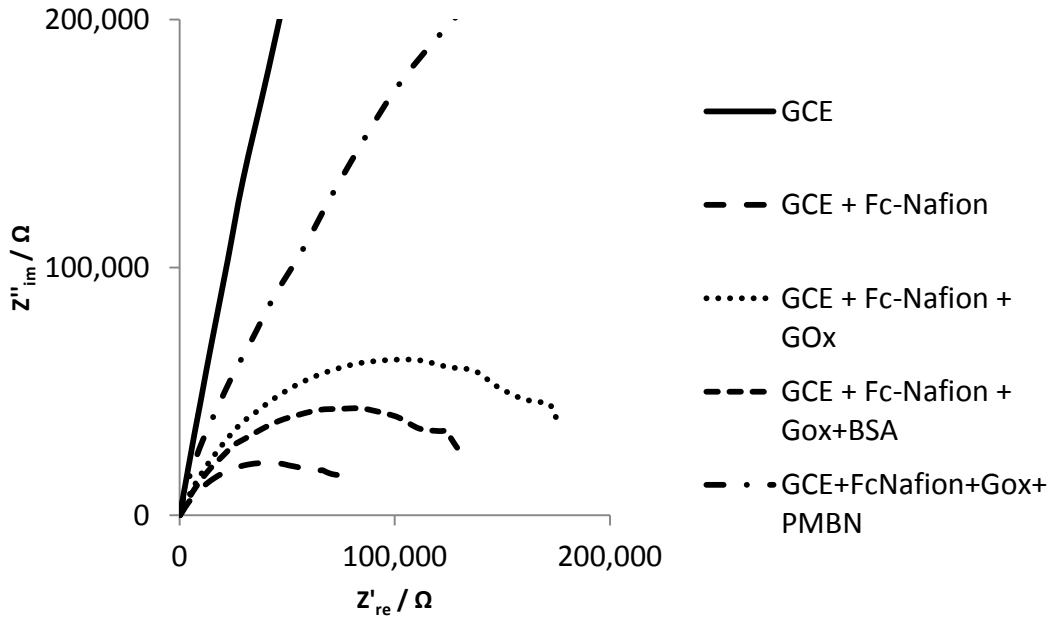

Figure 2.28: EIS spectra of the electrode at different stages of modification.

There is no Warburg diffusion line present in Figure 2.28, indicating that the diffusion of Fc through the film is a slow process (compared to the diffusion of a redox probe through

the film (see below)), as the diffusional process did not produce a Warburg impedance at the frequencies used in the experiment. Therefore the simplest possible equivalent circuit for this system is a resistor followed by a parallel combination of capacitor and resistor representing the solution resistance (R_S) the double layer capacitance (C_{DL}) and the charge transfer resistance (R_{CT}) respectively.

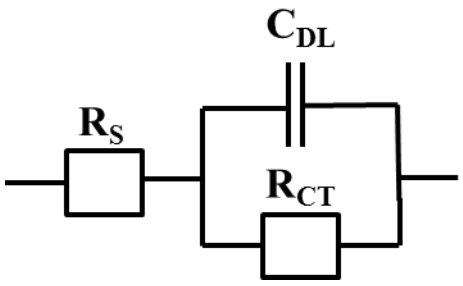

Figure 2.29: Equivalent circuit used to generate data shown in Figure 2.30.

The Nyquist plot shown in Figure 2.30 is derived from Figure 2.28 by fitting the data to the equivalent circuit shown in Figure 2.29. Table 2.1 shows values for R_S, C_{DL} and R_{CT} derived from Figure 2.30. R_S does not change significantly as the electrode is modified as described above. C_{DL} increases significantly when the FcNafion film is immobilised. This is attributed to the increase in surface charge associated with the FcNafion layer. The C_{DL} decreases when protein is immobilised on the surface as the presence of protein inhibits the formation of a well ordered double layer, reducing the ability of the double layer to store charge and hence reducing C_{DL}. The values for R_{CT} exhibit the trend described above for Figure 2.28.

Experiments Carried Out With a Redox Probe

Information about the blocking of an electrode surface by adsorbed or bound species can be obtained by adding a redox probe to the electrolyte before carrying out EIS experiments. Figure 2.31 shows a Nyquist plot for the EIS experiment carried out in the

presence of a redox probe. The experiment was carried out at the formal potential of the probe; therefore, unlike the experiments without a probe, there is no contribution from Fc redox reactions. The response is based on the redox reactions of the probe.

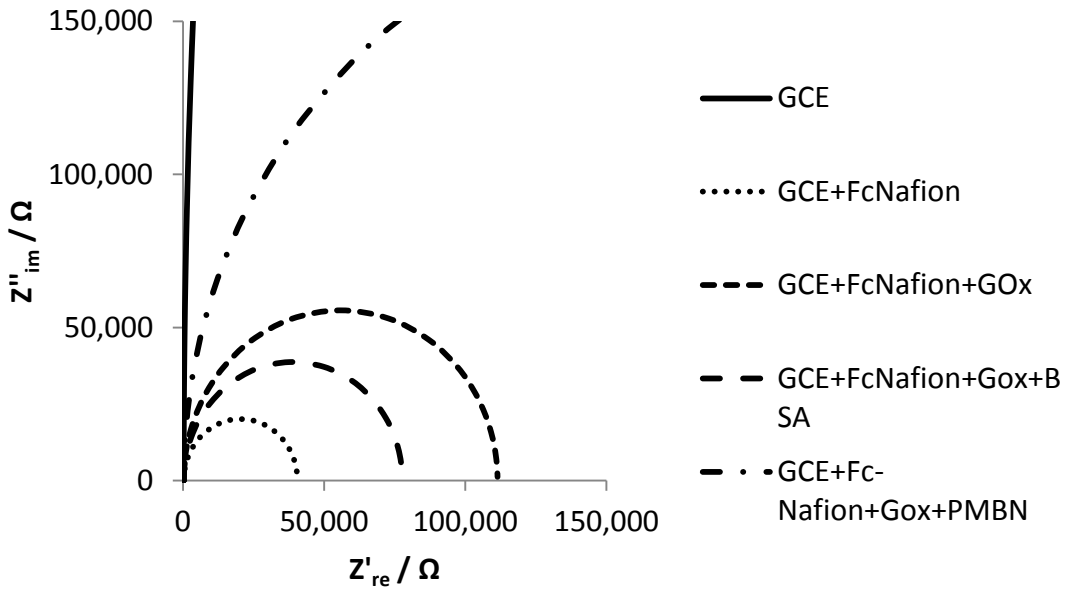

Figure 2.30: Data from Figure 2.28 fitted to equivalent circuit shown in Figure 2.29.

	R_S / Ω	C_{DL} / nF	R_{CT} / Ω	χ^2
GCE	222	969	6,830,000	6.71
GCE+FcNafion	254	2,700	40,300	12.02
GCE+FcNafion+GOx	222	1,580	111,000	10.35
GCE+FcNafion+GOx+BSA	224	1,690	77,500	10.45
GCE+FcNafion+GOx+PMBN	241	4680	373,000	6.05

Table 2.1: Data derived from Figure 2.30.

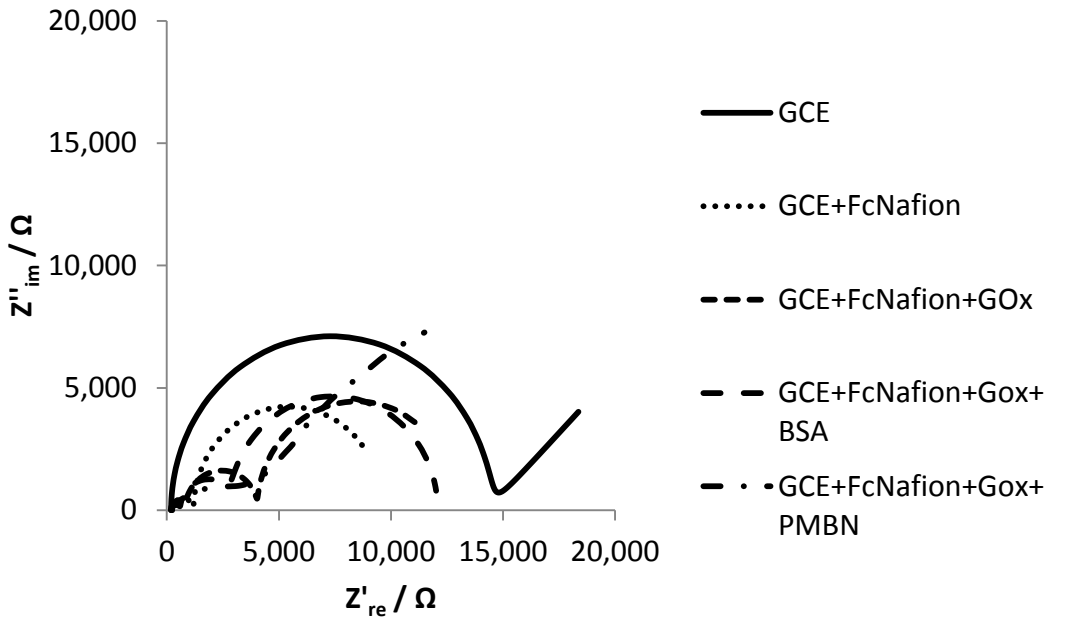

Figure 2.31: EIS spectra of the electrode at different stages of modification with the inclusion of 5mM $K_3[Fe(CN)_6]$ / $K_4[Fe(CN)_6]$ (1:1) in the electrolyte as a redox probe.

The bare electrode shows a semicircular ark along with a Warburg diffusion line under these conditions which is not expected for a bare electrode. This is attributed to the lower activity towards the redox probe of the GCE compared to other electrodes such as Au which were used with this redox probe[53] as described above. The data for the bare electrode in Figure 2.31 can be modelled with a Randles circuit (Figure 1.7) to give the Nyquist plot shown in Figure 2.32. Figure 2.32 can then be used to derive values for the various circuit elements. The values are shown in Table 2.2.

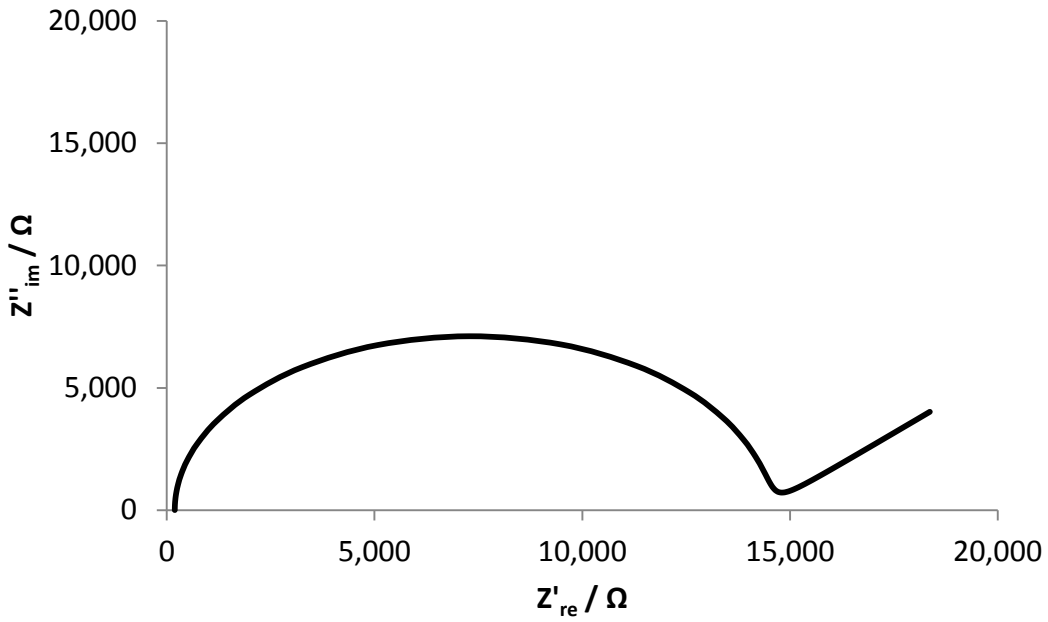

Figure 2.32: Nyquist plot based on data for the bare GCE shown in Figure 2.31 fitted to a Randles circuit.

R_S(+Rf) / Ω	C_{DL} / nF	R_{CT} / Ω	R_W / μS	χ^2
192	256	14,200	702	0.45

Table 2.2: Data derived from Figure 2.32.

In this case, the C_{DL} represents the capacitance of the double layer formed at the interface between the GCE and the electrolyte. The R_{CT} represents the charge transfer resistance caused by the redox reaction of the probe at the electrode surface and the R_W represents the impedance caused by the diffusion of the probe to the surface of the electrode. The χ^2 value is the squared sum of the difference between the data points of the fit and the experimental data points, i.e. a large χ^2 indicates that the observed data differs greatly from the data one would expect to get using a particular circuit. A χ^2 value of 0 indicates that the observed data exactly fits the data one would expect to get using a particular circuit.

The Nyquist plot for the FcNafion modified electrode cannot be modelled accurately with a Randles circuit.

Figure 2.33 shows that the Nyquist plot for the FcNafion modified electrode consists of two overlapping semicircles, one at high frequencies and another which forms as the frequency diminishes. The second semicircle does not intercept the real (x) axis at the frequencies used in the measurement.

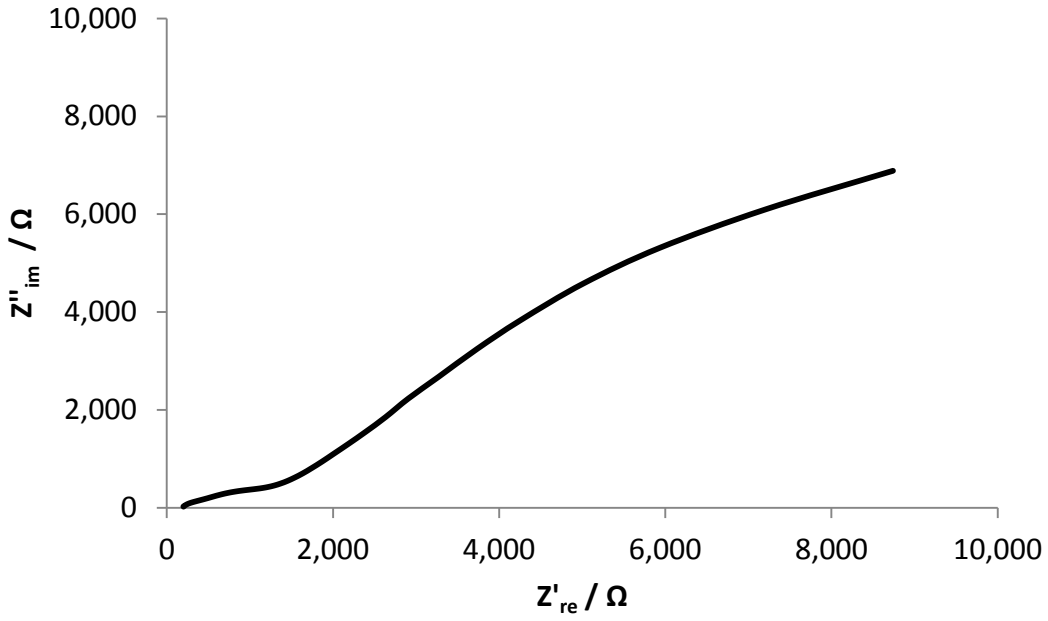

Figure 2.33: Nyquist plot for the FcNafion modified electrode (data from Figure 2.31).

The reason for the appearance of the two semicircles can be explained using the schematic diagram shown in Figure 2.34.

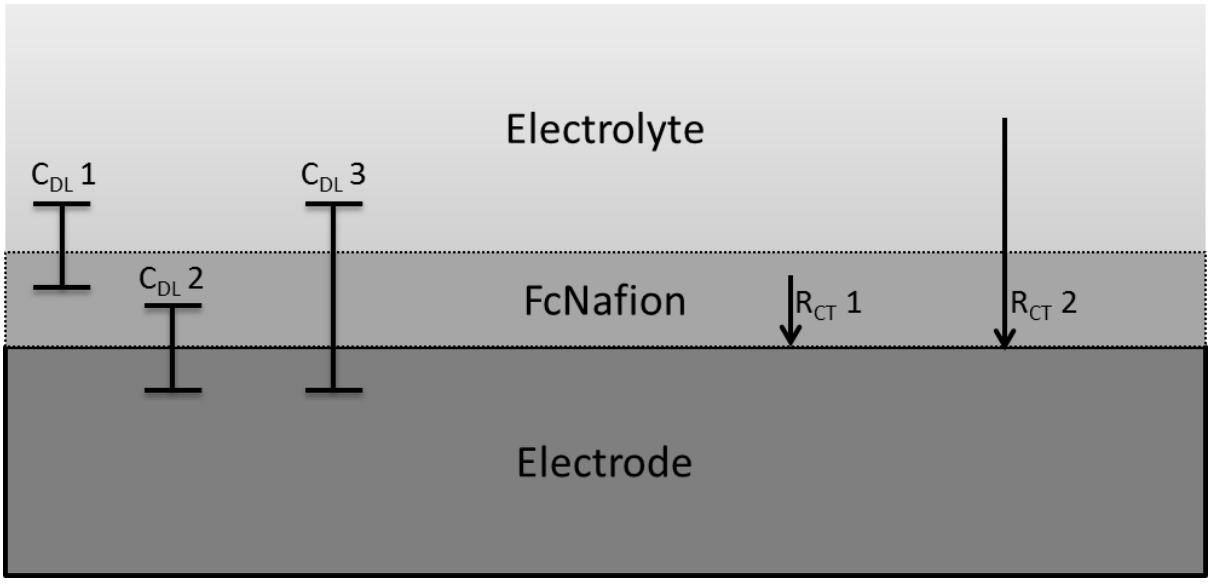

Figure 2.34: Diagram showing the various charge transfer resistances and capacitances that affect the Nyquist plot for the FcNafion modified GCE.

Figure 2.34 is a schematic representation of the origin of the various resistances and capacitances that give rise to the Nyquist plot for the FcNafion modified GCE observed in Figure 2.31. Figure 2.34 can be used to construct an equivalent circuit which can be applied to the data for the FcNafion modified GCE.

Figure 2.35 shows an equivalent circuit for the FcNafion modified GCE. $C_{DL}1$ arises from the interface between the FcNafion layer and the electrolyte. There is no associated charge transfer process at this interface. $C_{DL}2$ and $R_{CT}1$ represent the double layer capacitance and charge transfer resistance associated with the interface between the FcNafion layer and the electrode.

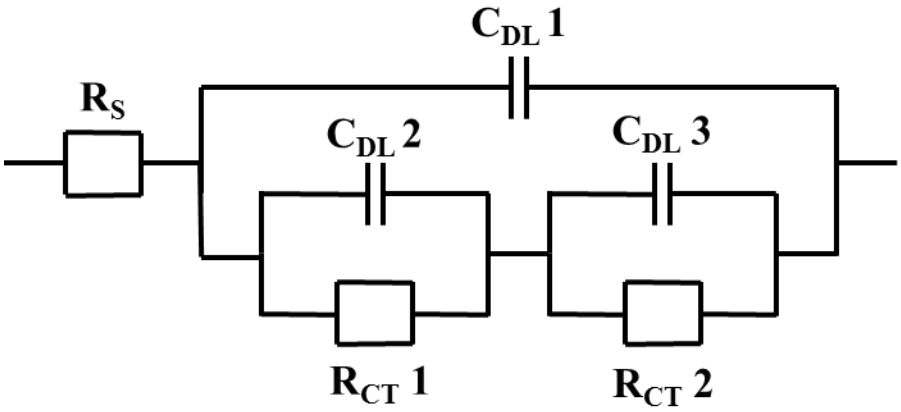

Figure 2.35: Equivalent circuit diagram for the FcNafion modified GCE.

$C_{DL}3$ and $R_{CT}2$ represent the double layer capacitance and charge transfer resistance associated with the combined capacitance and charge transfer resistance of the electrolyte|FcNafion interface and the FcNafion|electrode interface. The data for the FcNafion modified GCE can be fitted to the equivalent circuit shown in Figure 2.35 to give the Nyquist plot shown in Figure 2.36.

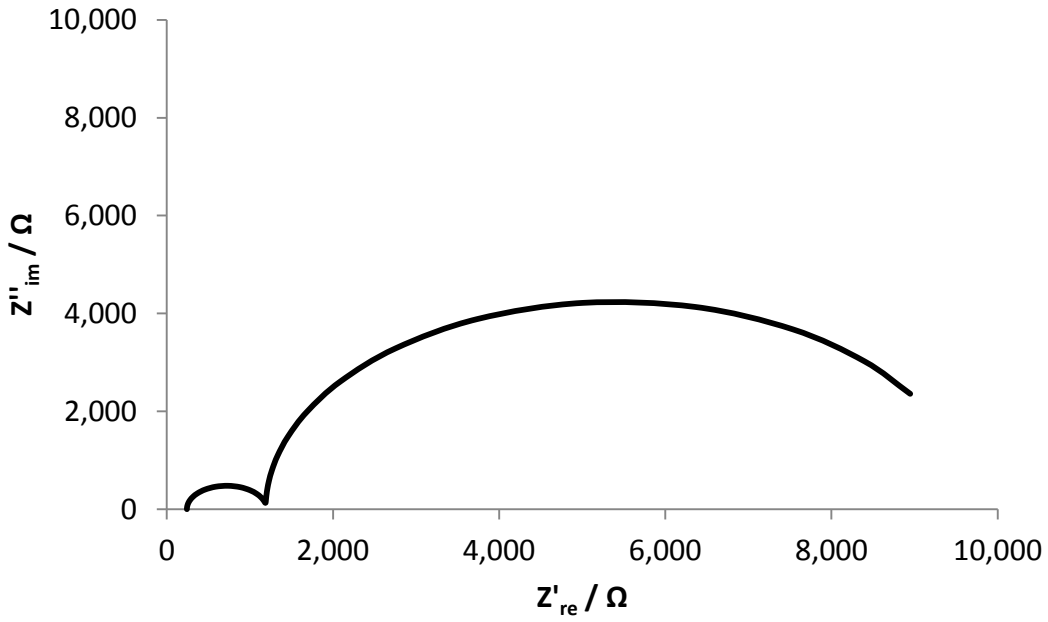

Figure 2.36: Nyquist plot based on data for the FcNafion modified electrode shown in Figure 2.31 fitted to the equivalent circuit shown in Figure 2.35.

Figure 2.36 can then be used to derive values for the various circuit elements. The values are shown in Table 2.3.

R_S(+Rf) / Ω	$C_{DL}1$ / nF	$C_{DL}2$ / nF	$C_{DL}3$ / nF	$R_{CT}1$ / Ω	$R_{CT}2$ / Ω	χ^2
242	2,160	495	569,000	956	8,470	4.03

Table 2.3: Data derived from Figure 2.36.

The Nyquist plots for GCE+FcNafion+GOx and GCE+FcNafion+GOx+BSA also cannot be modelled with a Randles circuit. These plots show three overlapping semicircles. This can be explained using the schematic diagram shown in Figure 2.37.

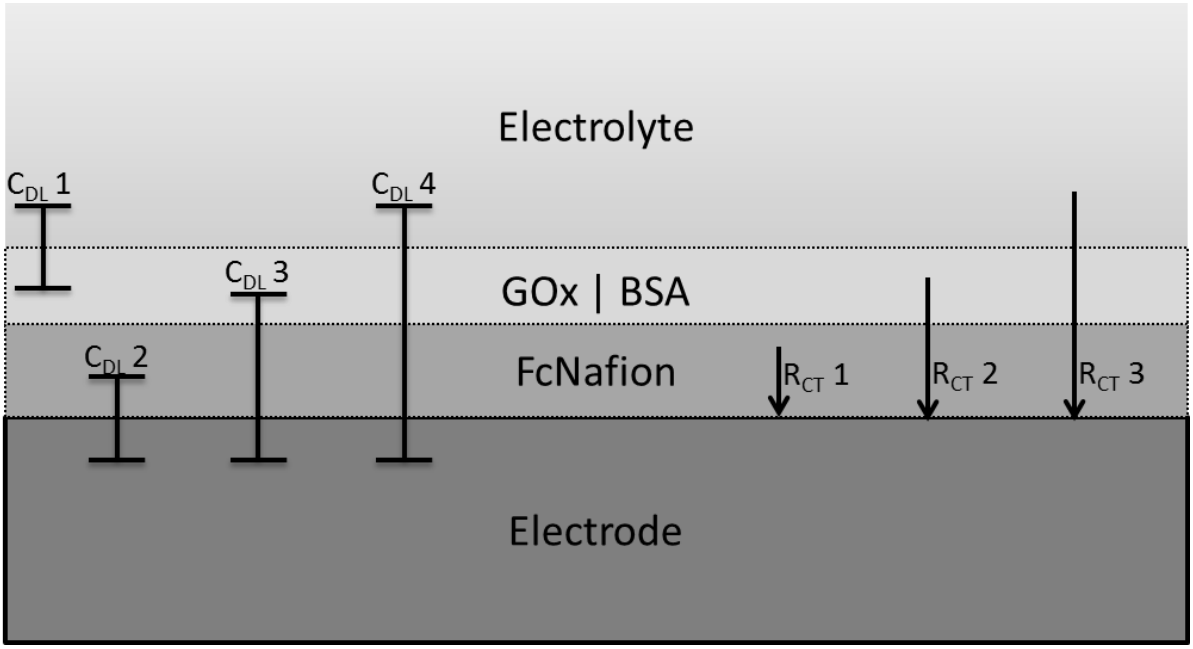

Figure 2.37: Diagram showing the various charge transfer resistances and capacitances that affect the Nyquist plots for GCE+FcNafion+GOx and GCE+FcNafion+GOx+BSA.

Figure 2.37 can be used to construct an equivalent circuit diagram which can be applied to the data for GCE+FcNafion+GOx and GCE+FcNafion+GOx+BSA.

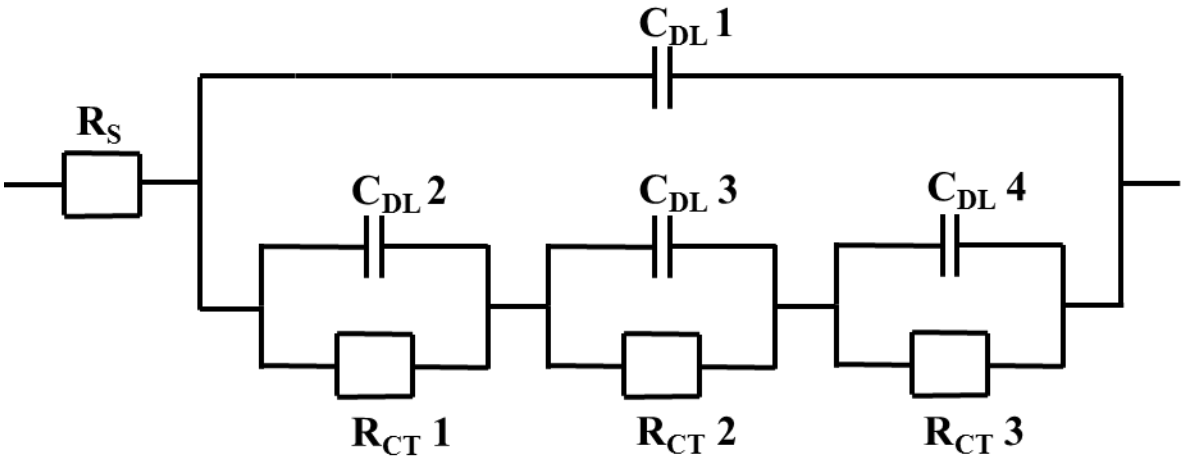

Figure 2.38: Equivalent circuit diagram for GCE+FcNafion+GOx and GCE+FcNafion+GOx+BSA.

Figure 2.38 shows an equivalent circuit for GCE+FcNafion+GOx and GCE+FcNafion+GOx+BSA. The values for the various circuit elements can be determined by comparing the data after each modification of the electrode. The values of each of the circuit elements fit the pattern expected based on the type of modification of the electrode. In Figure 2.38, $C_{DL}1$, $C_{DL}2$, and $R_{CT}1$ have the same origin as in Figure 2.34. $C_{DL}3$ and $R_{CT}2$ represent the double layer capacitance and charge transfer resistance associated with the combined capacitance and charge transfer resistance of the GOx/BSA|FcNafion interface and the FcNafion|electrode interface. $C_{DL}4$ and $R_{CT}3$ represent the capacitance and charge transfer resistance of all the interfaces between the electrode and the electrolyte combined. The data for GCE+FcNafion+GOx and GCE+FcNafion+GOx+BSA can be fitted to the equivalent circuit shown in Figure 2.38 to give the Nyquist plot shown in Figure 2.39

The same circuit can also be used to fit the data from the PMBN modified electrode. This shows that there is significant mixing of the GOx and PMBN after immobilisation.

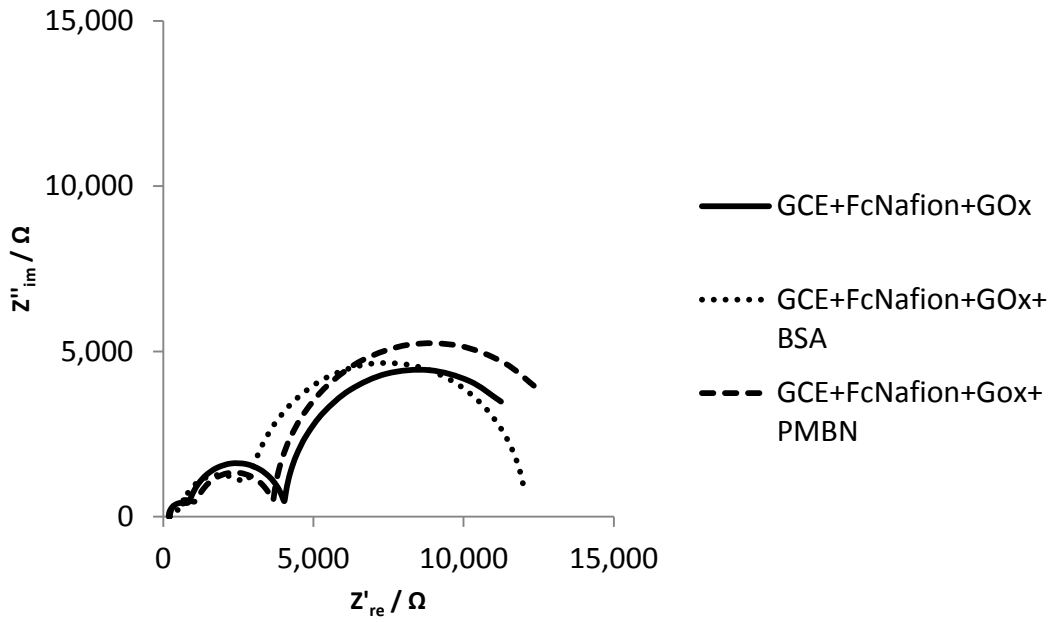

Figure 2.39: Nyquist plot based on data for GCE+FcNafion+GOx and GCE+FcNafion+GOx+BSA shown in Figure 2.31 fitted to the equivalent circuit shown in Figure 2.38.

Figure 2.39 can then be used to derive values for the various circuit elements. The values are shown in Table 2.4.

	R_S(+Rf) / Ω	C_{DL}1 / nF	C_{DL}2 / nF	C_{DL}3 / nF	C_{DL}4 / nF	R_{CT}1 / Ω	R_{CT}2 / Ω	R_{CT}3 / Ω	χ^2
GCE+FcNafion+GOx	179	432	16	4,480	864,000	822	3,040	8,880	0.89
GCE+FcNafion+GOx +BSA	213	337	35	8,740	148,000	418	2,220	9,240	1.08
GCE+FcNafion+GOx +PMBN	220	390	46	6,100	665,000	984	2,400	10, 500	1.12

Table 2.4: Data derived from Figure 2.39.

The value for $R_{CT}3$ for the electrode modified with PMBN is the highest because of the resistance of the phospholipid. The $C_{DL}4$ value is lower than GOx because the film has absorbed more electrolyte.

2.3.4 An FcNafionGOx Enzyme Electrode

As stated in section 2.1.2, enzymes can be suspended in water|ethanol|Nafion mixtures. One potential benefit of this method is resistance to common biological interferants such as ascorbic acid (AA) and urea.

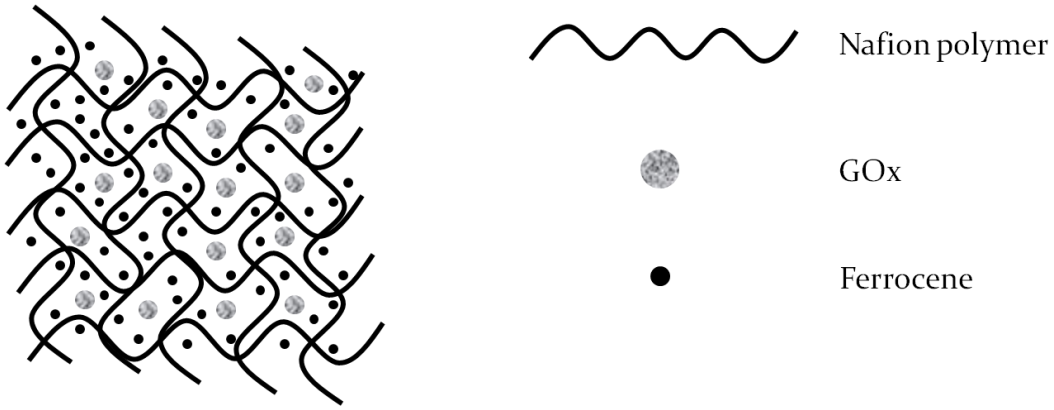

Figure 2.40: Enzymes such as GOx can be suspended directly in FcNafion mixtures whilst retaining their activity.

Therefore, an electrode was prepared by suspending GOx into an FcNafion solution (0.25% Nafion solution in 90% ethanol containing 5mM Fc) and protecting it with a layer of PMBN (See section 2.2.7). Firstly, the response of this electrode to changing glucose concentration was tested with CV and LSV.

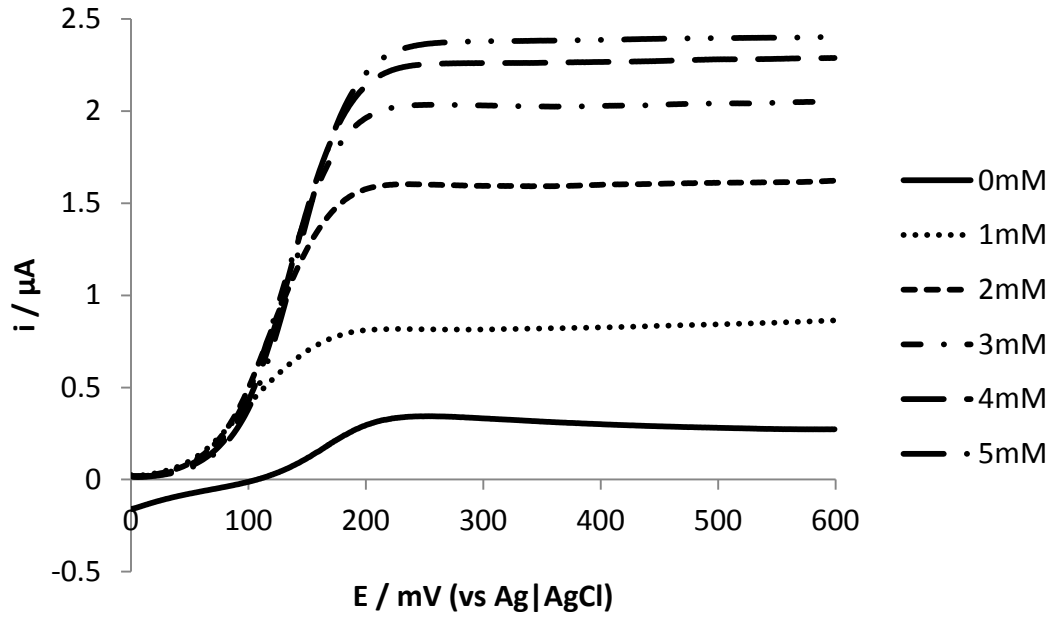

Figure 2.41: LSVs carried out on an FcNafionGOx|PMBN modified GCE with increasing concentrations of glucose; v = 1mV s^{-1}.

Figure 2.41 and Figure 2.42 show that the FcNafionGOx|PMBN modified GCE can detect changes in glucose concentration under scanning potential conditions up to 5mM.

Interference Study

A CA experiment was carried out on a GCE modified with FcNafion and FcNafion|PMBN (i.e. without the use of GOx). 0.13mM AA was added to the cell after 40 minutes in order to see how effective a layer of PMBN could be at reducing the interference of AA. The results are shown in Figure 2.43. The PMBN layer reduced the interference of AA by 76.5% (based on the decrease in j_{max} after the addition of AA). However there is also a significant mass transport limitation for the electrode modified with PMBN. This electrode took 6 minutes and 48s longer to reach j_{max}.

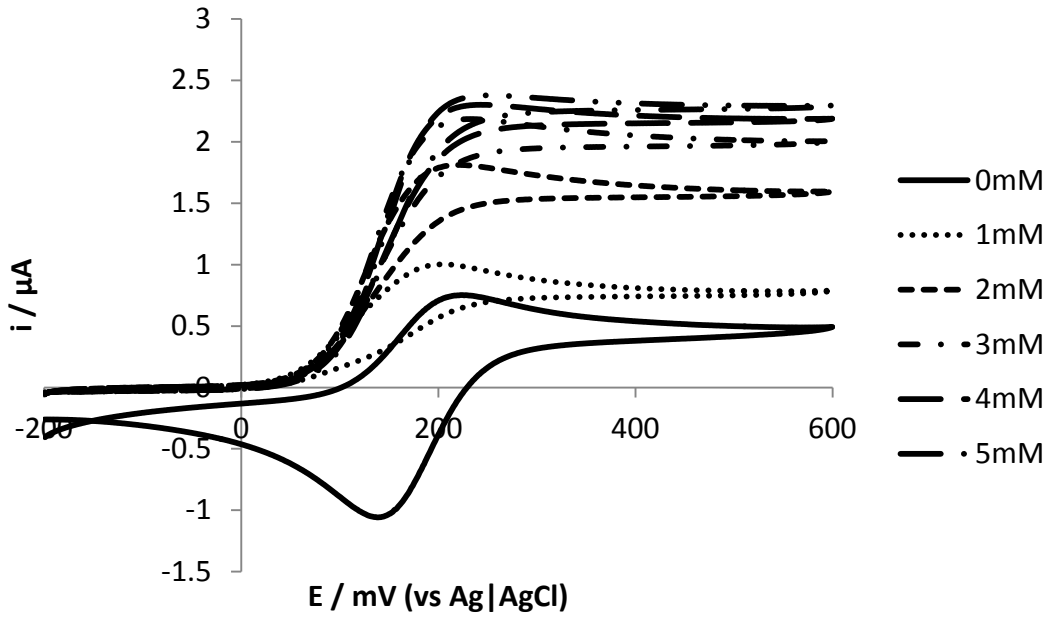

Figure 2.42: CV scans carried out on an FcNafionGOx|PMBN modified GCE with increasing concentrations of glucose; v = 5mV s^{-1}.

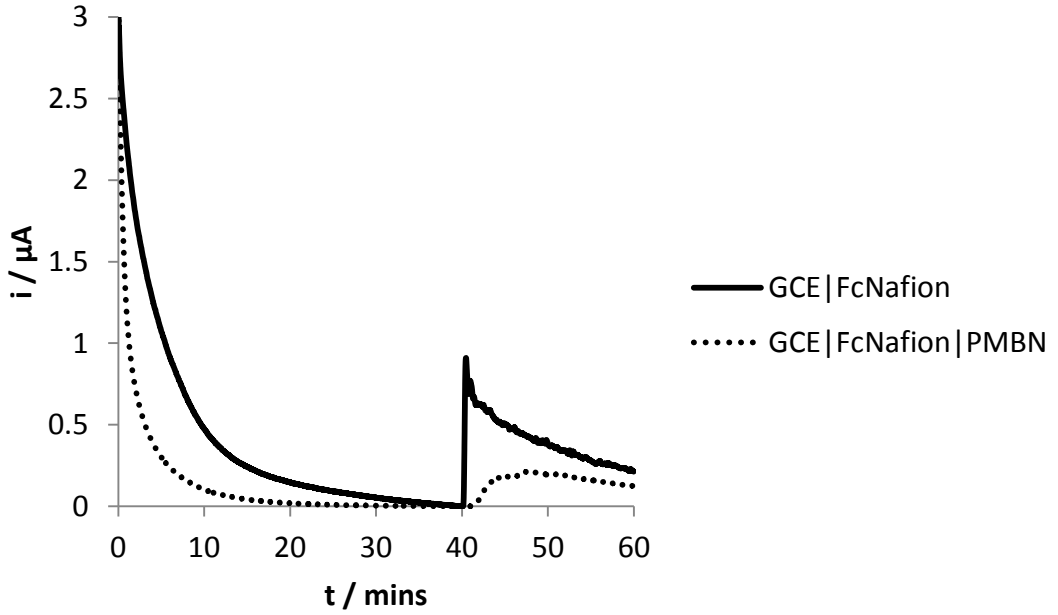

Figure 2.43: Chronoamperometry (CA) experiment for a FcNafion and FcNafion|PMBN modified GCE. The [AA] was changed to 0.13 mM after 40 minutes. Eapp = 0.37 V (vs Ag|AgCl). (Background current removed).

A CA experiment was then carried out on the GCE modified with FcNafionGOx with and without a coating of PMBN. The electrode was held at 0.37V.

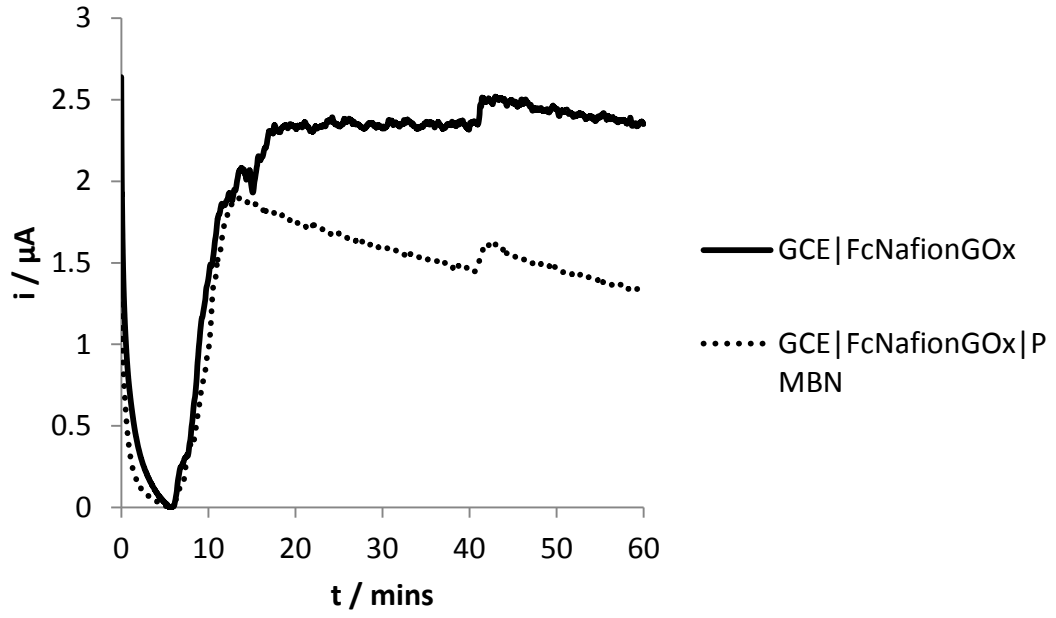

Figure 2.44: Chronoamperometry (CA) experiment for a FcNafionGOx and FcNafionGOx|PMBN modified GCE. The [glucose] was changed to 3mM after 5 minutes and the [AA] was changed to 0.13 mM after 40 minutes. Eapp = 0.37 V (vs Ag|AgCl). (Background current removed).

Figure 2.44 shows a CA trace for two FcNafionGOx modified GCEs, one with an additional protective layer of PMBN. The PMBN modified electrode shows a more stable response than the unprotected electrode. The i_{ss} remains constant during the experimental measurement whereas the i_{ss} of the unprotected electrode begins to drop immediately after reaching its peak value. This is attributed to the stabilising effect of PMBN on GOx. The cell [AA] was then changed to 0.13 mM (a biologically relevant concentration[16]), as with Figure 2.44, increased oxidation current was observed for both electrodes, but the electrode with the protective layer of PMBN showed a 4.91% increase in oxidation current upon the addition of AA, compared to a 8.88% increase for the unprotected

electrode, i.e. a 55.29% decrease in interference. Therefore the presence of the PMBN layer helped to reduce interference from AA. The reduction in interference is lower when GOx in incorporated into the immobilised film. This is attributed to the increase in solvent uptake by the film when GOx is used, due to the hydrophilic nature of GOx. Also the presence of GOx will reduce the uniformity of the film, leading to a higher susceptibility to interfering substances.

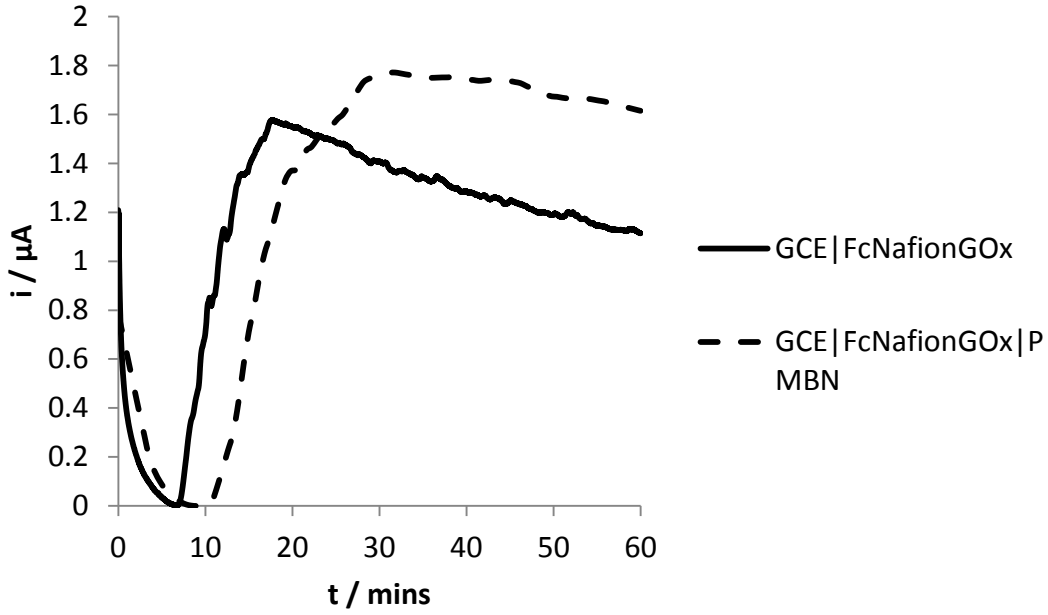

Figure 2.45: Chronoamperometry (CA) experiment for a FcNafionGOx and FcNafionGOx|PMBN modified GCE. The [glucose] was changed to 3mM after 5 minutes and the [urea] was changed to 0.2 mM after 40 minutes. Eapp = 0.37 V (vs Ag|AgCl). (Background current removed).

Figure 2.45 shows the result of a repeated experiment using urea as an interferants instead of AA. The concentration of urea in the cell was made up to 0.2mM (a biologically relevant concentration[16]) after 40 minutes. The PMBN modified electrode shows a longer initial response time (~ 5 minutes compared to ~ 1 minute for the unprotected electrode). This is attributed to the reduction in mass transport rate associated with the

PMBN layer. No increase in oxidation current upon the addition of urea was seen for either electrode, indicating that biologically relevant concentrations of urea have no effect on the response of the electrode. This is attributed to the presence of Nafion on the electrode surface, which has been shown to reduce interference from anionic compounds (see section 2.1.2).

2.3.5 A PMBN-HMDA-FcCOOH-PMBN-GOx (PHFPG) Electrode

In this section, the feasibility of introducing redox capability to PMBN via the covalent attachment of FcCOOH to the polymer will be investigated. The modified PMBN polymer is then tested as a potential polymer mediator for GOx.

General Properties of the PMBN-HMDA-FcCOOH (PHF) Film

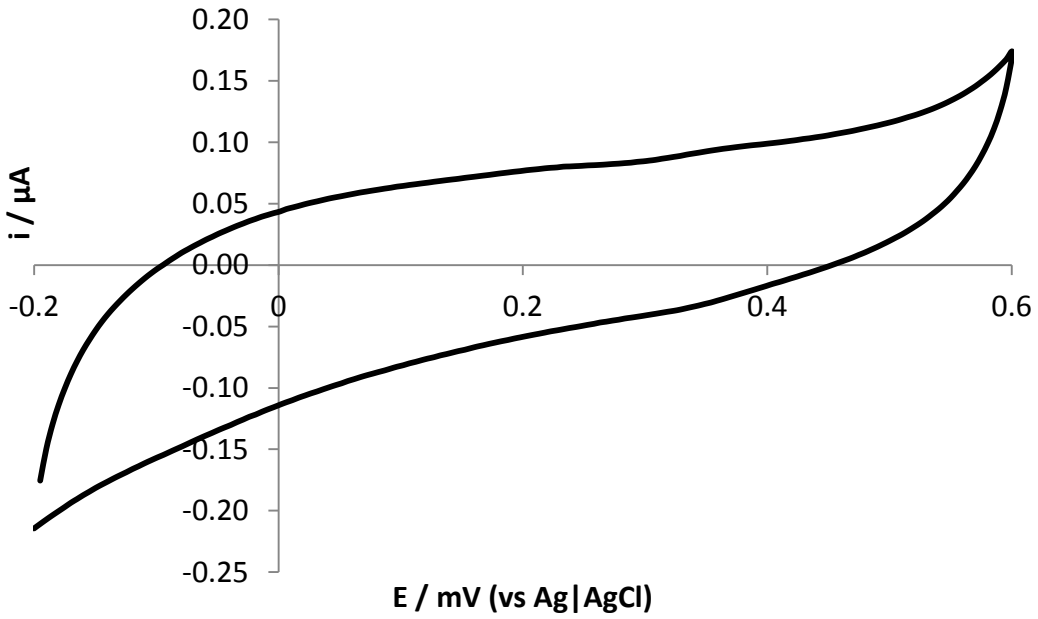

Figure 2.46: CV scan (v = 50mV s^{-1}) for the PMBN-HMDA-FcCOOH (PHF) modified GCE.

Figure 2.46 shows a CV scan for a PMBN-HMDA-FcCOOH (PHF) film prepared on a GCE using the procedure outlined in section 2.2.8. In this case 1µl of a 1 wt% PMBN

solution, 1µl of 1% wt HMDA (a.q.) and 1µl of the FcCOOH/EDC solution was used. It can be seen from Figure 2.46 that no redox response from the FcCOOH group is present. This may be due to rapid evaporation of the solvents involved in the film deposition process. This would not allow sufficient interaction time for the species involved in covalent bonding and therefore the FcCOOH groups will not attach successfully to the MEONP group of the PMBN. Therefore the same experiment was repeated except 5µl of the PMBN solution was added to an Eppendorf tube and 2µl of HMDA solution was then mixed with the PMBN. 2µl of this was added to the GCE. The electrode modified with a layer of PMBN-HMDA was then immersed in the FcCOOH/EDC solution overnight at 4°C.

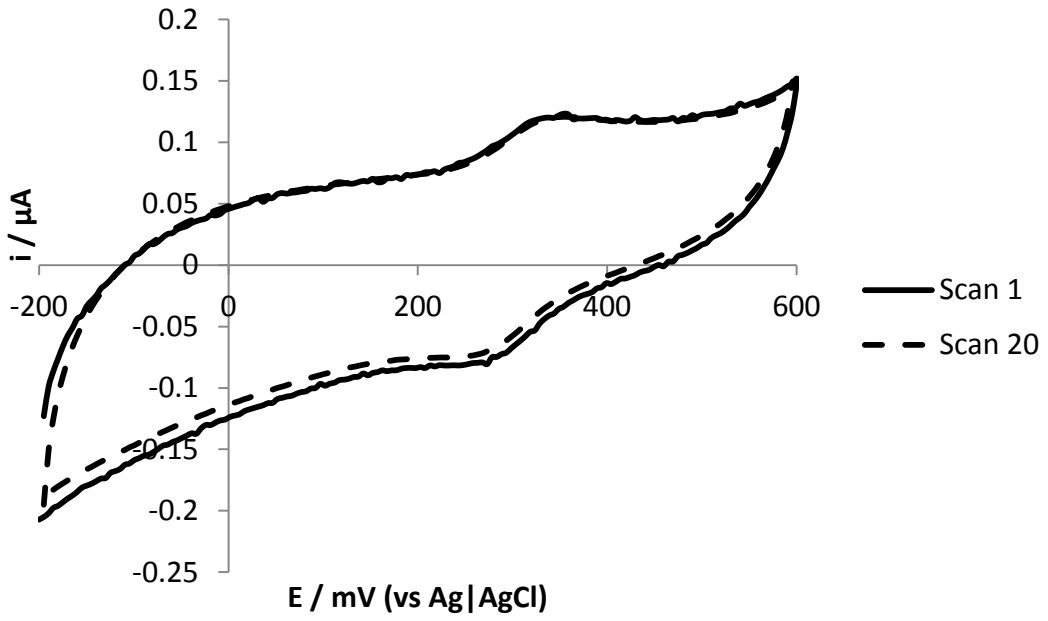

Figure 2.47: CV scans (v = 50mV s^{-1}) for the PHF modified GCE with overnight incubation.

Initial voltammograms obtained for the PHF electrode clearly show the presence of a redox peak associated with the redox of FcCOOH (E° = 337mV vs Ag|AgCl).[129] This

shows that increasing the amount of solution cast on the GCE surface and immersing the modified electrode in the FcCOOH/EDC solution overnight increased the FcCOOH binding to the HMDA.

Figure 2.47 shows typical CV curves of PHF in PBS (pH 6.8) at RTP. It shows oxidation and reduction current peaks at a scan rate (v) of 50 mV s^{-1}. The oxidation and reduction waves of the FcCOOH unit appear at ~ 334 mV and 283 mV (vs. Ag|AgCl), respectively. Initially, the ferric ions in the FcCOOH units exist in both the reduced form ($Fe^{(II)}$) and oxidized form ($Fe^{(III)}$). During the anodic scan, $Fe^{(II)}$ is oxidized to $Fe^{(III)}$, and subsequently an oxidation current peak is observed. During the cathodic scan, $Fe^{(III)}$ is reduced. The ΔE_p (at a scan rate of 50 mV s^{-1}) for PHF is ~ 50mV.

It is proposed that the FcCOOH groups would be facing the electrolyte due to their hydrophilicity compared to that of the PMBN (see Figure 2.48). Electron transfer to and from the electrode and the FcCOOH groups will be possible due to the mobility introduced by the HMDA linker and the fact that as the potential on the electrode is changed, the FcCOOH groups will be attracted to it via electrostatic forces.

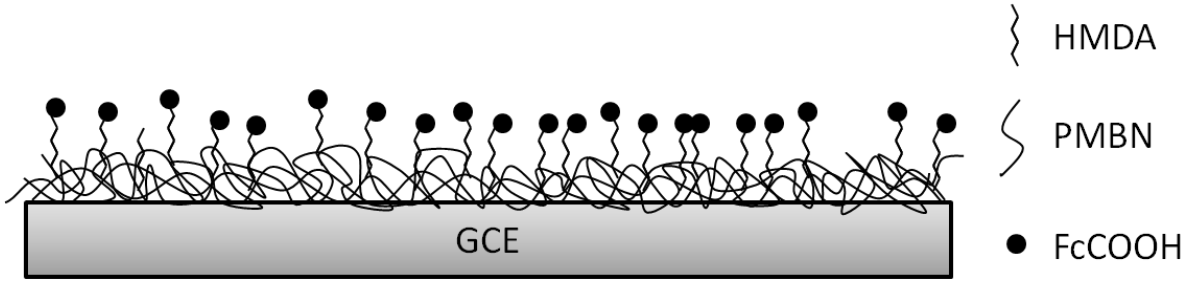

Figure 2.48: Schematic diagram of a layer of PHF on a GCE surface.

Figure 2.47 also shows that continued potential cycling has little effect on the shape and magnitude of the redox peaks, indicating that the film was electrochemically stable.

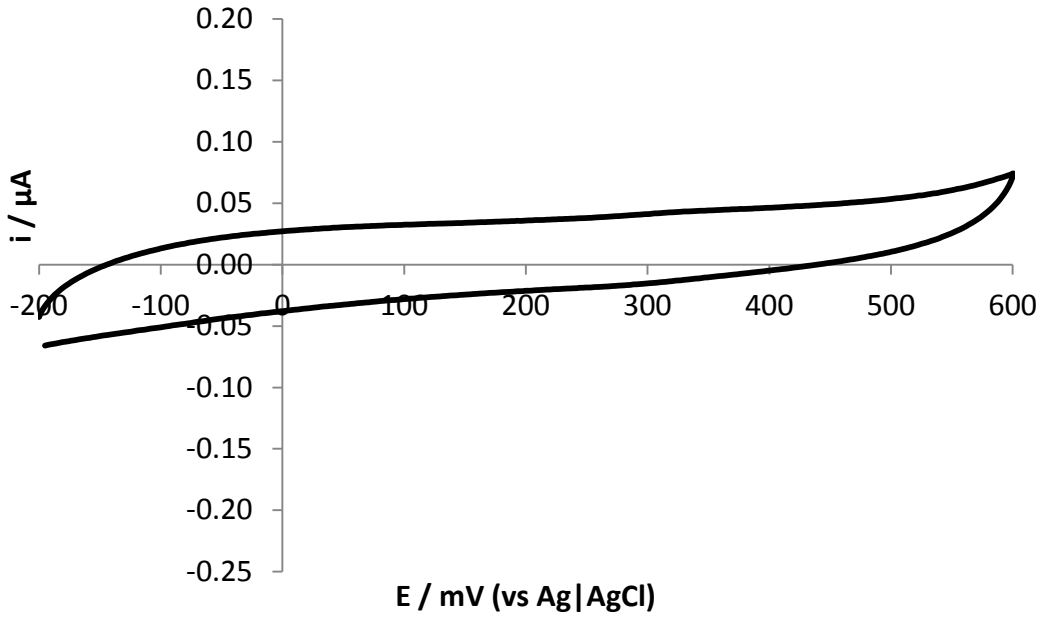

Figure 2.49: CV scan (v = 10mV s^{-1}) for the PHF modified GCE after 24hrs in 0.1M PBS (pH 6.8) at 4°C.

Figure 2.49 shows a CV scan for the GCE modified with 2µl of PHF after it had been immersed in PBS for 24hrs at 4°C. It is clear that the redox waves associated with the FcCOOH group are no longer present. This may be because a 2µl casting volume may not provide sufficient quantities of PMBN needed to bind efficiently with the GCE surface via hydrophobic interactions and electrostatic attractions. The fact that the capacitance of the electrode solution interface is smaller in Figure 2.49 than in Figure 2.47 indicates that the film has been depleted from the surface of the electrode.

Also, it has been noted[130] that much larger (up to 80mM) concentrations of EDC should be can be used for the immobilisation process and that these concentrations of EDC allow efficient linking of amides to carboxylic acids over time periods in minutes rather than hours. Therefore using higher concentrations of EDC could improve the linking of FcCOOH to HMDA and ensure the film stays redox active for longer periods.

Figure 2.50 shows CV scans for a GCE modified with 10µl of PMBN-HMDA solution and immersed in 5mM FcCOOH and 80mM EDC for 20 minutes.

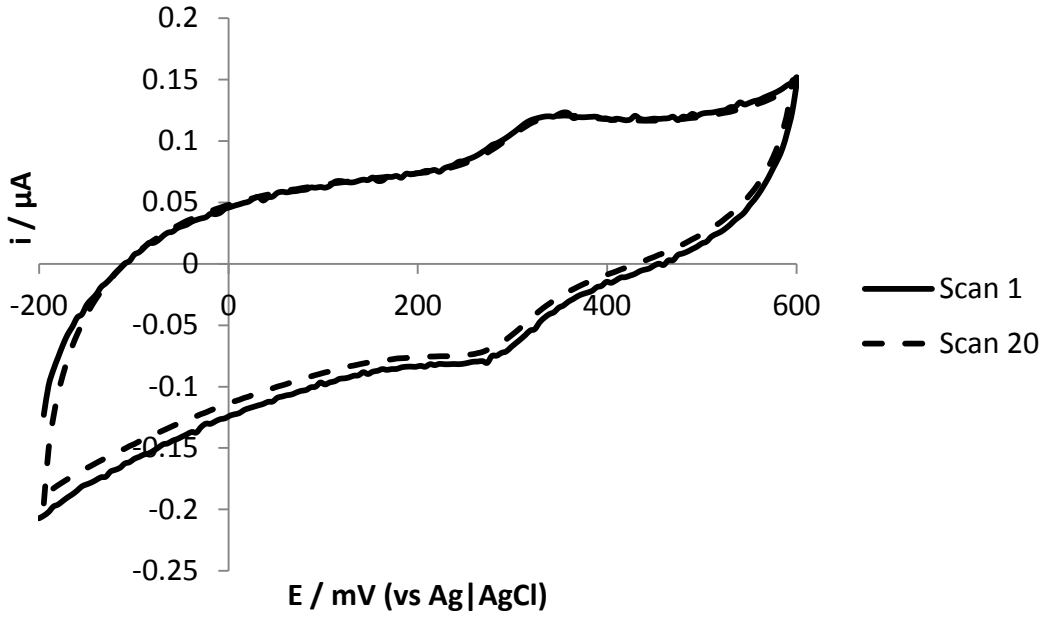

Figure 2.50: CV scans (v = 50 mV s^{-1}) for a GCE modified with 10µl of PMBN-HMDA solution and immersed in 5mM FcCOOH and 80mM EDC for 20 minutes.

Again it is noted that continued potential cycling has little effect on the shape and magnitude of the oxidation and reduction peaks of PHF, highlighting the films electrochemical stability. The slightly smaller (~ 0.01µA) reduction current of scan 20 in Figure 2.50 may be due to depletion of O_2 in the film. This is likely the case as the difference in reduction current between scan 1 and scan 20 is most prominent at more negative (<0mV) potentials as oxygen reduction current increases as the potential becomes more negative.

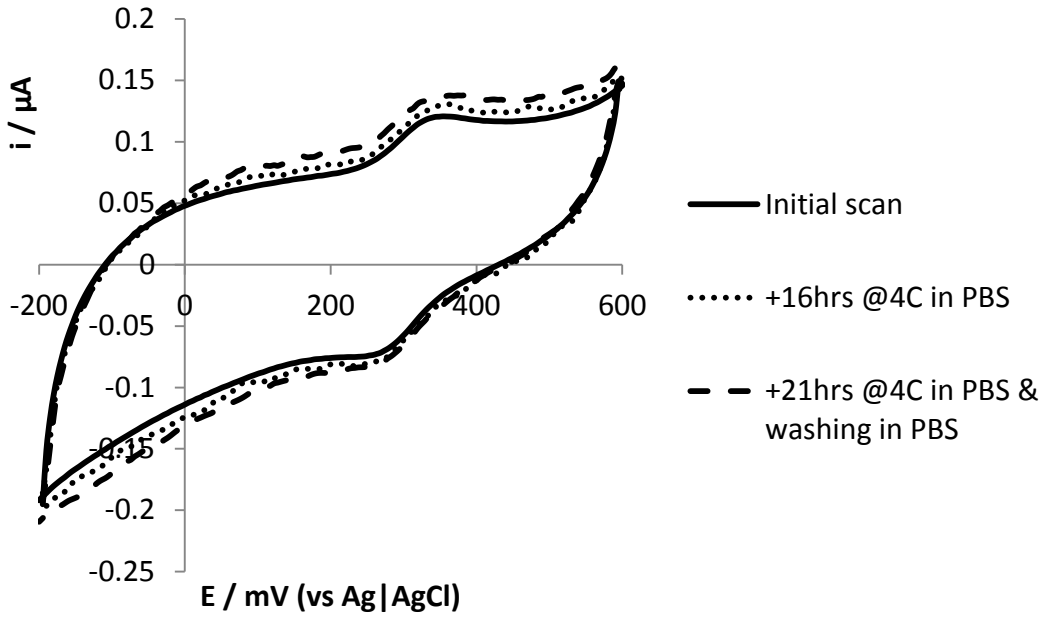

Figure 2.51: CVs of the PHF electrode (v = 50 mV s^{-1}) initially after 16hrs and after 22hrs immersed in PBS.

Figure 2.51: shows that the voltammetric waves remained unchanged after the electrode was immersed in PBS for several hours. There is a slight increase in current over the potential range of the scan after the electrode had been immersed in PBS for several hours. This may be due to the hydrogel properties of PMBN. The PMBN will adsorb electrolyte and therefore increase the capacitance of the film over time.

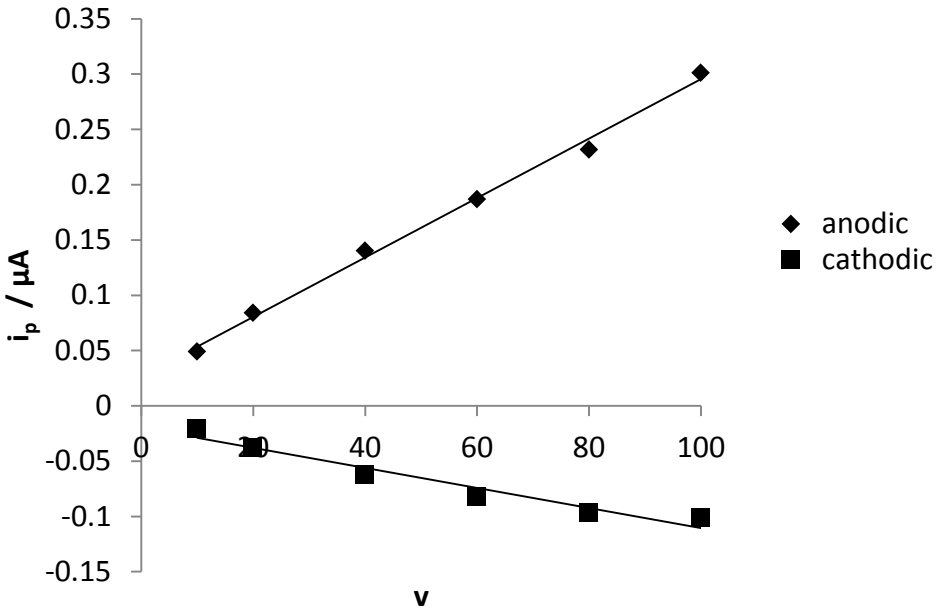

Figure 2.52: Peak current density vs. v for the PHF electrode.

Figure 2.52 shows a plot of peak current density vs v for the PHF electrode prepared using 10µl of PMBN-HMDA solution and immersed in 5mM FcCOOH and 80mM EDC for 20 minutes. There is a linear relationship which shows that the current is generated by a surface confined redox process.[131] Figure 2.53 shows the peak current densities for the same electrode plotted against √v. A plot of peak current density vs √v should be linear for a reversible system.[132] It can be seen from Figure 2.53 that there is a linear relationship up to high scan rates (100mV s^{-1}) indicating that there is efficient electron transfer between the FcCOOH groups and the electrode.

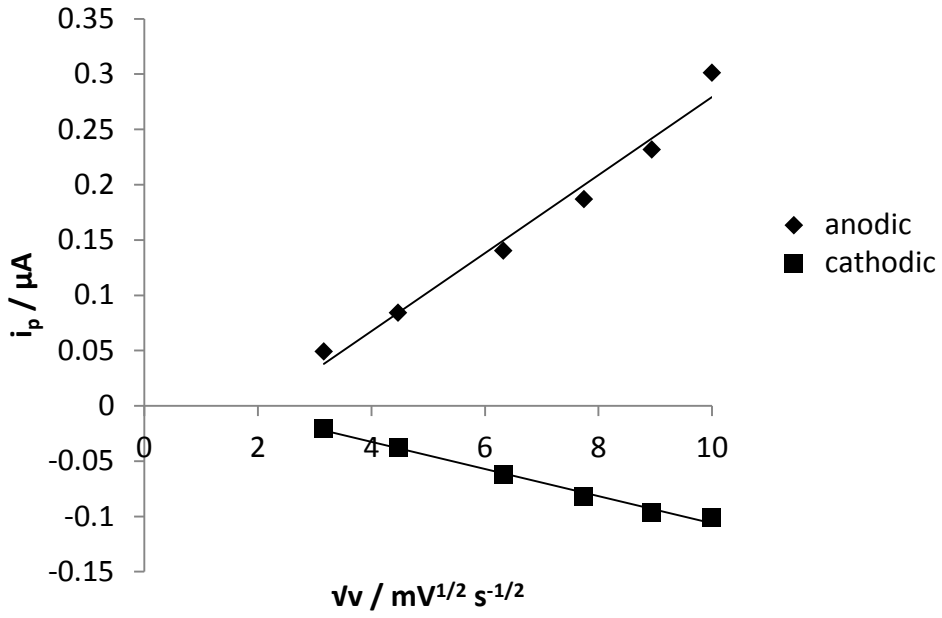

Figure 2.53: Peak current density vs. √v for the PHF electrode.

Response of the PMBN-HMDA-FcCOOH/PMBN-GOx (PHFPG) to Changing [Glucose]

In order to test the ability of PHF to act as a redox mediator, 10µl of PMBN-GOx (PG) was added to the PHF film. The composition of the PG layer was 5mg ml^{-1} GOx (1055 unit's ml^{-1}) in 0.9%wt. PMBN in 90% ethanol. This resulted in an enzyme loading of 50µg (10.55 units). Once the electrode was placed inside the cell, scans were carried out at various cell glucose concentrations.

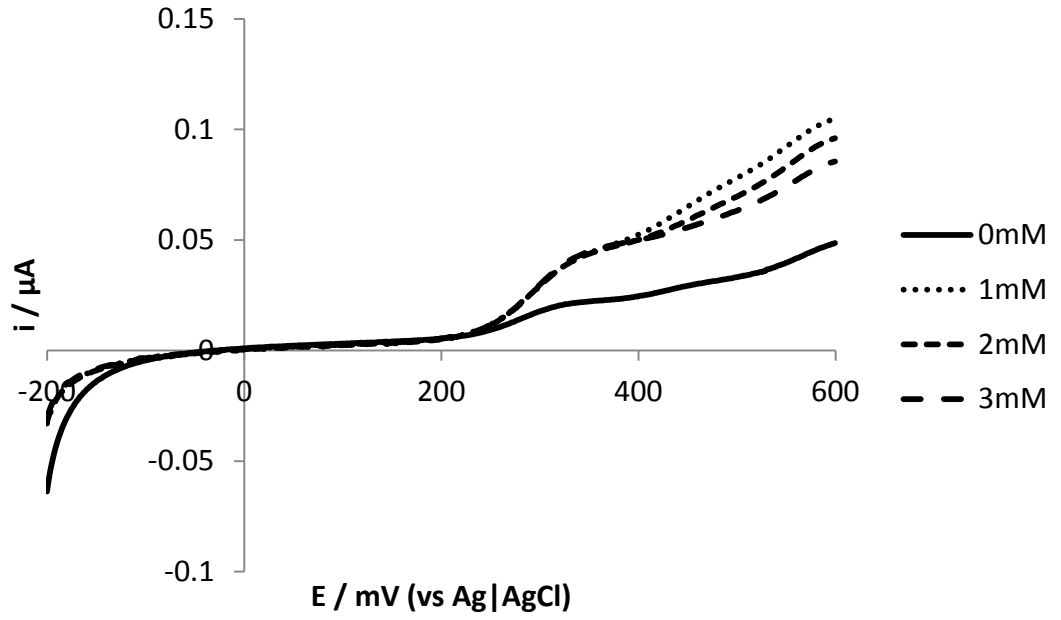

Figure 2.54: LSV's of the PHFPG electrode (v = 1 mV s^{-1}) at different glucose concentrations.

Figure 2.54 shows the response of the PHFPG electrode to different cell glucose concentrations. Both the current in the kinetic region (the current at the E° of FcCOOH (337mV)) and the diffusion limited current (the current at potentials >337mV) increases when glucose is added indicating that there is a larger concentration of $Fe^{(II)}$ at the electrode surface. The increase in [$Fe^{(II)}$] is caused by regeneration of $Fe^{(II)}$ from $Fe^{(III)}$ by the reduced enzyme. It can be seen from Figure 2.54 that the upper limit of detection for the electrode is 1mM as there is no subsequent increase in diffusion limited current as the glucose concentration is raised above 1mM.

Figure 2.55 shows a CA trace for glucose oxidation at the PHFPG electrode. The CA was carried out in the diffusion limited current region of the PHF film (370mV). In this experiment the upper limit of detection is 1mM, corresponding to the result shown in Figure 2.54.

In order to ensure efficient delivery of the substrate to the electrode surface, the electrolyte was stirred during the experiment.

Figure 2.56 shows a CA trace for the PHFPG electrode under stirred and quiescent conditions. The cell [glucose] was increased to 1mM after 5 minutes and the catalytic current recorded for 4hrs. There is a ~ 75% drop in the current measured for stirred conditions after 4hrs. The attenuation of catalytic current over the course of the experiment may be due to mechanical instability of the film. It is expected that the binding of the film to the electrode surface may not be sufficient to withstand the mechanical strain imparted on it during stirring of the electrolyte. Therefore the experiment was repeated under quiescent conditions.

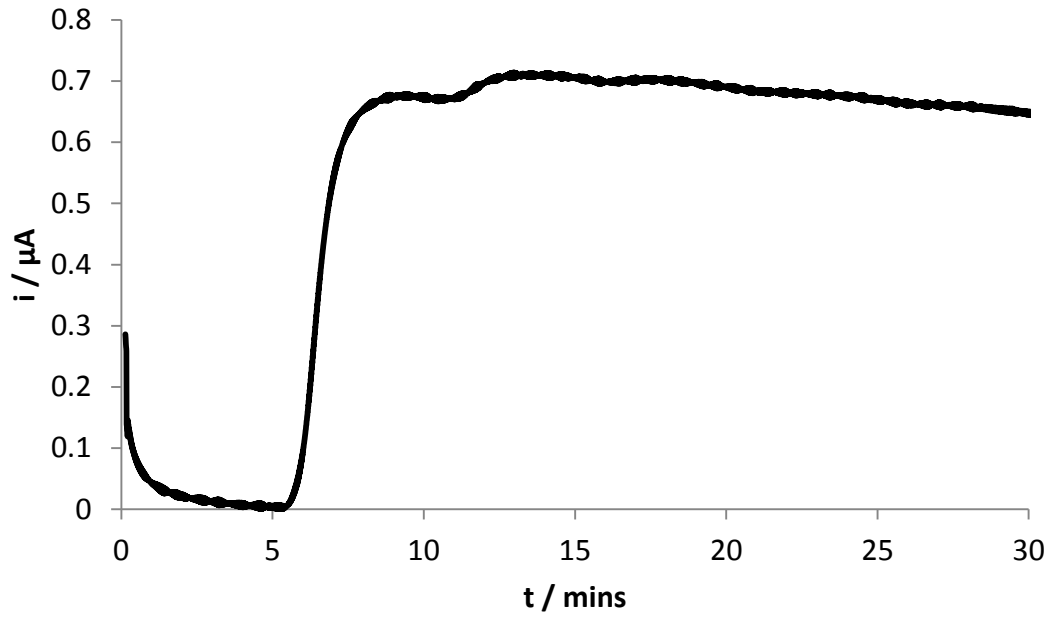

Figure 2.55: CA (E = 370m V) on the PHFPG electrode. The [glucose] was increased to 1mM after 5 minutes and increased by 1mM every 5 minutes thereafter (background current subtracted).

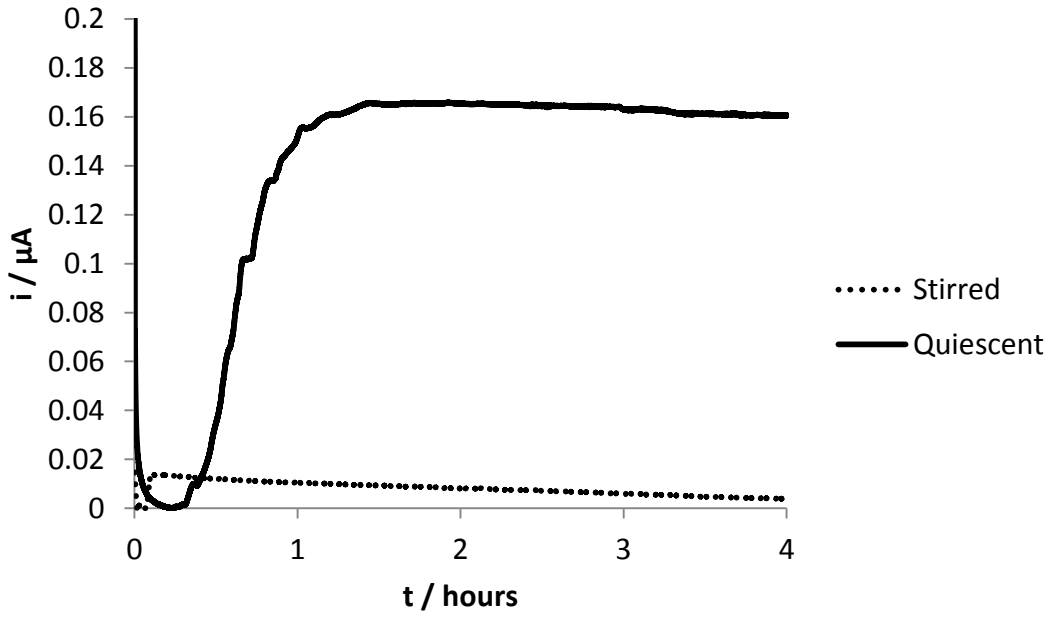

Figure 2.56: CA (E = 370m V) on the PHFPG electrode under stirred and quiescent conditions. The [glucose] was increased to 1mM after 5 minutes (stirred) and increased by 1mM every 5 minutes up to 3mM (quiescent) (background current subtracted).

The response to the injection of glucose is significantly longer for the quiescent case as opposed to the stirred case, as can be expected. No catalytic current was observed under quiescent conditions after 5 minutes, therefore more glucose was injected into the cell. A catalytic current was observed after 15 minutes. In stirred solution, the catalytic current dropped steadily over time. The catalytic current had dropped by 73.5% of its maximum value after 4 hours. For the quiescent case, the catalytic current had dropped by 2.9% of its maximum value after 4 hours. The improvement in the stability of the catalytic current for quiescent conditions is attributed to the lack of mechanical stress on the film due to the lack of stirring.

Figure 2.57 shows the stability of the PHFPG electrode that was used for the experiment shown in Figure 2.56 (quiescent) after being stored at 4°C in PBS for 48 and 72 hrs. The

activity of the electrode dropped steadily over three days and was completely inactive after four days. This may be due to gradual degradation of the PHFPG film.

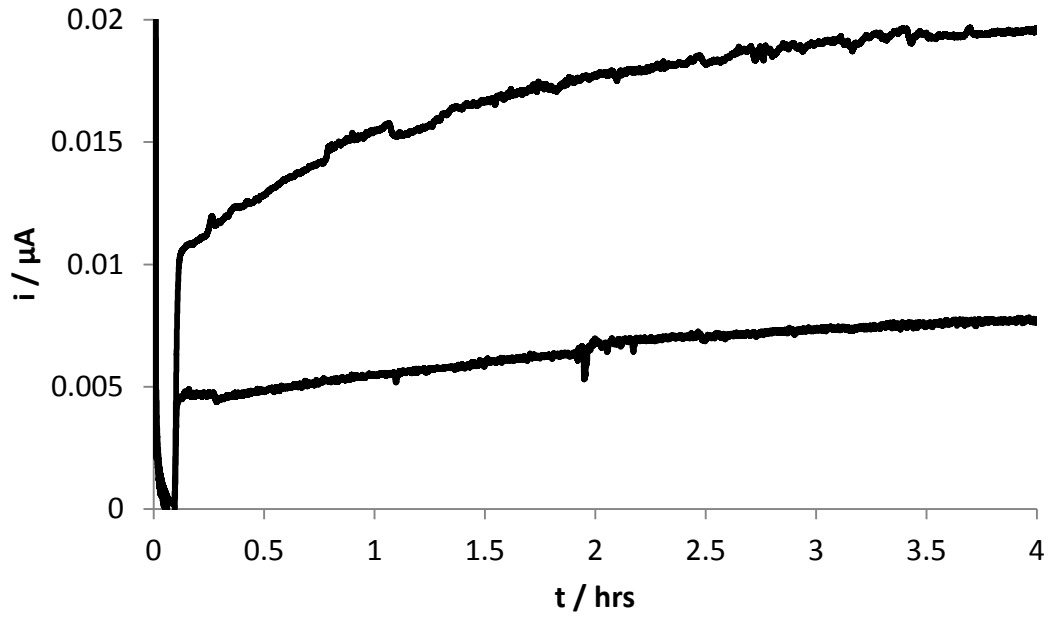

Figure 2.57: CA experiments on the PHFPG electrode used in Figure 2.56 (quiescent). E = 370mV (vs Ag|AgCl), 1mM glucose added after 5 minutes after storage in PBS at 4°C for 48 hrs (upper line) and 72 hrs (lower line) (background current subtracted).

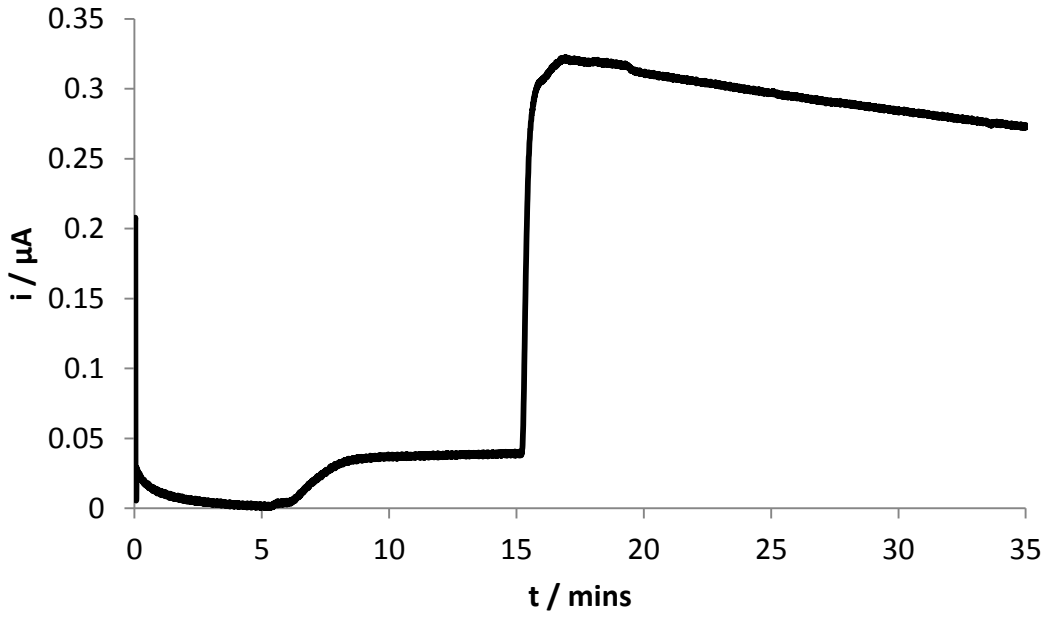

Figure 2.58: CA experiment on the PHFPG electrode, E = 370mV (vs Ag|AgCl), 1mM glucose added after 5 minutes, 0.13 mM AA added after 15 minutes, 0.2 mM urea added after 25 minutes.

The effect of common biological interferants on the catalytic response of the PHFPG electrode was investigated. AA and urea were added to the cell during a CA measurement at biologically relevant concentrations.[16, 133] The addition of AA clearly affects the response of the electrode (see

Figure 2.58) however the addition of urea did not affect the catalytic current.

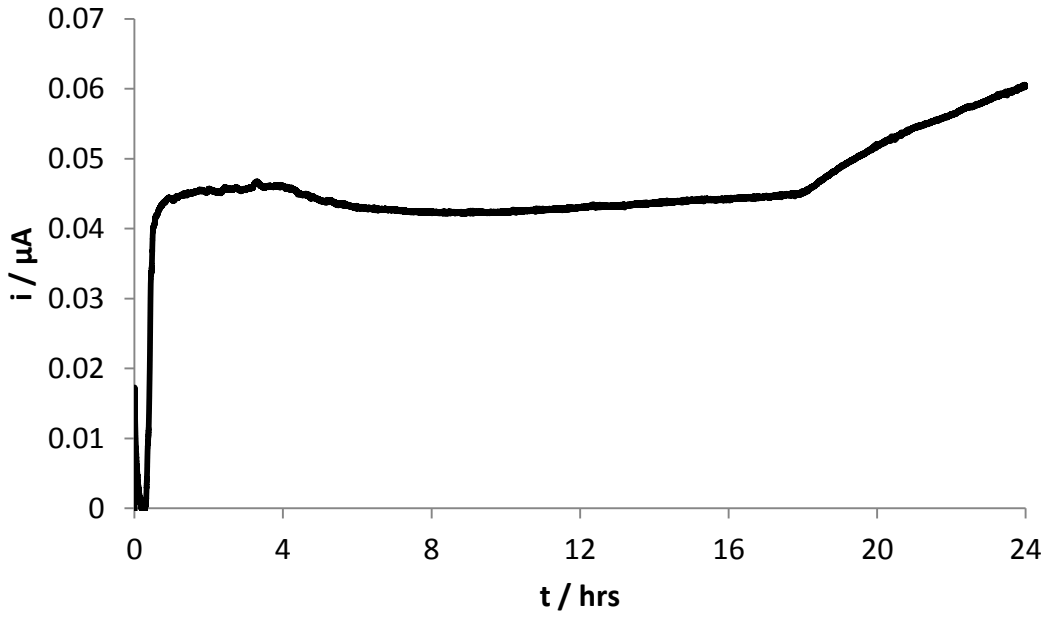

Figure 2.59: CA experiment on the PHFPG electrode, E = 370mV (vs Ag|AgCl) (Cell volume = 6ml), 3mM glucose added after 5 minutes.

Figure 2.59 shows the catalytic current response of the PHFPG electrode after increasing the electrolyte glucose concentration to 3mM after 5 minutes. The experiment was carried out with a working electrolyte volume of 6ml. The initial detection of glucose took ~ 9 minutes and a steady state current was reached ~ 20 minutes after the initial detection. For the same electrode but with electrolyte stirring, the initial detection of glucose was effectively instantaneous and a steady state current was reached after ~ 18 seconds. The current remained stable for 18 hours until an increase in catalytic current was seen. This may be due to evaporation of the electrolyte causing an increase in the concentration of glucose in the cell.

Figure 2.60 also shows the catalytic current response of the PHFPG electrode after increasing the electrolyte glucose concentration to 3mM after 5 minutes. Due to evaporation of the electrolyte in the previous experiment over 24 hours, the working

electrolyte volume was increased to 15ml. The timeframe of the experiment was also increased. The initial detection of glucose took 6 hours 18 minutes and 22 seconds and a steady state current was reached 3 hours 17 minutes and 38 seconds after the initial detection. This is compared to ~ 9 minutes for initial detection and then another ~ 20 minutes for steady state current to be reached with a working electrolyte volume of 6ml without stirring and effectively instantaneous initial detection of glucose and ~ 18 seconds for steady state current for a 6ml working electrolyte volume with stirring. The electrocatalytic current drops gradually after it has reached steady state until 19 hours 8 minutes and 40 seconds where it begins to increase again. This increase continues for 2 hours 36 minutes and 20 seconds after which time it begins to drop again. It then begins to rise again after 36 hours 25 minutes 50 seconds. These rises may be due to variations in electrolyte temperature over the course of the experiment, which can affect the enzymes catalytic activity.

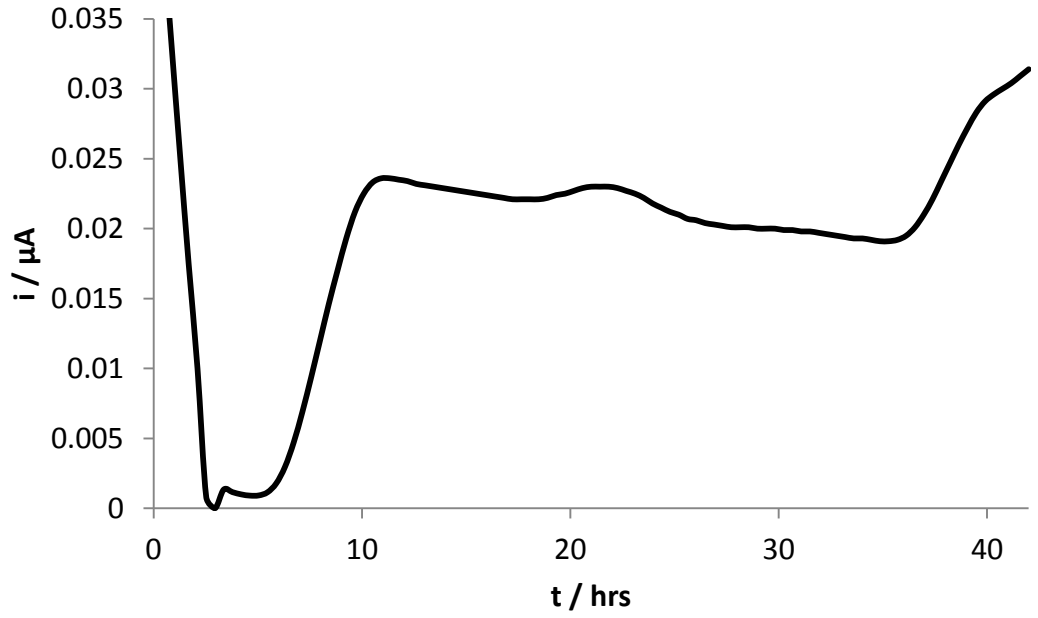

Figure 2.60: CA experiment on the PHFPG electrode, E = 370mV (vs Ag|AgCl), 3mM glucose added after 5 minutes.

2.3.6 Investigation of Different Mediators for use in Enzyme Electrodes

In order to reduce interference, it is desirable to have the most negative operating potential possible. This is also beneficial when using an enzyme electrode as the anode of a fuel cell. With this in mind, Nickelocene (Nc) (a structural analogue of Fc) and Coenzyme Q10 (Ubiquinone) (CQ_{10}) (which has been shown to exhibit anodic oxidation)[134] were tested for potential use in enzyme electrodes as they have more negative oxidation potentials than Fc.

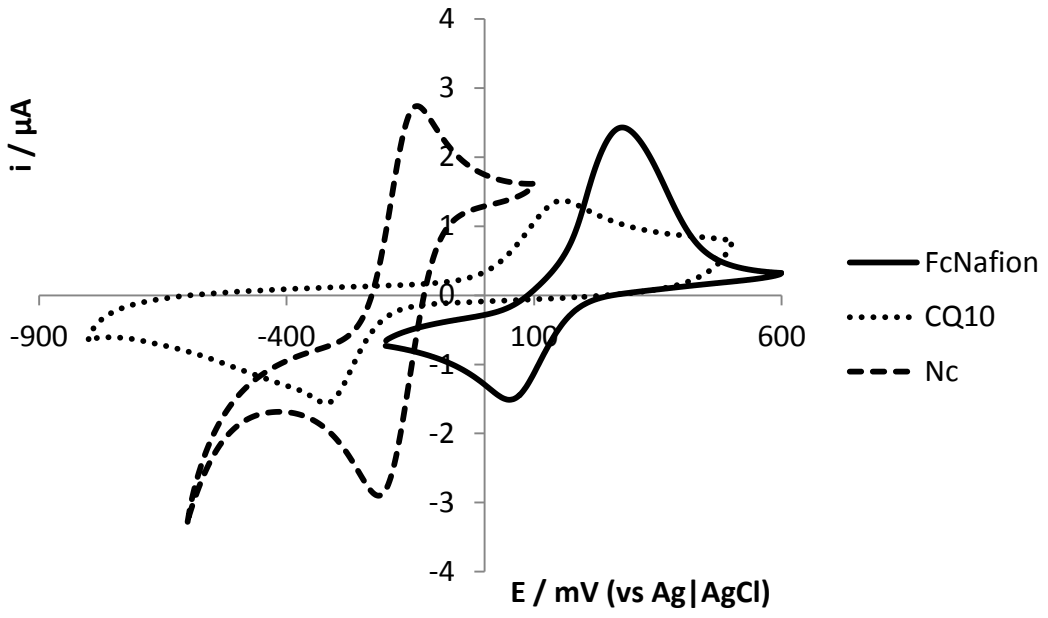

Figure 2.61: CVs of different immobilised mediators (v = 50mV s^{-1}). Electrolyte = 0.1M PBS (pH7). GCE WE, Pt CE, Ag|AgCl RE.

Mediator	**Oxidation E_p (mV vs Ag|AgCl)**
Fc	213
CQ_{10}	128
Nc	-157

Table 2.5: The oxidation potentials of Fc, CQ_{10} and Nc derived from Figure 2.61.

Figure 2.61 shows CV scans carried out for three different mediators. The oxidation potentials derived from Figure 2.61 are shown in Table 2.5.

The electrodes (prepared as described in Section 2.2.9) were tested with cyclic voltammetry over 20 cycles to investigate their electrochemical stability. Figure 2.62 shows that CQ_{10} remains stable over 20 cycles while Figure 2.63 and Figure 2.64 show

that there is a loss of Fc and Nc during the potential cycling process. This is attributed to Fc and Nc becoming soluble when oxidised.

The problem of Fc and Nc becoming soluble when oxidised can be solved by dissolving them in 0.25 wt% Nafion solution (in Ethanol) (as described in section 2.3.2). As CQ_{10} is not soluble in 0.25 wt% Nafion, the tests for Fc and Nc were carried out using Acetone for a fair comparison.

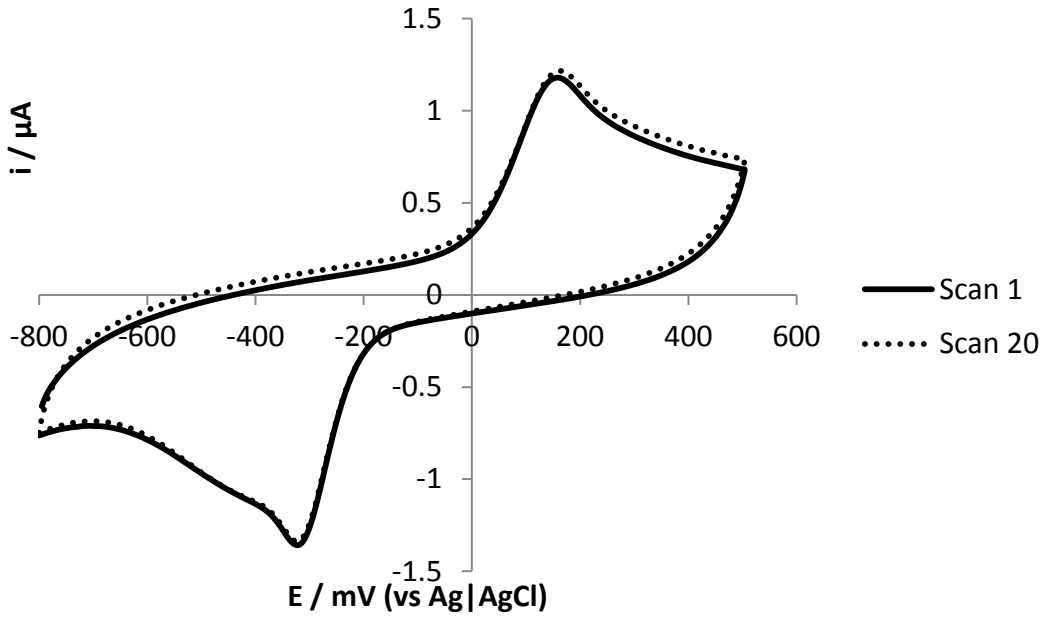

Figure 2.62: CVs showing the stability of a GCE modified with CQ_{10} (as described in Section 2.2.9), all conditions as in Figure 2.61.

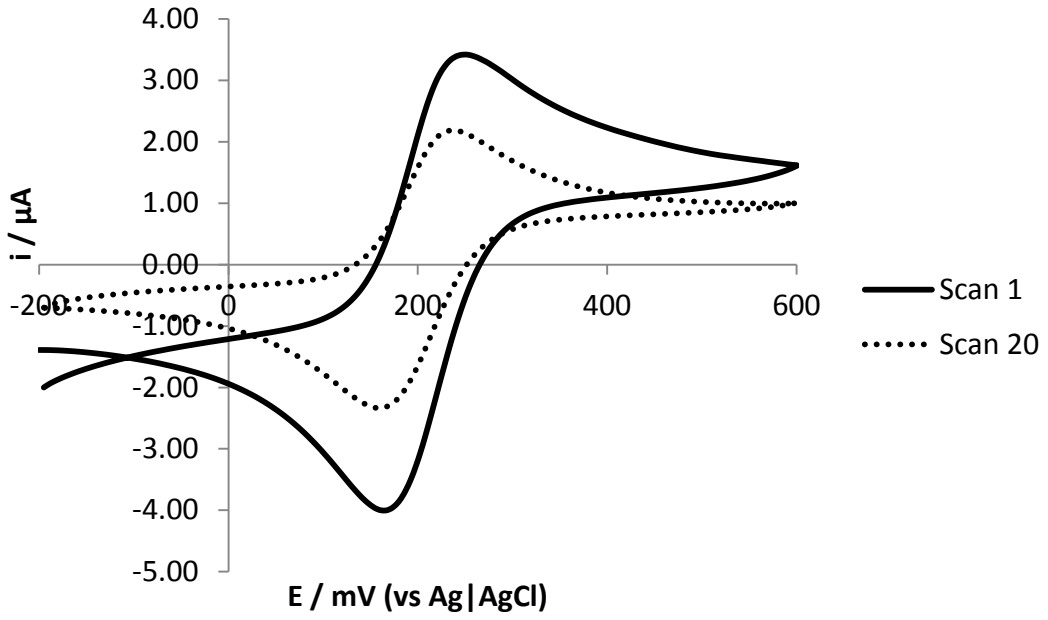

Figure 2.63: CVs showing the stability of a GCE modified with Fc (as described above), all conditions as in Figure 2.61.

The difference in the shape of the scan for Nc between Figure 2.61 and Figure 2.64 is attributed to the rapid oxidation of Nc in aerobic environments. This is especially obvious in Figure 2.65. The stability of the adsorbed CQ_{10} shown in Figure 2.62 is attributed to both oxidised and reduced forms of CQ_{10} being insoluble.

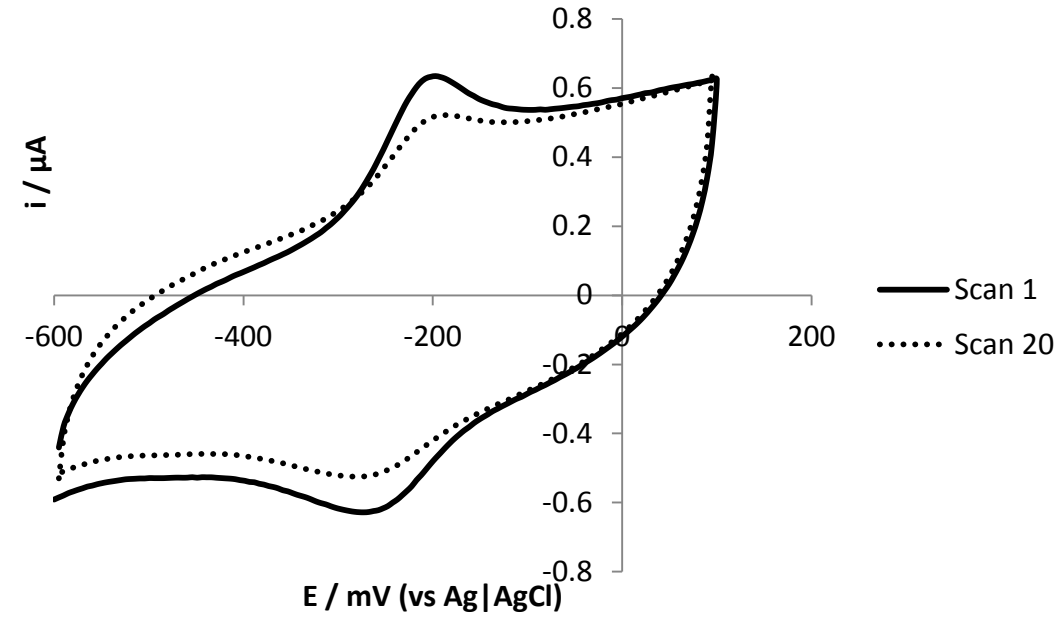

Figure 2.64: CVs showing the stability of a GCE modified with Nc (as described above), all conditions as in Figure 2.61.

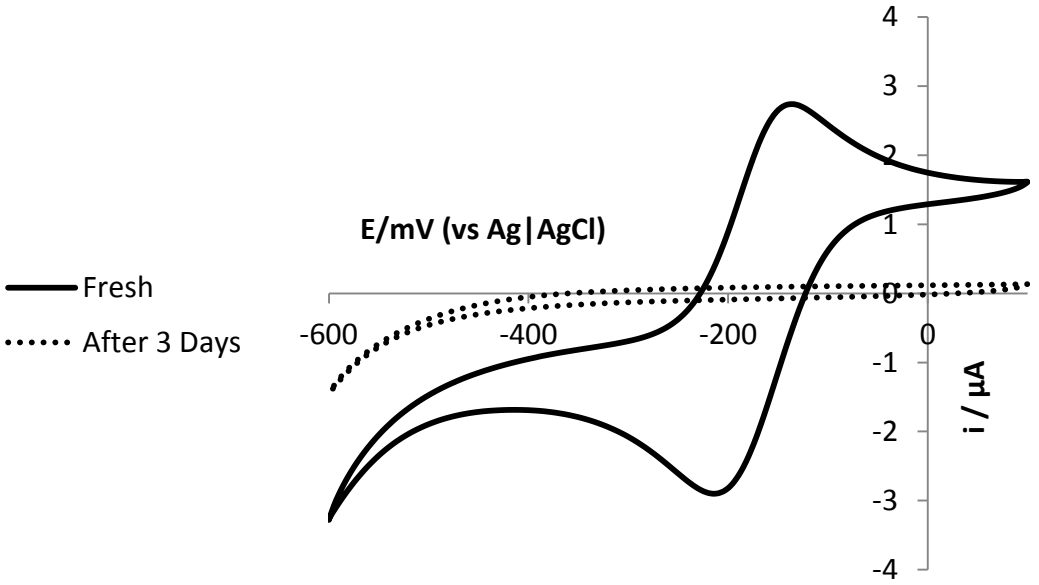

Figure 2.65: CVs for freshly prepared & 3 day old Nc solution (all other conditions as in Figure 2.61).

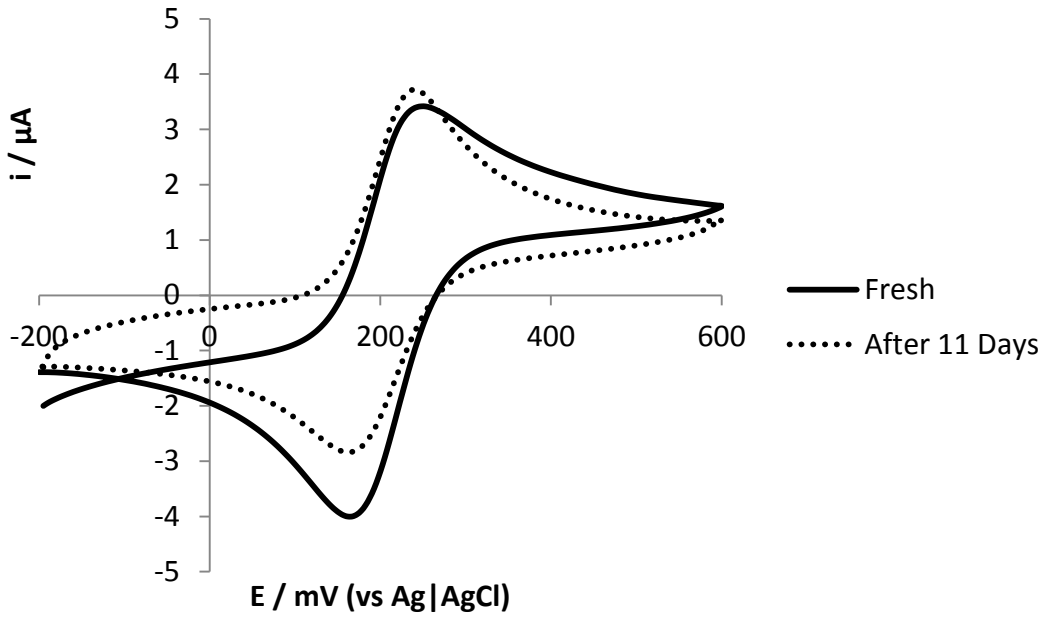

Figure 2.66 CVs for freshly prepared & 3 day old Fc solution (all other conditions as in Figure 2.61).

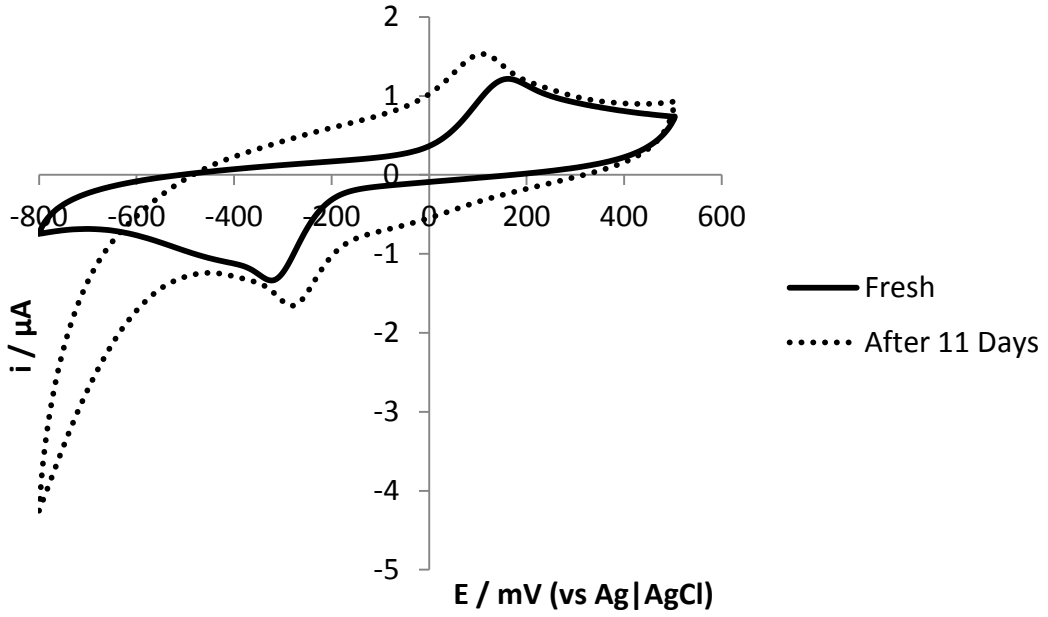

Figure 2.67: CVs for freshly prepared & 3 day old CQ_{10} solution (all other conditions as in Figure 2.61).

Figure 2.66 and Figure 2.67 show the redox response of freshly prepared and eleven day old solutions of Fc and CQ_{10}. The scans show that both Fc and CQ_{10} retain their redox

activity in solution over several days. Figure 2.65 shows that Nc is not stable in solution as no redox response is seen even after 3 days. This is because Nc is readily oxidised[135] which makes it difficult to use.

These results show that CQ_{10} is a promising mediator for use in enzyme electrodes due to its low oxidation potential (compared to Fc) and its electrochemical stability.

2.4 Conclusions

p(VFc-Co-HEMA) was tested as a redox polymer for the development of GOx enzyme electrodes. The polymer was shown to be unstable, primarily due to leaching of the mediator. Incorporation of the polymer into a graphite paste electrode could not prevent leaching of the mediator.

FcNafion was tested as a redox mediator and was shown to be stable, with good electron transfer properties, suggesting FcNafion could be a suitable redox mediator for a GOx enzyme electrode. The enzyme electrode can be stabilised using the phospholipid polymer PMBN.

EIS was successfully used to follow the fabrication process of FcNafion-GOx enzyme electrode and equivalent circuits were developed to model the EIS data.

GOx was then suspended directly in a FcNafion redox polymer, retaining the activity of the enzyme. The suspension of GOx in the Nafion layer prevented interference from urea but did not prevent interference from AA. Due to the relatively harsh environment created by FcNafion, PMBN can be used to stabilise the enzyme electrode.

Redox capability was successfully incorporated into PMBN using covalent attachment of a Fc derivative to PMBN. The resulting redox polymer was shown to be electrochemically stable. This was used as the basis for an enzyme electrode. This electrode was also shown to be resistant to interference from urea but not from AA.

Finally, Nc and CQ_{10} were tested as potential mediators for enzyme electrodes capable of operating at a more negative potential than those based on Fc. Nc has the more negative oxidation potential but was shown to be unstable when immobilised on an electrode surface. CQ_{10} proved to be the most stable upon immobilisation.

Chapter 3 - An Enzyme Electrode Based on CQ_{10}

The aim of the work carried out in this chapter was to develop an enzyme electrode based on the redox mediator Co-enzyme Q_{10} (CQ_{10}). The stability, electrochemical properties and electrocatalytic activity of a CQ_{10} based enzyme electrode was also investigated.

3.1 Introduction

2,3-dimethoxy-5-methyld-polyisoprenoid-1,4-benzoquinone (CQ_{10}) (a derivative of 2,3-dimethoxy-5-methyl-benzoquinone with a polyisoprenoid side-chain[136] in position six of the quinone ring,[134] the number of isoprene units ranges from zero to ten)[134] is part of a family of naturally occurring vitamin-like lipid-soluble molecules known as Ubiquinones. Ubiquinones carry out a variety of roles in biology and they are widely distributed in the cells of living organisms.[136] They have been shown to function as primary or secondary electron acceptors in photosynthetic reaction centres.[137] CQ_{10} has been shown to act as an electron carrier from flavoprotiens to cytochromes during ATP synthesis in the mitochondrial respiratory chain[25, 111, 136, 137b, 138] and also in the membranes of bacteria.[136] In this process, CQ_{10} is reduced to $CQ_{10}H_2$ via the semiubiquinone radical ($CQ_{10}H\bullet$).[134] The fully reduced form of CQ_{10} ($CQ_{10}H_2$) plays an important role as an antioxidant and thus protects lipid membranes against peroxidative damage.[134] It can also act as a proton transporter in the inner layer of biological membranes.[138d, 139] It is the most common coenzyme Q in long-lived mammals and coexists with its reduced form ($CQ_{10}H_2$ — ubiquinol or ubidecarenol) which is a predominant form in tissues.[134]

Most ubiquinones are present at a biological membrane-water interface[137a] at a concentration that normally falls in the range of 1-2 mol%.[140] The molecule contains a very polar quinone redox centre and a long (50Å)[140] isoprenoid chain, the length of the

side-chain in the molecule does not appreciably affect the redox properties of the CQ_{10}.[136] It is therefore an amphiphile and it has been suggested that its amphiphilic character is responsible for its location,[138b] in the central hydrophobic part of cellular membranes, i.e. between the double layers of phospholipid fatty acids.[141]

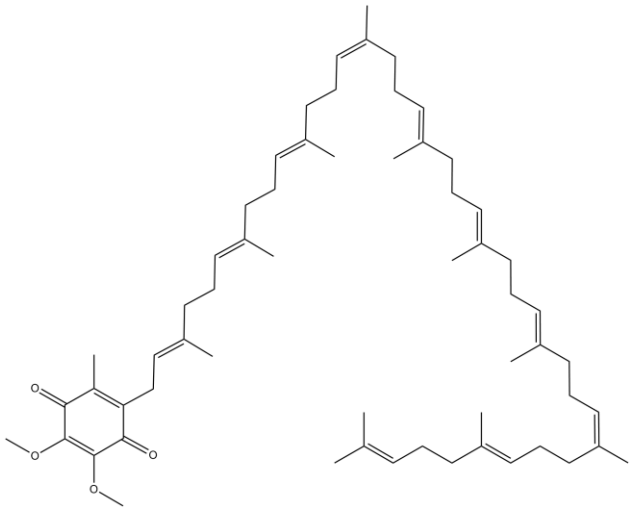

Figure 3.1: The chemical structure of CQ_{10}.

CQ_{10} has been immobilised in carbon paste onto which D-gluconate dehydrogenase from *Pseudomonas fluorescens* was immobilised.[142] The resulting electrode could oxidise d-gluconate electrocatalytically, with CQ_{10} serving as the electron transfer mediator between the carbon paste electrode and the immobilised enzyme. When immobilised, this enzyme creates a hydrophobic layer. This hydrophobic layer is able to dissolve high concentrations of CQ_{10} which improves the performance of the electrode.[142] It was shown that leakage of CQ_{10} from the enzyme layer into the solution was negligibly small since CQ_{10} is practically insoluble in aqueous solution. In this study the shape and magnitude of the cyclic voltammograms were not influenced by stirring the electrolyte and voltammetric waves remained unchanged for several hours of continuous potential cycling.[142]

CQ_{10} dissolved in carbon paste has also been shown to act as a mediator for GOx.[143] The biological activity of CQ_{10} results from its ability for reversible redox conversion.[136]It has been found[138a] that the stability of semiubiquinone in the pH range 7.0-11.3 confirms the idea that in the mitochondria CQ_{10} participates in one electron transfer processes. It has also been shown that CQ_{10} can be oxidised in a two electron process.[138c]

Although it presents a low solubility in aqueous solutions or in solutions similar to physiological media,[144]CQ_{10} can be dissolved in a phospholipidic matrix and its electrochemical response depends on its diffusion through the this matrix.[144] Therefore the approach in this work is based on dissolving CQ_{10} in PMBN solution in order to create a biocompatible redox polymer capable of mediating electron transfer with GOx for use as an enzyme electrode with a lower oxidation potential than Fc, bearing in mind that one concern of this approach is the restricted mass transfer properties of CQ_{10}.[137a]

Multi walled Carbon Nanotubes (MWCNT)

In this chapter, multiwalled carbon nanotubes (MWCNT) are used in the electrode assembly, in order to improve the electrical conductivity of the immobilised enzyme|mediator film. MWCNT are coaxial assemblies of graphene cylinders and have dimensions ranging from 2 to 30 nm in diameter and several microns in length.[145] From the perspective of electron-transfer properties, the open ends of carbon nanotubes (CNTs) have been likened to edge planes of highly oriented pyrolytic graphite (HOPG), while the walls are suggested to have properties similar to those of the basal planes of HOPG.[146] The surface of basal plane graphite is hydrophobic while edge plane graphite exhibits

oxygen functionalities such as carboxyl and carbonyl groups, hydroxides, phenols and quinols.[8] The exposed MWCNT ends should behave like a graphite edge-plane, resulting in a nanoelectrode ensemble for electroanalytical applications requiring fast electron transfer rates.[147]

CNTs have been demonstrated to be an effective interface in the promotion of electron transfer.[148] The efficiency of electron transfer through CNTs is demonstrated by electrodes modified with tubes cut to different lengths having the same electron transfer rate constant[146]. Also, studies indicate that MWCNTs have a fast electron transfer rate for various redox reactions[147] and generally, MWCNTs have larger diameters and better electrical conductivity compared to SWCNTs.[147]

CNT's can improve electrocatalysis in enzyme electrodes. The amount of improvement depends on CNT orientation and amount of oxygenation[8]. CNT have been used in a layer-by-layer self- assembly technique with the polymer chitosan, providing the unique characteristics of CNTs in promoting electron transfer and of chitosan in providing a biocompatible environment in which to construct an active microperoxidase-11 multilayer film.[148] CNT's have also been shown to be biocompatible.[148]

CNT have also been used with Teflon in electrode materials. This provided new capabilities for electrochemical devices by combining the advantages of CNTs and "bulk" composite electrodes.[149]

It has been suggested that MWCNTs enhance the efficiency of electron transfer between GOx and electrodes, resulting in high sensitivity in detecting glucose. [150]

Also, they can be cast onto GCE surfaces. During the adsorption of CNT's onto the GCE, the nanotubes tend to form bundles as the adsorption propagates, following a "nucleation adsorption mechanism".[151]

Gold Nanoparticles (AuNPs)

In this chapter AuNP's will also be used in the electrode assembly. AuNPs can act as a nanocollector of electrons.[152] They can then be used as a hopping bridge or relay of electrons generated from the enzyme catalytic redox reaction.[152] AuNPs therefore, can act as tiny conduction centres to facilitate electron transfer to realize sensitive enzyme electrodes.[117] AuNPs can also be used as electron transfer promoters in combination with CNT's.[153] The presence of AuNPs has been shown to increase the conductivity of sol-gel matrices, allowing enzymes to transfer electrons to electron acceptors quickly.[154] AuNPs can enhance the activity of proximally immobilised enzymes.[152a] They have been shown to act as relay units between the FAD centre of GOx and an electrode.[152b] This can increase the activity of GOx.[155] This has been attributed to the quantum size effect. When atoms contained in a particle decrease, the redox potential of the particle increases, which results in a stronger affinity to electrons.[155] The reason for this is the increase in the excess free energy of a small metal particle with dimensions Γ:

$$\Delta E = \frac{2\sigma V_m}{\Gamma F} \qquad 3.1$$

where Vm is the molar volume of the metal, σ is the specific free surface energy of the interface with the electrolyte and F is the Faraday constant.[155] According to this equation, the surface free energy will increase as the dimensions decrease. This is a proof

of the strong ability of small sized particles to accept electrons.[155] This increased ability to accept electrons can lead to direct electron transfer between GOx and AuNPs.[156]

The stabilisation of GOx by AuNPs has also been attributed to the fact that AuNPs can strongly adsorb the enzyme and thus prevent the leakage of enzyme.

Electron transfer through AuNPs is much faster than electron transfer to the native electron acceptor for GOx (O_2)[152b] therefore the presence of AuNPs in the electrode assembly reduces the negative effects caused by dissolved oxygen. This fast electron transfer of AuNPs can also help to reduce interference from ascorbic acid.[152b] AuNPs have also been shown to be biocompatible and non-toxic.[152a] Due to the possible benefits and effects of including AuNPs to the PMBNCQ_{10} film, AuNPs were included in the PMBNCQ_{10} based electrode in order to improve its conductivity and hence improve its performance.

3.2 Experimental

Materials

Coenzyme Q_{10} (CQ_{10}), $HAuCl_4$, Sodium citrate and $NaBH_4$, were obtained from Sigma-Aldrich (Dorset, UK) and used without further purification. Nitric acid, Sulphuric acid were obtained from Fisher Scientific, (Leicestershire, UK) and used without further purification. Polyethersulfone (PES) membranes were obtained from Pall Life Sciences. Multiwalled Carbon Nanotubes (MWCNT) (inner diameters of 20-50 nm and outer diameters of 70-200 nm) were obtained from Applied Sciences Inc. (Ohio, USA). All other materials were obtained as described in Section 2.2.

Electrode Fabrication Procedure

CQ_{10} can be dissolved in a phospholipid matrix. Therefore CQ_{10} was dissolved in 1% wt. PMBN in ethanol to make at 0.4mM CQ_{10} solution. This solution is designated $PMBNCQ_{10}$. 10µl of the $PMBNCQ_{10}$ solution was then dropped onto a polished GCE. The electrode was allowed to dry and tested in a three electrode cell (Pt CE, Ag|AgCl RE) in 0.1M PBS. The cell was sparged with N_2 and all experiments were carried out under a N_2 blanket.

2 µL of $PMBNCQ_{10}$ (0.4mM CQ_{10} in 1% wt. PMBN in ethanol) was dropped onto a polished GCE and allowed to dry. The electrode was then added to a three electrode cell containing 0.5 mg ml^{-1} GOx in 0.1M PBS (pH 6.8). The electrode was then tested at different concentrations of glucose after the cell had been sparged with N_2 for at least 10 minutes. A N_2 blanket was maintained throughout the experiments.

Electrode Preparation Procedure

Preparation of AuNP solution

An AuNP solution was prepared according the method of Zhou.[157] Briefly, $HAuCl_4 \cdot 4H_2O$ (1 mL, 1 wt %) was added to 90 mL H_2O. After mixing for 1 minute, sodium citrate (2 mL, 38.8 mM) was added, followed by stirring for another two minutes. An aqueous solution of 1 ml of 0.075 wt % $NaBH_4$ in sodium citrate (38.8 mM) was then added, and the reaction mixture was stirred for 5 minutes.

Estimation of Nanoparticle Concentration

The concentration of the AuNPs was estimated according to the method of Neiman.[158] Briefly, from the size of the nanoparticles (nominally 2nm) and the molar volume of Au (10.2 ml mol^{-1}) the number of Au atoms in a single nanoparticle can be estimated.

Knowing the original concentrations of the Au solutions and assuming 100% conversion to nanoparticles, the number of nanoparticles per litre can be calculated.

Preparation of MWCNT solution

The MWCNT solution was prepared according to the method of Liu.[151] Briefly, The nanotubes were cut into short pipes by chemical oxidation in a mixture of concentrated sulphuric and nitric acids (3:1, 98% and 70%, respectively) under ultrasonication for 4h. The reaction mixture was then diluted with water and allowed to stand overnight for precipitation. The supernatant was decanted, and the remains were diluted with H_2O and filtered with a 0.2µm diameter pore Polyethersulfone (PES) membrane under vacuum. The solid shortened CNT sample was obtained by washing the remains on the PES filter with deionised water until the filtrate pH became nearly neutral. The CNT pipes obtained were found to form stable colloidal suspensions in water and Dimethylformamide (DMF). Suspensions were prepared by ultrasonication without using surfactants, suggesting that relatively short nanotubes were made.

Fabrication of the MPCAG Electrode

10mg of GOx was dissolved in 200µl of (AuNP) solution (1.264µM, 2nm) to give a stock 50 mg ml^{-1} enzyme/AuNP solution. 2µl of this solution was then mixed with 18µl of PMBN(CQ_{10}) (0.4mM CQ_{10} in 1% wt. PMBN in ethanol). This solution was gently shaken for 30 minutes. Meanwhile 2.5µl of 2 mg ml^{-1} MWCNT (in DMF) were deposited onto a polished GCE. In order to increase the amount of enzyme loading on the electrode surface, 10µl of the previously prepared enzyme solution was then added to the modified GCE and allowed to dry. The modified electrode was then inserted into a three electrode cell (Pt CE, Ag|AgCl RE) containing 6ml of 0.1M PBS (pH 6.8). After this the cell was

sparged with N_2 and a N_2 blanket was maintained inside the cell throughout the experiment.

3.3 Results & Discussion

In this section, the characterisation of $PMBNCQ_{10}$ as a redox polymer for the immobilisation of GOx is described. This electrode was then tested for electrocatalytic activity towards glucose.

Initial Electrochemical Characterisation of $PMBNCQ_{10}$

Stability of PMBNCQ10

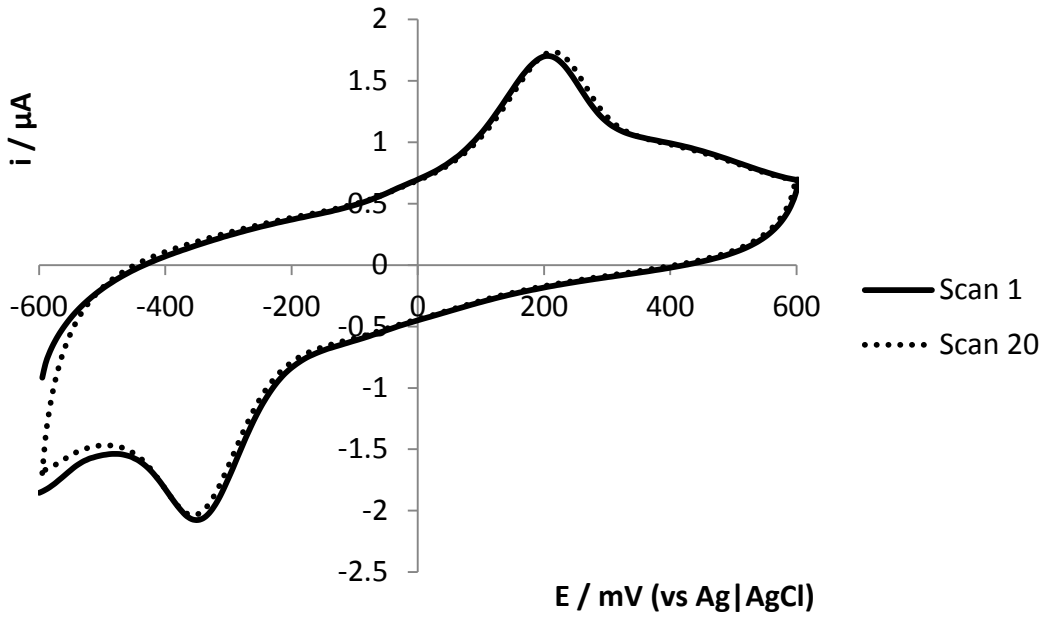

Figure 3.2: CVs of the $PMBNCQ_{10}$ electrode (v = 50 mV s^{-1}) after different numbers of scans (conditions as described in Section 3.2).

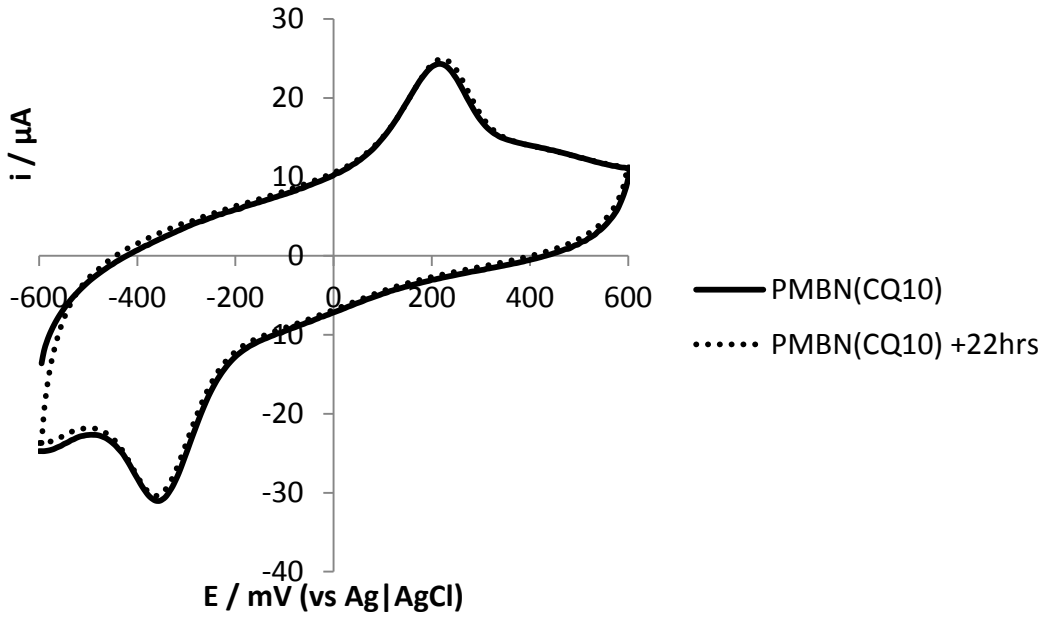

Figure 3.3: CVs of the PMBNCQ$_{10}$ electrode (v = 50 mV s^{-1}) initially and after 22hrs immersed in PBS (0.1M pH7).

One of the reasons CQ_{10} was chosen as a potential mediator for an enzyme electrode is its stability when immobilised onto electrode surfaces. As CQ_{10} is insoluble in aqueous solutions, leakage of the mediator into the electrolyte should be negligible. This claim is supported by Figure 3.2 which shows that the shape and magnitude of the oxidation peak is not influenced by continued potential cycling. Figure 3.3 shows that the voltammetric waves remained unchanged after the electrode was immersed in buffer solution for several hours.

Electrochemical Reversibility of PMBNCQ$_{10}$

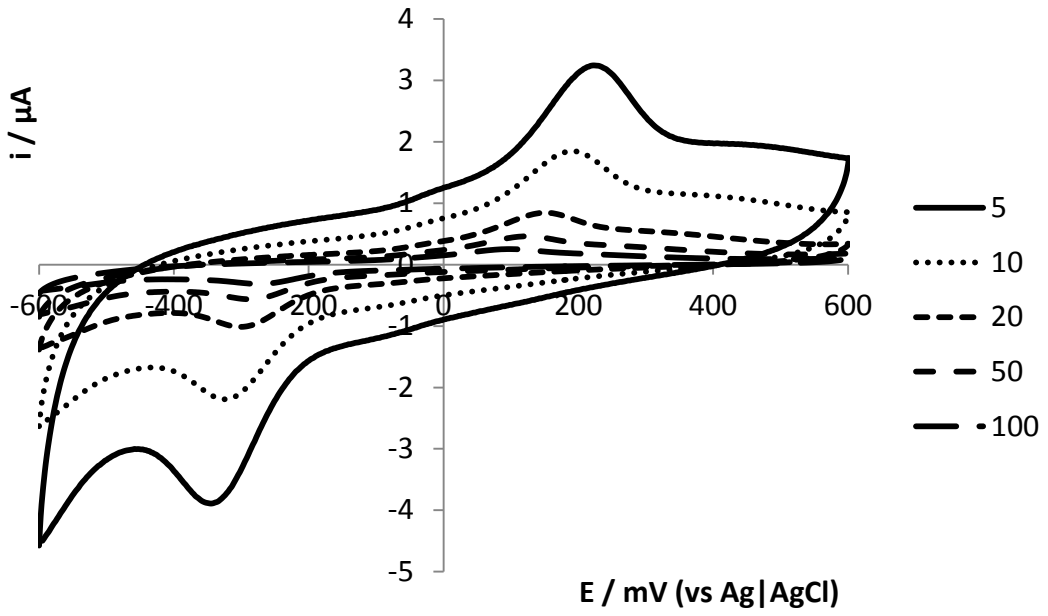

Figure 3.4: CVs of $PMBNCQ_{10}$ on a GCE at various v.

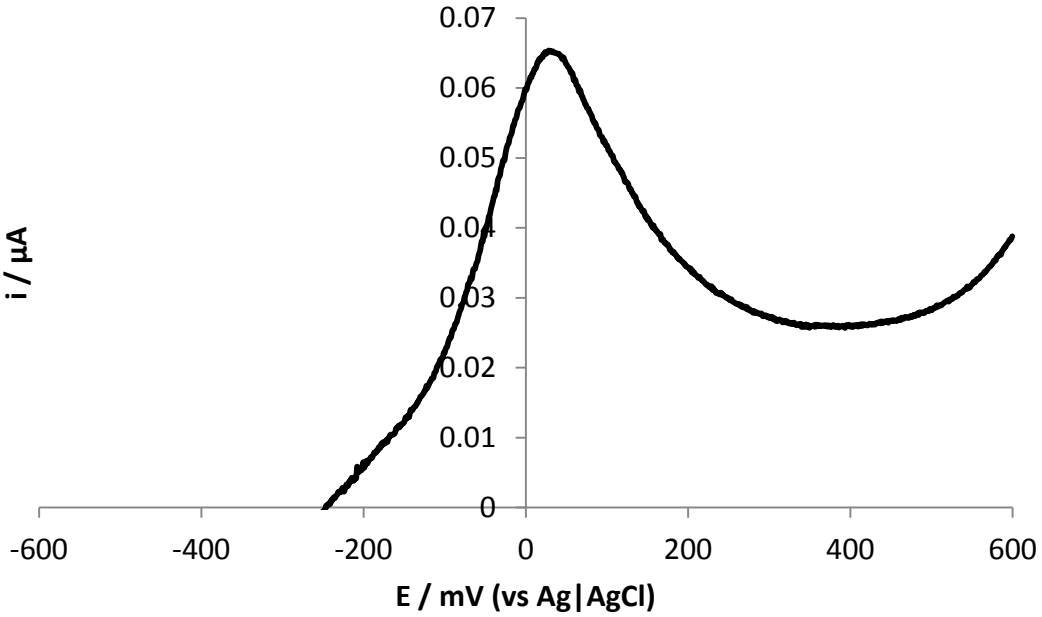

Figure 3.5: LSV of the $PMBNCQ_{10}$ modified GCE (v = 1mV s^{-1}).

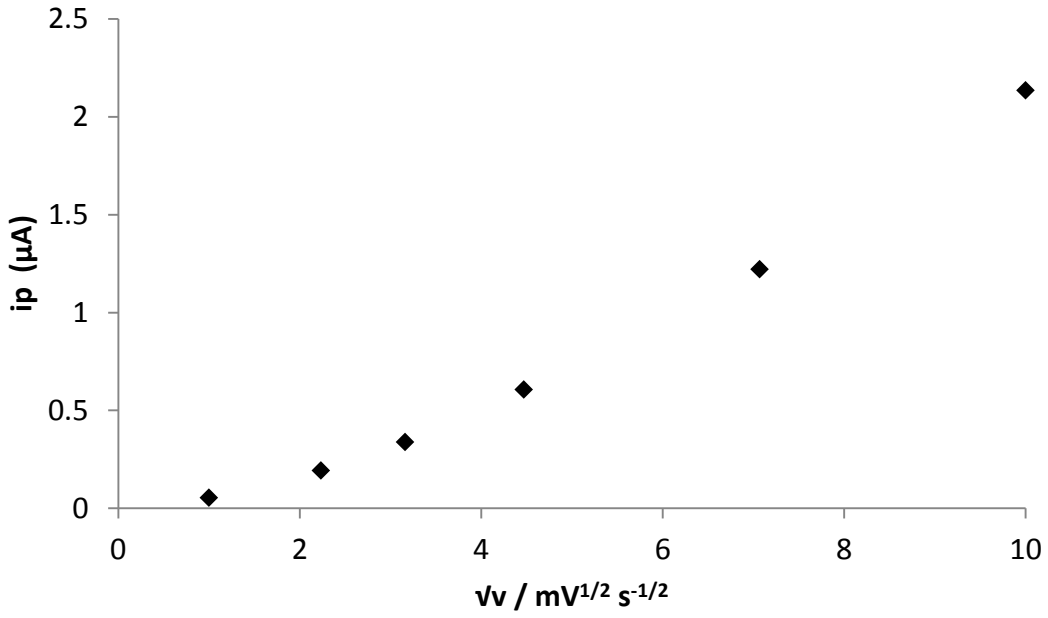

Figure 3.6: Anodic peak current density vs. square root of v for the PMBNCQ$_{10}$ modified GCE.

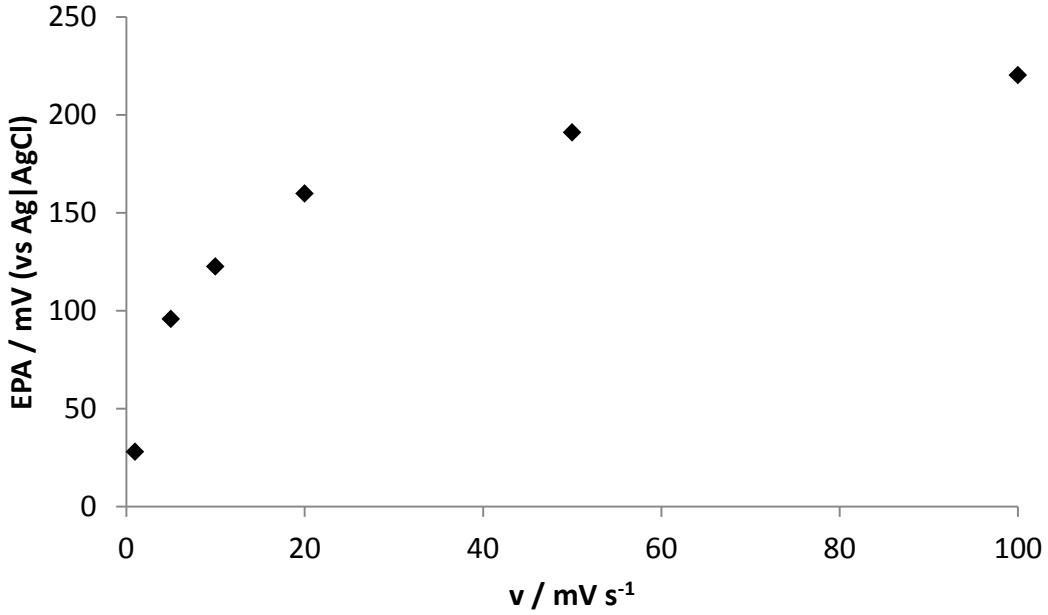

Figure 3.7: Anodic peak potential vs v for the PMBNCQ$_{10}$ modified GCE.

Figure 3.4 and Figure 3.5 show the electrochemical response of the PMBNCQ$_{10}$ electrode at various scan rates. Figure 3.4 shows a single reduction peak at ~ -350mV (vs Ag|AgCl)

corresponding to the single stage reduction of CQ_{10}. The oxidation peak at ~200mV (vs Ag|AgCl) corresponds to the oxidation of CQ_{10} as shown in equation 5.2. This data was used to generate Figure 3.6 and Figure 3.7. Figure 3.6 shows the relationship between the square root of the scan rate (v) and the anodic peak current density. The anodic peak current is proportional to the potential scan rate at $v < 10mV\ s^{-1}$ and overall the relationship is not linear, indicating the redox process is not highly chemically reversible. Figure 3.5 shows that the anodic peak potential becomes more positive as the scan rate is increased. This is also an indication of a lack of electrochemical reversibility. This lack of reversibility is likely due to complications in the electron transfer process. The complications most probably arise from the mechanistic complexity of the redox process for CQ_{10}. For example the two hydrogen two electron transfer may proceed through several possible routes, each one being more or less favoured by the nature of the environment.[159] As the redox process is taking place at the interface between a GCE and a phospholipid polymer, the availability of protons will affect the electrochemical reversibility of the redox molecule. Water molecules, protons and buffer components should all be able to interact with the immobilised CQ_{10}.[159] Therefore it was assumed that the availability of protons would not be an issue in this system.

Response of GCE|PMBNCQ$_{10}$ with GOx in Solution to Changing [Glucose]

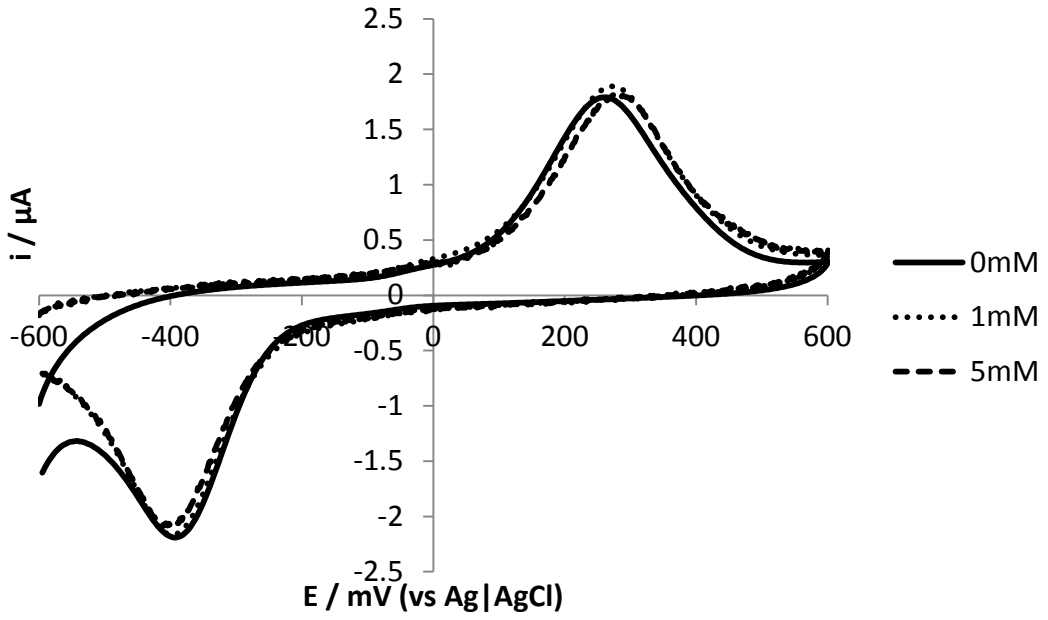

Figure 3.8: CVs of the PMBNCQ$_{10}$ electrode (v = 100 mV s^{-1}) in 0.1M PBS containing 0.5 mg ml^{-1} GOx at different glucose concentrations.

Figure 3.8 shows CVs of the PMBNCQ$_{10}$ electrode at different concentrations of glucose when 0.5 mg ml^{-1} of GOx was present in the electrolyte. The anodic peak current increases when the concentration of glucose in the electrolyte is raised to 1mM. This indicates that there is a larger concentration of $CQ_{10}H_2$ in the film attached to the electrode. This increase in the [$CQ_{10}H_2$] may be caused by regeneration of $CQ_{10}H_2$ from CQ_{10} by the reduced enzyme. The maximum anodic peak current is obtained at 1mM glucose concentration, consistent with the result obtained when GOx was immobilised (Section 2.3.5). Figure 3.8 also shows attenuation in cathodic peak current with increasing glucose concentration in the electrolyte. This may be due to a decrease in the availability of CQ_{10} caused by reduction of CQ_{10} by the reduced enzyme.

Figure 3.9 shows LSV data for the PMBNCQ$_{10}$ electrode at different concentrations of glucose when 0.5 mg ml^{-1} of GOx was present in the electrolyte. There is no increase in

anodic peak current when the cell glucose concentration is raised from 1 to 5mM as the enzyme is saturated with substrate and the reaction is taking place at its maximum rate. In order to check that this effect is not due to variations in peak current associated with multiple potential sweeps, potential sweeps were repeated for the same electrolyte concentration of glucose.

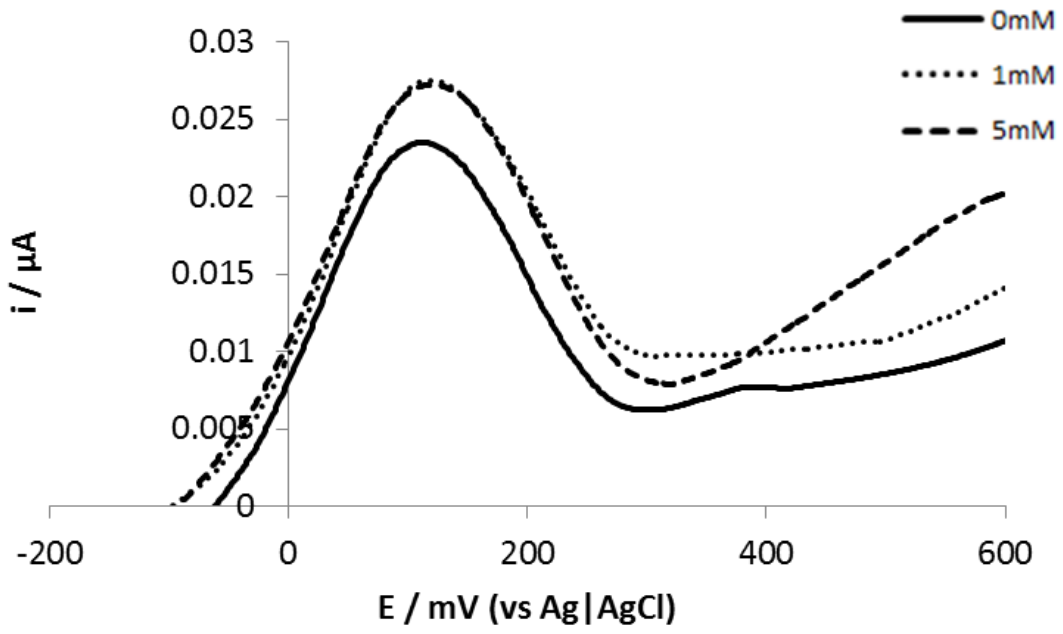

Figure 3.9: LSV's of the $PMBNCQ_{10}$ electrode (v = 1 mV s^{-1}) in 0.1M PBS containing 0.5 mg ml^{-1} GOx at different glucose concentrations.

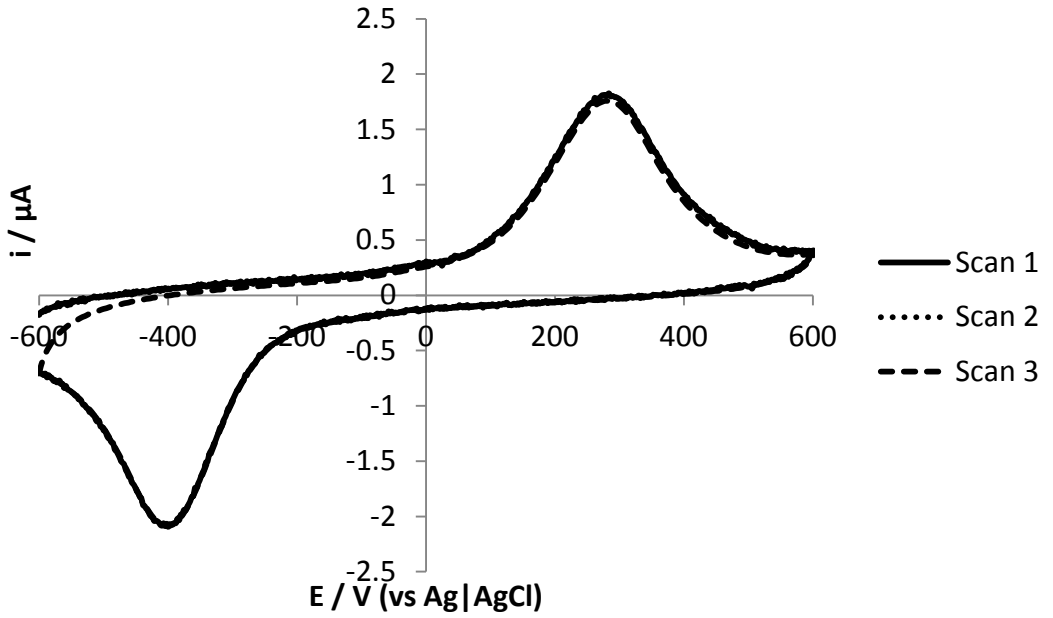

Figure 3.10: CVs of the PMBNCQ$_{10}$ electrode (v = 100 mV s^{-1}) in 0.1M PBS containing 0.5 mg ml^{-1} GOx, [glucose] = 1mM.

Figure 3.10: shows that there is virtually no variation in either anodic or cathodic peak current for multiple potential sweeps. This shows that PMBNCQ$_{10}$ may have be able to act as a redox polymer for GOx, however a significant proportion of the enzyme is unable to communicate with the CQ$_{10}$ although it remains enzymatically active.

It is therefore desirable to improve the electrical conductivity of the PMBN film to enhance the electron transfer from GOx to CQ$_{10}$ in the film. In order to improve the electrical conductivity of the PMBNCQ$_{10}$ film, multiwalled carbon nanotubes (MWCNT) and gold nanoparticles (AuNP) were incorporated into the film.

An MPCAG Electrode

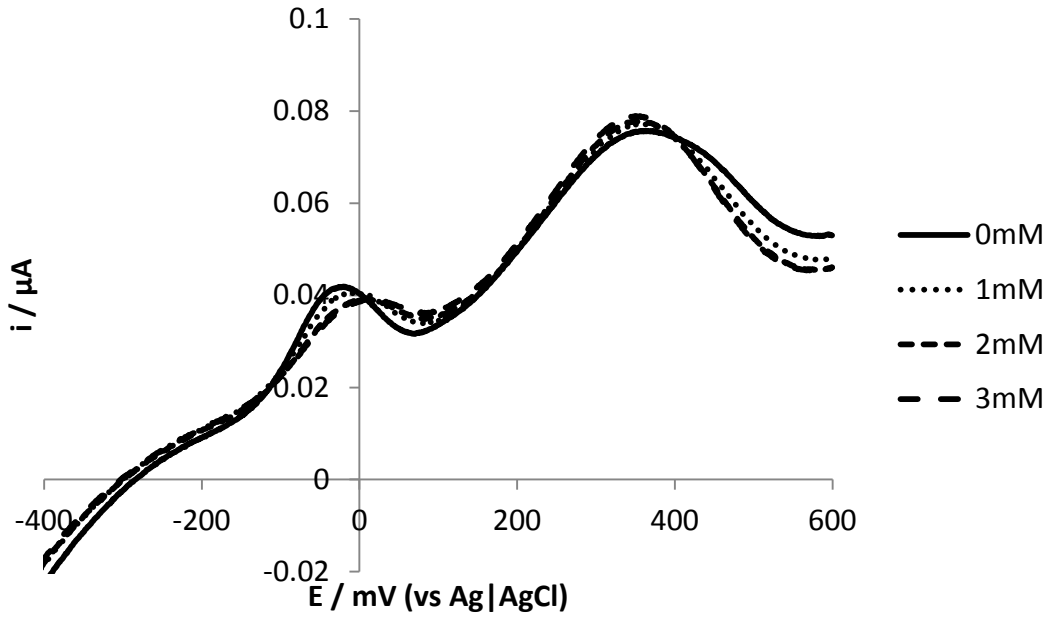

Figure 3.11: LSV's for a MPCA electrode (v = 1 mV s^{-1}) at different glucose concentrations.

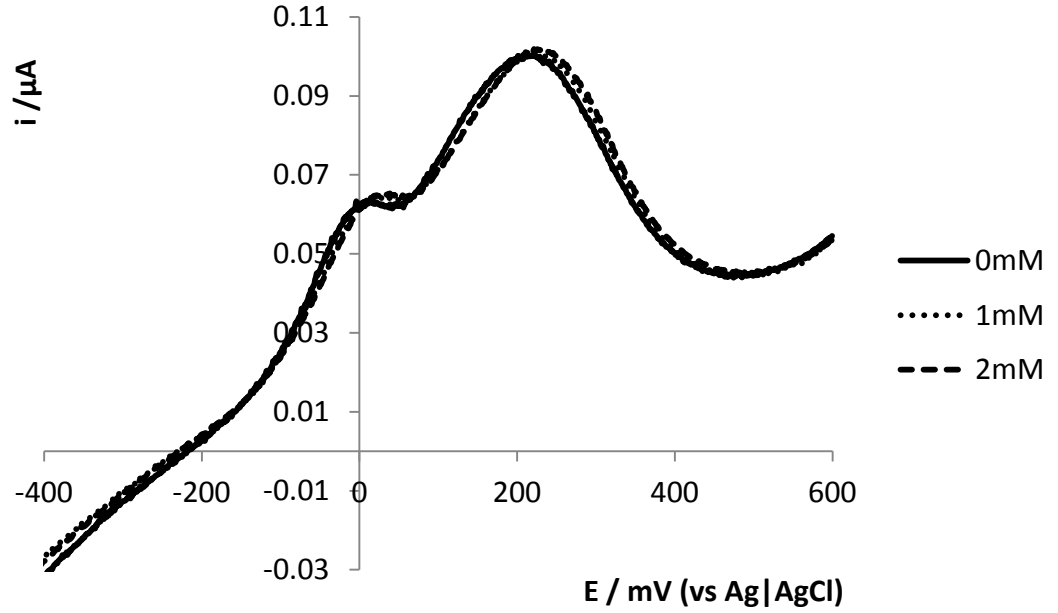

Figure 3.12: LSV's for a PCG electrode (v = 1 mV s^{-1}) at different glucose concentrations.

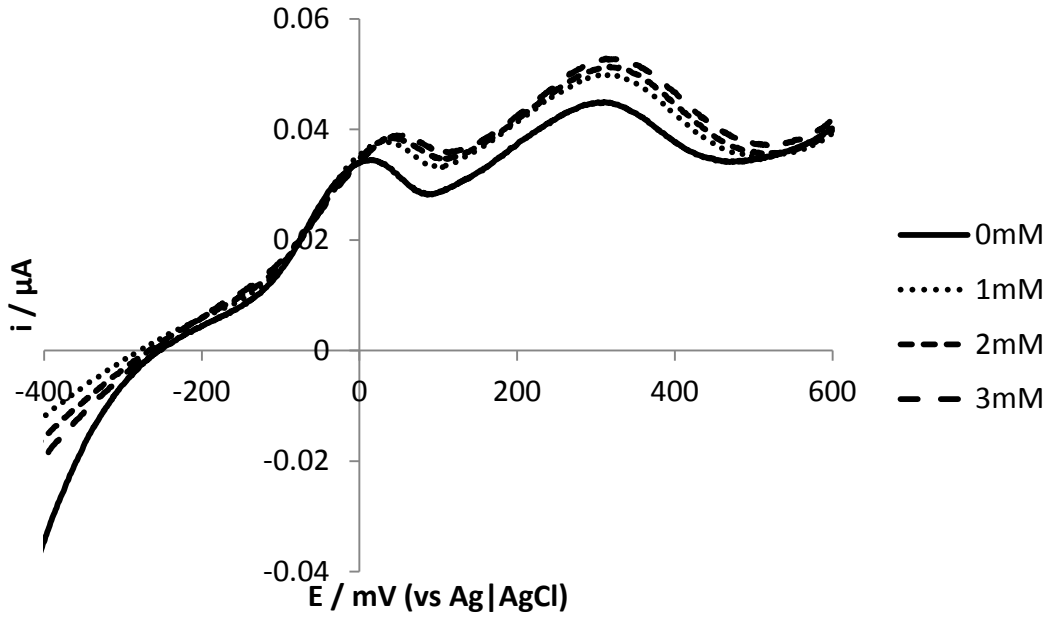

Figure 3.13: LSV's for a MPCAG electrode (v = 1 mV s^{-1}) at different glucose concentrations.

Figure 3.11 shows LSV data for a GCE modified with MWCNTs, $PMBNCQ_{10}$ and AuNPs at different glucose concentrations. This electrode is designated MPCA. Figure 3.12 shows LSV data for a GCE modified with $PMBNCQ_{10}$ and GOx at different glucose concentrations. This electrode is designated PCG. Both of these graphs show that no catalytic current response is seen when the glucose concentration is increased. The two oxidation peaks arise from the oxidation of $CQ_{10}H_2$ as in shown in equation 3.2:

$$CQ_{10}H_2 - 2e^- - 2H^+ \leftrightarrow CQ_{10} \qquad 3.2$$

The complex electrochemistry of CQ_{10} confined in a lipidic environment is very strongly dependent upon the pH and the environment surrounding the quinone redox head.[138c] The overall two-electron, two-proton transfer may proceed through several different pathways, depending on the nature of the environment.[138d] It has been proposed[111] that the two oxidation peaks seen in the CV scans are derived from:

1. Inter- and/or intra-molecular proton transfer process occurring at monolayer sites of an immobilised CQ_{10} film.
2. Electron transfer process between adjacent CQ_{10} molecules taking place at the inner layer of multilayer sites of the film.

Based on observations made using different concentrations of CQ_{10} in an immobilised film, the authors[111] concluded that the more positive oxidation peak corresponds to electron transfer from CQ_{10} molecules adsorbed onto the electrode as a multilayer. The less positive oxidation peak was assigned to CQ_{10} molecules residing in a monolayer on the electrode surface. Due to the slow mass transport of CQ_{10} through immobilised films, the charge transfer from CQ_{10} immobilised in a multilayer is most likely based on electron hopping, rather than diffusion of CQ_{10} to the electrode surface.

There are alternative explanations for these two oxidation peaks at neutral pH. It has been suggested that the two peaks correspond to two single discrete electron transfer steps, with a stable semiubiquinone as an intermediate between the reduced and oxidised form of CQ_{10}.[160]

It has been determined[134] that the electrons originate from positions two and three of the quinone ring, with the first transfer proceeding from the methoxy group in position three. The authors[134] proposed that the oxidation produces a dication with a positive charge localised on oxygen atoms of the methoxy groups of CQ_{10}.

It is most likely that the hydrophobic region of PMBN would be facing the GCE. Therefore the quinone ring of CQ_{10} must reside in this region as no redox response would be observed if the quinone ring was facing towards the electrolyte,[161] unless the quinone moiety had direct access to the electrode surface via pinhole defects in the phospholipid

film [162] and it has been shown[140] that such defects exist in phospholipid films. These pinhole defects could be induced by existing defects in the electrode surface.[140] In the case of diffusion through pinhole defects, the mass transport of CQ_{10} in the phospholipid film is related to the films structural integrity.[162]

Figure 3.13 shows data for a GCE modified with MWCNTs PMBNCQ_{10} AuNPs and GOx at different glucose concentrations. This electrode is designated MPCAG. This graph shows that there is an increased concentration of $CQ_{10}H_2$ detected when glucose is present in the cell. This arises from reduction of CQ_{10} by the reduced enzyme, demonstrating mediated electron transfer from GOx via CQ_{10} to the electrode. The combined effect of enzyme, MWCNTs and AuNPs gives rise to the electrocatalytic activity as Figure 3.11 and Figure 3.12 show that no electrocatalytic activity is seen when one or more of these components is missing. This can be attributed to an improvement in electron transfer between the enzyme and the mediator by the MWCNTs and the AuNPs.

The largest increase in oxidation current came with the first increase in glucose concentration from 0 to 1mM. Therefore the experiment was repeated with smaller increases in glucose as can be seen in Figure 3.14. This graph shows an increase in catalytic activity on going from 0 to 0.5mM glucose but does not show the same trend seen in Figure 3.13. This lack of reproducibility may arise from the heterogeneous nature of the enzyme-mediator-polymer mixture as it is composed of both hydrophilic and hydrophobic materials.[29]

Electrocatalytic activity could only be detected at scan rates of 1 mV s^{-1}. Therefore despite the presence of MWCNTs and AuNPs, the electron transfer kinetics for this material are still rather slow.

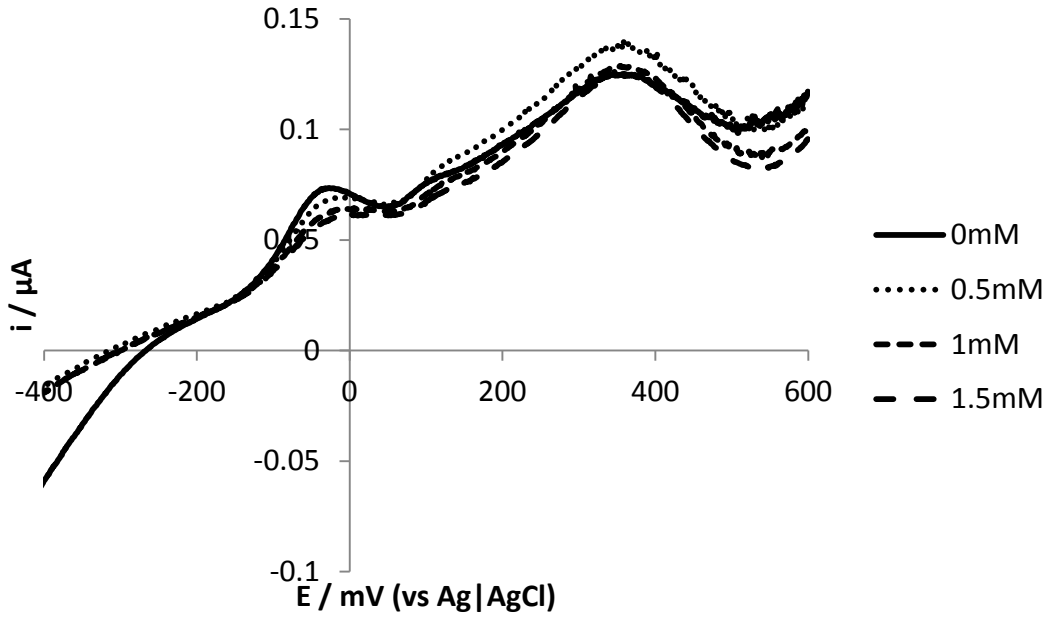

Figure 3.14: LSV's for a MPCAG electrode (v = 1 mV s^{-1}) at different glucose concentrations.

Figure 3.15 shows the response of the MPCAG electrode when increasing the electrolyte glucose concentration by 0.5mM every 5 minutes. The initial detection of was effectively instantaneous (stirred electrolyte) and a steady state current was reached 4 minutes and 21 seconds after the initial detection of the substrate. No further increases in concentration were seen after 0.5mM and it was assumed that the immobilised enzyme was saturated, i.e. reacting at its maximum rate and not capable of catalysing any further substrate.

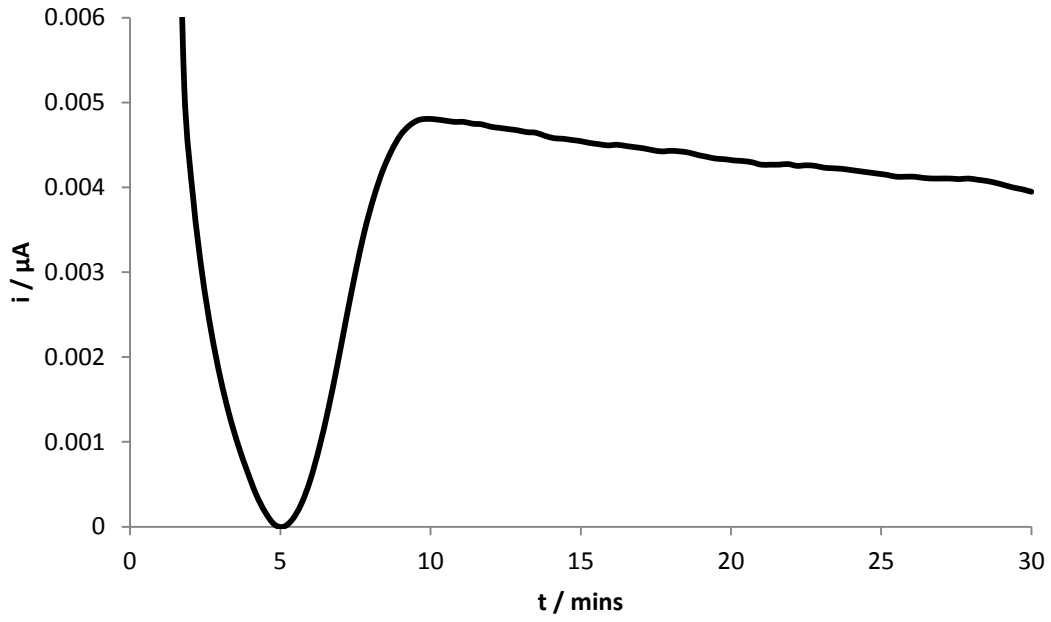

Figure 3.15: CA (E = 400mV (vs. Ag|AgCl)), 0.5mM glucose added every 5 minutes for the MPCAG electrode.

3.4 Conclusions

$PMBNCQ_{10}$ was shown to be electrochemically stable and could act as a redox mediator for GOx in solution. However the redox process is not highly chemically reversible. MWCNT and AuNPs were added to the electrode design to try to improve electron transfer within the $PMBNCQ_{10}$ film.

The MPCAG (MWCNT|$PMBNCQ_{10}$|AuNP|GOx) electrode showed electrocatalytic activity towards glucose. However the efficiency of mediation is not high enough compared to Fc. The long polyprenyl side chain in CQ_{10} is beneficial in producing redox polymers that do not suffer from mediator leaching, as the solubility of CQ_{10} is so low, however the diffusional restriction this places on the mediator is too severe to act as an efficient mediator for GOx.

Chapter 4 - Direct Electron Transfer with Glucose Oxidase

The aim of the work carried out in this chapter was to investigate the possibility of direct electron transfer (DET) between the active site of GOx and an electrode. An investigation into the electrocatalytic activity of an electrode based on DET was also carried out.

4.1 Introduction

Direct electron transfer (DET) can be considered as an enzyme catalysed electrode process. The electrode can be considered as an enzyme co-substrate. Enzymatic and electrode reactions form stages in the bioelectrocatalytic reaction mechanism. The catalytic effect of the enzyme is the reduction of the over potential for the reaction of the substrate with the electrode.

Traditionally mediators have been used to impose electron contact between the redox enzymes and electrodes. However DET is more attractive because it can not only help to understand the intrinsic redox behaviours of enzymes, but also to develop mediatorless biosensors and biofuel cells which are simple to manufacture and can produce high sensitivities/power outputs.[163] Also, systems utilising DET can be operated at potentials either at or close to the redox potential of the enzyme itself. The detection of DET is achieved by measuring the redox current associated with the FAD active site.

DET i.e. electron exchange between an enzyme and an electrode without the use of mediators has been observed between covalently immobilised GOx and a cyanuric chloride modified graphite electrode.[164] This was the first example of DET for covalently immobilised GOx. DET has also been observed for GOx absorbed onto anodised carbon electrodes, however the enzyme lost its activity due to denaturation.[165]

DET between immobilized GOx and an aminophenyl boronic acid modified GCE has been observed.[166] This was achieved by modifying the surface of glassy carbon rods with carboxylic acid groups.[166] (3-Aminophenyl)boronic acid (APBA) was then coupled to the carboxylic acid functions after activation with water-soluble carbodiimide to give GCE-APBA electrodes.[166] Interaction with GOx furnished GCE-APBA-GOx electrodes.[166] The authors presumed the enzyme was immobilised via formation of a complex between the sugar portion of the enzyme and boronic acid groups on the GCE surface.[166] The complexation apparently improved the accessibility of the FAD cofactor to DET with the electrode surface.[166] This report was also the first example of immobilisation of an enzyme via boronate groups.

APBA has been shown to promote DET between GOx and graphite by preventing the detachment of FAD from enzymes which are well situated and/or oriented to transfer electrons to the electrode.[167] However the authors stated that a significant driving force (overpotential) was needed in order to see any direct electron transfer using electrodes treated with APBA.[167]

It has been suggested that CNTs can be used to achieve DET due to the similarity in length scales between nanotubes and redox enzymes leading to DET favourable interactions.[168] As CNTs can be treated with acid in order to produce carboxylic and possibly phenolic groups on their surfaces, while also increasing their surface area, special opportunities can arise for the adsorption and entrapment of biological molecules in order to achieve DET.[168]

GOx has been found to spontaneously adsorb onto SWCNT bundles cast onto a GCE.[168] This was shown to give rise to DET, with the enzyme retaining its activity towards glucose.[168] The authors suggested that the DET arose from the nanotube fibrils becoming positioned within electron tunnelling distance of the cofactors.[168] The nanoscale dendrites of the CNTs project outwards from the surface and can act like bundled ultra-microelectrodes that allow access to the active site and permit DET to the adsorbed enzyme.[168] During the process of enzyme adsorption, the authors suggest small assemblies of CNTs (possibly individual nanotubes) can approach and be physically located within the electron tunnelling distance of the prosthetic group FAD of the enzyme.[168] Thus because of the nanostructured topology of CNT surfaces, the electrode can be positioned close to the enzymes active site whilst retaining the enzymes structure.[168] A useful analogy is provided by the authors, they liken the carbon nanotube to a needle which can be carefully inserted into a balloon such that it doesn't pop, and the needle is now free to interact with the contents of the balloon, while the balloon still retains its air and its shape.[168] The skin of the balloon being the enzymes glycoprotein shell, and the contents of the balloon being the FAD centre. Such access is not provided by smooth, polished electrode surfaces.[168]

Dispersing CNTs with a surfactant such as cetyltrimethylammonium bromide has promotion effects on DET with GOx when immobilised onto a surface of CNTs immobilised onto a GCE.[169] A similar effect was observed using 3-Aminopropyltriethoxysilane as the surfactant.

Also, SWCNT can be immobilised onto a Au surface by modifying the surface first with cysteamine and then aligning shortened SWCNT to the electrode surface via self-assembly.[170] The nanotubes can then be plugged into GOx in one of two ways[170]:

1) native GOx is covalently attached to the ends of the aligned tubes which allowed close approach to FAD and DET to be observed.

2) FAD was attached to the ends of the tubes and the enzyme reconstituted around the surface immobilized FAD, which gave rise to more efficient electron transfer.

DET has also been observed using CNT powder microelectrodes.[171] The authors proposed that the detection of DET using CNTs is improved by the high local electron density at topological defects in CNT lattices.[171]

Use of Nanoparticles for DET

A colloidal gold modified GCE has been shown to promote DET with GOx.[172] The achievement of DET using colloidal gold can be attributed to the properties of this material as described in Section 3.1. It also provides an environment similar to that of redox proteins in native systems and gives the protein molecules more freedom in orientation, thus reducing the insulating property of the protein shell for DET and facilitating the electron transfer through the conducting tunnels of colloidal gold.[172]

In a similar approach, GOx can be co-deposited onto a GCE with nickel-oxide nanoparticles in order to achieve DET.[173] The authors suggest that the DET resulted from the efficient electrical conductivity of the nickel-oxide nanoparticles in a similar way to AuNPs, with the possibility that the nickel-oxide nanoparticles could act as molecular wires, similar to CNTs, due to their size.[173] DET with GOx can also be achieved by entrapping both CNTs and GOx in a biological polymer such as chitosan.[174]

The authors suggest that entrapment in chitosan produces a conformational change in GOx which improves access to the active site, giving rise to DET.[174] DET with GOx can be revealed by combining the beneficial effects of chitosan, AuNPs and CNTs on an electrode surface.[175]

Biofuel cells have been developed utilising DET for GOx on the anode.[163] This was achieved using MWCNT modified electrode surfaces. MWCNT are an attractive material for DET based electrodes as they have all the benefits of SWCNT such as excellent stability and nanoscale structure but also exhibit higher conductivity than SWCNT.[163] The authors found that immobilising GOx onto a MWCNT surface resulted in partial denaturation of the enzyme, providing increased access to the active site, facilitating DET.[163] An electrode utilising MWCNT incorporated into a cellulose matrix along with GOx has been shown to exhibit DET.[176]

Chitosan

Chitosan (β-1,4-poly-d-glucosamine) is an amine and carboxyl containing crystalline polysaccharide.[174, 177] It has one amino group and two hydroxyl groups in a repeating hexosamide residue.[178] It is derived from deacetylation of natural chitin.[174] When exposed to aqueous solution, it displays the properties of a hydrogel.[177a] Chitosan has various desirable properties for use in enzyme electrodes, e.g. biocompatibility, low toxicity, excellent film forming ability, high permeability towards water, good adhesion, chemical inertness and high mechanical strength.[179] It is also in-expensive.[180] Chitosan molecules also contain lots of amino groups, which have high affinity for AuNPs.[179a] It has been shown to be a convenient polymeric scaffold for enzyme immobilization[181] as

well as being able to stabilise AuNPs, improving the performance of AuNP/chitosan based enzyme electrodes.[180] Depositing chitosan and AuNPs can provide a biocompatible microenvironment for GOx to withstand changes in external conditions such as solution pH.[179b]

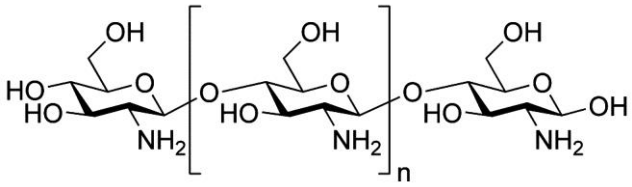

Figure 4.1: The chemical structure of chitosan.

The entrapment of GOx and AuNPs in a chitosan matrix at an electrode surface can increase the retention of GOx at the electrode surface and also increase the effective surface area of the electrode.[180] Also chitosan deposited onto a GCE surface has been shown to be mechanically stable.[182]

Chitosan has been modified with Fc to create a redox polymer mediator. Electron transfer in the polymer mediator was increased with the addition of MWCNTs. The fast electron transfer in the CS-Fc/MWCNT film was attributed to the charge hopping between neighbouring conductive MWCNTs and Fc redox sites that mediate the effective charge migration thorough the polymer[28].

4.2 Experimental

Materials

Chitosan was obtained from Sigma-Aldrich (Dorset, UK), all other materials were obtained as described in Section 2.2 and Section 3.2.

Electrode Preparation Procedure

2.5µl of 2mg ml^{-1} MWCNT (in DMF) were added to a polished GCE. The DMF was then evaporated using a lamp. Next 1ml of a 1.264µM AuNP solution (2nm) was added to 1ml of 1% w/v chitosan solution. The resulting solution was 632 nM AuNP / 0.5% w/v chitosan. 10mg of GOx was then added to this solution giving an enzyme concentration of 5mg ml^{-1}. This solution was added to a three electrode cell (Pt CE, Ag|AgCl RE) and the cell was sparged with N_2. A CA was then carried out for 5 minutes at -0.3V to deposit the chitosan film, incorporating the AuNPs and the GOx.

4.3 Results & Discussion

In this section, DET between immobilised GOx and an electrode, facilitated by MWCNTs and AuNPs will be investigated.

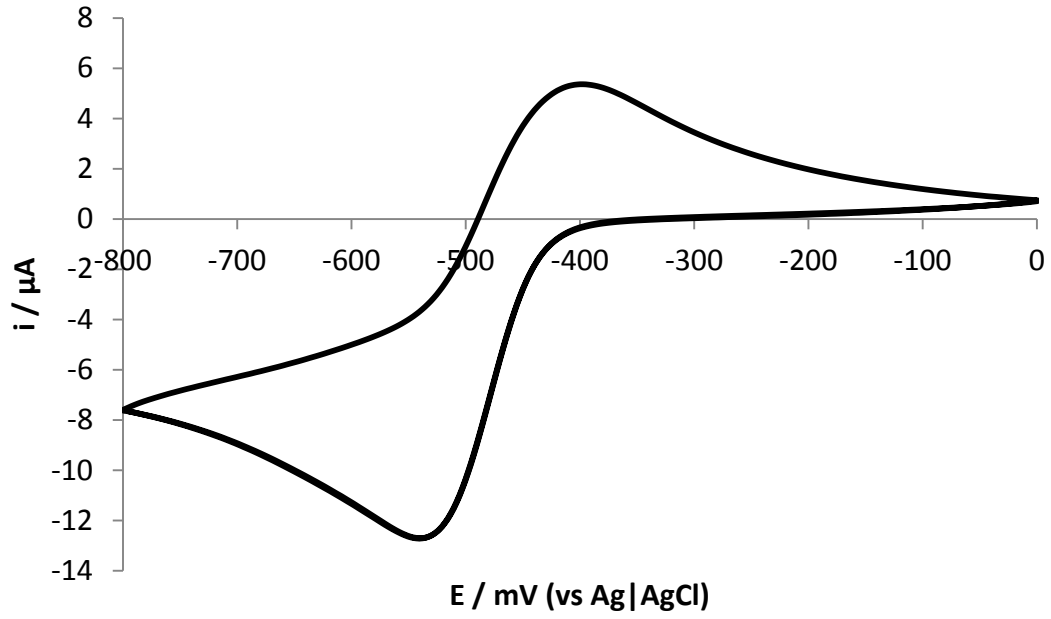

Figure 4.2: CV (v = 5mV s^{-1}) for 5mM FAD in 0.1M PBS (pH7).

Figure 4.2 shows CV data for FAD dissolved in PBS. The $E_{1/2}$ is ~ - 470mV (vs. Ag|AgCl). Therefore if the MWCNT|Chitosan-AuNP-GOx (MCAG) electrode exhibits direct electron transfer the $E_{1/2}$ from the CV data should be in this region.

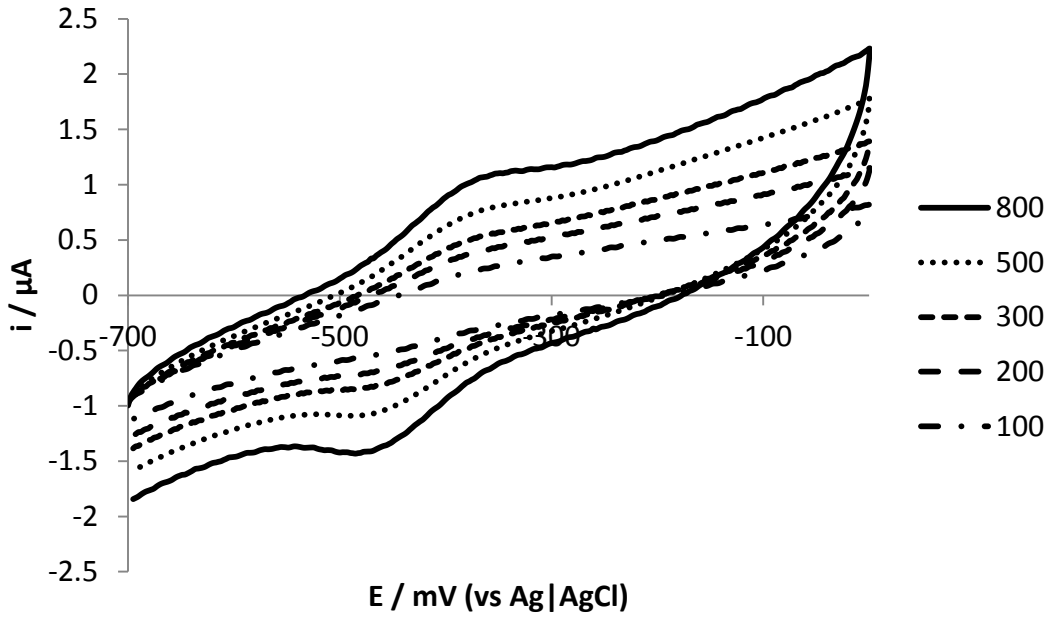

Figure 4.3: CVs for the MCAG electrode in N_2 PBS (pH 6.8) at various scan rates.

Figure 4.3 shows CV scans for the MCAG electrode. The $E_{1/2}$ is ~ - 450mV (vs. Ag|AgCl) indicating that this redox peak arises from the FAD centre of the bound GOx. The scan rate dependence of the redox peak currents was studied, and the results are shown in Figure 4.4.

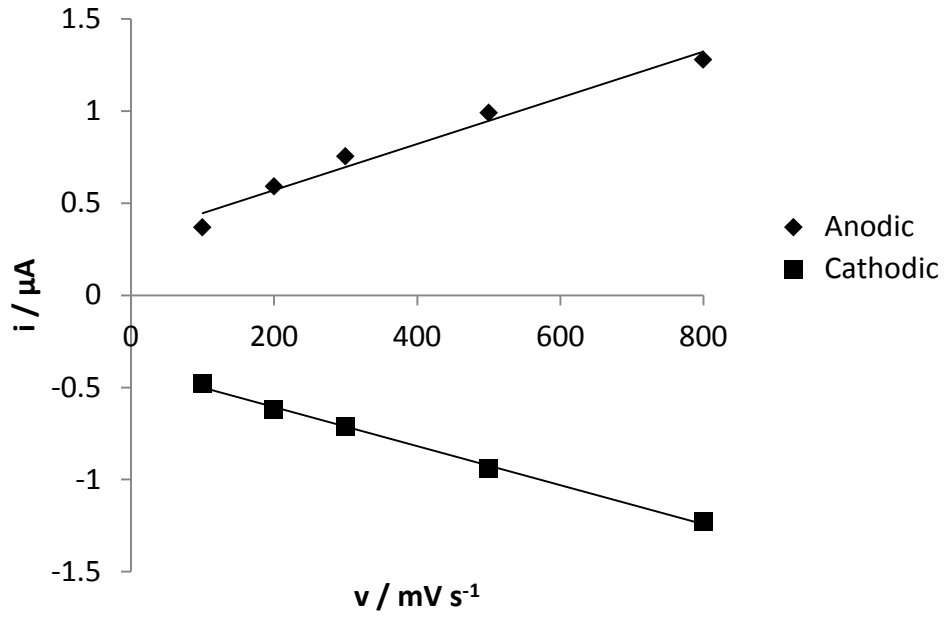

Figure 4.4: Plots of peak current densities vs. scan rate for the MCAG electrode.

The anodic and cathodic peak currents for the immobilised GOx were both linearly proportional to the scan rate in the range 100 to 800 mV s^{-1} indicating a surface controlled electrochemical process. Also, i_{pa}/i_{pc} ~ 1 indicating good reversibility.

The CV scans of the different modified electrodes were studied in deaerated PBS and two redox peaks with a formal potential of ~ -450mV (vs. Ag|AgCl) were observed for the GOx modified electrode as shown in Figure 4.5. In contrast, no such peak was observed for the electrode modified with the same materials except without the enzyme. Thus confirming that the redox peaks observed at the enzyme modified electrode arise from the direct electrochemistry of GOx.

The decrease in capacitance seen in Figure 4.5 for the electrode containing the enzyme is attributed to the inhibition of electrical conduction between the electrode and the CNTs by the insulating enzyme.

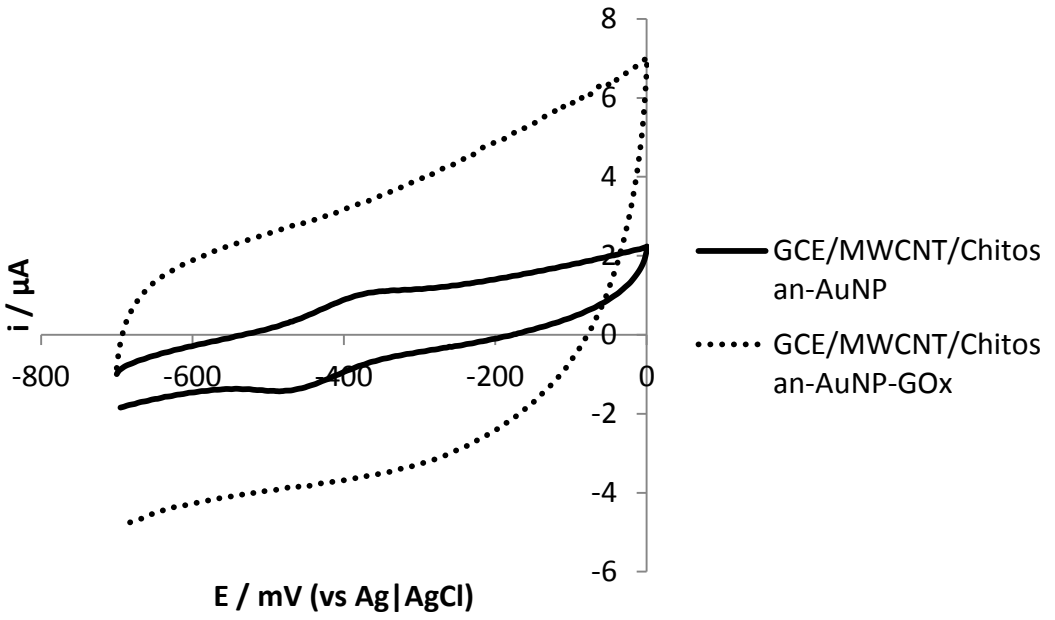

Figure 4.5: CV scans of the MCA and MCAG modified electrodes (v = 800mV s^{-1}) in N_2 saturated PBS (pH 6.8).

Note also that the redox peaks associated with the enzyme cannot be seen at scan rates lower than 100mV s^{-1}. This shows that the electron transfer rate between the enzyme active site and the electrode is very fast and cannot be detected with slower scan rates. The resistance of the chitosan film is also very high as the CV scans in Figure 4.3 show. The shape of the scan is similar to that of a pure resistor.

The Response of the Enzyme Electrode to Glucose

To confirm whether the immobilised GOx retains its enzymatic activity while demonstrating DET, glucose was added to the deaerated PBS in the cell. As can be seen from Figure 4.6, the oxidation peak current of GOx increased with the addition of glucose, suggesting that the immobilised enzyme retained its enzymatic activity while exhibiting direct electrochemistry.

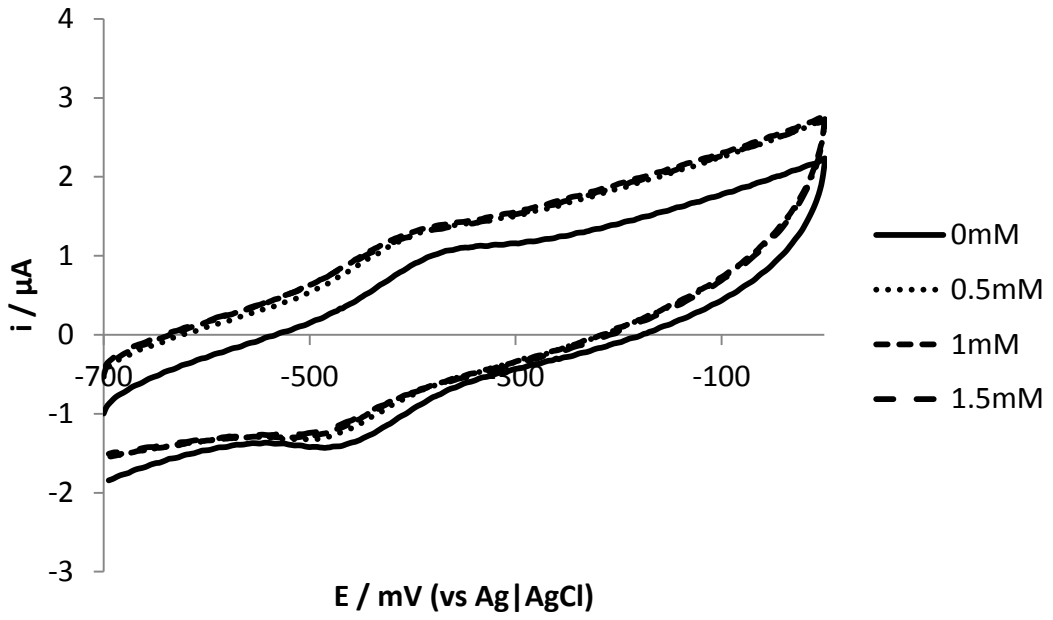

Figure 4.6: CV scans for the MCAG modified electrode at different concentrations of glucose (v = 800 mV s^{-1}).

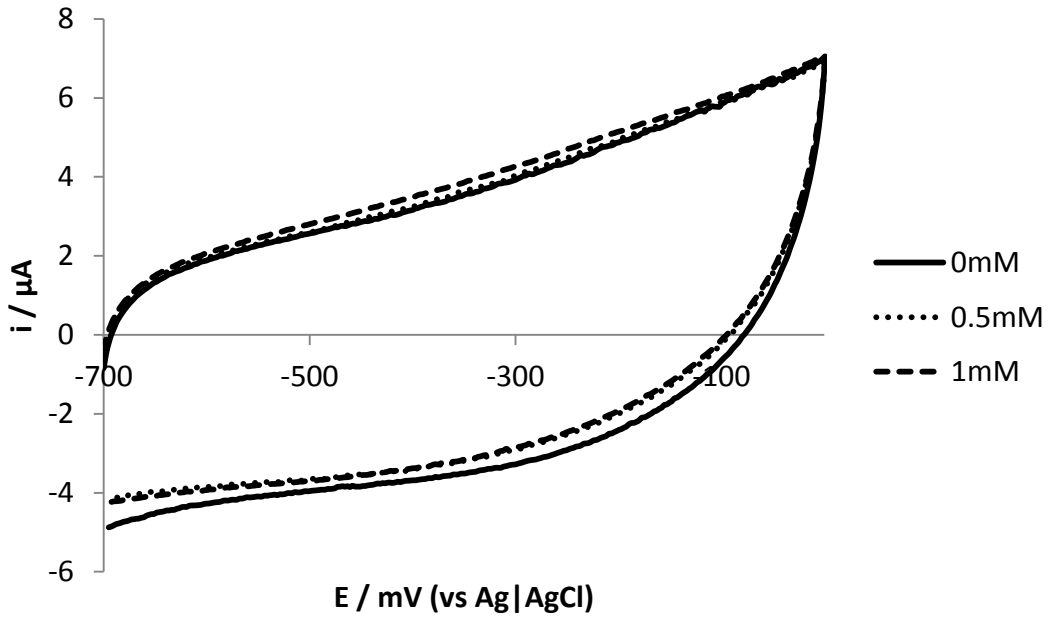

Figure 4.7: CV scans for the MCA modified electrode at different concentrations of glucose (v = 800 mV s^{-1}).

Figure 4.7 shows the response of the same electrode except without the enzyme to different concentrations of glucose. No increase in oxidation peak current can be seen in

Figure 4.7 confirming that the electrocatalytic activity seen in Figure 4.6 comes from the immobilised enzyme.

It can be seen in Figure 4.6 that the electrode is not sensitive to changes in glucose concentration above 0.5mM. This may be due to the high scan rates needed to observe the redox activity of the enzyme. This means that the observed current is under kinetic control and therefore mass transfer of the substrate will not be able to influence the observed current.

4.4 Conclusions

An MCAG electrode was fabricated and exhibited DET from the active site of GOx to the electrode surface, with good reversibility. When exposed to glucose, the electrode was shown to be electrocatalytically active. However, the electrode was not sensitive to changes in glucose concentration above 0.5mM. This may be due to the high resistance of the chitosan film. There is also an issue with DET regarding access of the active site to substrate, when CNTs are used to achieve DET. The presence of the nanotube in the vicinity of the active site makes DET possible; however this then blocks access for glucose, limiting the electrodes catalytic activity.

Chapter 5 - A Glucose|Air Fuel Cell with GOx and Bilirubin Oxidase Enzyme Electrodes

The aim of the work carried out in this chapter was to develop and test a glucose|air enzymatic biofuel cell (EBC). The enzyme electrodes in the fuel cell are based on GOx and Bilirubin Oxidase (BOD). An additional aim of this chapter was to base the fuel cell design on screen printed electrodes in order to reduce the complexity of the fabrication procedure for the cell, which can be an issue in EBC design. Once fabricated, the performance of the fuel cell was tested.

5.1 Introduction

An enzymatic biofuel cell (EBC) is a fuel cell which uses organic matter as fuel and enzymes as electrode catalysts, converting chemical potential energy into electrical energy via electrochemical reactions involving biochemical pathways.[183] This electrochemical transduction is accomplished by utilizing enzymes to bio-catalyse oxidation and reduction reactions.[184]

EBCs have many advantages over conventional fuel cells, chiefly the ability to operate in physiological conditions. Due to the high selectivity of enzymes, membranes are not needed in EBC design, unlike fuel cells which utilise noble metal catalysts, as neither the crossover of glucose to the cathode compartment nor the crossover of O_2 to the anode compartment prevents the operation of the cell.[2] The reproducible, low cost manufacture of membranes and cases of sub-millimetre dimensions (as would be needed for implantable devices) is difficult.[185]

The fact that separation of fuel and oxidant is not needed in EBCs means they can be significantly scaled down in size and can therefore find applications in biologically

implantable devices, making use of fuels and oxidants present in such environments. With the added advantage of reaction products being tolerable to organisms and only present in low concentrations.[1]

It has been estimated that, using EBCs the number of conventional components of fuel cells can be reduced by eight, with no need for a case, case seal, membrane, membrane seal, ion conducting electrolyte (e.g. phosphoric acid), plumbing to the cathode compartment and plumbing to the anode compartment.[186]

Because glucose is present in all tissues and organs, the fuel-storing reservoir, plumbing for fuel delivery and fuel pump are not needed.[186] Because O_2 is present in all organs and tissues, air breathing membranes for cathode compartments are not needed.[186] Two components of conventional fuel cells and batteries which are difficult to miniaturize are the case (usually made of stainless steel) and its seal.[186] The case confines the strongly acidic or basic electrolyte and the gaseous, volatile or reactive reactants of fuel cells and batteries. Because EBCs can operate in a physiological fluid and the reactants are glucose and O_2, and because gluconate, the glucose electrooxidation product, is non-toxic, no case is needed.[186] In the absence of the case there is no need for the case seal and for the air-breathing membrane of the cathode compartment, which is hydrophobic on the air-side (to prevent the electrolyte from oozing out by capillary action) and is wetted by the catholyte on the inside (for rapid delivery of O_2 to the catholyte).[186] The two components which are particularly difficult to miniaturize, the membrane separating the anode and cathode compartments of conventional fuel cells and its seal, are eliminated.[186]

EBCs have another advantage over fuel cells utilising noble metal catalysts, cost. Enzymes are derived from natural sources and can be manufactured at very low cost using well-established fermentation techniques.[1] However, the cost of conventional noble metal catalysts, particularly platinum, is expected only to increase with increased production and demand.[1]

The exploitation of ambient fuels is attractive in situations where power needs for small electronic devices are distributed, disconnected, and long-term.[1] This might be true for electronic sensor systems for monitoring of plant health, air quality, weather, or the presence of biohazards.[1] In principle, the fuel can be derived from carbohydrates contained in plants or from effluent of human or animal processes.[1] Mammalian blood is also an excellent source of glucose and oxygen that can be utilized as a reactant and oxidant, respectively, in a fuel cell to produce power.[18] The concentration of O_2, an important substrate of GOx based EBCs is ~ 45 µM in human blood and ~ 200 µM in aq. solutions in air.[187]

Enzymes such as GOx and Bilirubin oxidase (BOD) have no known toxicity in the milligram quantities considered for EBCs, and some synthetic species have received "Generally Recognized as Safe" (GRAS) status from the U.S. Food and Drug Administration (FDA).[1] EBCs as energy sources in implantable devices are particularly attractive compared to conventional power sources (usually batteries) as the energy supply is potentially unlimited as it is derived from physiologically ambient sugars.

By immobilising the enzyme and mediator onto the electrode surface, and taking advantage of ambient convection in physiological environments, it is possible to create EBCs that do not need to be housed in any sort of compartment, again leading to the

possibility of significant miniaturisation of EBC devices. Also, the lack of any compartment means that the design of any such device is much simpler than conventional fuel cells.

It is desirable to contain enzymes and electron-transfer mediators within an electrode volume to maintain concentration and activity.[1] In the case of diffusional mediators, this requires the use of semipermeable barriers such as polymer membranes, intended to prevent flux of mediator species out of the electrode.[1] The use of redox polymers that contain biocompatible materials is also essential. Frequently complexes of osmium are used as electron mediators. This is undesirable as the neat tetroxide of osmium is a strong oxidizer and is considered "highly toxic" in the U.S. and "very toxic" by the European Union.[1] Therefore EBCs that do not use this material are desirable.

Bilirubin oxidase (BOD)

Bilirubin oxidase (BOD) is used as the O_2 reducing catalyst on the cathode of the EBC studied in this chapter. It is produced by a range of organisms including fungi, bacteria and animals and catalyses the oxidation of Bilirubin (the yellow breakdown product of haem catabolism, responsible for the yellow colour of bruises and the background straw-yellow colour of urine, amongst other things) to biliverdin as well as the oxidation of other tetrapyrroles, diphenols and aryl diamines, with the concomitant reduction of dioxygen to water.[188] It has a molar mass of 60-64 kDa and is a monmeric multi-copper oxidase containing type 1, type 2, and type 3 coppers (in the ratio 1:1:2) (the labels type 1 (T1) type 2 (T2) and type 3 (T3) are derived from the spectroscopic and magnetic properties of the copper atoms in their enzyme active site environment) similar to

Laccase, ascorbate oxidase, and ceruloplasmin.[188a, 189] It catalyses the four electron electroreduction of O_2 to H_2O without producing reactive intermediates such as H_2O_2 or $O_2^{\cdot -}$.[186, 188a, 188c, 189]

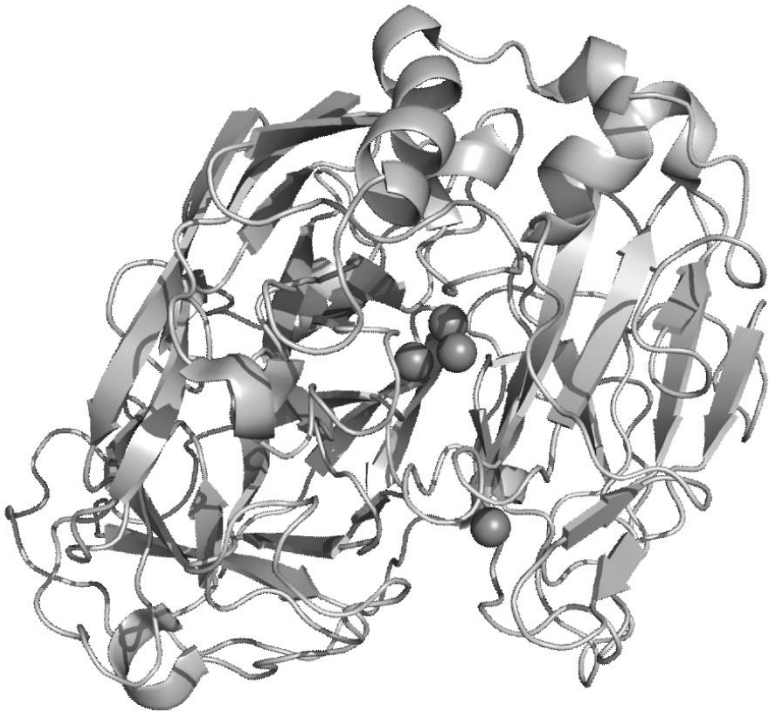

Figure 5.1: The structure of BOD showing the four Cu atoms at its centre.

It has been shown that the T1 site (lying in a shallow cleft on the surface of the enzyme) is the primary centre, at which electrons are accepted from reducing substrates.[188b, 188d] Electrons are transferred, one at a time, via internal pathways to the trinuclear T2/T3 cluster which converts O_2 into H_2O in a four electron reaction.[188d, 190] The unique characteristic of immobilised BOD is the absence of inhibition of the copper based enzyme at pH 7.2 or by chloride, differentiating it from both Laccase and dissolved BOD, which are inhibited.[191] Both Laccase and BOD have four $Cu^{+/2+}$ redox centres. One of

the Laccase centres (the T2 centre) is inactive at neutral pH and is inhibited by Cl^-.[191] BOD has also been shown to be much less sensitive to high concentrations of bromide, which deactivates Laccase.[1] This makes BOD promising for use in implantable devices as it will be active under the conditions imposed by blood serum.[18] An important feature of BOD is its ability to catalyse the reduction of oxygen without producing toxic oxygen intermediates.[190] The highest activity for BOD has been reported at low pH (pH 4), however, the reaction can also be catalysed in the neutral pH range.[190] Other advantages of the enzyme are its ability to retain a high activity in the presence of high concentrations of molecular oxygen and its comparatively good stability.[190] Thus, BOD is an interesting and promising candidate for application in biofuel cells and biosensors.

BOD also has important biochemical properties for biotechnological applications, such as high activity, stability, and low extent of glycosylation.[188b] BOD has a redox potential at pH 7 under air of 530 mV (vs Ag|AgCl).[185] This may be positive enough to generate a useful cell voltage when used in conjunction with a Fc mediated GOx electrode in an EBC. When adsorbed on spectrographic graphite, BOD has been shown to largely decrease the overvoltage needed for the electroreduction of molecular oxygen.[188b] A positive sign for the use of BOD on other carbon electrodes. An electron transfer from a redox mediator into the T1 centre of BOD has already been reported.[190] The authors stated that this site is also interesting for a heterogeneous electron transfer at electrodes.[190] The distance between the electrode-contacting enzyme surface and the T1 site at its closest approach can be less than 10 Å, short enough for electrons to be transferred from the electrode to the T1 site, but only when the enzyme is uniquely oriented.[188c] The electron is then intra-molecularly transferred by a Cys-2His pathway to

the T2/T3 cluster, across a distance of ~ 13 Å, where it reduces the copper-cluster-bound O_2.[188c] Another positive sign is the fact that DET has been observed for BOD on carbon electrodes.[188b] Immobilisation of BOD on plastic formed carbon by electrostatic entrapment in the cationic polymer poly-l-lysine (taking advantage of the fact that BOD has a net negative charge in neutral solution, because of its isoelectric point of 4.2) was shown to give rise to DET from BOD to the electrode surface.[192] The authors suggest that the DET could either arise from BOD adsorbed in a monolayer at the surface of the electrode or that BOD is free to diffuse within the polymer to exchange electrons with the electrode surface. The authors also note that BOD exhibits a high affinity for negatively charged molecules, suggesting that the vicinity of the active centre of BOD would be positively charged. This is good news for DET to carbon based materials as they tend to have highly oxygenated surfaces, providing an electrostatic attraction for the active site of BOD, facilitating DET. It has been confirmed independently that the active site of BOD is indeed surrounded by positively charged patches, resulting from a positively charged arginine residue close to the active site, as well as other hydrophilic residues in this surface area.[193] It has been shown that the inclusion of CNTs in the design of an enzyme electrode can promote DET from BOD to an electrode surface.[194] The nanotubes provide docking places for the enzyme and thus, can effectively replace the natural substrate of BOD – Bilirubin, which is delivering electrons for the oxygen reduction in the catalytic cycle.[190] Direct adsorption of BOD onto MWCNT immobilised on a Au electrode has been shown to give rise to DET.[195] Pyrene-functionalised SWCNTs have also been shown to promote DET with BOD.[196] DET from BOD to an electrode surface has also been shown for Au electrodes modified with 3-mercaptopropionic acid.[188c] BOD

adsorbed onto Au(111) electrodes modified with C_3–$SO3_H$ and C_n–COOH (n = 2, 5 and 7), showed the electrocatalytic currents of dioxygen reduction based on DET,[197] with the authors noting that negatively charged electrode surfaces can give a suitable molecular orientation for DET. DET can also be achieved by immobilising BOD onto AuNPs.[198] Modifying Au electrodes with MWCNT can enable DET from BOD to the electrode surface, with the MWCNT replacing Bilirubin as the substrate of BOD.[199] The authors stated that a high activity of BOD could be retained when using MWCNTs, and that the electron transfer from the electrode to the enzyme was efficient.[199] BOD is superior to pure platinum as an electrocatalyst of the four-electron electroreduction of O_2 to H_2O. Not only is its overpotential for O_2 reduction lower, but unlike platinum, it is not affected by organic compounds like glucose, or the oxidation product of glucose, gluconolactone.[2, 200]

Pyrene

In the EBC developed in this chapter, pyrene is used in the cathode preparation procedure to facilitate the immobilisation of BOD and improve the electron transfer properties of the electrode.

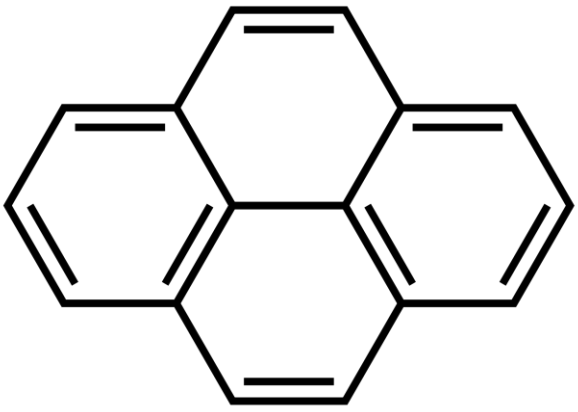

Figure 5.2: The structure of pyrene.

Pyrenyl groups have been shown to have strong π- π interactions with the sidewalls of nanotubes.[130] SWCNT functionalised with pyrene have been shown to improve direct electron transfer to enzymes such as BOD.[196]

5.2 Experimental

Materials

1-pyrenebutyric acid, N-hydroxysulfosuccinimide (Sulfo-NHS) were purchased from Sigma-Aldrich (Dorset, UK) and used without further purification.

Bilirubin oxidase (BOD) from *Myrothecium verrucaria* (Amano Enzyme Inc.), purified by hydrophobic interaction chromatography using a HiTrap™ Phenyl HP hydrophobic column (GE Healthcare) was kindly donated by collaborators in Oxford, UK.[130]

Carbon screen printed electrodes (CSPE) modified with a layer of single walled carbon nanotubes (SWCNT) were purchased from Dropsens (Oviedo, Spain).

All other materials were purchased as described in Section 2.2.

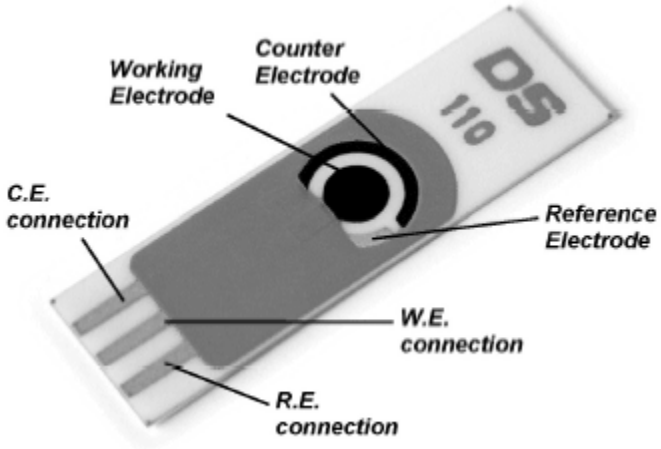

Figure 5.3: This figure shows the CSPE used in this study.

5.2.1 Anode Preparation

A CSPE was modified with FcNafionGOx (1% w/w Nafion in 90% ethanol containing 5mM Fc and 50mg ml^{-1} GOx (12,500 units ml^{-1})), similar to the method outlined in Section 2.2.7 except with a higher GOx content (50mg ml^{-1} as opposed to 5mg ml^{-1}) in order to increase the performance of the fuel cell.

5.2.2 Cathode Preparation

The cathode preparation method was based on a method described previously.[130] Briefly, 15µl of 1-pyrenebutyric acid solution (10mM in DMF) was added to a CSPE modified with a layer of SWCNT. This was left in the dark for one hour to generate strong π-π stacked interactions between the SWCNT and the Pyrene. The electrode was then washed with distilled water. Next, 15µl of EDC|Sulfo-NHS solution (0.4M EDC, 0.1M Sulfo-NHS) was added to the electrode and left for 20 minutes. The electrode was again washed with distilled water. Then 15µl of an 8mg ml^{-1} BOD solution (in 0.1M PBS, pH7) was then added to the electrode. This was then kept at 4°C overnight to allow covalent linking of the activated carboxylic acid groups on the Pyrene and BOD.

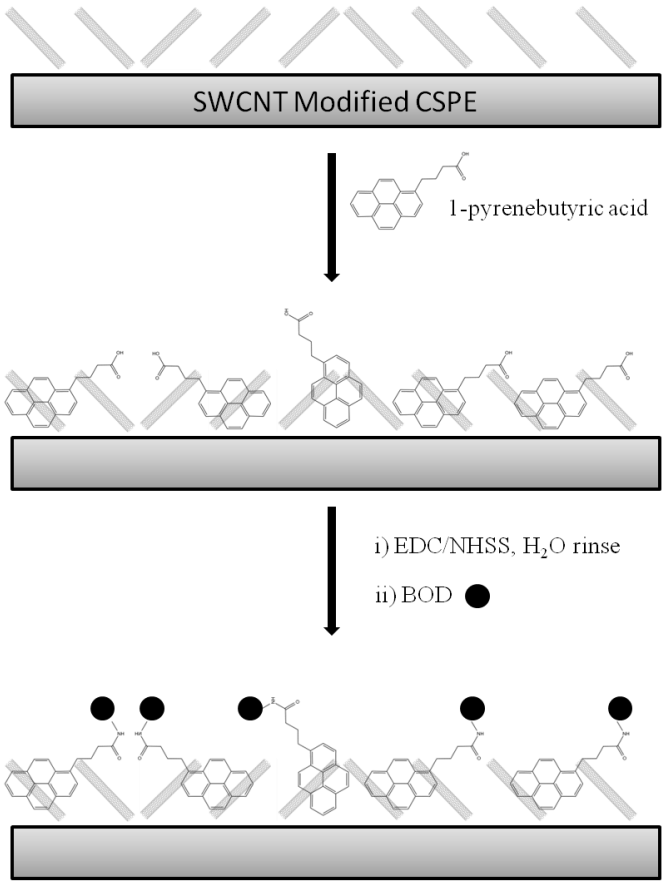

Figure 5.4: Schematic representation of the cathode preparation procedure.

5.2.3 Electrochemical Test

The power output and current production of the cell were tested using a resistor box and a multimeter. The resistor box was placed between the anode and the cathode in the circuit with the cell electrolyte completing the circuit. The resistance between the anode and the cathode was lowered from 10MΩ to 0.2MΩ in sequential steps while the cell voltage was measured using the multimeter. The cell voltage was recorded 30s after each change in resistance. The cell glucose concentration was made up to 10mM before the start of the experiment.

5.3 Results & Discussion

In this section, the performance of a glucose|air EBC, fabricated using screen printed electrodes (SPEs) is discussed. GOx was used as the glucose oxidising enzyme on the anode and BOD was used as the O_2 reducing enzyme on the cathode.

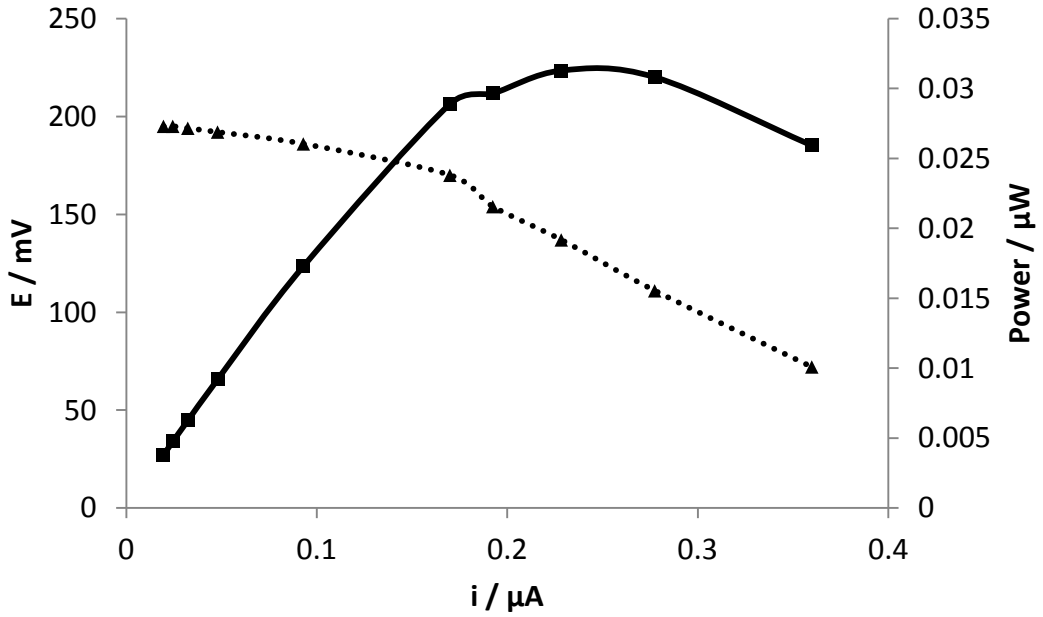

Figure 5.5: Polarization curve (solid line) and power performance curve (dotted line) for the enzymatic biofuel cell. Glucose concentration = 10mM.

Figure 5.5 shows the performance of the enzymatic biofuel cell constructed from the glucose oxidising anode and O_2 reducing cathode. The results are summarised in Table 5.1.

R_{OPT} / MΩ	E_{OPT} / mV	i_{MAX} / µA	P_{MAX} / µW	OCP / mV
0.60	137	0.360	0.031	195

Table 5.1: Summary of results from Figure 5.5.

The performance of the cell was hampered by the lack of a sufficient seal between the anode and cathode compartments. This caused electrolyte to leak from the cell. The effect of the leaking is seen in the ohmic loss region which is unusually short.

Rubber gaskets were then added to the cell to improve the seal between the two compartments. The electrochemical test was then repeated and the results are shown in Figure 5.6.

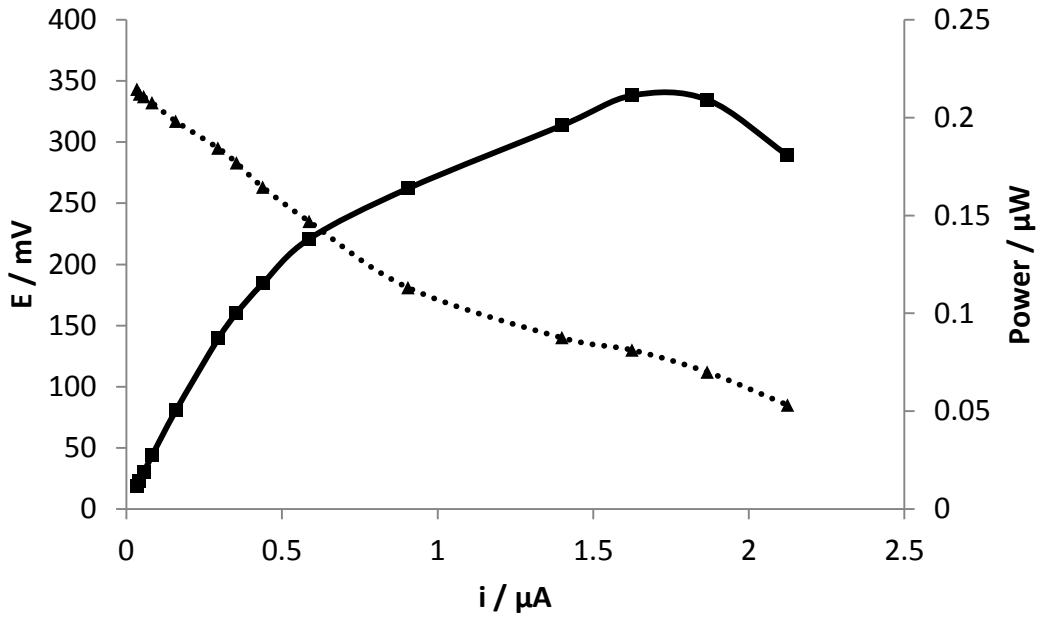

Figure 5.6: Polarization curve (solid line) and power performance curve (dotted line) for the enzymatic biofuel cell including rubber gaskets. Glucose concentration = 10mM.

	R_{OPT} / MΩ	E_{OPT} / mV	i_{MAX} / uA	P_{MAX} / µW	OCP / mV
Test 1	0.60	137	0.360	0.031	195
Test 2	0.08	130	2.130	0.211	343

Table 5.2: Summary of results from Figure 5.6 (Test 2) and from the previous test (Test 1, Figure 5.5).

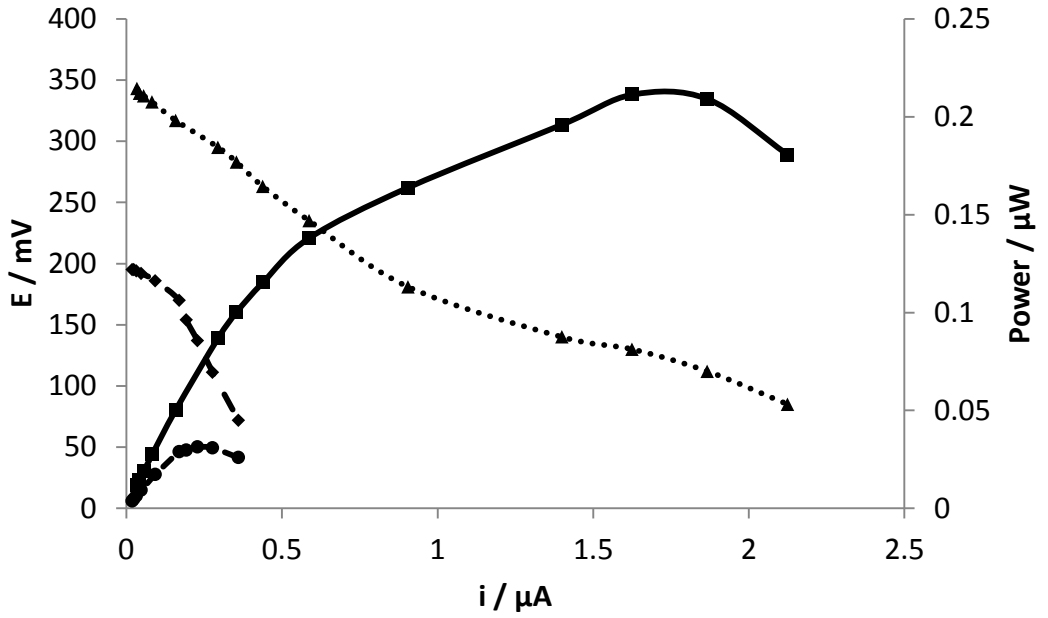

Figure 5.7: Data from Figure 5.6 compared with polarisation curve (dashed line) and power performance curve (large dashes) from previous test (Test 1).

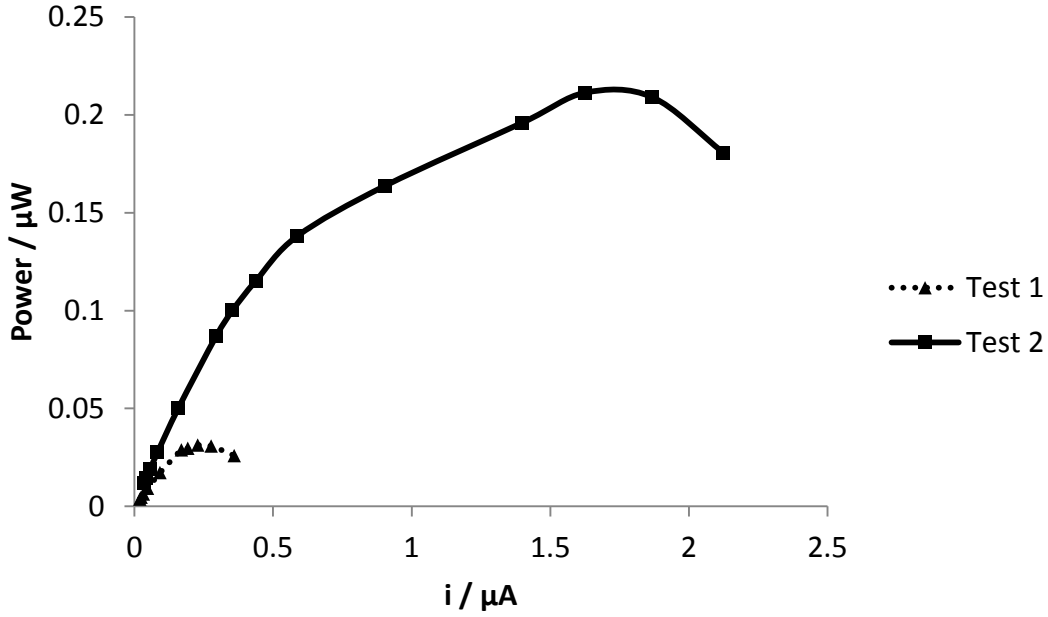

Figure 5.8: Power performance curves for Test 1 and Test 2.

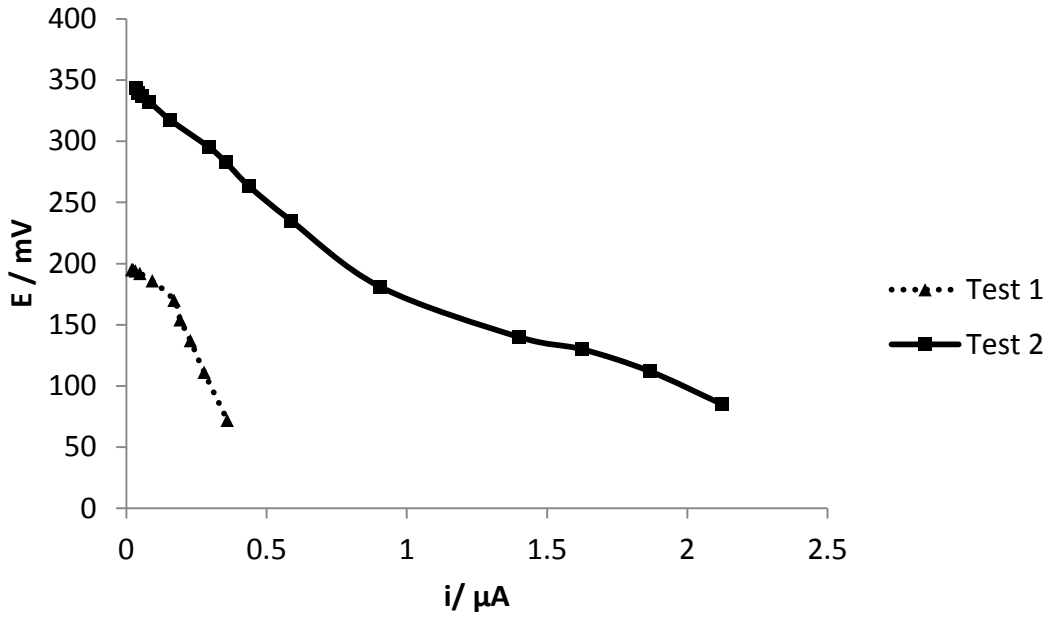

Figure 5.9: Polarisation curves for Test 1 and Test 2.

The test was then repeated using SWCNT modified CSPE on both the anode and cathode in order to improve the conductivity of the anode and therefore improve the performance of the cell. The results of this test are shown in Figure 5.10.

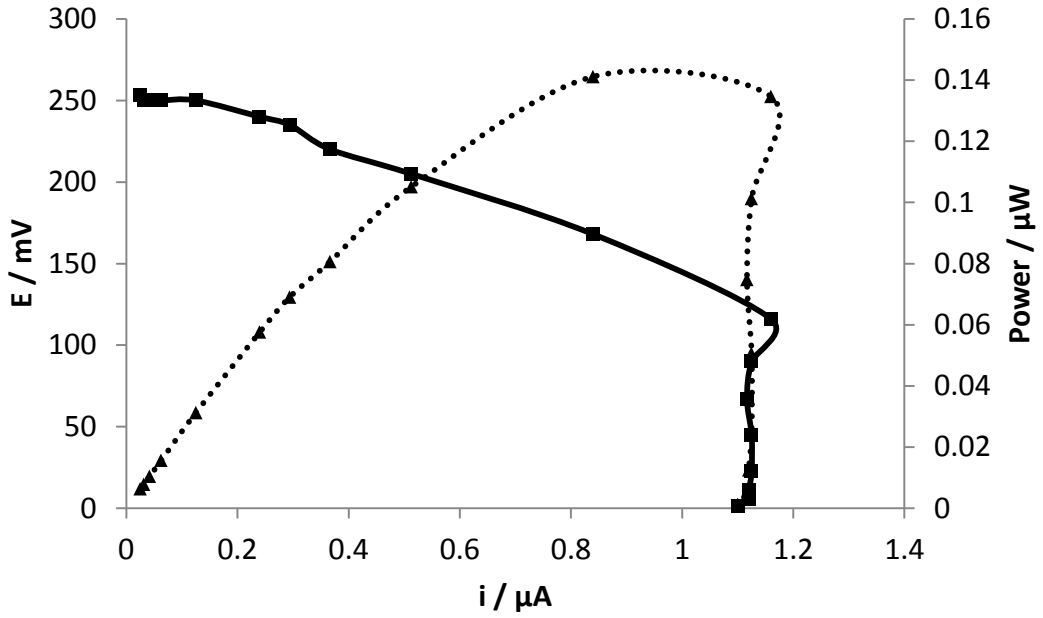

Figure 5.10: Polarization curve (solid line) and power performance curve (dotted line) for the enzymatic biofuel cell using SWCNT modified CSPE for both the anode and the cathode. Glucose concentration = 10mM.

	R_{OPT} / MΩ	E_{OPT} / mV	i_{MAX} / uA	P_{MAX} /µW	OCP / mV
Test 1	0.60	137	0.360	0.031	195
Test 2	0.08	130	2.130	0.211	343
Test 3	0.20	168	1.120	0.141	253

Table 5.3 Summary of results from Figure 5.10 (Test 3) and from the previous tests.

It can be seen that using SWCNT on both the anode and the cathode does not have an effect on the performance of the cell. This indicates that the performance of the cell is limited by the enzyme containing redox polymer on the anode and not the conductivity of the anode electrode substrate.

5.4 Conclusions

A glucose|air fuel cell was fabricated using CSPEs. GOx was used as the catalyst on the anode and BOD was used as the catalyst on the cathode. The SPEs were housed in

custom made perspex holding blocks. Initially, the performance of the cell was hampered by the lack of a sufficient seal between the anode and cathode compartments. This caused electrolyte to leak from the cell.

Rubber gaskets were then added to the cell to improve the seal between the two compartments. The presence of the gaskets prevented electrolyte leaking from the cell and this improved the cells power output.

Tests were then carried out using SWCNT modified CSPEs for both anode and cathode in order to improve the conductivity of the anode and therefore improve the performance of the cell. This did not have an effect on the performance of the cell. This indicates that the performance of the cell is limited by the enzyme containing redox polymer on the anode and not the conductivity of the anode electrode substrate.

Chapter 6 - Application of a GOx Enzyme Electrode for Simultaneous Detection of Glucose and NEFA

The aim of the work carried out in this chapter was firstly to investigate the possibility of using the layer by layer (LBL) electrode fabrication method to successfully immobilise GOx. The electrocatalytic activity of a GOx enzyme electrode based on this fabrication method was investigated. Further to this the possibility of the simultaneous detection of two analytes (glucose and non-esterified fatty acids) from a single mixed sample using enzyme electrodes was investigated.

6.1 Introduction

In this chapter, the feasibility of an electrochemical enzyme based biosensor for the simultaneous detection of non-esterified fatty acids (NEFA) and glucose is investigated. The detection of NEFA is based on the layer by layer (LBL) modification of CSPEs with multilayer films of poly(dimethyldiallyammonium chloride) (PDA) wrapped MWCNTs and two enzymes, acyl-CoA synthatase (ACS) and acyl-CoA oxidase (ACOD).

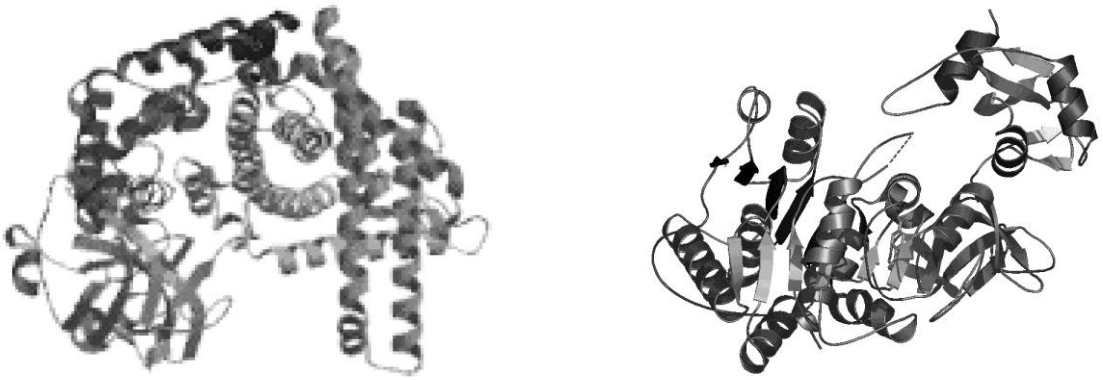

Figure 6.1: The structures of ACOD (left) and ACS.

The detection of glucose is based on FcNafionGOx modified CSPEs. The rapid simultaneous detection of NEFA and glucose can provide useful information for the

treatment of diabetes. Currently there is a lack of suitable technology to characterise and measure such complex biomarker combinations outside of the laboratory. Diabetes is increasingly understood as disordered energy metabolism involving both sugar and fat utilisation. Patients with Type 2 diabetes (T2D) often show a higher level of non-esterified fatty acids (NEFA), associated with increased insulin resistance (IR) and poor glucose disposal rate (GDR). NEFA is an important skeletal muscle fuel source. The change in plasma NEFAs is a useful indicator of the rate of lipolysis. An increase in plasma NEFAs can induce insulin resistance by inhibition of muscle glucose transport, resulting in the reduction in the rate of muscle glycogen synthesis. Therefore it is important to monitor the concentrations of NEFA and glucose levels in T2D patients. In a healthy adult heart, NEFA, glucose and lactate are metabolized for ATP production in the mitochondria.[201] However, in a diabetic heart, glucose and lactate oxidation are decreased and fatty acid oxidation is increased, increasing the oxygen requirement per ATP molecule produced. T2D patients with apparently normal cardiac function have impaired myocardial and skeletal muscle energy metabolism related to changes in circulating metabolic substrates. Another reason why information relating to the concentrations of these substances is important for the treatment of T2D. Plasma NEFA levels are slightly affected by the immediate eating of fatty foods.[202] As well as being a vital energy source, circulating blood NEFAs can affect the regulatory function on pancreatic β-cells and skeletal and smooth muscle metabolism of glucose. A small increase in blood NEFA levels maintains basal insulin secretion throughout fasting and is crucial in keeping a normal insulin secretory response to glucose. The levels of NEFA seen during fasting can predict the change from normal glucose tolerance to impaired

glucose tolerance (IGT) and the reverse. Plasma NEFA concentration is therefore used as a diagnostic marker for identification of people at greater risk of developing T2D prior to the appearance of IR and insulin secretion defects. This is of particular importance in providing early diagnoses of T2D, assessing the degree of myocardial infarction and other obesity-related illnesses. NEFA, like glucose can reflect acute change of the energy status from an individual, thus its concentration in blood can be used as a biomarker for diabetes. Diabetes research in Newcastle studied the second-meal phenomenon and effect of exercises in T2D monitoring both NEFA and glucose concentration changes, and suggested that dietary manipulation and exercise could have considerable implications in people with diabetes.[203] Existing diabetes management promotes self-monitoring of blood glucose for disease management and secondary prevention. The monitoring of the changes of both sugar and NEFA during metabolic processes would provide a more accurate means of diagnosis, prediction of the risk and subsequently, more effective means of disease prevention.[204] Moreover, it would offer more comprehensive information of the patient's metabolic profile, for both patient and clinician, and would therefore lead to better disease management. This shows that there is a significant benefit in the development of an electrochemical biosensor allowing simultaneous monitoring of both NEFA and glucose. The LBL technique used in the fabrication of the NEFA detecting electrode is one of the most promising methods for surface modification and biomolecule immobilisation because it is simple, versatile and can be applied to a wide range of materials that can be used for film assembly.[205] The method is mostly based on electrostatic assembly of oppositely charged polyelectrolytes to a charged solid surface. It has been widely used for modifying materials with functional coatings, materials

encapsulation, biosensing and other applications.[206] Enzymes are polyelectrolytes and therefore their charge depends on their pKa and the solution pH. Knowledge of both the enzyme pKa and polymer pKa allows the facile immobilisation of enzymes into LBL films, allowing the activity of the immobilised enzyme to be maintained.[207] An issue with commonly used polyelectrolytes for LBL immobilisation onto electrodes is a lack of electrical conductivity.[206c, 208] This problem can be alleviated by incorporating CNTs into the LBL film.

PDA is a strong polycation that can be well adsorbed on carbon or gold electrodes.[209]

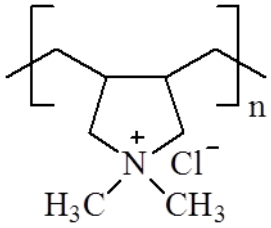

Figure 6.2: The chemical structure of PDA.

It has been reported to have good affinity for CNTs and AuNPs.[210] By incorporating carbon nanotubes into PDA, a conductive composite can be formed which can be used to immobilize enzymes in the LBL manner for electrochemical biosensor applications.[209b, 211]

6.2 Experimental

Materials

Oleoyl coenzyme A lithium salt (OACoA), Palmitoyl coenzyme A (PACo-A), coenzyme A sodium salt hydrate (CoA), adenosine 5′-triphosphate disodium salt hydrate (ATP), and glucose were purchased from Sigma-Aldrich (Dorset, UK). Oleic acid (OA) and acyl-CoA synthatase (ACS) were from the Wako HR-series NEFA-HR(2) enzymatic NEFA

assay kit (Neuss, Germany). Acyl-CoA oxidase (ACOD) was purchased from Wako (Japan). Palmitic acid (PA) was purchased from Cayman Chemical Company. PDA (Mw= 200-250 kDa) was kindly provided by Surflay Nanotech GmbH (Berlin, Germany). Carbon screen printed electrodes (CSPE) were purchased from Dropsens (Oviedo, Spain). Parafilm was purchased from (Bemis Flexible Packaging).

6.2.1 Fabricating a PDA-MWCNT|GOx Electrode

15 µl of PDA-MWCNT solution was dropped onto the working electrode of a Dropsens CSPE at 4°C for 30 minutes. The electrode was then washed with 15 µl of PBS (0.1M, pH 6.8) twice to remove the excess PDA-MWCNTs that did not adsorb or were weakly adsorbed. Next, 15 µl of 50mg ml^{-1} (12,500 units ml^{-1}) GOx solution (in PBS) was dropped onto the PDA-MWCNT modified electrode and also kept at 4°C for 30 minutes. The electrode was again washed with 15 µl of PBS to complete the first (PDA-MWCNT|GOx) double layer coating on the electrode. Two double layers of (PDA-MWCNT|GOx) were assembled on the electrode. The multilayer film was assembled without drying during each deposition step.

6.2.2 Entrapment of GOx in a layer of PDA-MWCNT

In order to trap GOx in a layer of PDA-MWCNT, 20µl of a sonicated mixture of PDA-MWCNT was mixed with 1mg of GOx to form a 50mg ml^{-1} (12,500 units ml^{-1}) PDA-MWCNT-GOx solution. 15µl of this solution was then added to a Dropsens CSPE and kept at 4°C for 30 minutes. The solution was then removed from the electrode and the electrode was then washed with 15 µl of PBS (0.1M, pH 6.8) twice to remove the excess PDA-MWCNT-GOx that did not adsorb or was weakly adsorbed. Finally the

electrode was placed in a cell containing 500µl of PBS. The cell was sparged with N_2 and a N_2 blanket was maintained throughout the experiment.

6.2.3 Fabrication of the PACo-A/OAcoA detecting Electrode

The fabrication of the PACo-A/OAcoA detecting electrode (the NEFA detecting electrode) was based on the method described in Section 6.2.1. Briefly, four double layers of ACOD and PDA-MWCNT were immobilised on the NEFA detecting electrode. The coating solutions were ACOD (4 units ml^{-1} in PBS) and 1% wt. PDA containing 0.6 mg ml^{-1} MWCNT. 15µl of each solution was added to the NEFA detecting electrode every 30 minutes. The electrode was kept at 4°C between each coating step. The electrode was washed with PBS (0.1M pH7) between each coating step.

The fabrication of the glucose detecting electrode was as described in Section 5.2.1.

The electrodes were tested using Chronoamperometry at 0.3V (vs Ag QRE) and CV (v = 100mV s^{-1}) in a perspex cell containing 300µL of PBS (0.1M, pH 6.8).

6.2.4 Preparation of standard solution of PA

OA is available commercially as a solution and can therefore be used as received but is more expensive than PA. PA is available as a solid and is much cheaper. However it is sparingly soluble in aqueous solution and it is therefore necessary to dissolve it in ethanol before it can be used in electrochemical tests.

25.6 mg of PA (256.42 g/mol) was weighed into a 10 ml volumetric flask and dissolved in about 2 ml of warm ethanol (35-40^{o}C). The volumetric flask was immediately sealed with Parafilm and allowed to cool to 15-25^{o}C. About 8 ml of PBS was added to the solution, with slow stirring to avoid the formation of microcrystals at the point of entry. It

was then stirred using a magnetic stirrer for a further 30 minutes and made up to the mark with PBS. The standard had a concentration of 10 mM (glucose was added to this solution to make a 0.1M glucose solution).

6.2.5 Fabrication of the PA/OA Detecting Electrode

The fabrication of the PA/OA detecting electrode (the NEFA detecting electrode) is based on the method outlined in Section 6.2.1 except using ACOD and ACS as the enzymes to be immobilised, briefly, one double layer of ACOD and PDA-MWCNT was immobilised on the NEFA detecting electrode. The coating solutions were 1% wt. PDA containing 0.6 mg ml^{-1} MWCNT, ACOD (4 units ml^{-1} in PBS) and ACS (4 units ml^{-1} in PBS). 15µl of PDA-MWCNT solution was added to the NEFA detecting electrode and kept at 4°C for 30 minutes. The electrode was washed with PBS (0.1M pH7). This process was repeated with ACOD solution, followed again by PDA-MWCNT solution, followed by ACS solution to give a final electrode film composition of CSPE|PDA-MWCNT|ACOD|PDA-MWCNT|ACS.

The glucose detecting electrode was fabricated using the procedure outlined in Section 5.2.1.

The electrodes where tested with CA and CV in a perspex cell containing 9ml of PBS with 3.2mM ATP and 0.23mM CoA.

6.3 Results & Discussion

6.3.1 Using the LBL Method with GOx

The LBL method was initially tested with GOx to determine if it was possible to detect DET based on the fact that CNTs would be in close proximity to GOx upon immobilisation.

It was initially thought that DET from the FAD active site of GOx to the electrode would be possible due to the presence of MWCNTs in the polymer layer. However, Figure 6.3 shows that no DET was detected. Figure 6.3 also shows that it is possible to detect changes in [glucose] indirectly via the oxidation of hydrogen peroxide as in Equation 6.1.

$$H_2O_2 \rightarrow O_2 + 2H^+ + 2e^- \qquad 6.1$$

Figure 6.4 shows a calibration curve derived from Figure 6.3 for the detection of glucose by the $(PDA|MWCNT|GOx)_2$ modified CSPE. The sensitivity of the electrode was 1.22μA mM^{-1}. Figure 6.5 shows a reciprocal plot derived from Figure 6.4. This was used to determine the K_m of the immobilised GOx as 2.98mM. Therefore the K_m of GOx immobilised using PDA-MWCNT via the LBL method is 61.3% lower than GOx in solution.[120a]

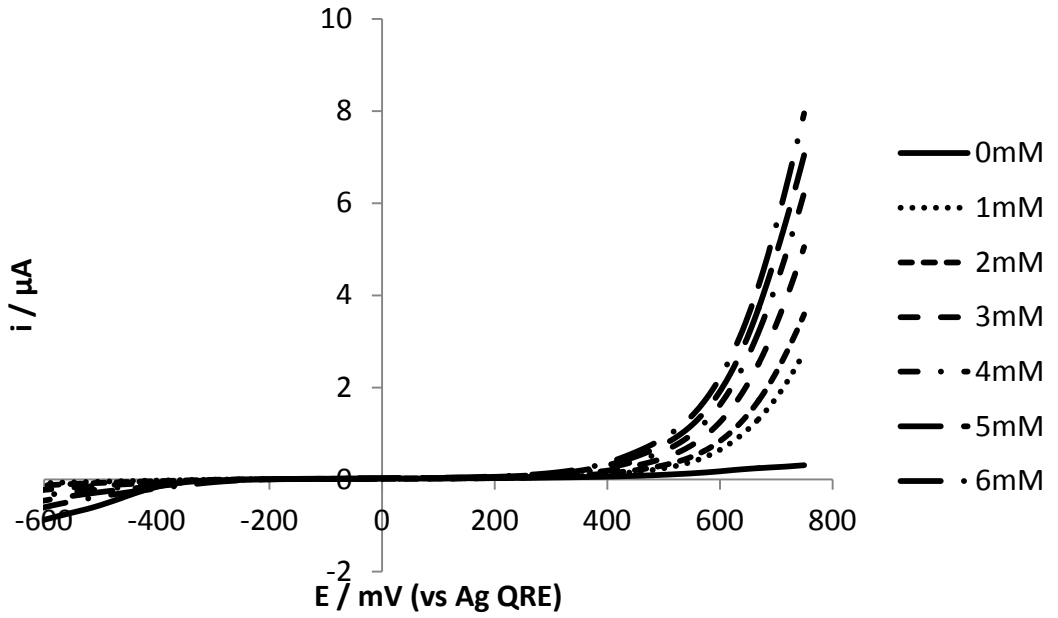

Figure 6.3: LSVs (v = 1mV s^{-1}) for different [glucose] measured at a CSPE modified with $(PDA|MWCNT|GOx)_2$.

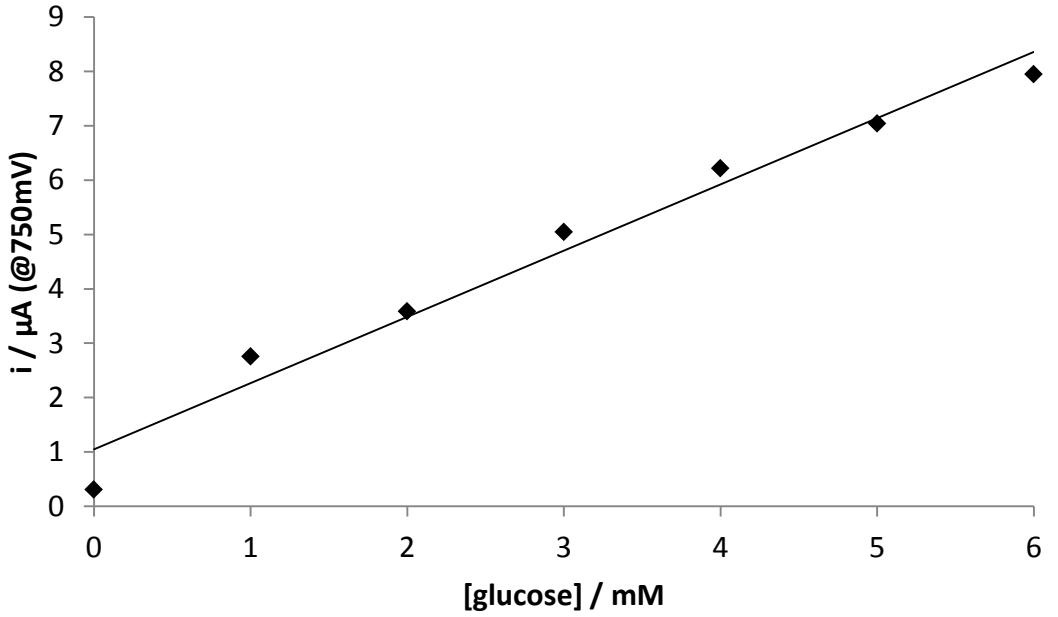

Figure 6.4: Calibration curve for $(PDA|MWCNT|GOx)_2$ modified CSPE for different [glucose] at E= 750mV.

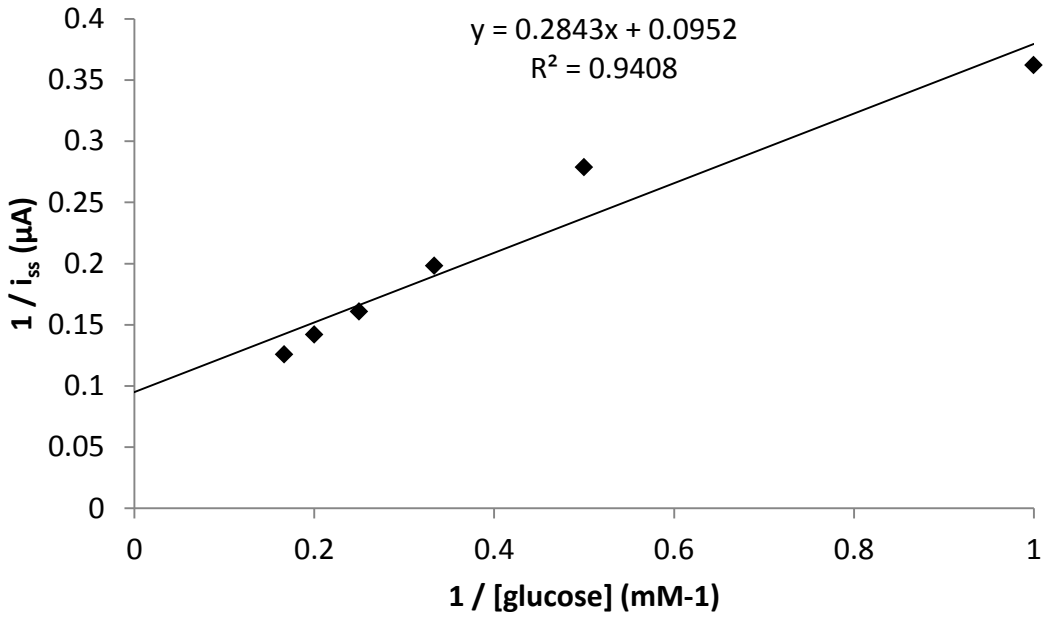

Figure 6.5: Plot of 1/ i_{ss} (at 750mV) and 1/[glucose] derived from Figure 6.4.

A variation of the experiment was then attempted, utilising entrapment of GOx in PDA-MWCNT, similar to the method described above for FcNafionGOx (see Section 5.2.1). The experimental procedure for the entrapment of GOx in PDA-MWCNT is described in Section 6.2.2. This electrode was also tested for DET.

Figure 6.6 shows that DET from the GOx active site (E° = -416mV vs Ag|AgCl)[60] was not detected at a scan rate of 1mV s^{-1}. Changes in [glucose] were detected via oxidation of H_2O_2 produced during the oxidation of glucose by GOx at potentials > 500mV. No DET was detected even at higher scan rates (1000mV s^{-1}, Figure 6.7) It is possible that the wrapping of the MWCNTs by the PDA polymer reduces the ability of the MWCNTs to come into contact with the FAD centre of GOx. DET was observed using PMBN as the containing polymer and PMBN will not wrap MWCNTs in the same way as PDA due to its amphiphilic nature.

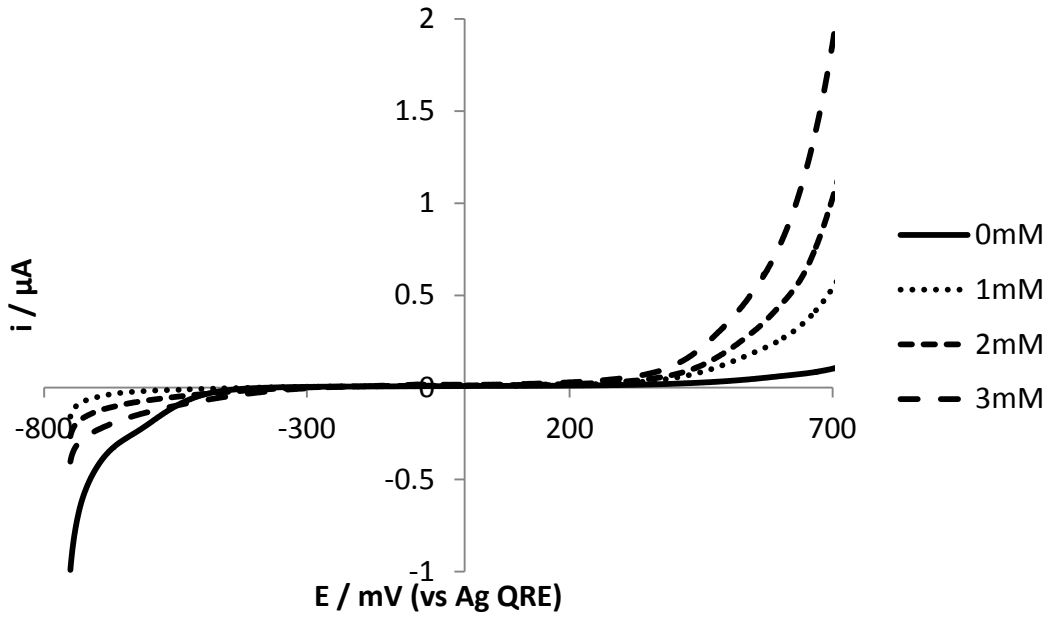

Figure 6.6 LSVs (v = 1mV s^{-1}) for different [glucose] measured at a CSPE modified with (PDA-MWCNT-GOx).

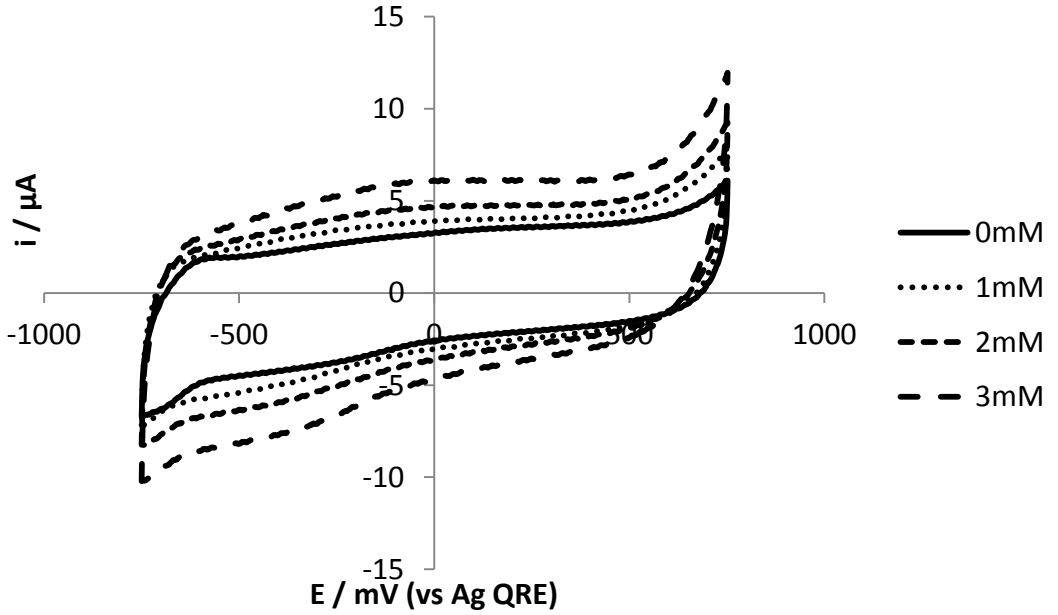

Figure 6.7: CVs (v = 1000mV s^{-1}) for different [glucose] measured at a CSPE modified with (PDA-MWCNT-GOx).

Another variation of the experiment was attempted using a different polycation, Polyethylenimine modified with FcCOOH using EDC/NHSS coupling. An investigation was carried out to determine if the FcCOOH modified Polyethylenimine (PEI-Fc) could act as a polymer mediator for the oxidation of glucose by GOx immobilised with PEI-Fc using the LBL technique. An electrode was prepared as described in Section 6.2.1, using PEI-Fc in the place of PDA-MWCNT.

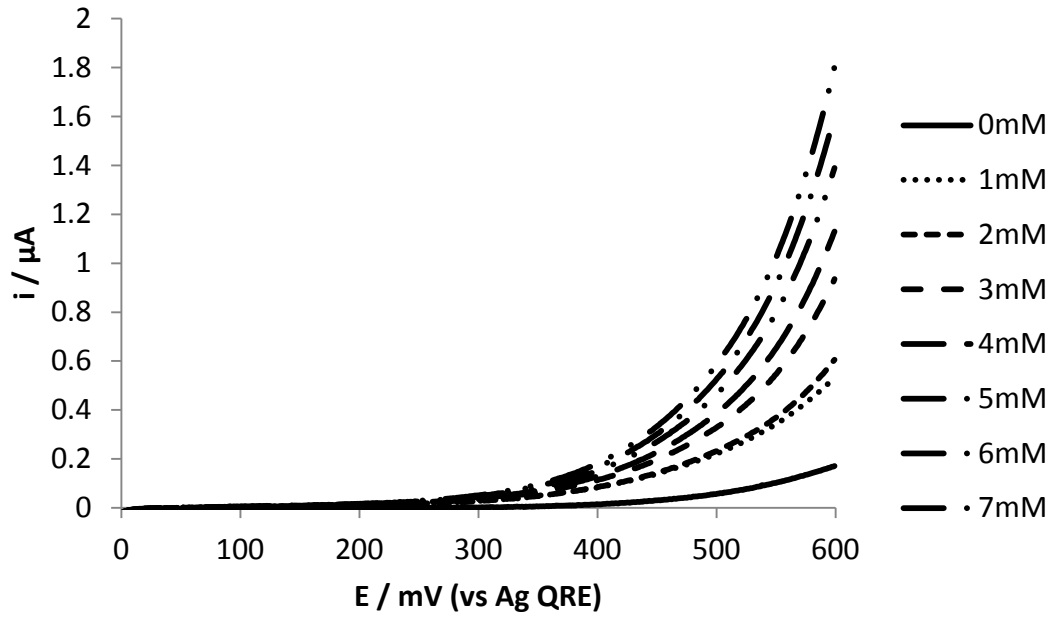

Figure 6.8: LSVs (v = 1mV s^{-1}) for different [glucose] measured at a CSPE modified with $(PEI\text{-}Fc\text{-}GOx)_2$.

Figure 6.8 shows that no Fc redox peak (E° = 247mV vs Ag|AgCl)[88] was detected. Changes in [glucose] were detected via oxidation of H_2O_2 produced during the oxidation of glucose by GOx at potentials > 500mV.

Figure 6.9 shows a calibration graph based on data collected in Figure 6.8.

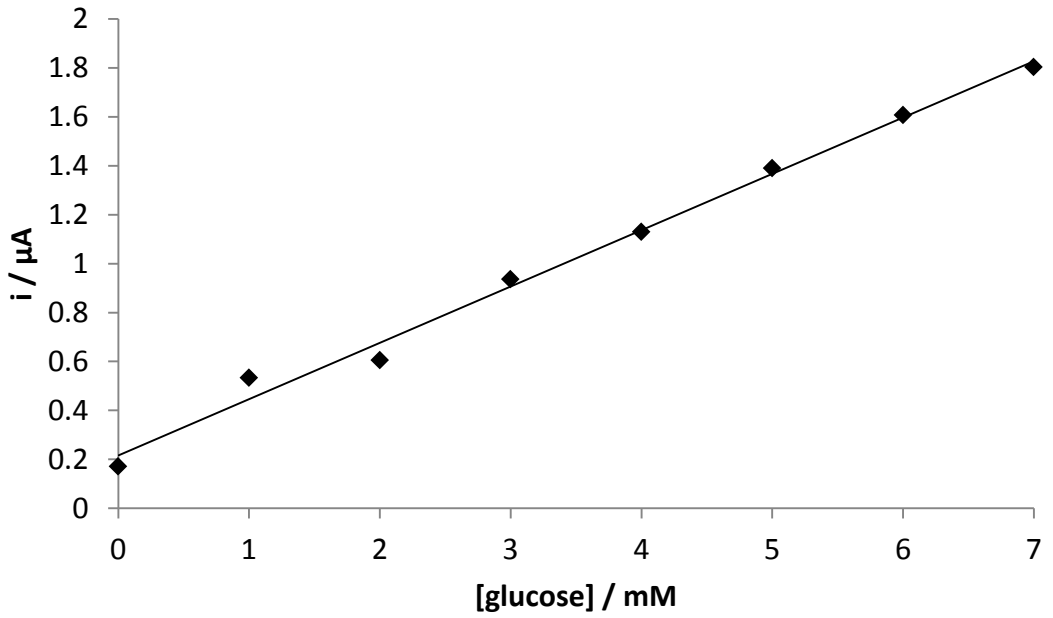

Figure 6.9: Calibration curve for Dropsens-(PEI-Fc-GOx)$_2$ modified CSPE for different [glucose] at E= 600mV.

6.3.2 Simultaneous Determination of PACo-A/OAcoA and Glucose Concentration Using Duel Electrode System

The experiments described in this section were carried out with the aim of achieving simultaneous measurement of Palmitoyl coenzyme A / Oleoyl coenzyme A (PACo-A/OAcoA) (the thioester analogues of the Acyl-CoA product of the oxidation of fatty acids by ACS (Acetyl—CoA Synthetase) and glucose concentrations from a single mixed sample. A screen printed electrode with two working electrodes was used. Each working electrode was modified with enzymes that oxidise PACoA or glucose and the oxidation current detected at each of these electrodes with various methods should be related to the concentration of the analytes.

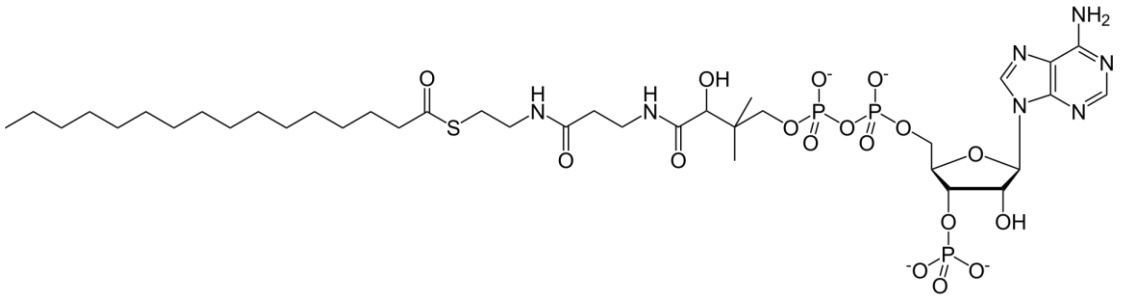

Figure 6.10: The chemical structure of palmitoyl coenzyme A.

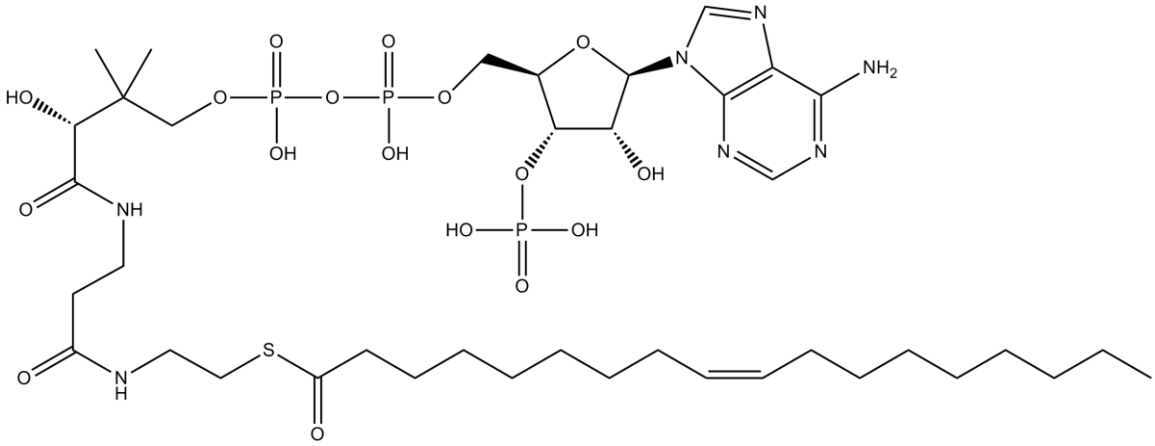

Figure 6.11: The chemical structure of oleoyl coenzyme A (identical to that of palmitoyl coenzyme A (Figure 6.10) except with an unsaturated carbon bond.

Figure 6.12 shows a CA carried out on the modified SPE. Both CA traces seem to follow a similar pattern. The amount of glucose added after the first addition is at the upper end of detection for FcNafionGOx. The concentration of the PACoA|Glucose solution was chosen to highlight the ACOD catalysis rather GOx. It was expected that the oxidation current would peak and then level off for the glucose detecting electrode (GOx) and continuously rise in a stepwise fashion for the NEFA detecting electrode (ACOD). However a response similar to what was expected for the glucose detecting electrode was seen on both electrodes. The increase in PACoA concentration is quite small and therefore it was expected that little current response would be seen until after several

additions of PACoA|Glucose solution. The fact that this was not seen indicates that the response is dominated by glucose oxidation on both electrodes.

Figure 6.13 shows CV scans carried out after the CA shown in Figure 6.12. There is a clear Fc oxidation peak on the glucose detecting electrode along with a reduction peak that is much smaller than the oxidation peak, typical for mediated enzyme electrodes during substrate catalysis. There is also a smaller Fc oxidation peak on the NEFA detecting electrode. This indicates that some Fc from the FcNafion crossed over from the glucose detecting electrode to the NEFA detecting electrode. The test was repeated with only FcNafionGOx immobilised on the glucose detecting electrode.

Figure 6.14 shows the results of the repeated CA experiment with only the glucose detecting electrode modified. The oxidation current increases on both electrodes after the addition of the glucose|PACoA solution. In this case, the oxidation current on the NEFA detecting electrode is larger than that of the glucose detecting electrode. This is likely due to the fact that the NEFA detecting electrode is unmodified and therefore has unrestricted access to the electrolyte, whereas the glucose detecting electrode is modified with an FcNafionGOx film.

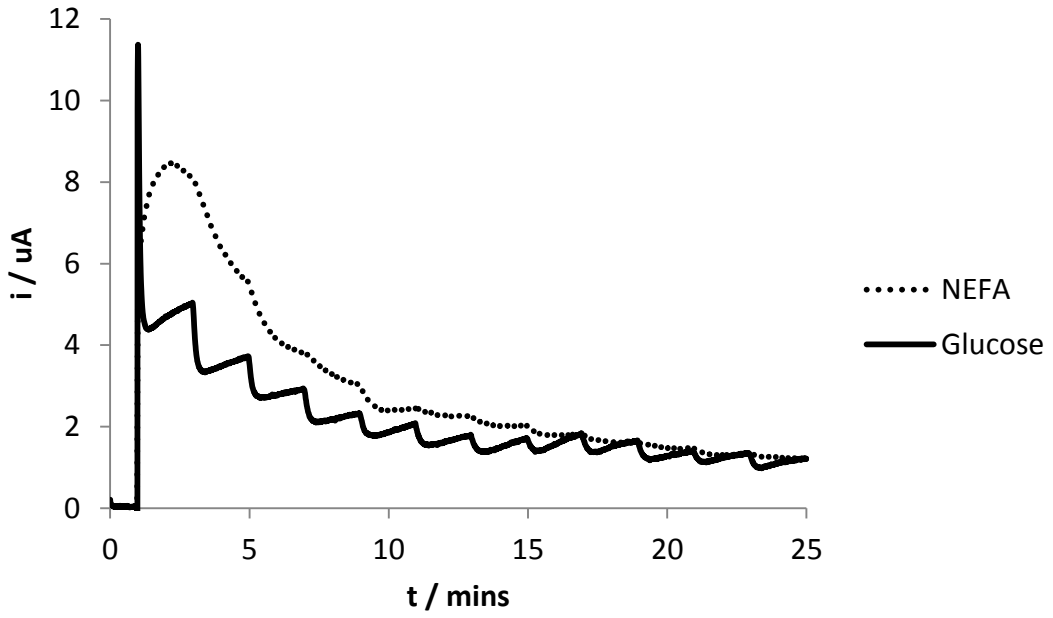

Figure 6.12: CA carried out on modified SPE. E = 0.3V. 1.5µl of a 10mM PACoA solution and 1M glucose solution (in PBS) was added after 1 minute and then every 2 minutes, corresponding to a concentration increase of 0.05mM for PACoA and 5mM for glucose.

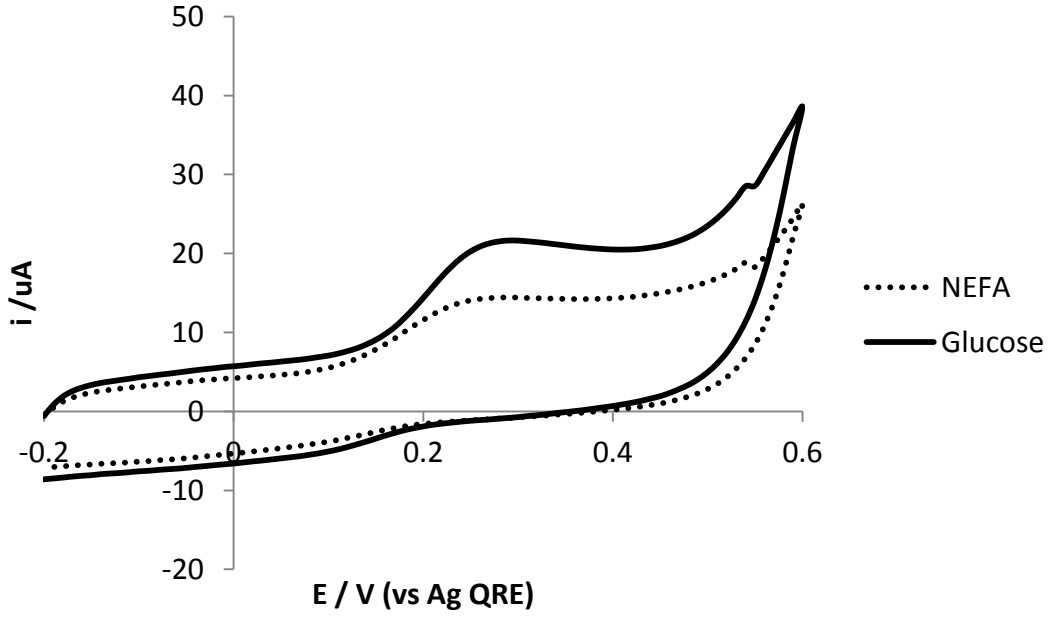

Figure 6.13: CV scans (v = 100mV s^{-1}) performed after the CA shown in Figure 6.12.

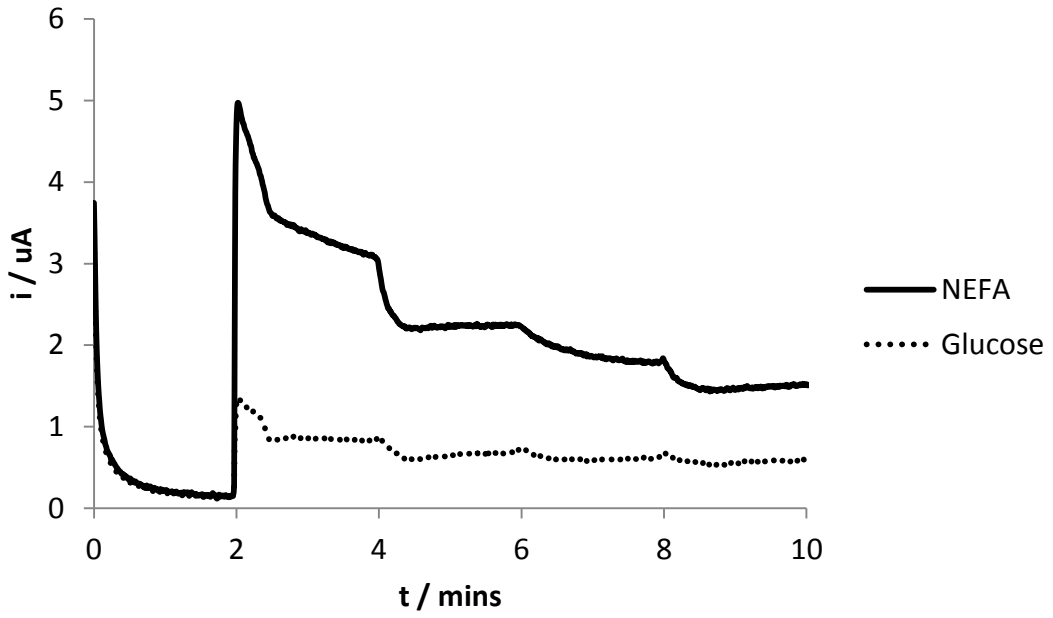

Figure 6.14: CA carried out under the same conditions as in Figure 6.12 except with only the glucose detecting electrode modified. Glucose|PACoA solution added after 2 minutes and every 2 minutes subsequently.

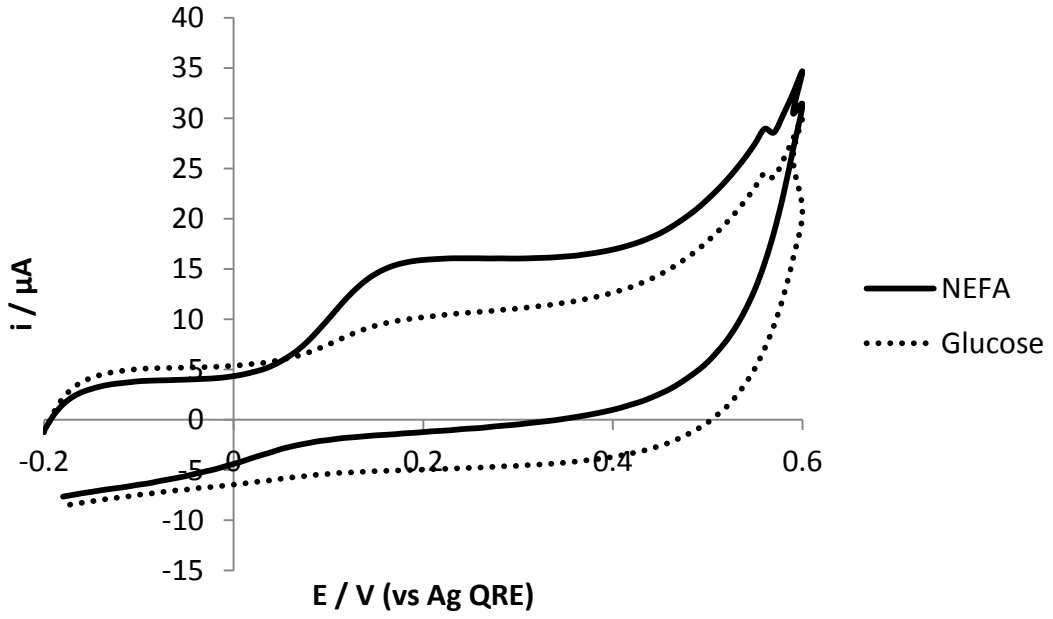

Figure 6.15: CV scans (v = 100mV s^{-1}) performed after the CA shown in Figure 6.14.

Figure 6.15 shows CV scans carried out after the CA shown in Figure 6.14. The Fc oxidation peak is larger for the NEFA detecting electrode than for the glucose detecting

electrode. This could be due to a small amount of FcNafion solution remaining in the cell after immobilisation. The presence of a Fc oxidation peak on the NEFA detecting electrode shows that the oxidation current measured during the CA experiment is likely due to a combination of Fc and H_2O_2 oxidation. In order to remove any residual FcNafion solution left over from the immobilisation procedure, the test was repeated with an additional washing step.

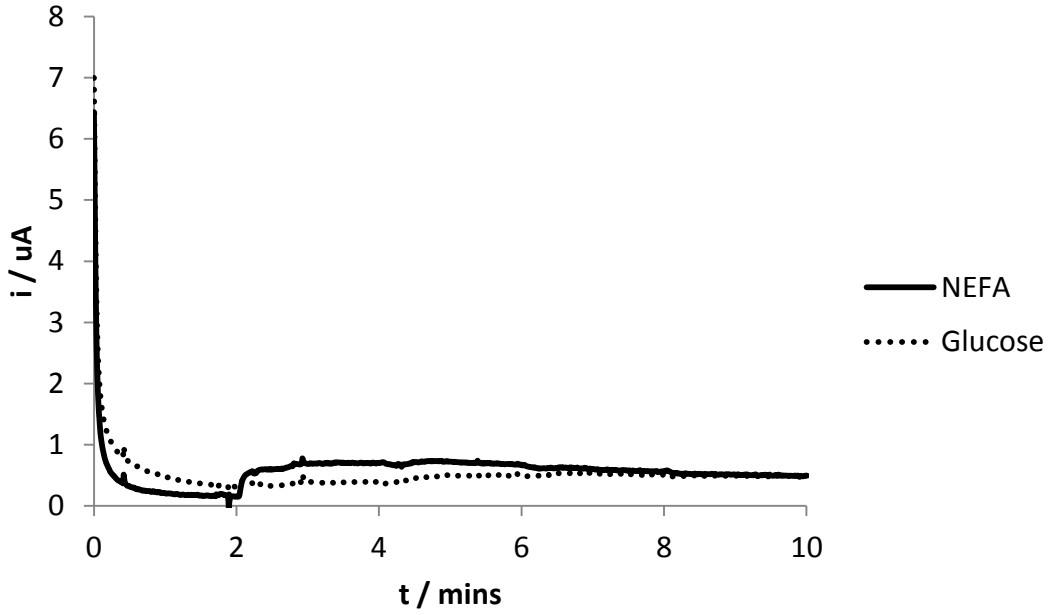

Figure 6.16: CA carried out under the same conditions as in Figure 6.14 except with an additional washing step after the immobilisation procedure.

Figure 6.16 shows the results of a CA experiment carried out under the same conditions as in Figure 6.14 except with an additional washing step after the immobilisation procedure. There is a much lower current response compared to the previous experiments, likely due to the removal of the FcNafionGOx material during washing. However the current from the NEFA detecting electrode is still higher than the glucose detecting electrode.

Figure 6.17 shows CV scans carried out after the CA experiment shown in Figure 6.16. It appears that the additional washing step reduces the crossover of Fc onto the NEFA detecting electrode as the Fc oxidation peak on the glucose detecting electrode is higher on the glucose detecting electrode than on the NEFA detecting electrode as should be expected. The peak current at E = 0.6V is consistent throughout all the CV experiments carried out in this study; Indicating that the current response at this potential is dependent only on H_2O_2 oxidation. It is expected that the presence of the PDA-MWCNT|ACOD film at the surface of the NEFA detecting electrode would help to reduce interference from H_2O_2 produced from the glucose detecting electrode and vice versa. Therefore it may be beneficial to carry out the CA experiment with the NEFA detecting electrode at 0.6V and the glucose detecting electrode at 0.3V. This methodology was avoided at first to try to minimise the complexity of the method.

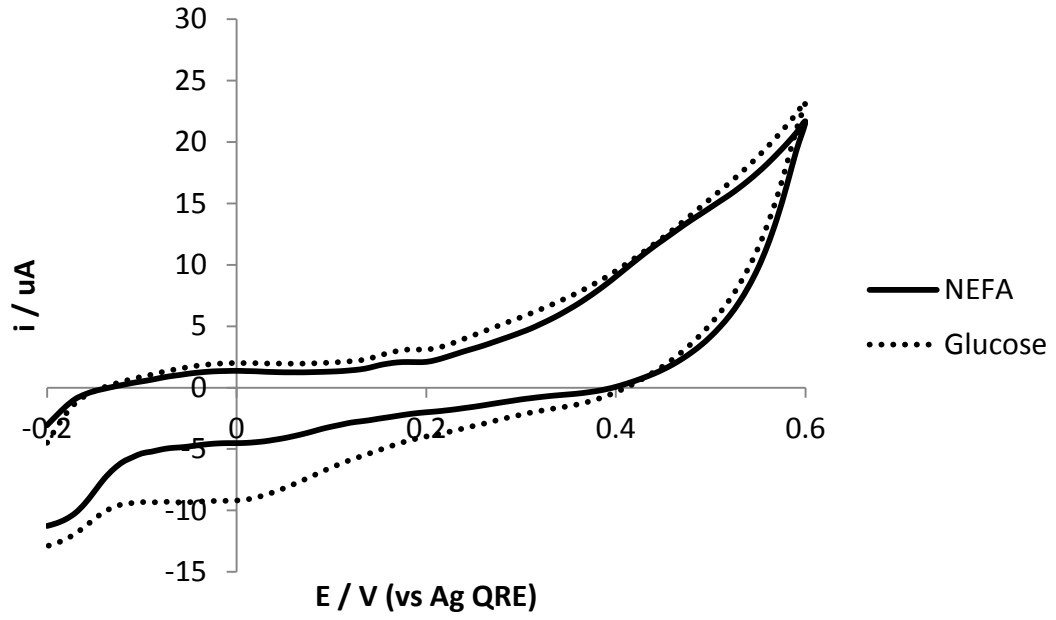

Figure 6.17: CV scans (v = 100mV s^{-1}) performed after the CA shown in Figure 6.16.

Figure 6.17 shows additional un-accounted for redox processes at E ~ - 0.1V. Therefore additional CV scans were carried out with a larger potential range to investigate the additional peaks. These scans are shown in Figure 6.18.

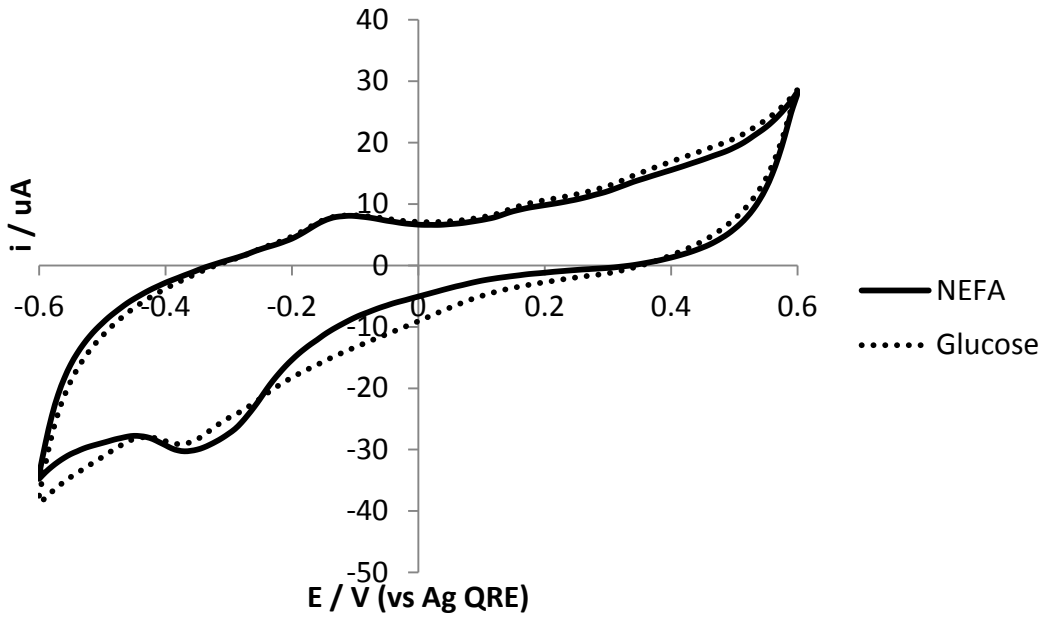

Figure 6.18: CV scans (v = 100mV s^{-1}) performed after the CV shown in Figure 6.17.

Once the redox potential of the additional peaks had been determined (~ - 0.26 V), additional scans were carried out to determine if the redox peaks were affected by the number of scans performed.

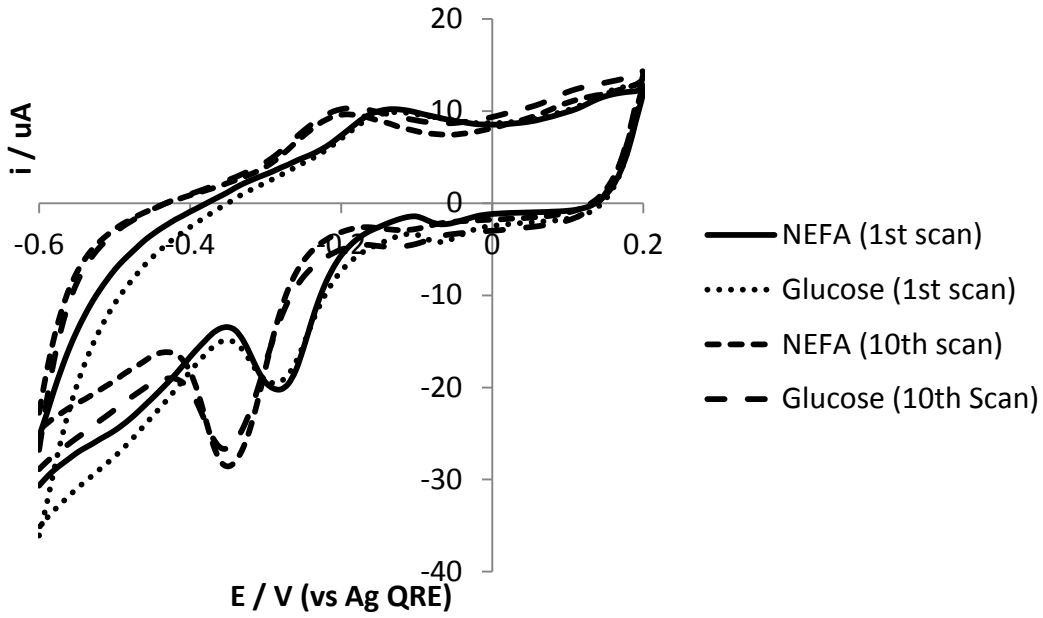

Figure 6.19: CV scans (v = 100mV s^{-1}) carried out using the same conditions as all previous CVs.

Figure 6.19 shows the results of 10 CV scans carried out with a lower positive potential limit on the electrode used in Figure 6.18. This shows that the redox peaks shift to more negative potential as the number of scans increases. Also, the reduction of peak potential increases with increasing scan number.

In order to determine if this redox peak was due to a component of the immobilized film (FcNafionGOx) or if it was an artefact of the electrode material, the same procedure was carried out on an unmodified electrode.

Figure 6.20 shows the results of this scan. The redox peaks observed in Figure 6.18 and Figure 6.19 were not as obvious in Figure 6.20. In order to determine if this was an effect of the potential scan range, additional scans were carried out with a larger potential scan range.

The results of these scans are shown in Figure 6.21. Figure 6.21 shows that increasing the potential scan range to more positive potentials had the effect of increasing the reduction peak potential for the blank electrode at ~ - 0.18V. This reduction peak is most apparent in the NEFA detecting electrode. The differences between the scans for the NEFA detecting electrode and the glucose detecting electrode are attributed to the different distances between the RE and the two electrodes. The presence of the additional peaks seen in Figure 6.17 are therefore attributed to redox species on the surface of the SPEs, most likely quinone groups.

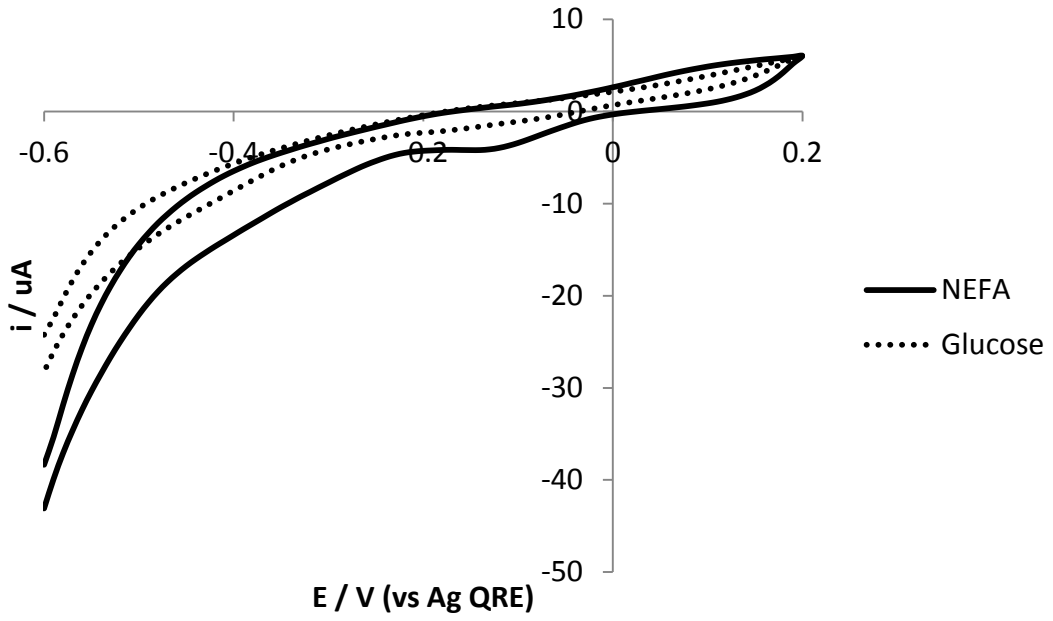

Figure 6.20: CV scans (v = 100mV s^{-1}) carried out on a blank carbon screen printed duel electrode in PBS.

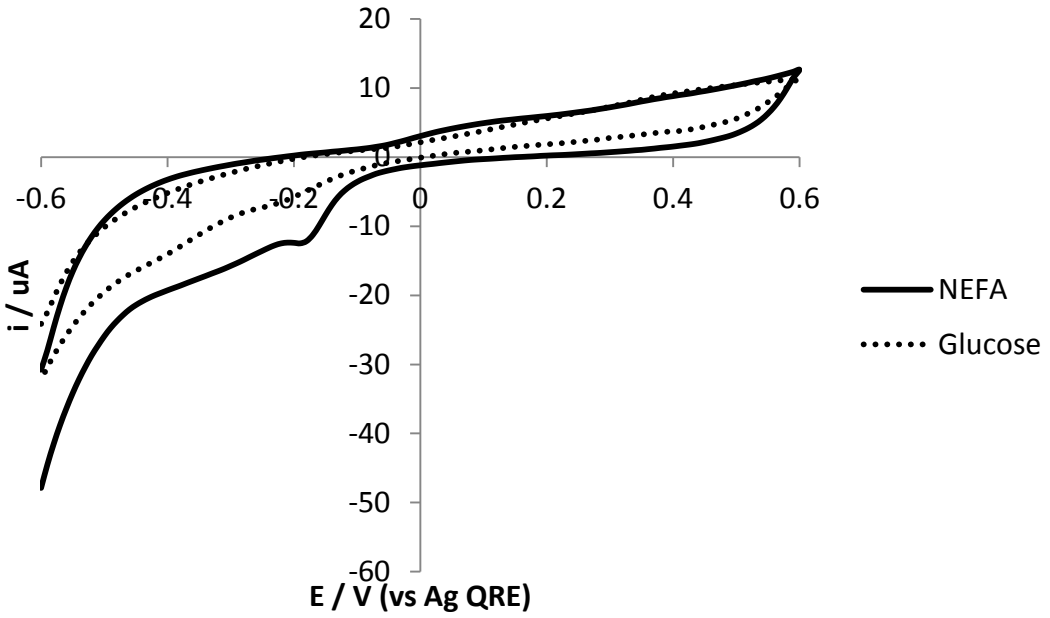

Figure 6.21: CV scans (v = 100mV s^{-1}) carried out under the same conditions as in Figure 6.20 except with a larger potential scan range.

Finally, a CA test was carried out on the unmodified electrodes with the addition of glucose|PACoA solution. The results of this test are shown in Figure 6.22. Figure 6.22 shows that the current response seen in previous CA experiments is due to the catalytic effect of the enzyme.

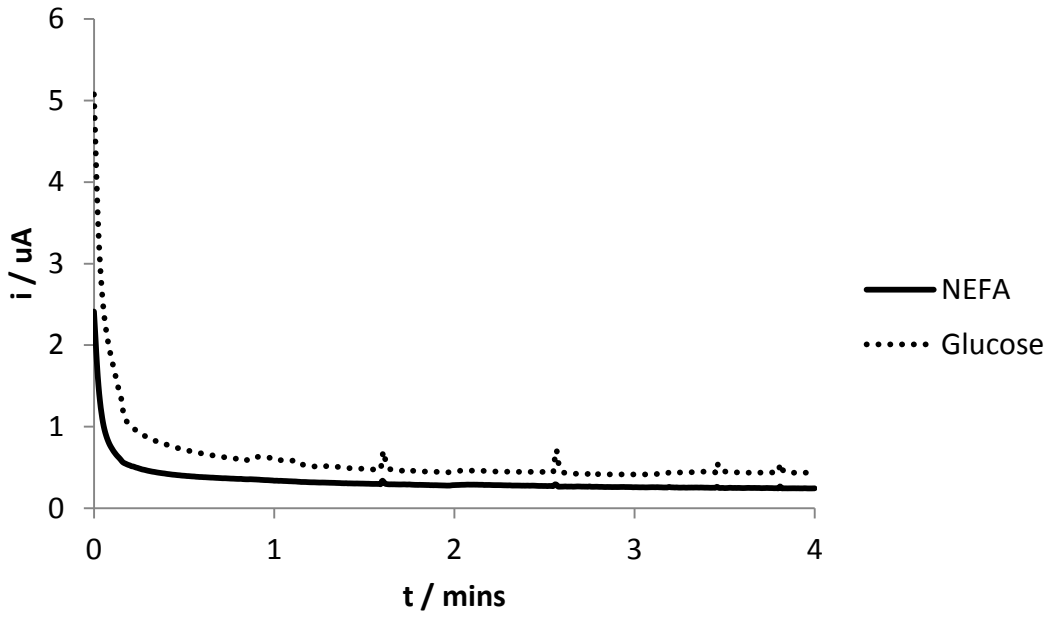

Figure 6.22: CA carried out under the same conditions as all previous CAs except with unmodified (blank) electrodes. Cell concentration increased by 0.05mM for PACoA and 5mM for glucose after 2 minutes.

An experiment was then carried out to investigate differences between electrodes modified with one and two layers of PDA-MWCNT|ACOD using CA and CV techniques. A CSPE with two working electrodes was modified according to the procedure outlined in Section 6.2.3, with one working electrode (the NEFA detecting electrode) modified with one layer of PDA-MWCNT and ACOD and the other working electrode (the glucose detecting electrode) modified with two layers. The electrodes were tested with CV in a perspex cell containing 300µl of PBS (pH7, 0.1M).

Figure 6.23: The CSPE with two working electrodes.

The experiment was first carried out using rubber washers to isolate each working electrode during modification. During the process it was noted that the enzyme-polymer immobilisation mixture was transferring from one WE to another. This was due to an insufficient seal between the washers and the electrode surface. Therefore the experiment was repeated using an inert putty to separate the two working electrodes.

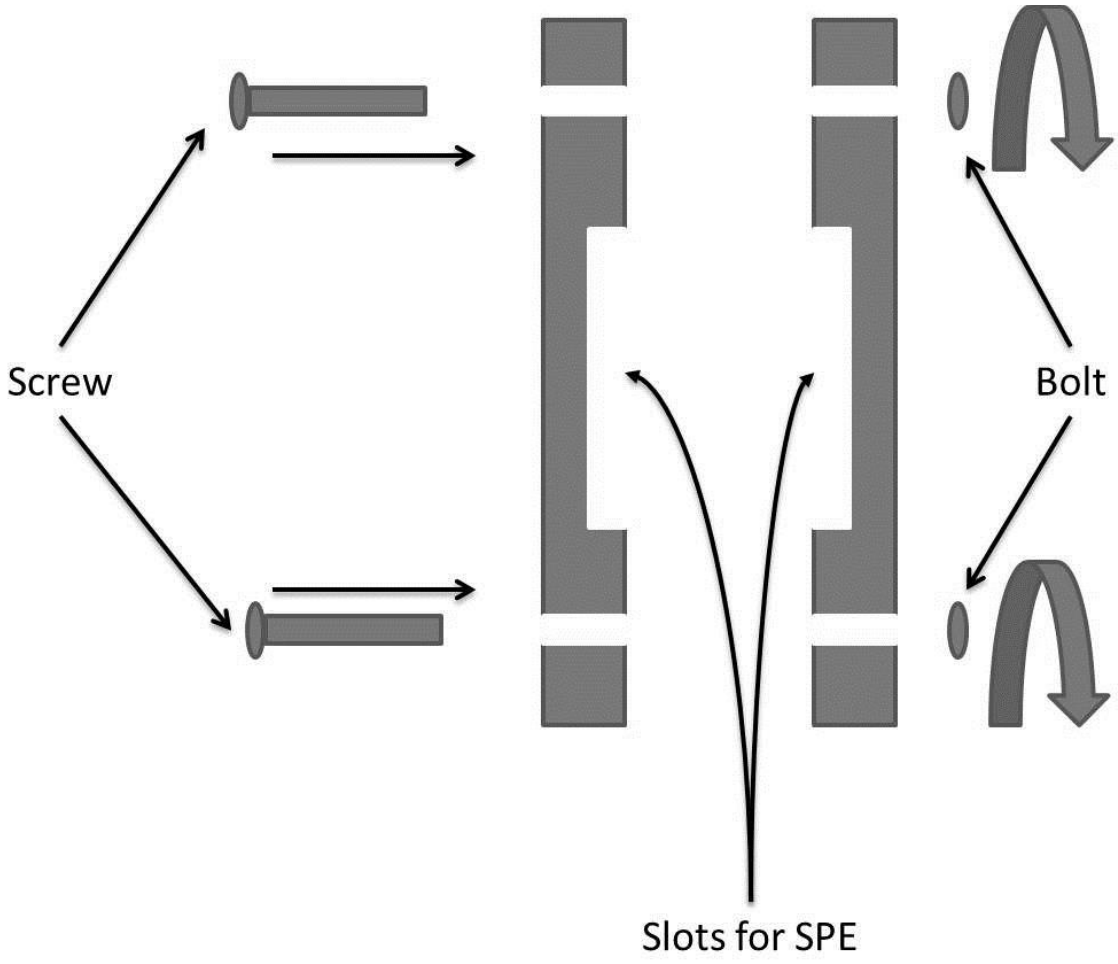

Figure 6.24: Birds eye view diagram of the cell setup used for two SPE's.

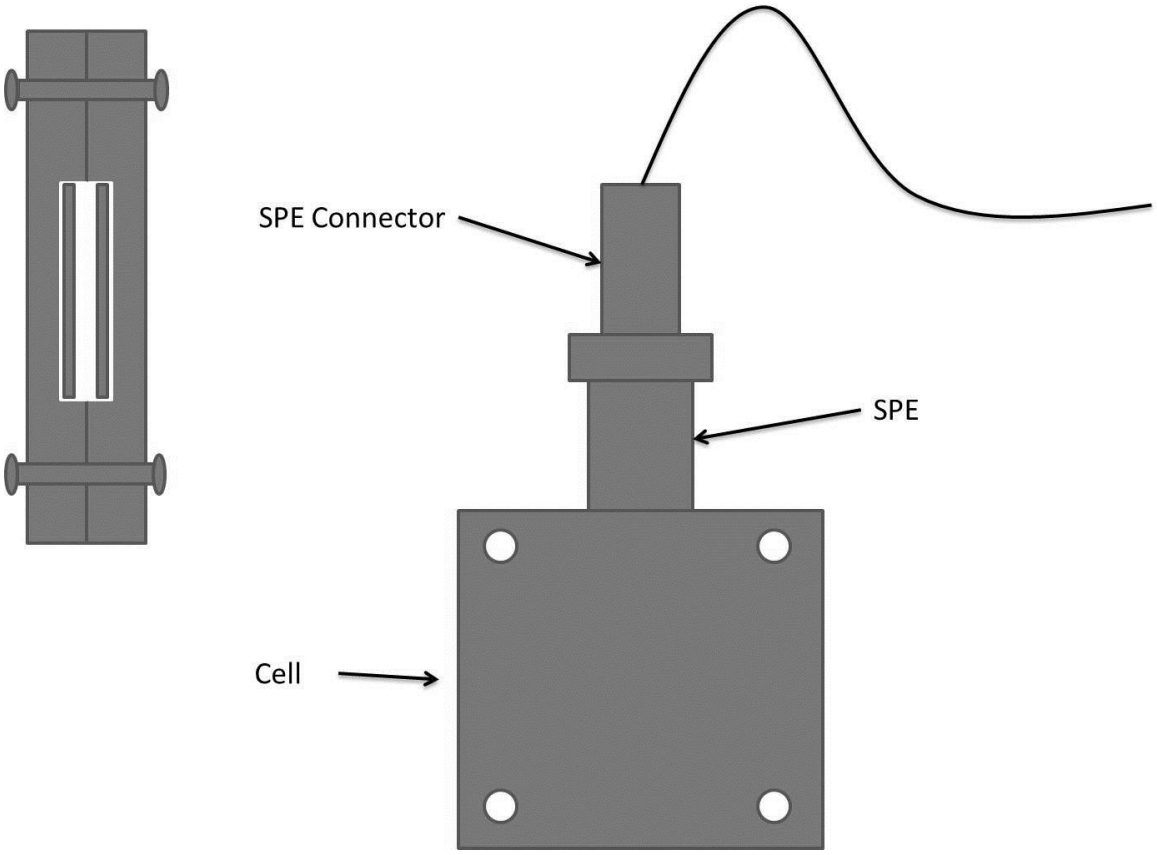

Figure 6.25: Side on view of the cell (with birds eye view (insert) of the closed cell).

This reduced but did not completely prevent transfer of the enzyme-polymer mixture. A CV scan was carried out to determine if each working electrode had a different current response (e.g. capacitance). However, the presence of the putty (which was difficult to remove after immobilisation) greatly reduced the access of the glucose detecting electrode to the counter electrode, hence the much larger current recorded in the CV shown in Figure 6.26.

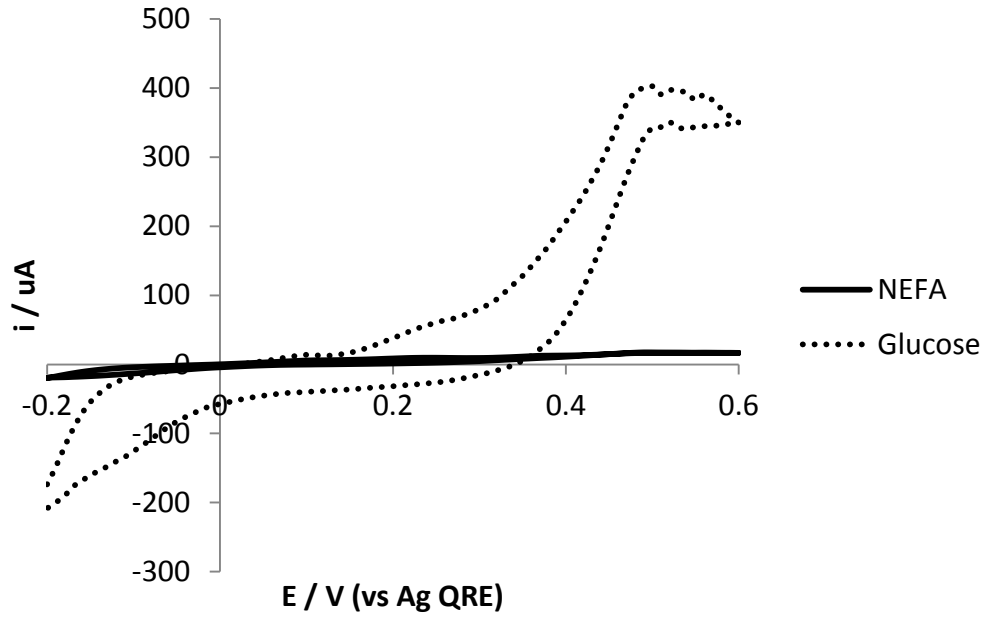

Figure 6.26: CV scans for the modified electrodes v = 100 mV s^{-1}, electrolyte = 0.1M PBS (pH7).

Therefore it was decided that two separate CSPEs each containing one working electrode (as shown in Figure 5.3) should be used for simultaneous detection experiments.

An experiment was then carried out using two separate CSPEs modified with FcNafionGOx and PDA|ACOD. CAs were carried out simultaneously on both the ACOD and GOx modified electrodes. The ACOD electrode was held at 0.5V. The GOx electrode was held at 0.3V. Aliquots of a single mixture of OACoA and glucose were added to the cell at regular intervals and the steady state current was measured.

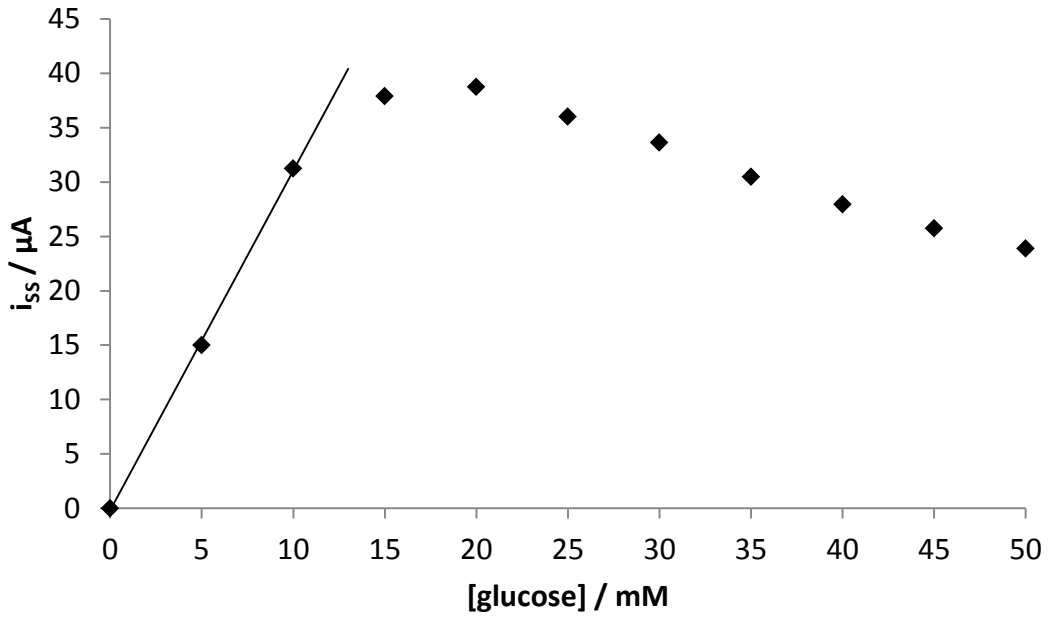

Figure 6.27: Calibration graph for a CSPE modified with FcNafionGOx with the addition aliquots of a single mixture of OACoA and glucose (E = 0.3V).

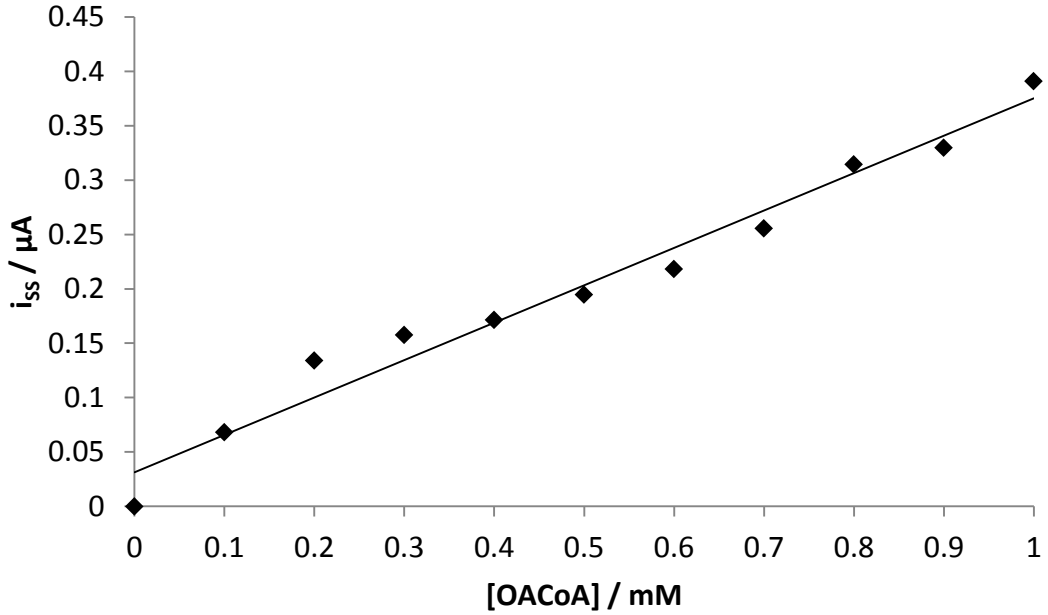

Figure 6.28: CA (E = 0.5V) for a CSPE modified with PDA-MWCNT|ACOD with the addition of aliquots of a single mixture of OACoA and glucose.

The concentration of glucose was increased rapidly (5mM per addition) while the concentration of OACoA was increased gradually (0.1mM per addition), in order to show

that two separate signals could be recorded corresponding to the concentrations of two separate analytes. The fact that the CA profiles of the two different analytes (Figure 6.27 and Figure 6.28) are so different indicates that both analytes can be detected from the same sample without interfering with each other.

6.3.3 Simultaneous Detection of PA/OA & Glucose

The aim of this investigation was to detect palmitic acid (PA) or oleic acid (OA) (NEFA markers) and glucose simultaneously using two SPEs and a bi-potentiostat. The use of two SPEs requires a larger cell and therefore a larger volume of electrolyte. This requires larger volumes of substrate and therefore PA was used as the NEFA marker, as using large volumes (>5ml) of acyl-CoA is unfeasible.

This requires both ACOD (acyl-CoA oxidase) and acyl-CoA synthetase (ACS) to produce H_2O_2 for electrochemical detection based on the reactions shown in Figure 6.29.

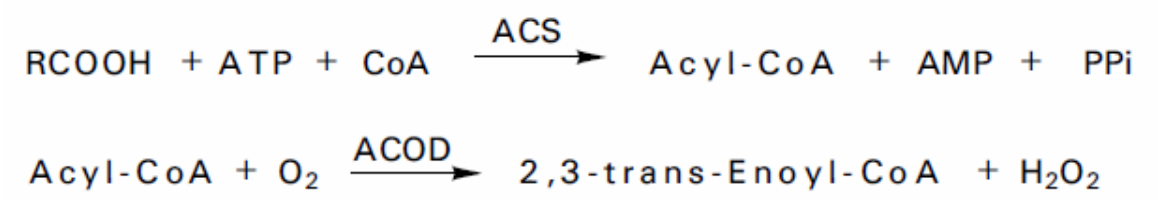

Figure 6.29: NEFA represented here by RCOOH, when treated with ACS in the ATP and CoA form the thiol esters of CoA known as acyl-CoA along with the by-products adenosine monophosphate (AMP) and pyro-phosphate (PPi). Acyl-CoA can then be oxidised by ACOD to produce H_2O_2.

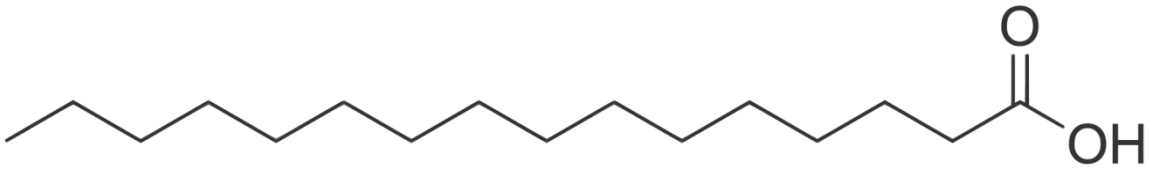

Figure 6.30: The chemical structure of PA (compare to Figure 6.10).

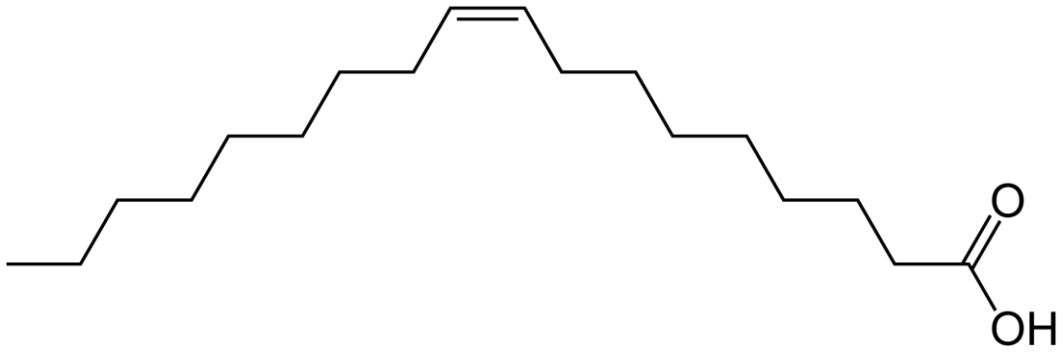

Figure 6.31: The chemical structure of OA (compare to Figure 6.11).

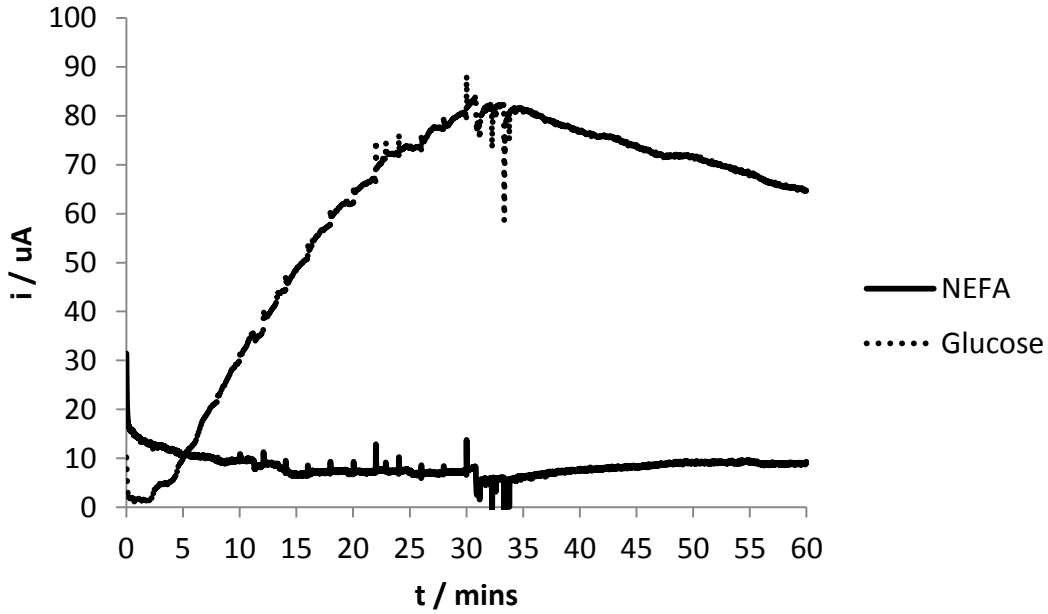

Figure 6.32: CA carried out on the modified SPEs. The NEFA detecting electrode E = 0.5V (vs Ag QRE) and the glucose detecting electrode E = 0.3V (vs Ag QRE). Substrate solution was added every two minutes up to thirty minutes so as to increase the cell concentration of glucose by 1mM and PA by 0.1mM.

Figure 6.32 shows a CA experiment carried out using the two modified CSPEs. Substrate solution was added every two minutes up to thirty minutes, increasing the cell PA concentration by 0.1mM and glucose concentration by 1mM with each addition. A current response was seen for the glucose detecting electrode (FcNafionGOx) as

expected. No response was seen for the NEFA detecting electrode (PDA-MWCNT|ACOD|PDA-MWCNT|ACS). The noise at approximately thirty two minutes is due to the magnetic stirrer becoming unstable in the cell. The spikes in current which appear every two minutes, coinciding with the addition of substrate solution are attributed to vibration of the electrodes during the substrate addition.

CV scans were then recorded before and after the CA experiment.

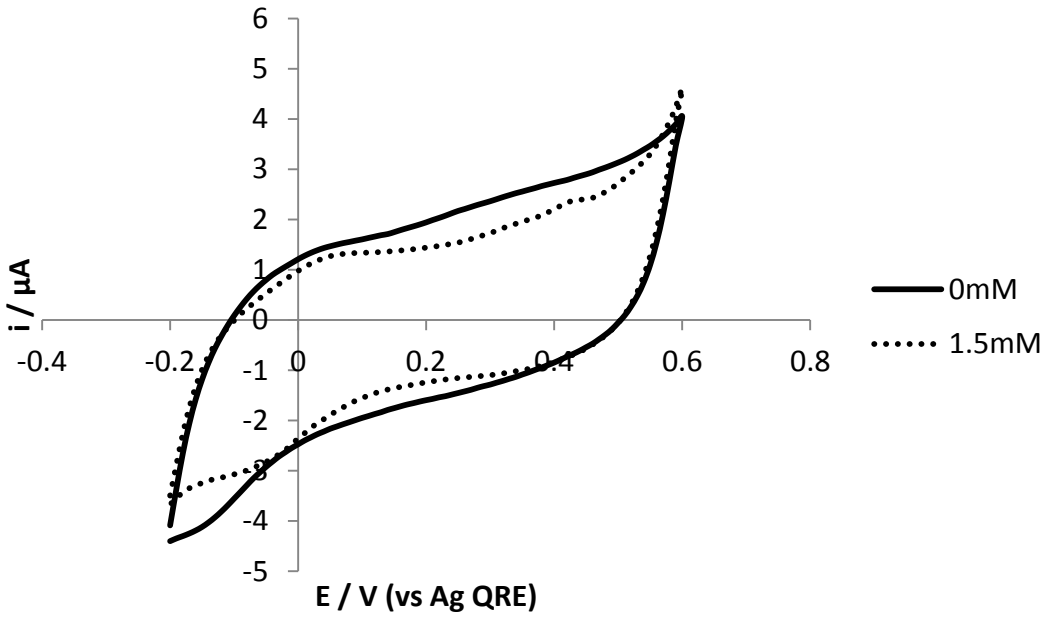

Figure 6.33: scans (v = 100mV s^{-1}) for the NEFA detecting electrode before (0mM) and after (1.5mM) the CA experiment shown in Figure 6.32.

Figure 6.33 shows the before and after scans for the NEFA detecting electrode. The capacitance of the electrode is slightly lower after the CA experiment (1.5mM in Figure 6.33, the concentrations refer to PA). This may be due to some slight decomposition of the film over the course of the CA experiment. There is a noticeable increase in oxidation current at 0.6V. This is attributed to the oxidation of H_2O_2. It is not clear if this oxidation current comes from H_2O_2 produced from the enzymatic reaction at the NEFA detecting

electrode or the glucose detecting electrode. It is unlikely to come from the NEFA detecting electrode as no oxidation current was detected during the CA experiment. Figure 6.34 shows the before and after scans for the NEFA detecting electrode (the concentrations in the legend refer to glucose). This figure is dominated by the catalytic current generated from the oxidation of Fc which has been reduced by oxidised GOx. Figure 6.35 shows a calibration curve calculated from data measured from the glucose detecting electrode in Figure 6.32. It can be seen that the FcNafionGOx electrode has a linear response to glucose up to 8mM with a sensitivity of 0.938 µA mM^{-1}.

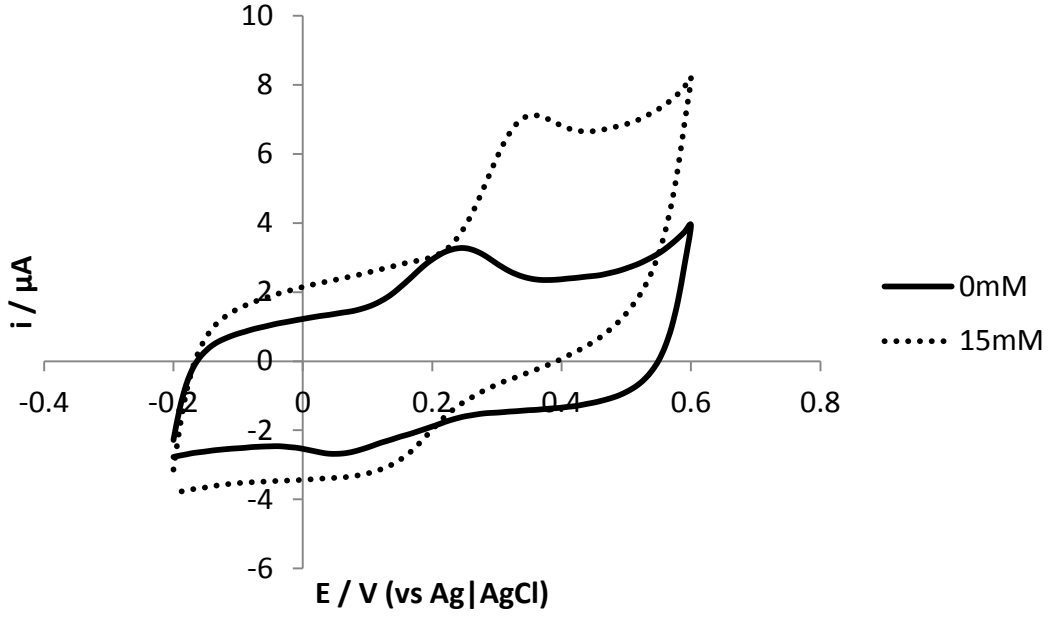

Figure 6.34: CV scans (v = 100mV s^{-1}) for the glucose detecting electrode before (0mM) and after (15mM) the CA experiment shown in Figure 6.32.

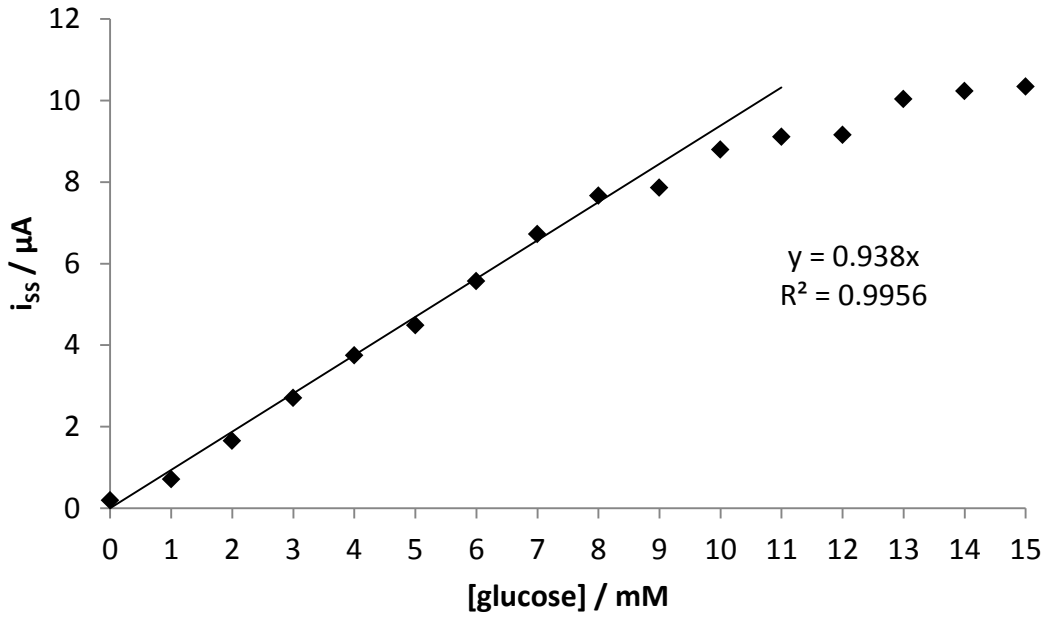

Figure 6.35: Calibration curve based on data measured for the glucose detecting electrode shown in Figure 6.32.

The cell was setup again with freshly prepared electrodes and CAs were carried out simultaneously on both ACOD|ACS and GOx modified electrodes. The ACOD electrode was kept at 0.5V. The GOx electrode was held at 0.3V. Aliquots of a single mixture of OA and glucose were added to the cell at regular intervals and the steady state current was measured. Both NEFA and glucose were detected electrochemically using enzyme electrodes from single mixed analyte sample (Figure 6.36 and Figure 6.37).

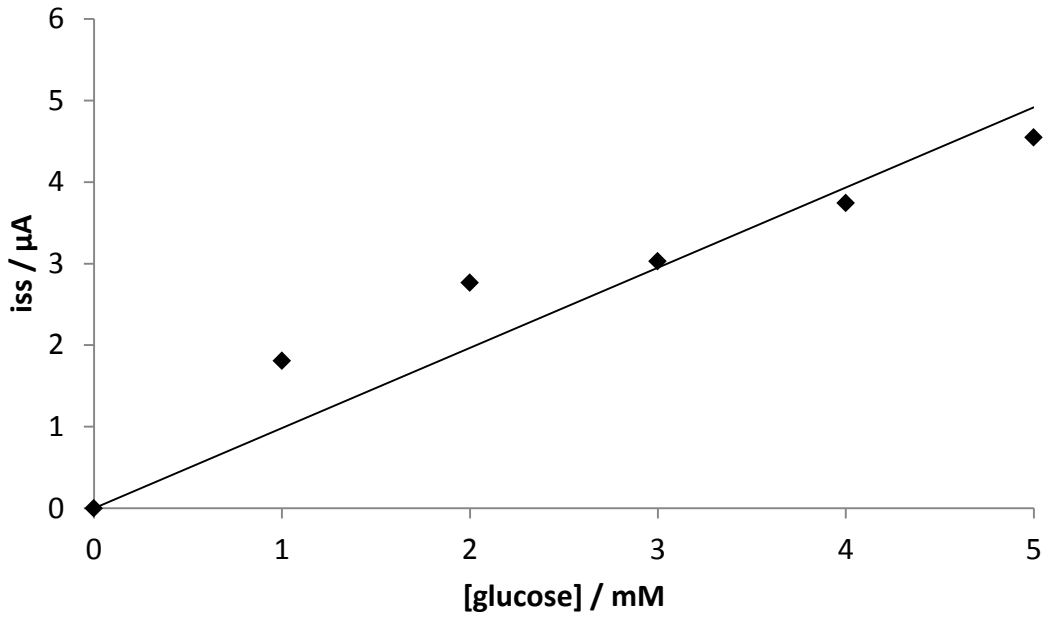

Figure 6.36: CA (E = 0.3V) for a CSPE modified with FcNafionGOx with the addition aliquots of a single mixture of OA and glucose.

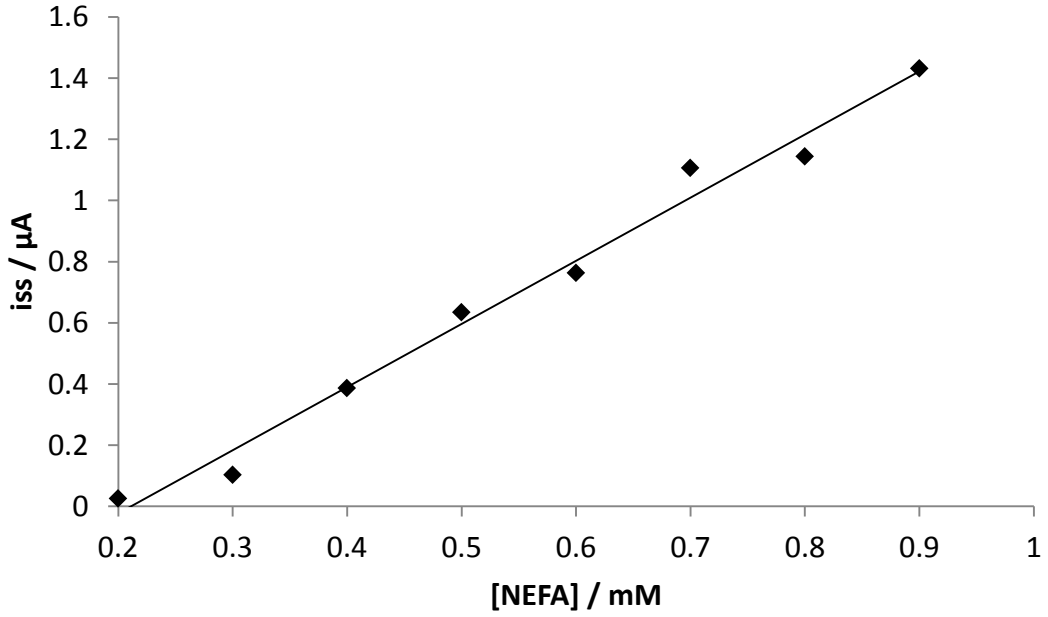

Figure 6.37: CA (E = 0.5V) for a CSPE modified with PDA-MWCNT|ACOD|PDA-MWCNT|ACS with the addition of aliquots of a single mixture of OACoA and glucose.

6.3.4 Investigation of the effect of PA on FcNafionGOx

An experiment was then carried out to investigate the influence of PA on the current response of a FcNafionGOx modified carbon screen printed electrode (CSPE) using CA. An electrode was prepared according to the method outlined in Section 5.2.1. This electrode was then added to a perspex cell containing 9 ml of PBS (0.1M pH 7). A CA was then carried out at 0.3V (vs Ag QRE).

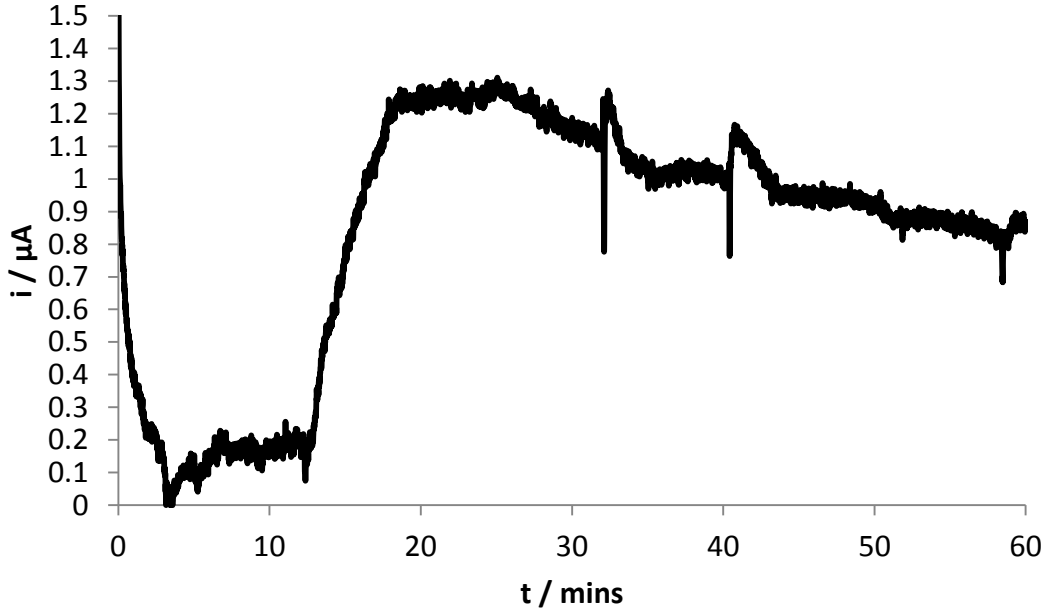

Figure 6.38: CA (E = 0.3V vs Ag QRE) for the FcNafionGOx modified CSPE. Baseline current subtracted.

Figure 6.38 shows a CA trace carried out on the FcNafionGOx modified CSPE. The [glucose] in the cell was increased to 1mM after two minutes. There was no discernible response , this is attributed to the configuration of the cell which is different to that used previously, in which two electrodes were used. The configuration used in this experiment resulted in longer mixing times for the glucose solution and this affects the current response.

The cell [glucose] was then increased again to 2mM after twelve minutes. Shortly after this point (~ 12 minutes 30s) the oxidation current density increased as expected for the catalytic conversion of glucose to gluconolactone by GOx mediated by Fc.

The [PA] was then increased to 0.1mM after 32 minutes and then to 0.2mM after 42 minutes. This was achieved with the addition of 90 µl of 10mM PA solution in 20% ethanol. There is a slight (~ 0.1 µA) increase in oxidation current upon the addition of the PA solution (see Figure 6.39).

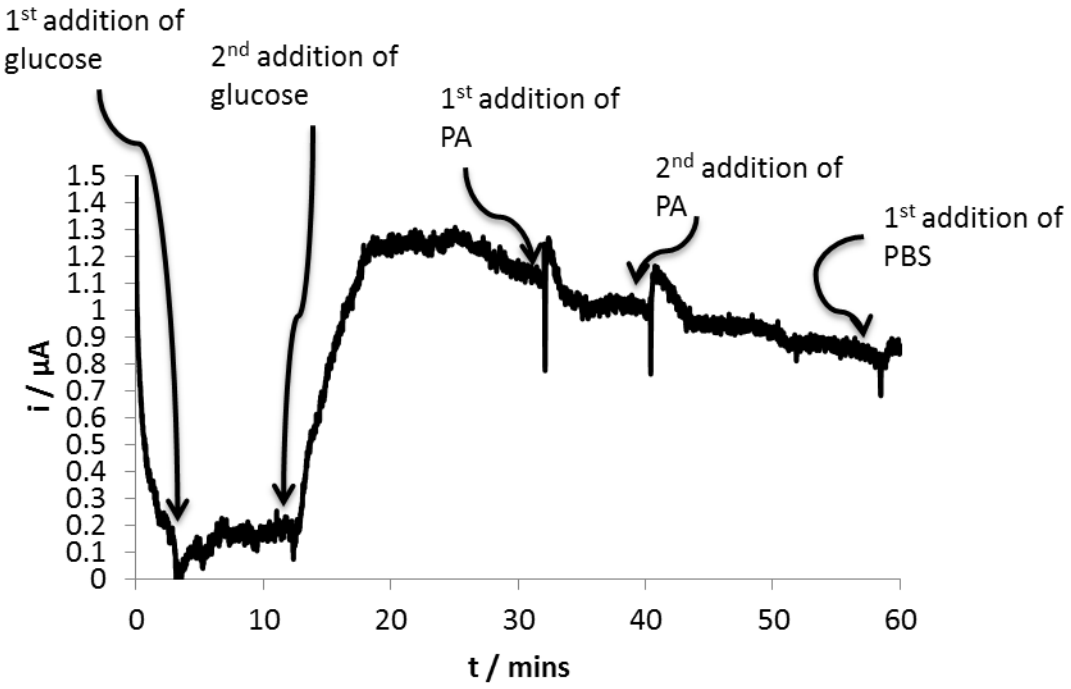

Figure 6.39: Data from Figure 6.38 annotated to show additions of different substrates to the cell.

6.3.5 The Activity of CSPEs and FcNafion Modified CSPEs towards EtOH

It is important to rule out any influence of EtOH on the current response of the CSPEs and those modified with FcNafion, as EtOH is the solvent used to dissolve NEFA for electrochemical analysis.

A plane CSPE was added to a perspex cell containing 9 ml of PBS (0.1M pH 7). A CA was then carried out at 0.3V (vs Ag QRE). The same procedure was carried out for a CSPE modified as described in Section 5.2.1.

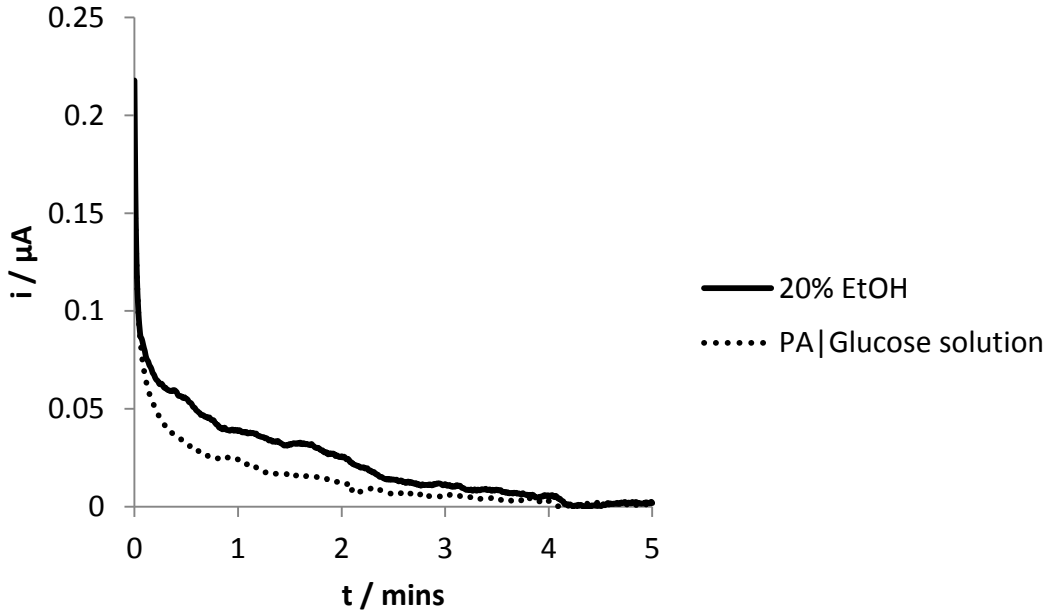

Figure 6.40: CA (E = 0.3V vs Ag QRE) for an unmodified CSPE in a perspex cell containing 9 ml of 0.1M PBS (pH7) (baseline current subtracted).

Figure 6.40 shows a CA trace carried out using an unmodified CSPE. 9 µl of 20% EtOH (in PBS) was added to the cell after two and four minutes respectively (solid line). It is clear that this electrode has no activity towards EtOH at this potential. The same test was repeated the addition of 90 µl of 10mM PA solution in 20% ethanol (in PBS) containing

0.1M glucose after two and four minutes respectively (dotted line). Again no increase in oxidation current is seen.

Figure 6.41: shows a repeat of the experiment shown in Figure 6.40 except with an FcNafion modified CSPE. The initial oxidation current is an order of magnitude larger than that of the unmodified CSPE due to the presence of Fc on the surface of the electrode. This experiment also shows no oxidation current due to EtOH or PA.

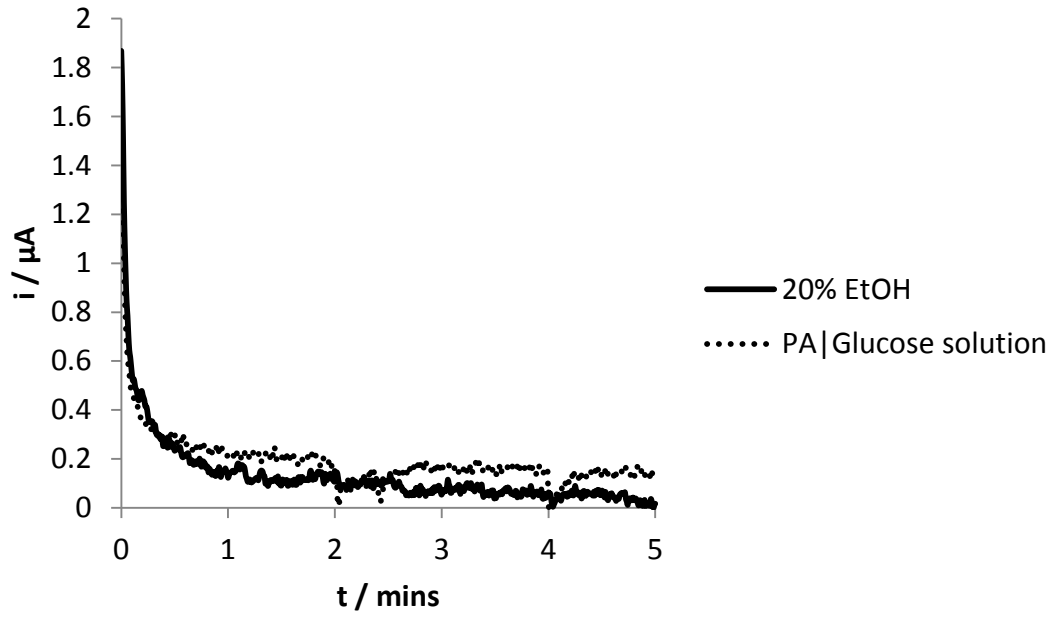

Figure 6.41: CA (E = 0.3V vs Ag QRE) for a CSPE modified with FcNafion in a perspex cell containing 9ml of 0.1M PBS (pH7) (baseline current subtracted).

6.3.6 Investigation of the effect of Glucose on NEFA sensing with ACOD

It is important to investigate the interference of glucose on the NEFA sensing electrode. Therefore the influence on the current response of a CSPE modified with PDA-MWCNT and ACOD after the addition of Oleoyl coenzyme A (an analogue of the Acyl-CoA

product of the oxidation of fatty acids by ACS (Acetyl—CoA Synthetase) was investigated.

A CSPE was modified according to the procedure outlined in Section 6.2.3. The modified CSPE was then placed in a perspex cell containing 500µl of 0.1M PBS (pH7). A CA was carried out on the electrode at 0.5V (vs Ag QRE). The cell OACoA concentration was increased by 0.5mM after 2 minutes, the cell glucose concentration was increased by 5mM after 4 minutes.

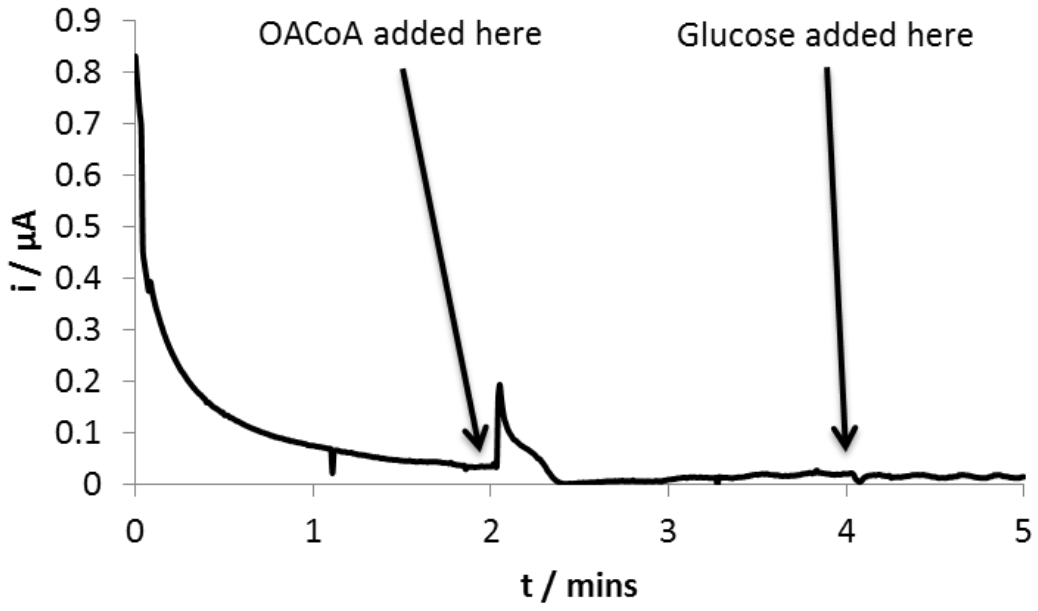

Figure 6.42: CA (E = 0.5V vs Ag QRE) for the CSPE|(PDA-MWCNT|ACOD)$_2$ in a perspex cell containing 500µl of 0.1M PBS (pH7) (baseline current subtracted).

Figure 6.42 shows the result of the CA experiment carried out on CSPE|(PDA-MWCNT|ACOD)$_2$. 25µl of 10mM OACoA solution was added to the cell after two minutes resulting in a 0.5mM cell concentration. An increase in oxidation current is seen immediately corresponding to the oxidation of H_2O_2 produced in the second step of the reaction shown in Figure 6.29.

2.5µl of 1M glucose solution was added to the cell after four minutes, resulting in a cell concentration of 5mM. No change in oxidation current is seen after the addition of glucose indicating that glucose does not interfere in this reaction. The CA experiment was continued for 10 more minutes (not shown) in order to see if there was any change in the current response but no further change was seen.

Investigation of the Effect of Glucose on the Process

Glucose is commonly present in the blood serum samples. Therefore there is a possibility that it can be a physiological interferants for NEFA detection. To investigate the effect of glucose on NEFA detection, 5 mM glucose was added to the cell with 0.5 mM OACoA on a (PDA-MWCNT|ACOD)$_2$ modified electrode to investigate its interference. Negligible current was observed after addition of glucose The presence of 5mM glucose increased the oxidation current by 0.0364µA (18.38%) at 500mV (Figure 6.43). On the contrary, when using a bare carbon electrode, having OACoA and ACOD present in solution, 5mM glucose has induced an increase of oxidation current at 500 mV of 0.09 µA (62.46%) (Figure 6.44). This indicates that the multilayer polymer and enzyme immobilised on the electrode surface can suppress non-specific adsorption of glucose on the electrode. This is a desired property for a sensor device to only produce a signal from its substrate specifically.

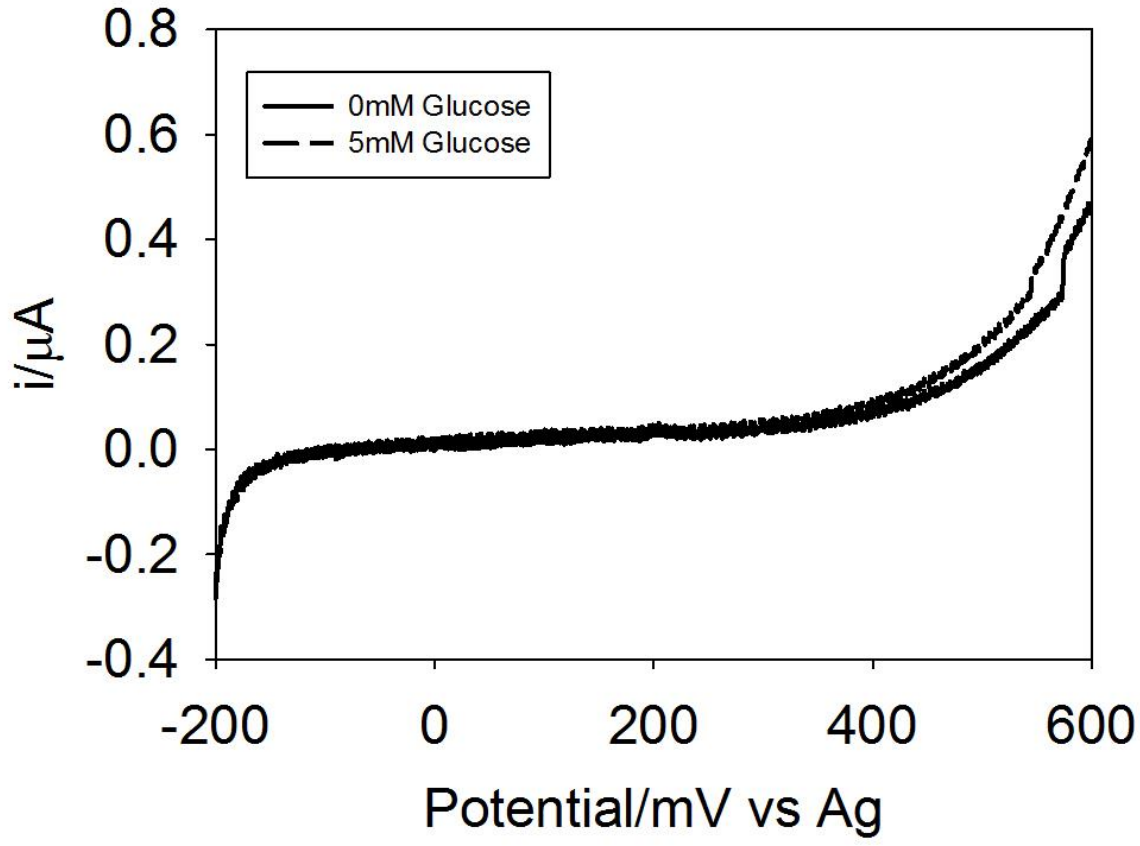

Figure 6.43: LSVs (scan rate = 10mV s^{-1}) for 0mM and 5mM concentrations of glucose measured at a (PDA-MWCNT|ACOD)$_2$ modified electrode in a cell containing 0.5mM OACoA.

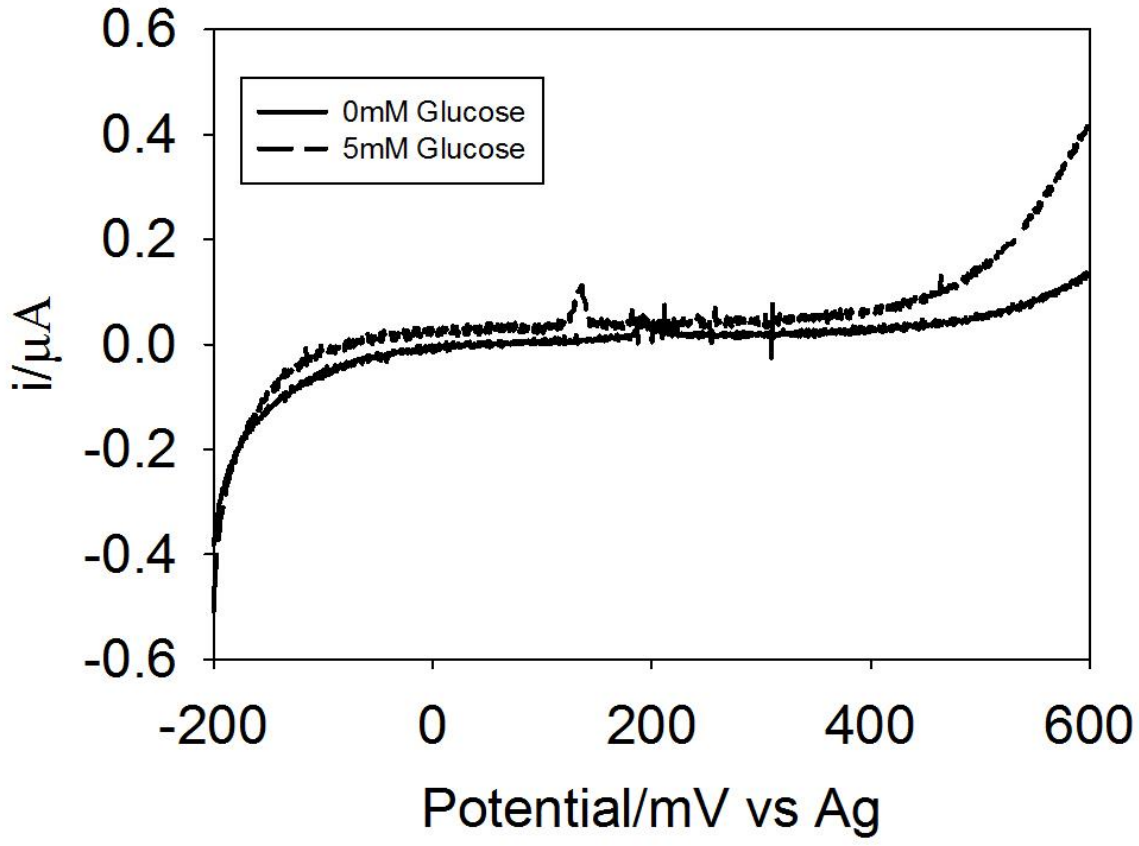

Figure 6.44: LSVs (scan rate = 10mV s^{-1}) for 0mM and 5mM concentrations of glucose measured at a bare CSPE in a cell containing 0.5mM OACoA and 0.4 units ml^{-1} ACOD.

6.4 Conclusions

The LBL method was initially tested with GOx to determine if it was possible to detect DET based on the fact that CNTs would be in close proximity to GOx upon immobilisation. No DET was detected, however, GOx retained its activity when immobilised using the LBL method, as evidenced by the oxidation of H_2O_2, produced during the enzymes catalytic cycle in the presence of glucose, which could be detected by the electrode.

Entrapment of GOx in a layer of PDA-MWCNT also did not produce DET but the GOx retained its activity, as evidenced by the detection of H_2O_2 oxidation at the electrode

surface, in the presence of glucose. Experiments carried out using two SPEs modified with ACOD for the detection of thioester analogues of the Acyl-CoA product of the oxidation of fatty acids by ACS and GOx for the detection of glucose indicated that both analytes can be detected from same sample without interfering with each other. Subsequent experiments then showed that both NEFA and glucose can be detected electrochemically using enzyme electrodes from a single mixed analyte sample.

Chapter 7 - Conclusions & Recommendations for Future Work

The main work of this study was to fabricate and characterise enzyme electrodes for potential use in implantable medical devices such as biofuel cells and biosensors. Enzyme electrodes were fabricated using various methods with different configurations. An electrochemical investigation into the stability, activity, susceptibility to interference, ease of fabrication and feasibility of use in novel applications such as multi analyte sensors of various enzyme electrodes was carried out. The characterisation and analysis of materials for use in enzyme electrodes was accomplished along with tests on enzyme electrodes in various different scenarios such as half-cell tests, fuel cell tests and multi analyte sensing. The conclusions drawn from this study are as follows.

One of the most promising ways to improve the performance of GOx based enzyme electrodes is to create mutant forms of the enzyme with improved characteristics for enzyme electrode design.[113] This was the starting point for the project and such mutant enzymes where characterised using the redox polymer Poly(vinylferrocene-co-2-hydroxyethyl methacrylate) (p(VFc-Co-HEMA). However the redox polymer suffered from poor stability and this proved problematic for the characterisation of mutant enzymes. Therefore attention was focused on improving the stability of redox polymers for enzyme electrodes and these were tested with commercially available GOx.

One attempt to improve the stability of the GOx based enzyme electrode involved the use of the phospholipid polymer poly(2-methacryloyloxyethyl phosphorylcholine-co-n-butyl methacrylate (PMBN). This polymer was modified with Ferrocene Carboxylic acid in order to produce a biocompatible redox polymer for use in enzyme electrode design. This

redox polymer was shown to be electrochemically stable and stable in solution for several hours whilst immobilised onto an electrode surface. When GOx was immobilised onto this redox polymer, electrocatalytic activity was observed, albeit up to a relatively low glucose concentration (3mM). The enzyme electrode was also shown to give a stable response to glucose over several hours and retain its activity over several days, although the activity was substantially reduced.

It is well known that the presence of polymers at the surface of electrode can help make them more resistant to unwanted electrochemical signals. Therefore the ability of this enzyme electrode to resist interference from AA and urea was also tested. The enzyme electrode was found to be capable of resisting interference from urea, however it was not resistant to interference from AA.

Another attempt to improve the stability of GOx based enzyme electrodes involved the use of a mixture of Ferrocene and Nafion (FcNafion) as a redox polymer. This redox polymer was shown to be electrochemically stable and when GOx was immobilised onto a layer of FcNafion a linear electrocatalytic response to glucose up to 4mM was seen. Attempts to increase the linear range of this enzyme electrode using the enzyme stabilising protein bovine serum albumin, but this was shown to interfere with the detection of glucose.

Therefore the phospholipid polymer PMBN was used to stabilise the enzyme, which increased the linear glucose detection range of the electrode to 10mM.

The enzyme was then immobilised directly into a mixture of FcNafion and the enzyme was shown to retain activity even in the presence of the Nafion ionomer dissolved in ethanol. By combining the beneficial effects of both Nafion and PMBN into the electrode design the resistance to interference and stability of the electrode was improved.

The relatively positive oxidation potential of Fc can be problematic for use in biosensor and biofuel cell applications as it leads to problems with interference and lowers the operating voltage of any potential fuel cell using this mediator. Therefore investigations were carried out into the use of mediators with lower oxidation potentials such as coenzyme Q_{10} (CQ_{10}). A redox polymer was fabricated using PMBN and CQ_{10} and was shown to be electrochemically stable. GOx was then added to the redox polymer and the resulting enzyme electrode was shown to be electrocatalytically active towards glucose. However the mass transport limitations associated with CQ_{10} meant that the performance of this enzyme electrode did not match that of those fabricated using Fc.

The operating potential of a GOx based enzyme electrode can be brought close to the redox potential of the FAD active site itself by achieving direct electron transfer (DET) from the FAD centre to electrode surfaces. This greatly reduces the problem of electrochemical interference and maximises the operating voltage of any subsequent fuel cell utilising DET. Investigations were carried out using the biocompatible polymer chitosan modified with CNTs and AuNPs in association with GOx in order to achieve DET and fabricate a working DET based enzyme electrode. DET from GOx was detected

with this electrode but the electrode did not show any electrocatalytic activity towards glucose.

The FcNafionGOx based enzyme electrode was then used in conjunction with a Bilirubin oxidase based enzyme electrode to create a simple enzymatic biofuel cell using only screen printed electrodes. The cell produced a power output of 0.211µW.

Finally the FcNafionGOx based enzyme electrode was used as a glucose sensor along with a NEFA sensing electrode in a duel analyte sensing system. Demonstrating the feasibility of the simultaneous real time electrochemical detection of multiple analytes from single mixed samples.

7.1 Recommendations for Future Work

7.1.1 Enzymes

GOx has many advantages for use in enzyme electrodes. However there are alternative enzymes that may offer more promising alternatives to GOx. One such enzyme is Pyranose 2 Oxidase (P2O).

P2O is an FAD dependent oxidase fungi and has a proposed role in the oxidative events of lignin degradation.[212] It is a homotetrameric enzyme with a molecular mass of 270 kDa, where each of the four subunits carries one FAD molecule covalently bound to a Histadine group,[212] and one active site.[213]

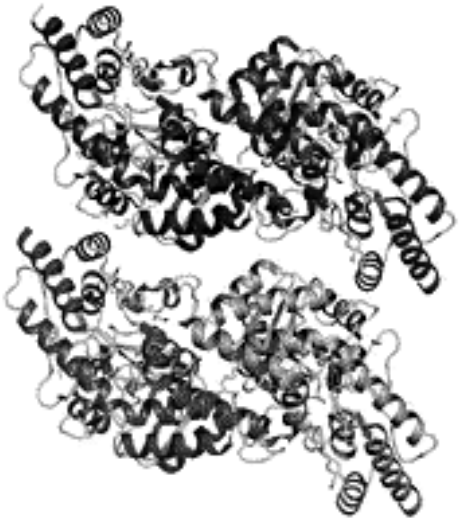

Figure 7.1: The structure of P2O.

Like GOx, P2O can transfer electrons to a wide variety of acceptors.[214] One of the advantages of P2O over GOx is the fact that P2O can oxidise a wide range of carbohydrate substrates.[212] This means that if P2O is used as the enzyme in the anode of an enzymatic biofuel cell, the fuel cell will be able to utilise a wider range of fuels and could therefore produce a higher power output than GOx based EBCs.

The reactivity of P2O towards O_2 can also be reduced by modifying its active site via the replacement of certain amino acid residues.[215] This could possibly enhance its performance in enzyme electrodes.

The feasibility of using modified P2O in enzyme electrodes was tested after a sample of a T169G (the Threonine 169 amino acid reside was replaced with a Glycine group)[215] mutant of P2O was kindly donated by collaborators from Thailand.

The enzyme was immobilised using the FcNafion method outlined in Section 5.2.1, with the exception that 0.125% w/w Nafion solution in 45% ethanol containing 2.5mM Fc (FcNafion) and 6.7 mg ml^{-1} T169G P2O was used.

Figure 7.2 shows CVs recorded using a CSPE modified with FcNafion containing the T169G mutant of P2O. It can be seen that the modified enzyme reduced by glucose can transfer electrons to Fc and generate catalytic current. This is very encouraging and it would be interesting to see further studies using this modified enzyme as the catalyst for a sugar oxidising anode in an EBC.

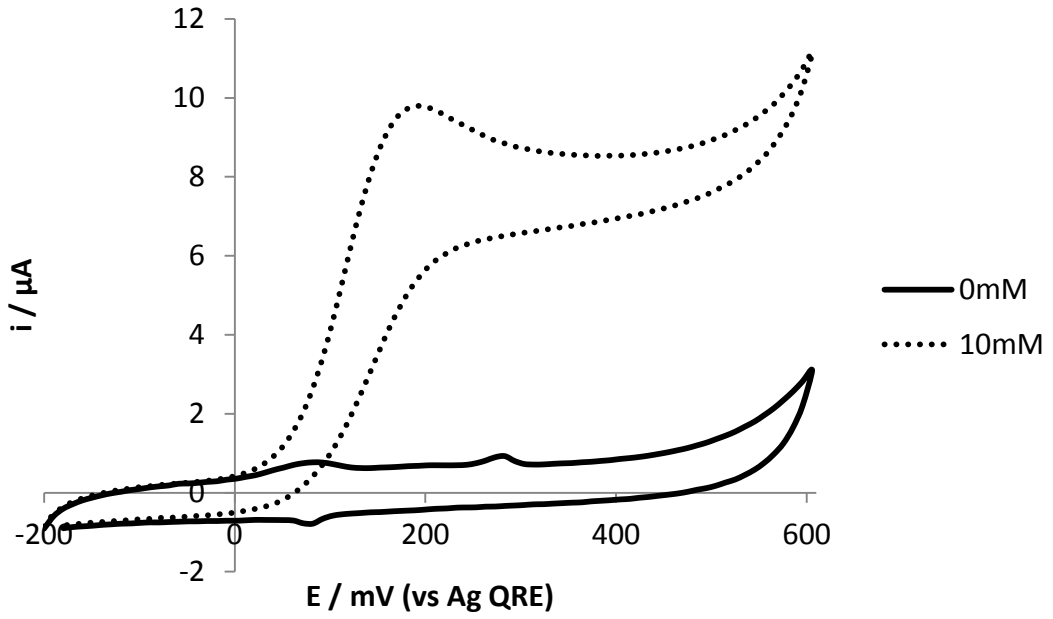

Figure 7.2: CVs (v = 10mV s^{-1}) at 0mM and 10mM glucose for immobilised T169G P2O.

7.1.2 Mediators

As discussed in Chapter 2, Fc has many advantages for use in enzyme electrodes based on GOx and the best results were obtained using this mediator. However the relatively positive oxidation potential of this mediator is problematic. Other mediators with lower oxidation potentials than Fc have been used successfully with GOx, however, they tend to be plagued by low diffusion coefficients, limiting their usefulness. Therefore, electrode fabrication methods that can take advantage of the relatively negative oxidation potentials

of quinone based redox mediators, whilst avoiding the problems associated with low diffusion coefficients will provide a substantial increase in the performance of enzyme electrodes.

7.1.3 *In Vivo* Studies

Due to the nature of enzyme electrodes, their main application is likely to be in biologically implantable devices. Therefore it would be interesting to investigate the performance of the enzyme electrodes fabricated in this work in real physiological solutions and subsequently *in vivo* studies. This will be particularly interesting for the dual detection system outlined in Chapter 6, as this technology has the potential to substantially improve current medical diagnosis.

References

[1] S. Calabrese Barton, J. Gallaway and P. Atanassov, *Chemical Reviews* **2004**, *104*, 4867-4886.

[2] A. Heller, *Analytical and Bioanalytical Chemistry* **2006**, *385*, 469-473.

[3] W. E. Farneth and M. B. D'Amore, *Journal of Electroanalytical Chemistry* **2005**, *581*, 197-205.

[4] L. C. Clark and C. Lyons, *Annals of the New York Academy of Sciences* **1962**, *102*, 29-45.

[5] S. J. Updike and G. P. Hicks, *Nature* **1967**, *214*, 986-988.

[6] E. Katz, A. Riklin, V. Heleg-Shabtai, I. Willner and A. F. Bückmann, *Analytica Chimica Acta* **1999**, *385*, 45-58.

[7] Y. Degani and A. Heller, *Journal of the American Chemical Society* **1988**, *110*, 2615-2620.

[8] J. Davis, *Engineering the Bioelectronic Interface*, Royal Society of Chemistry, **2009**, p.

[9] C. Bourdillon, J. P. Bourgeois and D. Thomas, *Journal of the American Chemical Society* **1980**, *102*, 4231-4235.

[10] P. Kavanagh and D. Leech, *Physical Chemistry Chemical Physics* **2013**, *15*, 4859-4869.

[11] a) H. J. Hecht, D. Schomburg, H. Kalisz and R. D. Schmid, *Biosensors & Bioelectronics* **1993**, *8*, 197-203; b) H. J. Hecht, H. M. Kalisz, J. Hendle, R. D. Schmid and D. Schomburg, *Journal of Molecular Biology* **1993**, *229*, 153-172.

[12] Y. Degani and A. Heller, *The Journal of Physical Chemistry* **1987**, *91*, 1285-1289.

[13] A. T. Yahiro, S. M. Lee and D. O. Kimble, *Biochimica et Biophysica Acta (BBA) - Specialized Section on Biophysical Subjects* **1964**, *88*, 375-383.

[14] A. L. Crumbliss, H. A. O. Hill and D. J. Page, *Journal of Electroanalytical Chemistry* **1986**, *206*, 327-331.

[15] T. Saito and M. Watanabe, *Reactive and Functional Polymers* **1998**, *37*, 263-269.

[16] A. E. G. Cass, G. Davis, G. D. Francis, H. A. O. Hill, W. J. Aston, I. J. Higgins, E. V. Plotkin, L. D. L. Scott and A. P. F. Turner, *Analytical Chemistry* **1984**, *56*, 667-671.

[17] H. Sakai, T. Nakagawa, Y. Tokita, T. Hatazawa, T. Ikeda, S. Tsujimura and K. Kano, *Energy & Environmental Science* **2009**, *2*, 133-138.

[18] J. Kim, J. Parkey, C. Rhodes and A. Gonzalez-Martin, *Journal of Solid State Electrochemistry* **2008**, *13*, 1043-1050.

[19] E. Katz, D. D. Schlereth and H.-L. Schmidt, *Journal of Electroanalytical Chemistry* **1994**, *367*, 59-70.

[20] M. G. Loughran, M. H. Jenny and P. F. T. Anthony, *Electroanalysis* **1996**, *8*, 870-875.

[21] E. Yu, Y. Himuro, M. Takai and K. Ishihara, *Applied Biochemistry and Biotechnology* **2009**, *160*, 1094-1101.

[22] H. Shinohara, G. F. Khan, Y. Ikariyama and M. Aizawa, *Journal of Electroanalytical Chemistry* **1991**, *304*, 75-84.

[23] E. Katz, V. Heleg-Shabtai, B. Willner, I. Willner and A. F. Bückmann, *Bioelectrochemistry and Bioenergetics* **1997**, *42*, 95-104.

[24] I. Willner, E. Katz and B. Willner, *Electroanalysis* **1997**, *9*, 965-977.

[25] S. Michalkiewicz, *Bioelectrochemistry* **2008**, *73*, 30-36.

[26] Y. Kajiya and H. Yoneyama, *Journal of Electroanalytical Chemistry* **1992**, *341*, 85-92.

[27] S. Dong, B. Wang and B. Liu, *Biosensors and Bioelectronics* **1992**, *7*, 215-222.

[28] R. P. Liang, L. X. Fan, R. Wang and J. D. Qiu, *Electroanalysis* **2009**, *21*, 1685-1691.

[29] J. Kulys and H. E. Hansen, *Biosensors and Bioelectronics* **1994**, *9*, 491-500.

[30] C. M. Moore, N. L. Akers, A. D. Hill, Z. C. Johnson and S. D. Minteer, *Biomacromolecules* **2004**, *5*, 1241-1247.

[31] P. Schläpfer, W. Mindt and P. H. Racine, *Clinica Chimica Acta* **1974**, *57*, 283-289.

[32] J. R. Macdonald, *Annals of Biomedical Engineering* **1992**, *20*, 289-305.

[33] a) S. R. Taylor and E. Gileadi, *CORROSION* **1995**, *51*, 85-94; b) I. Rubinstein, J. Rishpon and S. Gottesfeld, *Journal of The Electrochemical Society* **1986**, *133*, 729-734.

[34] K. E. Johnson, *Electrochimica Acta* **1964**, *9*, 653-657.

[35] G. Inzelt and G. Lang, *Electrochimica Acta* **1991**, *36*, 1355-1361.

[36] M. M. Musiani, *Electrochimica Acta* **1990**, *35*, 1665-1670.

[37] R. M. Penner and C. R. Martin, *The Journal of Physical Chemistry* **1989**, *93*, 984-989.

[38] R. Ehret, W. Baumann, M. Brischwein, A. Schwinde, K. Stegbauer and B. Wolf, *Biosensors and Bioelectronics* **1997**, *12*, 29-41.

[39] J. E. B. Randles, *Discussions of the Faraday Society* **1947**, *1*, 11-19.

[40] B. Lindholm, *Journal of Electroanalytical Chemistry and Interfacial Electrochemistry* **1990**, *289*, 85-101.

[41] S. Panero, P. Prosperi, S. Passerini, B. Scrosati and D. D. Perlmutter, *Journal of the Electrochemical Society* **1989**, *136*, 3729-3734.

[42] J. Tanguy, N. Mermilliod and M. Hoclet, *Journal of the Electrochemical Society* **1987**, *134*, 795-802.

[43] R. D. D. Armstrong, B. Lindholm and M. Sharp, *Journal of Electroanalytical Chemistry and Interfacial Electrochemistry* **1986**, *202*, 69-74.

[44] T. B. Hunter, P. S. Tyler, W. H. Smyrl and H. S. White, *Journal of the Electrochemical Society* **1987**, *134*, 2198-2204.

[45] J.-P. Candy, P. Fouilloux, M. Keddam and H. Takenouti, *Electrochimica Acta* **1981**, *26*, 1029-1034.

[46] a) C. Deslouis, M. M. Musiani and B. Tribollet, *Journal of Electroanalytical Chemistry and Interfacial Electrochemistry* **1989**, *264*, 37-55; b) W. J. Albery, Z. Chen, B. R. Horrocks, A. R. Mount, P. J. Wilson, D. Bloor, A. T. Monkman and C. M. Elliott, *Faraday Discussions of the Chemical Society* **1989**, *88*, 247-259.

[47] C. M. A. B. a. A. M. O. Brett, *Electrochemistry: Principles, Methods, and Applications*, Oxford University Press, **1993**, p. 231-235.

[48] J. H. Sluyters, *Recueil des Travaux Chimiques des Pays-Bas* **1960**, *79*, 1092-1100.

[49] E. J. Calvo, R. Etchenique, C. Danilowicz and L. Diaz, *Analytical Chemistry* **1996**, *68*, 4186-4193.

[50] a) B. Lindholm, M. Sharp and R. D. Armstrong, *Journal of Electroanalytical Chemistry and Interfacial Electrochemistry* **1987**, *235*, 169-177; b) G. Lang and G. Inzelt, *Electrochimica Acta* **1991**, *36*, 847-854.

[51] C. Gabrielli, H. Takenouti, O. Haas and A. Tsukada, *Journal of Electroanalytical Chemistry and Interfacial Electrochemistry* **1991**, *302*, 59-89.

[52] T. T. N. Lien, T. D. Lam, V. T. H. An, T. V. Hoang, D. T. Quang, D. Q. Khieu, T. Tsukahara, Y. H. Lee and J. S. Kim, *Talanta* **2009**, *80*, 1164-1169.

[53] M. Knichel, P. Heiduschka, W. Beck, G. Jung and W. Gopel, *Sensors and Actuators B: Chemical* **1995**, *28*, 85-94.

[54] N. Nakajima and Y. Ikada, *Bioconjugate Chemistry* **1995**, *6*, 123-130.

[55] K. De Wael, H. Buschop, L. De Smet and A. Adriaens, *Talanta* **2008**, *76*, 309-313.

[56] M. A. Lange and J. Q. Chambers, *Analytica Chimica Acta* **1985**, *175*, 89-97.

[57] L. Gorton, H. I. Karan, P. D. Hale, T. Inagaki, Y. Okamoto and T. A. Skotheim, *Analytica Chimica Acta* **1990**, *228*, 23-30.

[58] M. J. Green and H. A. O. Hill, *Journal of the Chemical Society, Faraday Transactions 1* **1986**, *82*, 1237-1243.

[59] M. Watanabe, H. Nagasaka and N. Ogata, *The Journal of Physical Chemistry* **1995**, *99*, 12294-12300.

[60] A. Badia, R. Carlini, A. Fernandez, F. Battaglini, S. R. Mikkelsen and A. M. English, *Journal of the American Chemical Society* **1993**, *115*, 7053-7060.

[61] Y. Himuro, M. Takai and K. Ishihara, *Sensors and Actuators B: Chemical* **2009**, *136*, 122-127.

[62] D. J. Harrison, R. F. B. Turner and H. P. Baltes, *Analytical Chemistry* **1988**, *60*, 2002-2007.

[63] J. K. Harkness, O. J. Murphy and G. D. Hitchens, *Journal of Electroanalytical Chemistry* **1993**, *357*, 261-272.

[64] A. Vishnyakov and A. V. Neimark, *The Journal of Physical Chemistry B* **2001**, *105*, 9586-9594.

[65] H. L. Yeager and A. Steck, *Journal of the Electrochemical Society* **1981**, *128*, 1880-1884.

[66] N. P. Blake, M. K. Petersen, G. A. Voth and H. Metiu, *The Journal of Physical Chemistry B* **2005**, *109*, 24244-24253.

[67] a) R. F. B. Turner, D. J. Harrison, R. V. Rajotte and H. P. Baltes, *Sensors and Actuators B: Chemical* **1990**, *1*, 561-564; b) A. A. Karyakin, E. A. Kotel'nikova, L. V. Lukachova, E. E. Karyakina and J. Wang, *Analytical Chemistry* **2002**, *74*, 1597-1603.

[68] A. A. Karyakin, E. E. Karyakina, L. Gorton, O. A. Bobrova, L. V. Lukachova, A. K. Gladilin and A. V. Levashov, *Analytical Chemistry* **1996**, *68*, 4335-4341.

[69] I. Rubinstein and A. J. Bard, *Journal of the American Chemical Society* **1980**, *102*, 6641-6642.

[70] I. Rubinstein, *Analytical Chemistry* **1984**, *56*, 1135-1137.

[71] A. Malinauskas, Kuzmarskyt, R. Meskys and A. Ramanavicius, *Sensors and Actuators B: Chemical* **2004**, *100*, 387-394.

[72] H. S. White, J. Leddy and A. J. Bard, *Journal of the American Chemical Society* **1982**, *104*, 4811-4817.

[73] M. Vaillancourt, J. Wei Chen, G. Fortier and D. Bélanger, *Electroanalysis* **1999**, *11*, 23-31.

[74] a) M. J. Schrenk, R. E. Villigram, N. J. Torrence, S. J. Brancato and S. D. Minteer, *Journal of Membrane Science* **2002**, *205*, 3-10; b) T. J. Thomas, K. E. Ponnusamy, N. M. Chang, K. Galmore and S. D. Minteer, *Journal of Membrane Science* **2003**, *213*, 55-66.

[75] H. W. Rollins, F. Lin, J. Johnson, J.-J. Ma, J.-T. Liu, M.-H. Tu, D. D. DesMarteau and Y.-P. Sun, *Langmuir* **2000**, *16*, 8031-8036.

[76] C. R. Martin and H. Freiser, *Analytical Chemistry* **1981**, *53*, 902-904.

[77] M. W. Espenscheid, A. R. Ghatak-Roy, R. B. Moore, R. M. Penner, M. N. Szentirmay and C. R. Martin, *Journal of the Chemical Society, Faraday Transactions 1: Physical Chemistry in Condensed Phases* **1986**, *82*, 1051-1070.

[78] M. A. F. Robertson and H. L. Yeager, *Macromolecules* **1996**, *29*, 5166-5171.

[79] A. Lindheimer, J. Molenat and C. Gavach, *Journal of Electroanalytical Chemistry and Interfacial Electrochemistry* **1987**, *216*, 71-88.

[80] Y. Zhang, Y. Hu, G. S. Wilson, D. Moatti-Sirat, V. Poitout and G. Reach, *Analytical Chemistry* **1994**, *66*, 1183-1188.

[81] G. A. Gerhardt, A. F. Oke, G. Nagy, B. Moghaddam and R. N. Adams, *Brain Research* **1984**, *290*, 390-395.

[82] J. Redepenning and F. C. Anson, *The Journal of Physical Chemistry* **1987**, *91*, 4549-4553.

[83] C. E. W. Hahn, H. A. O. Hill, M. D. Ritchie and J. W. Sear, *Journal of the Chemical Society, Chemical Communications* **1990**, 125-126.

[84] J. Weber, L. Kavan and M. Štícha, *Journal of Electroanalytical Chemistry and Interfacial Electrochemistry* **1991**, *303*, 237-244.

[85] A. Heller, *Accounts of Chemical Research* **1990**, *23*, 128-134.

[86] P. Atanasov, A. Kaisheva, S. Gamburzev and I. Iliev, *Sensors and Actuators B: Chemical* **1992**, *8*, 59-64.

[87] S. Koide and K. Yokoyama, *Journal of Electroanalytical Chemistry* **1999**, *468*, 193-201.

[88] V. S. Tripathi, V. B. Kandimalla and H. Ju, *Biosensors and Bioelectronics* **2006**, *21*, 1529-1535.

[89] M. Snejdarkova, M. Rehak and M. Otto, *Analytical Chemistry* **1993**, *65*, 665-668.

[90] A. Anine, J. M. Kauffmann, G. J. Patriarche and G. G. Guilbault, *Analytical Letters* **1989**, *22*, 2403-2411.

[91] J. A. Hayward and D. Chapman, *Biomaterials* **1984**, *5*, 135-142.

[92] N. Nakabayashi and D. F. Williams, *Biomaterials* **2003**, *24*, 2431-2435.

[93] T. Matsuda, J. Nagase, A. Ghoda, Y. Hirano, S. Kidoaki and Y. Nakayama, *Biomaterials* **2003**, *24*, 4517-4527.

[94] S. P. Ho, N. Nakabayashi, Y. Iwasaki, T. Boland and M. LaBerge, *Biomaterials* **2003**, *24*, 5121-5129.

[95] J. Watanabe and K. Ishihara, *Colloids and Surfaces B: Biointerfaces* **2008**, *65*, 155-165.

[96] K. T. Kinnear and H. G. Monbouquette, *Analytical Chemistry* **1997**, *69*, 1771-1775.

[97] A. L. Lewis, *Colloids and Surfaces B: Biointerfaces* **2000**, *18*, 261-275.

[98] T. Morisaku, J. Watanabe, T. Konno, M. Takai and K. Ishihara, *Polymer* **2008**, *49*, 4652-4657.

[99] T. Ueda, H. Oshida, K. Kurita, K. Ishihara and N. Nakabayashi, *Polymer Journal* **1992**, *24*, 1259-1269.

[100] K. Ishihara, S.-I. Ohta, T. Yoshikawa and N. Nakabayashi, *Journal of Polymer Science Part A: Polymer Chemistry* **1992**, *30*, 929-932.

[101] a) K. Takei, T. Konno, J. Watanabe and K. Ishihara, *Biomacromolecules* **2004**, *5*, 858-862; b) K. Ishihara, R. Aragaki, T. Ueda, A. Watenabe and N. Nakabayashi, *Journal of Biomedical Materials Research* **1990**, *24*, 1069-1077; c) K. Ishihara and M. Takai, *Journal of The Royal Society Interface* **2009**, *6*, S279-S291-S279 -S291.

[102] K. Ishihara, Y. Iwasaki and N. Nakabayashi, *Materials Science and Engineering: C* **1998**, *6*, 253-259.

[103] K. Ishihara, Y. Goto, M. Takai, R. Matsuno, Y. Inoue and T. Konno, *Biochimica et Biophysica Acta (BBA) - General Subjects* **2010**, *In Press*.

[104] M. Chu, H. Kudo, T. Shirai, K. Miyajima, H. Saito, N. Morimoto, K. Yano, Y. Iwasaki, K. Akiyoshi and K. Mitsubayashi, *Biomedical Microdevices* **2009**, *11*, 837-842.

[105] Y. Xu, M. Takai and K. Ishihara, *Annals of Biomedical Engineering* **2010**, *38*, 1938-1953.

[106] K. Ishihara, H. Oshida, Y. Endo, T. Ueda, A. Watanabe and N. Nakabayashi, *Journal of Biomedical Materials Research* **1992**, *26*, 1543-1552.

[107] K. Sakai-Kato, M. Kato, K. Ishihara and T. Toyo'oka, *Lab on a Chip* **2004**, *4*, 4-6.

[108] Y. Goto, R. Matsuno, T. Konno, M. Takai and K. Ishihara, *Biomacromolecules* **2008**, *9*, 828-833.

[109] K. Nishizawa, T. Konno, M. Takai and K. Ishihara, *Biomacromolecules* **2008**, *9*, 403-407.

[110] K. Ishihara and M. Takai, *Journal of The Royal Society Interface* **2009**, *6*, S279 -S291.

[111] K. Takehara and Y. Ide, *Bioelectrochemistry and Bioenergetics* **1991**, *26*, 297-305.

[112] A. Matsushima, Y. Kodera, M. Hiroto, H. Nishimura and Y. Inada in *Polyethylene Glycol-Modified Enzymes in Hydrophobic Media*, *Vol.* **2001**, pp. 49-64.

[113] E. Yu, R. Prodanovic, G. Güven, R. Ostafe and U. Schwaneberg, *Applied Biochemistry and Biotechnology* **2011**, *165*, 1448-1457.

[114] D. R. Thevenot, K. Toth, R. A. Durst and G. S. Wilson, *Pure and Applied Chemistry* **1999**, *71*, 2333-2348.

[115] F. R. Shu and G. S. Wilson, *Analytical Chemistry* **1976**, *48*, 1679-1686.

[116] Y.-M. Uang and T.-C. Chou, *Biosensors and Bioelectronics* **2003**, *19*, 141-147.

[117] P. Pandey, S. P. Singh, S. K. Arya, V. Gupta, M. Datta, S. Singh and B. D. Malhotra, *Langmuir* **2007**, *23*, 3333-3337.

[118] a) P. V. Sundaram, A. Tweedale and K. J. Laidler, *Canadian Journal of Chemistry* **1970**, *48*, 1498-1504; b) X. Liu, K. G. Neoh, L. Cen and E. T. Kang, *Biosensors and Bioelectronics* **2004**, *19*, 823-834.

[119] C. He, J. Liu, L. Xie, Q. Zhang, C. Li, D. Gui, G. Zhang and C. Wu, *Langmuir* **2009**, *25*, 13456-13460.

[120] a) H. H. Weetall, *Analytical Chemistry* **1974**, *46*, 602A-615a; b) A. Petrigliano, A. Tronin and C. Nicolini, *Thin Solid Films* **1996**, *284-285*, 752-756.

[121] G. Hermanson, *Bioconjugate Techniques*, **2008**, p.

[122] F. M. Richards and J. R. Knowles, *Journal of Molecular Biology* **1968**, *37*, 231-233.

[123] R. A. Kamin and G. S. Wilson, *Analytical Chemistry* **1980**, *52*, 1198-1205.

[124] E. J. Lahoda, C. C. Liu and L. B. Wingard, *BIOTECHNOLOGY AND BIOENGINEERING* **1975**, *17*, 413-422.

[125] D. Thomas, G. Broun and E. Sélégny, *Biochimie* **1972**, *54*, 229-244.

[126] B. Solomon, N. Lotan and E. Katchalski-Katzir, *Biopolymers* **1977**, *16*, 1837-1851.

[127] W. Furst and A. Banerjee, *The Annals of Thoracic Surgery* **2005**, *79*, 1522-1528.

[128] a) C. C. Liu, E. J. Lahoda, R. T. Galasco and L. B. Wingard, *BIOTECHNOLOGY AND BIOENGINEERING* **1975**, *17*, 1695-1696; b) J. C. Pickup, G. W. Shaw and D. J. Claremont, *Biosensors* **1989**, *4*, 109-119; c) E. F. Jansen, Y. Tomimatsu and A. C. Olson, *Archives of Biochemistry and Biophysics* **1971**, *144*, 394-400; d) A. F. S. A. Habeeb, *Archives of Biochemistry and Biophysics* **1967**, *119*, 264-268.

[129] A. D. Ryabov, V. N. Goral, L. Gorton and E. Csoregi, *Chemistry-a European Journal* **1999**, *5*, 961-967.

[130] S. Krishnan and F. A. Armstrong, *Chemical Science* **2012**, *3*, 1015-1023.

[131] Š. Komorsky-Lovrić and M. Lovrić, *Electroanalysis* **1996**, *8*, 959-962.

[132] A. J. Bard and L. Faulkner, *Electrochemical Methods: Fundamentals and Applications*, John Wiley & Sons, **2001**, p.

[133] I. Willner, E. Katz, B. Willner, R. Blonder, V. Heleg-Shabtai and A. F. Bückmann, *Biosensors and Bioelectronics* **1997**, *12*, 337-356.

[134] M. Slawomir, *Bioelectrochemistry* **2011**, *82*, 103-111.

[135] A. Jaworska-Augustyniak and J. Wojtczak, *Monatshefte fur Chemie* **1979**, *110*, 1113-1121.

[136] O. S. Ksenzhek, S. A. Petrova and M. V. Kolodyazhny, *Bioelectrochemistry and Bioenergetics* **1982**, *9*, 167-174.

[137] a) T. Erabi and M. Tanaka, *Bulletin of the Chemical Society of Japan* **1983**, *56*, 15-18; b) M. Kawakami, K. Tanaka, N. Uriuda and S. Gondo, *Bioelectrochemistry* **2000**, *52*, 51-56.

[138] a) R. S. Schrebler, A. Arratia, S. Sánchez, M. Haun and N. Durán, *Journal of Electroanalytical Chemistry and Interfacial Electrochemistry* **1990**, *298*, 81-91; b) G. J. Gordillo and D. J. Schiffrin, *Journal of the Chemical Society, Faraday Transactions* **1994**, *90*, 1913-1922; c) G. J. Gordillo and D. J. Schiffrin, *Faraday Discussions* **2000**, *116*, 89-107; d) M. R. Moncelli, R. Herrero, L. Becucci and R. Guidelli, *Biochimica et Biophysica Acta (BBA) - Bioenergetics* **1998**, *1364*, 373-384.

[139] K. Takehara, H. Takemura, Y. Ide and S. Okayama, *Journal of Electroanalytical Chemistry and Interfacial Electrochemistry* **1991**, *308*, 345-350.

[140] M. R. Moncelli, L. Becucci, A. Nelson and R. Guidelli, *Biophysical Journal* **1996**, *70*, 2716-2726.

[141] S. Michalkiewicz, *Bioelectrochemistry* **2007**, *70*, 495-500.

[142] T. Ikeda, K. Miki, F. Fushimi and M. Senda, *Agricultural and Biological Chemistry* **1987**, *51*, 747-754.

[143] M. Kawakami, N. Uriuda, H. Koya and S. Gondo, *Analytical Letters* **1995**, *28*, 1555-1569.

[144] S. Sanchez, A. Arratia, R. Córdova, H. Gomez and R. Schrebler, *Bioelectrochemistry and Bioenergetics* **1995**, *36*, 67-71.

[145] J. M. Nugent, K. S. V. Santhanam, A. Rubio and P. M. Ajayan, *Nano Letters* **2001**, *1*, 87-91.

[146] J. J. Gooding, R. Wibowo, Liu, W. Yang, D. Losic, S. Orbons, F. J. Mearns, J. G. Shapter and D. B. Hibbert, *Journal of the American Chemical Society* **2003**, *125*, 9006-9007.

[147] J. Li, A. Cassell, L. Delzeit, J. Han and M. Meyyappan, *The Journal of Physical Chemistry B* **2002**, *106*, 9299-9305.

[148] Z. Xu, N. Gao, H. Chen and S. Dong, *Langmuir* **2005**, *21*, 10808-10813.

[149] J. Wang, M. Musameh and Y. Lin, *Journal of the American Chemical Society* **2003**, *125*, 2408-2409.

[150] S. G. Wang, Q. Zhang, R. Wang, S. F. Yoon, J. Ahn, D. J. Yang, J. Z. Tian, J. Q. Li and Q. Zhou, *Electrochemistry Communications* **2003**, *5*, 800-803.

[151] Z. Liu, Z. Shen, T. Zhu, S. Hou, L. Ying, Z. Shi and Z. Gu, *Langmuir* **2000**, *16*, 3569-3573.

[152] a) F. Zhang, S. S. Cho, S. H. Yang, S. S. Seo, G. S. Cha and H. Nam, *Electroanalysis* **2006**, *18*, 217-222; b) Y. Xiao, F. Patolsky, E. Katz, J. F. Hainfeld and I. Willner, *Science* **2003**, *299*, 1877-1881.

[153] H. Zhang, R. Liu, Q. Sheng and J. Zheng, *Colloids and Surfaces B: Biointerfaces* **2010**, *82*, 532-535.

[154] Q. Xu, C. Mao, N.-N. Liu, J.-J. Zhu and J. Sheng, *Biosensors and Bioelectronics* **2006**, *22*, 768-773.

[155] X.-y. Chen, J.-r. Li, X.-c. Li and L. Jiang, *Biochemical and Biophysical Research Communications* **1998**, *245*, 352-355.

[156] M. Iwamoto, S. Tokonami, H. Shiigi and T. Nagaoka, *Research on Chemical Intermediates* **2009**, *35*, 919-930.

[157] X. Zhou, W. Xu, Y. Wang, Q. Kuang, Y. Shi, L. Zhong and Q. Zhang, *Journal of Physical Chemistry C* **2010**, *114*, 19607-19613.

[158] B. Neiman, E. Grushka and O. Lev, *Analytical Chemistry* **2001**, *73*, 5220-5227.

[159] D. Marchal, W. Boireau, J. M. Laval, J. Moiroux and C. Bourdillon, *Biophysical Journal* **1997**, *72*, 2679-2687.

[160] R. S. Schrebler, A. Arratia, S. SÃ¡nchez, M. Haun and N. DurÃ¡n, *Journal of Electroanalytical Chemistry and Interfacial Electrochemistry* **1990**, *298*, 81-91.

[161] K. Takehara, H. Takemura, Y. Ide and S. Okayama, *Journal of Electroanalytical Chemistry and Interfacial Electrochemistry* **1991**, *308*, 345-350.

[162] J.-M. Laval and M. Majda, *Thin Solid Films* **1994**, *244*, 836-840.

[163] D. Ivnitski, B. Branch, P. Atanassov and C. Apblett, *Electrochemistry Communications* **2006**, *8*, 1204-1210.

[164] R. M. Ianniello, T. J. Lindsay and A. M. Yacynych, *Analytical Chemistry* **1982**, *54*, 1098-1101.

[165] Q. Chi, J. Zhang, S. Dong and E. Wang, *Electrochimica Acta* **1994**, *39*, 2431-2438.

[166] K. Narasimhan and L. B. Wingard, *Analytical Chemistry* **1986**, *58*, 2984-2987.

[167] M. Alvarez-Icaza and R. D. Schmid, *Bioelectrochemistry and Bioenergetics* **1994**, *33*, 191-199.

[168] A. Guiseppi-Elie, C. Lei and R. H. Baughman, *Nanotechnology* **2002**, *13*, 559-564.

[169] C. Cai and J. Chen, *Analytical Biochemistry* **2004**, *332*, 75-83.

[170] J. Liu, A. Chou, W. Rahmat, M. N. Paddon-Row and J. J. Gooding, *Electroanalysis* **2005**, *17*, 38-46.

[171] Y.-D. Zhao, W.-D. Zhang, H. Chen and Q.-M. Luo, *Analytical Sciences* **2002**, *18*, 939-941.

[172] S. Liu and H. Ju, *Biosensors and Bioelectronics* **2003**, *19*, 177-183.

[173] A. Salimi, E. Sharifi, A. Noorbakhsh and S. Soltanian, *Biosensors and Bioelectronics* **2007**, *22*, 3146-3153.

[174] Y. Liu, M. Wang, F. Zhao, Z. Xu and S. Dong, *Biosensors and Bioelectronics* **2005**, *21*, 984-988.

[175] X. Luo, A. Killard and M. Smyth, *Electroanalysis* **2006**, *18*, 1131-1134.

[176] X. Wu, F. Zhao, J. R. Varcoe, A. E. Thumser, C. Avignone-Rossa and R. C. T. Slade, *Bioelectrochemistry* **2009**, *77*, 64-68.

[177] a) R. Fernandes, L.-Q. Wu, T. Chen, H. Yi, G. W. Rubloff, R. Ghodssi, W. E. Bentley and G. F. Payne, *Langmuir* **2003**, *19*, 4058-4062; b) S. D. Minteer, B. Y. Liaw and M. J. Cooney, *Current Opinion in Biotechnology* **2007**, *18*, 228-234.

[178] B.-Y. Wu, S.-H. Hou, F. Yin, J. Li, Z.-X. Zhao, J.-D. Huang and Q. Chen, *Biosensors and Bioelectronics* **2007**, *22*, 838-844.

[179] a) C.-X. Lei, S.-Q. Hu, G.-L. Shen and R.-Q. Yu, *Talanta* **2003**, *59*, 981-988; b) X.-L. Luo, J.-J. Xu, Y. Du and H.-Y. Chen, *Analytical Biochemistry* **2004**, *334*, 284-289.

[180] Y. Du, X.-L. Luo, J.-J. Xu and H.-Y. Chen, *Bioelectrochemistry* **2007**, *70*, 342-347.

[181] M. Zhang, A. Smith and W. Gorski, *Analytical Chemistry* **2004**, *76*, 5045-5050.

[182] A. K. Sarma, P. Vatsyayan, P. Goswami and S. D. Minteer, *Biosensors and Bioelectronics* **2009**, *24*, 2313-2322.

[183] R. A. Bullen, T. C. Arnot, J. B. Lakeman and F. C. Walsh, *Biosensors and Bioelectronics* **2006**, *21*, 2015-2045.

[184] J. Lim, P. Malati, F. Bonet and B. Dunn, *Journal of the Electrochemical Society* **2007**, *154*, A140-A145.

[185] H.-H. Kim, N. Mano, Y. Zhang and A. Heller, *Journal of the Electrochemical Society* **2003**, *150*, A209-A213.

[186] A. Heller, *Physical Chemistry Chemical Physics* **2004**, *6*, 209-216.

[187] P. Cinquin, C. Gondran, F. Giroud, S. Mazabrard, A. Pellissier, F. Boucher, J.-P. Alcaraz, K. Gorgy, F. Lenouvel, S. Mathé, P. Porcu and S. Cosnier, *PLoS One* **2010**, *5*, e10476-e10476.

[188] a) S. Tsujimura, H. Tatsumi, J. Ogawa, S. Shimizu, K. Kano and T. Ikeda, *Journal of Electroanalytical Chemistry* **2001**, *496*, 69-75; b) S. Shleev, J. Tkac, A. Christenson, T. Ruzgas,

A. I. Yaropolov, J. W. Whittaker and L. Gorton, *Biosensors and Bioelectronics* **2005**, *20*, 2517-2554; c) P. Ramírez, N. Mano, R. Andreu, T. Ruzgas, A. Heller, L. Gorton and S. Shleev, *Biochimica et Biophysica Acta (BBA) - Bioenergetics* **2008**, *1777*, 1364-1369; d) L. dos Santos, V. Climent, C. F. Blanford and F. A. Armstrong, *Physical Chemistry Chemical Physics* **2010**, *12*, 13962-13974.

[189] N. Mano, H.-H. Kim and A. Heller, *The Journal of Physical Chemistry B* **2002**, *106*, 8842-8848.

[190] M. C. Weigel, E. Tritscher and F. Lisdat, *Electrochemistry Communications* **2007**, *9*, 689-693.

[191] N. Mano, F. Mao and A. Heller, *Journal of the American Chemical Society* **2002**, *124*, 12962-12963.

[192] S. Tsujimura, K. Kano and T. Ikeda, *Journal of Electroanalytical Chemistry* **2005**, *576*, 113-120.

[193] V. Climent, J. Zhang, E. P. Friis, L. H. Østergaard and J. Ulstrup, *The Journal of Physical Chemistry C* **2011**, *116*, 1232-1243.

[194] F. Gao, Y. Yan, L. Su, L. Wang and L. Mao, *Electrochemistry Communications* **2007**, *9*, 989-996.

[195] G. Göbel and F. Lisdat, *Electrochemistry Communications* **2008**, *10*, 1691-1694.

[196] M. Jönsson-Niedziolka, A. Kaminska and M. Opallo, *Electrochimica Acta* **2010**, *55*, 8744-8750.

[197] M. Tominaga, M. Ohtani and I. Taniguchi, *Physical Chemistry Chemical Physics* **2008**, *10*, 6928-6934.

[198] K. Murata, K. Kajiya, N. Nakamura and H. Ohno, *Energy & Environmental Science* **2009**, *2*, 1280-1285.

[199] K. Schubert, G. Goebel and F. Lisdat, *Electrochimica Acta* **2009**, *54*, 3033-3038.

[200] C. Kang, H. Shin, Y. Zhang and A. Heller, *Bioelectrochemistry* **2004**, *65*, 83-88.

[201] M. Scheuermann-Freestone, P. L. Madsen, D. Manners, A. M. Blamire, R. E. Buckingham, P. Styles, G. K. Radda, S. Neubauer and K. Clarke, *Circulation* **2003**, *107*, 3040-3046.

[202] J. S. Hansen, J. K. Villadsen, M. Gaster, N. J. FÃ¦rgeman and J. Knudsen, *Analytical Biochemistry* **2006**, *355*, 29-38.

[203] a) E. J. Stevenson, P. E. Thelwall, K. Thomas, F. Smith, J. Brand-Miller and M. I. Trenell, *American Journal of Physiology-Endocrinology and Metabolism* **2009**, *296*, E1140-E1147; b) A. Jovanovic, J. Gerrard and R. Taylor, *Diabetes Care* **2009**, *32*, 1199-1201; c) A. Jovanovic, E. Leverton, B. Solanky, B. Ravikumar, J. E. M. Snaar, P. G. Morris and R. Taylor, *Clinical Science* **2009**, *117*, 119-127.

[204] A. Heller and B. Feldman, *Chemical Reviews* **2008**, *108*, 2482-2505.

[205] a) F. Caruso, *Advanced Materials* **2001**, *13*, 11-+; b) G. Decher, M. Eckle, J. Schmitt and B. Struth, *Current Opinion in Colloid & Interface Science* **1998**, *3*, 32-39; c) J. W. Ostrander, A. A. Mamedov and N. A. Kotov, *Journal of the American Chemical Society* **2001**, *123*, 1101-1110; d) M. Schonhoff, *Current Opinion in Colloid & Interface Science* **2003**, *8*, 86-95.

[206] a) K. Ariga, Q. Ji and J. P. Hill in *Enzyme-Encapsulated Layer-by-Layer Assemblies: Current Status and Challenges Toward Ultimate Nanodevices*, *Vol. 229* (Ed. F. Caruso), **2010**, pp. 51-87; b) R. M. Iost and F. N. Crespilho, *Biosensors & Bioelectronics* **2012**, *31*, 1-10; c) J. Kang, M. Loew, A. Arbuzova, I. Andreou and L. Daehne, *Advanced Materials* **2010**, *22*, 3548-+; d) J. L. Lutkenhaus and P. T. Hammond, *Soft Matter* **2007**, *3*, 804-816; e) G. H. Zeng, Y. B. Xing, J. A. Gao, Z. Q. Wang and X. Zhang, *Langmuir* **2010**, *26*, 15022-15026.

[207] P. Bertrand, A. Jonas, A. Laschewsky and R. Legras, *Macromolecular Rapid Communications* **2000**, *21*, 319-348.

[208] F. Caruso, K. Niikura, D. N. Furlong and Y. Okahata, *Langmuir* **1997**, *13*, 3422-3426.

[209] a) N. Alexeyeva and K. Tammeveski, *Analytica Chimica Acta* **2008**, *618*, 140-146; b) L. Zhang, W. Gong, Y. Pan and Y. Zhang, *Russian Journal of Electrochemistry* **2008**, *44*, 1271-1279.

[210] a) Y. Y. Wang, X. S. Wang, B. Y. Wu, Z. Zhao, F. Yin, S. Li, X. Qin and Q. Chen, *Sensors and Actuators B-Chemical* **2008**, *130*, 809-815; b) W. Xue, T. Cui and Ieee, *Deposition and characterization of layer-by-layer self-assembled carbon nanotube multilayer thin nano films*, **2007**, p. 77-82; c) S. X. Zhang, W. W. Yang, Y. M. Niu, Y. C. Li, M. Zhang and C. Q. Sun, *Analytical and Bioanalytical Chemistry* **2006**, *384*, 736-741.

[211] a) M. Eguilaz, R. Villalonga, L. Agui, P. Yanez-Sedeno and J. M. Pingarron, *Journal of Electroanalytical Chemistry* **2011**, *661*, 171-178; b) M. L. Guo, J. H. Chen, J. Li, L. H. Nie and S. Z. Yao, *Electroanalysis* **2004**, *16*, 1992-1998.

[212] M. Kujawa, H. Ebner, C. Leitner, B. M. Hallberg, M. Prongjit, J. Sucharitakul, R. Ludwig, U. Rudsander, C. Peterbauer, P. Chaiyen, D. Haltrich and C. Divne, *Journal of Biological Chemistry* **2006**, *281*, 35104-35115.

[213] B. Martin Hallberg, C. Leitner, D. Haltrich and C. Divne, *Journal of Molecular Biology* **2004**, *341*, 781-796.

[214] C. Leitner, J. Volc and D. Haltrich, *Applied and Environmental Microbiology* **2001**, *67*, 3636-3644.

[215] W. Pitsawong, J. Sucharitakul, M. Prongjit, T.-C. Tan, O. Spadiut, D. Haltrich, C. Divne and P. Chaiyen, *Journal of Biological Chemistry* **2010**, *285*, 9697-9705.